



River Research Institute

ISSN 1606-9277

TECHNICAL JOURNAL

Vol. 10 No. 01 May 2006

**RIVER RESEARCH INSTITUTE
FARIDPUR, BANGLADESH**

TECHNICAL JOURNAL

Vol. 10

No. 01

May 2006

**RIVER RESEARCH INSTITUTE
FARIDPUR, BANGLADESH**

TECHNICAL JOURNAL

Vol. 10, No. 1, 1917

NEW YORK
PUBLISHED BY THE
AMERICAN SOCIETY OF MECHANICAL ENGINEERS

TECHNICAL JOURNAL
RIVER RESEARCH INSTITUTE, FARIDPUR
May, 2006

EDITORIAL BOARD

CHAIRMAN

Md. Quamruzzaman

MEMBERS

Md. Hanif Mazumder
Md. Abdus Samad

EXECUTIVE EDITOR

Md. Rafiqul Alam

PUBLICATION ASSOCIATES

Md. Azizul Haque Podder
Fatima Rukshana

OFFICE MANAGER

Md. Azmal Hossain Fakir

TECHNICAL STAFF
RIVER RESEARCH INSTITUTE
1960

EDITORIAL BOARD

CHAIRMAN

MEMBERS

MEMBERS

MEMBERS

EXECUTIVE EDITOR

MEMBERS

PUBLICATION ASSOCIATES

MEMBERS

MEMBERS

OFFICE MANAGER

MEMBERS

**TECHNICAL JOURNAL
RIVER RESEARCH INSTITUTE, FARIDPUR**

Vol. 10, No. 01, May 2006

CONTENTS

Sl.No.	Title of the Paper with Author's Name	page
1.	River Geometry and Bankline Movement of The Ganges River in Bangladesh A.K.M. Ashrafuzzaman, Md. Lutfor Rahman, Md. Azizul Haque Podder and Md. Asadul Bari	1
2.	Verification of Hydraulic Jump Performances for Various Glacises Md. Hazrat Ali, Binoy Kumar Paul, and Ehsan Ahmed	15
3.	Flume Tests of Roughness Co-Efficient for a Mobile Bed Channel Md. Lutfor Rahman, Md. Azizul Haque Podder and Md. Alauddin Hossain	25
4.	A Hydrological Study on The Padma A K M Ashrafuzzaman, Md. Azizul Haque Poddar, Md. Alauddin Hossain and Md. Asadul Bari	31
5.	Improvement of Existing Solid Waste Management Practice of Dhaka City Corporation Md. Niamul Bari, Md. Mujibur Rahman and Mohammad Harunur Rashid	42
6.	Geotechnical Investigation of South Western Zone of Bangladesh and Correlation between Some Index Properties Uma Saha, Fatima Rukshana, Md. Matiar Rahman Mondol and Shailen Kumer Ghosh	55

7. Triaxial Extension Test and Nonlinear Model Parameters of Barind Soil	66
Syed Abdul Mofiz	
8. Effectiveness of Revetment using Physical Modeling: A Case Study of Arial Khan Roadway Bridge	80
Md. Abdus Samad, A K M Ashrafuzzaman, Md. Rafiqul Alam, Swapan Kumar Das and Md. Azizul Haque Poddar	
9. Morphological Aspects of the Alluvial River Gorai-Madhumati	92
Md. Kayser Habib, Md. Shofiul Islam, Pintu kannungoe, Syed Md. Anwaruzzaman A. S. Anwarul Islam and Md. Nazrul Islam Seddique	
10. Interpretation of Geoelectric Soundings in Deciphering Aquifer in Kushtia Municipality	105
M. Shahinuzzaman and M. Nozibul Haque	
11. Compaction Characteristics of Embankment Soils of Jamalpur Priority Project: A Case Study	120
Md. Rafiqul Alam and A.S. Anwarul Islam	
12. Rainwater Harvesting in Bangladesh: A Sustainable Source of Safe Water	134
Md. Alauddin Hossain ¹ , and A.K.M. Ashrafuzzaman	
13. Optimising the Planning and Engineering Design of Hydraulic Structures for Shrimp Culture in Bangladesh	144
Faruq Ahmed Mohiuddin, and Wahiduzzaman	
14. Determination of the uplift pressure of Teesta Barrage by electric analogy method	151
A.S Anwarul Islam, Md Rafiqul Alam and Dibakar Chakma	

River Geometry and Bankline Movement of The Ganges River in Bangladesh

A.K.M. Ashrafuzzaman¹, Md. Lutfor Rahman²,
Md. Azizul Haque Podder¹ and Md. Asadul Bari³

Abstract

A study was undertaken to investigate river geometry and bankline movement of the Ganges river from Indo-Bangladesh border to Aricha confluence. The study included analysis of river geometry in terms of cross-sectional area, depth, width, thalweg level (deepest point) & mean bed level (MBL), and quantifying bankline movement using satellite images. The study showed that the geometry of the river has undergone considerable change over a period of 1984 to 2000. Various amount of bankline movement of the Ganges river had been occurred at the selected locations within the study reach.

Introduction

Bangladesh is a land of rivers interlaced by numerous tributaries and distributaries of the three great river systems: the Ganges-Padma, the Brahmaputra-Jamuna and the Meghna. The Ganges is an international river with its basin spreading over China, Nepal, India and Bangladesh.

The Ganges carries massive discharge and huge sediment load. In the lean flow periods there is a tendency of silting up of the bed. As a result there are changes in cross-section, width, depth, bankline, slope, thalweg etc of the river. These altogether cause significant change to geomorphic and other hydraulic parameters of the river. Thus a study on river geometry and bankline movement of the Ganges river in Bangladesh is extremely important in connection with the river bank stabilization, navigation, flood control and also for the development of any water resources project. The study area was from Indo-Bangladesh Border to Aricha confluence.

Literature Review

About 500 years ago, the river swung to the east along recent multiple faults between Rajmahal Hills and Dinajpur Shield, to enter Bangladesh at Godagari (Khan, 1991). Until then, the course had coincided with the present Hoogly river. A hydraulic flow regime analysis of the Ganges by FAP4 shows that it is now in a dynamic equilibrium. However, it also shows that the sinuosity of the river is decreasing and that the river, especially the part downstream of Hardinge Bridge, is behaving as a wandering river, changing its platform between meandering and braiding. The bank erosion rate of the Ganges river is quite high. ISPAN (1993) analyzed satellite imagery of 1984 and 1993, and found almost similar values as that for the Jamuna River. Numerous studies on the Ganges relating hydrology, morphology and sediment transport have been undertaken and some of these studies are described in the following section.

¹ Senior Scientific Officer, ² Principal Scientific Officer & ³ Scientific Officer, River Research Institute, Faridpur

Hydrologic Study

Bangladesh Water Development Board (BWDB) normally collects hydrologic data and publishes it in different reports like 'water level and discharge observation records', 'water level records' and 'Gauge and discharge observation' under water supply papers. Moreover, the hydrological yearbook of Bangladesh Water Development Board contains hydrological data including rainfall and evaporation.

Some of the available data was analyzed during the feasibility study and planning and designing of the major projects on the Ganges such as Ganges-Kobadak Project; Survey of Faridpur-Barisal Scheme and Ganges Barrage, 1963; Ganges Barrage Design Project; Vol. I and II, 1970, and so on. Moreover, the consultant of East Pakistan Water and Power Development Authority (EPWAPDA) had compiled the hydrological data for master plan. Master Plan Organization (MPO) and its consultants did some studies while evaluating surface water availability of Bangladesh. Alam and Ahmed (1980) conducted flood frequency analysis for the Ganges using mean monthly and annual maximum discharge at Hardinge Bridge for the years 1935 to 1959. Hossain (1987) studied the maximum and minimum discharges of the Ganges at Hardinge Bridge before and after the construction of the Farraka Barrage in India at 18km upstream of Indo-Bangladesh border. He conducted his study taking the data from 1956 to 1986. He found that average peak discharge had increased by about 12% compared to the average peak flow before 1976. On the other hand the average annual lowest discharge had decreased by about 60% compared to the average annual lowest flow after 1976.

Morphological Study

BWDB, morphology division collects morphological data. Historical maps for banklines of the Ganges was studied by the Water Investigation Directorate of BWDB for the years 1780, 1855 and 1868 for this reach.

Dad (1977) studied the course-shifting pattern of the reach of the Ganges from the point of its entry into Bangladesh upto Goalundo. According to his investigation, study reach showed predominantly irregular and flat meandering pattern. The sinuosity of the river is getting flatter and the river has a tendency to develop breaching in some of its meandering reaches. He also stated that the shifting of bankline is erratic and gradual and it is due to the frequent shifting of thalweg in different years. The shifting of thalweg is due to the movement of sand bars, mid-channel islands and aggradation.

Rahman (1978) had studied the erosion pattern of the river reach, its migrating tendency and direction of movement, formation and movement of sand bars and mid-channel islands on its bed for the river Padma from Ganges-Brahmaputra confluence to Padma-Meghna confluence. He stated that the frequent wandering of the thalweg from position to another is due to the great magnitude of discharge during flood and movement of sand bars and mid-channel islands. He also stated that the shifting of the banklines is erratic and due to aggradation of the channel bed and the movement of the thalweg. He found that the maximum rate of erosion is about 1100ft per year and the maximum rate of deposition is about 850ft per year, both occurring on the right bank.

Hossain (1989) studied the erosion-deposition pattern, shifting characteristics and rate

of change of cross-section and thalweg movement, including sediment transport of the Ganges. He stated that bankline migration is very erratic in nature and varies very widely from bend to bend as well as from year to year. The analysis also show that the Ganges is becoming more sinuous in the upper reaches and less sinuous tending to straight-braided pattern in the lower reaches. The study reveals that there is a trend of rise in mean bed level in the upper reach and fall in the lower reach and net volume of material deposited during 1967-68 to 1979-80 within the study reach was about $4.26 \times 10^8 \text{ m}^3$. The short term migration of the bends were erratic in nature and varied very widely from about 20m per year to as much as 645m per year which corresponds to a minimum shift of 0.25km at one bend and a maximum shift of 9km at other bend during 1973 to 1897 period. The trend of the migration rate with R_c/W for the Ganges showed a general agreement with the trend of bed migration found in the case of another river. The mean gradient of the riverbed had increased from 5.18cm/km in 1967-68 to 7.14cm/km in 1979-80 within the study reach. He also developed some meander relationships.

Sediment Transport Study

Bari (1978) analyzed the sediment data of the Ganges river at Kalikapur for the years 1970, 1972 and 1973. He concluded that Colby and Engelund-Hansen formula yield a result, which may be comparable with the measured. He also developed rating curves for the Ganges at this station. Alam and Ahmed (1980) have analyzed the sediment data at Kalikapur for the year from 1969 to 1972. They also compared the measured sediment flow with those predicted by the various sediment transport equation and Colby's equation was found to be the best.

BWDB had analyzed the suspended sediment data of the Ganges at Goalundo utilizing the data of 1966 to 1969 (BWDB, 1972). According to their analysis the total annual suspended load was found to vary from 42million tons to about 675million tons with a mean value of 451million tons. The average daily minimum and maximum concentration was reported to be about 67ppm and 2344ppm respectively. According to Coleman (1969) the suspended sediment load varied from 257million tons to about 735million tons per year estimated on the basis of data from 1958 to 1962. Khan and Matin (1986) found that the Ganges carries about 30 percent of the suspended load as sand load, whereas 90 percent of the suspended load of the Brahmaputra is sand. Hossain (1989) studied that the annual suspended flow through the Ganges, which may be taken to vary from 181million tons to 304million tons. The total annual sediment load was found to vary from 220million tons to 368million tons. Hossain (1991) also found that the total annual sediment flow of the Ganges at Hardinge Bridge was found to vary between 350 to 600million tons. The highest and lowest daily sediment flow was found to be 10million tons and 9000 tons respectively.

The Ganges System

The source of the Ganges is at Gangotri in the Uttar Khashi district of India and is located at an elevation of 7010m. The Ganges is one of the major and most important rivers of the world. The Ganges is not known by this name either at the beginning or at the end. In India it is mostly known as the Ganges and in Bangladesh the river is known as the Padma. But in many literature it is called as the Ganges upto its confluence with the Brahmaputra (Jamuna) near Aricha and from there up to its confluence with the

Meghna is known as the Padma.

After traversing through seven states of India (Uttar Pradesh, Himachal, Punjab and Haryana, Rajasthan, Madhya Pradesh, Bihar and West Bengal) the Ganges enters Bangladesh at Lalgola, 18km downstream of the Farakka Barrage. Then the river travels along the common border of Indo-Bangladesh for a distance of about 100km from Jalangighat and then for a further distance of 125km from Jalangighat to Aricha where it meets the Brahmaputra (Jamuna). The river known as the Padma travels further downstream to meet the Meghna near Chandpur and the combined discharge finally falls into the Bay of Bengal through a number of estuary channels.

The total length of the Ganges from its source to outfall into the sea measured along the Hooghly is about 2525km and along the Padma-Meghna is about 2650km. The drainage area of the Ganges upto Goalundo confluence is approximately 977044km^2 of which about 7 percent (67395km^2) lies above the Goalundo confluence and bounded by the Bhagirathi-Hooghly on the west and the Ganges-Meghna in the east (Das, 1992). The Ganges river basin is shown in **Figure 1**.

River Geometry

The geometry and shape of an alluvial river are the results of the interaction among water discharge, the quantity and characteristics of sediment discharge, composition of bed and bank material etc. The bed and banks of alluvial rivers are mostly composed of non-cohesive granular materials. The erosion and subsequent transportation-deposition mainly result from the interaction of moving fluid and its loose boundary. Prolonged interactions tend to achieve the equilibrium or in regime status. A river in regime exists in a state of dynamic equilibrium, self-adjusting its river pattern, cross-sectional geometry, slope and bed form. These adjustments occur as the river's ability to transport sediment, balance the available sediment load. Also the characteristics of the river valleys and river flood plains play an important role in river geometry (Das, 1992).

Factors Influencing River Geometry

The factors that govern the geometry and roughness of an alluvial river are numerous and inter-related. Their nature is such that, it is not possible to isolate and study the role of an individual variable. Thus, if one attempts to evaluate the effect of increasing river depth on average velocity, additional related variables respond to change in depth. Similarly, not only will the velocity respond to change in depth, but also the form of bed roughness, the position and shape of alternate, middle and point bars, the shape of cross section, the magnitude of sediment discharge and so on. Consequently the study of the mechanics of flow in alluvial rivers and the response of river geometry have been the subject of study by many investigators at various time.

There are several variables, which influence the geometry of alluvial rivers. Some of the important variables are as follows: V , D , S , ρ , μ , g , d , σ , ρ_s , S_p , S_R , S_c , f_s , C_T .

Where,

V = Velocity, D = Depth, S = Slope of energy grade line, ρ = Density of water-sediment mixture, μ = Apparent dynamic viscosity of the water-sediment mixture,

g = Acceleration due to gravity, d = Grain size of the bed materials, σ = Measure of size distribution of bed materials, ρ_s = Density of sediment, S_p = Shape factor of the particles, S_R = Shape factor of the reach of the stream, S_c = Shape factor of the cross-section of the stream, f_s = Seepage force in the bed of the stream, C_T = Concentration of bed material discharge

Bankline Movement

Bankline movement through erosion-deposition processes in an alluvial river is a characteristic feature and one of the most conspicuous changes affecting fluvial landscapes. At a meander bend high velocity occurs in the outer bank causing recession of bank and also the spiral flow tends to deepen the outer bank. In a river rates of such bank erosion can be rather high but such rates apply to certain bends only, others on the same river at the same time shift more slowly. Generally, the rate of bank shifting is determined by the strength of the bank on one hand and the fluid forces on the other hand. Under natural conditions regular pattern of bank shifting cannot survive. This is due to the fact that apart from the effects of river flow variations, river and valley floor sediments are rarely uniform and the lateral redistribution associated with bank cutting and point bar construction introduces size sorting. Continued shifting with spatially variable boundary conditions must inevitably lead to distortion of the waveform with some bends, or parts of bends, eroding faster than others as the pattern as a whole becoming irregular. A deterministic analysis of meander development is extremely complicated because an irregular meander pattern is even less likely to be in a steady state. However, a statistical equilibrium can be envisaged in which the pattern retains its aggregate characteristics despite changes in detail. If some bends grow, but others decline or are eliminated, the scale and degree of meandering, and the overall level of irregularity, may remain more or less constant over the years. The river occupies different positions at different times and experiences different spatial sequences of disturbances about the average condition. The precise course of the channel depends on the detailed pattern of these disturbances, but the overall nature of the waveform need not alter. But such a statistical equilibrium is possible only if no change occurs in hydrologic regime of sediment load and the disturbance sequences are realizations of a single stationary stochastic process. If changes take place the problems in approaching to establish whether lateral movement of channels can be discerned from the various forms of evidence available are questions on their spatial and temporal distributions; questions about the controls on movement, including the effect of specific disturbances such as alteration can be analyzed based on the knowledge of the relationship between form and movement and on identification of stable forms (Islam et al., 1999).

Methodology

Eighteen standard BWDB cross-sections of the Ganges river were considered in the present study. These were G1, G2, G3, G4, G5, G6, G7, G8, G9, G10, G11, G12, G13, G14, G15, G16, G17 and G18. The index map showing the location of these cross-sections is shown in **Figure 3**. The cross-sectional area of each cross-section in 1984 was compared with that of 2000. The thalweg level is the deepest point of the cross-section and was determined for 1984 and 2000 to observe its variation.

The mean bed level (MBL) was determined by subtracting the average depth from the average bank level of each cross-section for 1984 and 2000 to observe its variation.

From the satellite images, the banklines of 1973 & 1984, 1984 & 1993 and 1993 & 1999 were superimposed. For this purpose eight representative sections were selected within the study reach. These sections were about 13, 42, 59, 97, 125, 142, 171 & 198km downstream of Indo-Bangladesh border near Shibganj upazila under Chapai Nawabganj district. The amount of bankline movement and also the rate of erosion/deposition were determined along the representative sections.

Results and Discussion

Variation of cross-sectional area, average depth and top width

Each of the cross-sectional maps was superimposed for 1984 and 2000, which clearly shows the shifting of thalweg, change in width as well as the location of the thalweg. A typical cross-section at G11 is shown in **Figure 4**. The variation of cross-sectional area, average depth and top width of the selected cross-sections shown in **Figure 5, 6 & 7**.

The cross-sectional area at cross-sections G1, G3, G6, G7, G8, G13, G14 & G16 had a decreasing trend indicating aggradation while there had an increasing trend at cross-sections G2, G4, G5, G9, G10, G11, G12, G15, G17 & G18 indicating degradation during the period from 1984 to 2000.

The maximum change in cross-sectional area was observed at cross-section G18 where the cross-sectional area in 2000 was increased by 2.36 times the corresponding cross-sectional area in 1984. The minimum change in cross-sectional area is observed at the cross-section G11. The total cross-sectional areas calculated were 741976m^2 and 916614m^2 in 1984 and 2000 respectively indicating overall erosion in 2000 with respect to 1984. The net increase in cross-sectional area was about 23.5%. The average depth & top width in 2000 was more than that of 1984.

Variation of thalweg level

The position as well as shifting of thalweg measured from left bank of river for the cross-sections over a period of 1984 to 2000 is shown in **Table 1**. The thalweg at cross-section G1, G6, G7, G9, G10, G12 & G15 was shifted to the right whereas the thalweg at cross-section G2, G3, G4, G5, G8, G11, G13, G14, G16, G17 & G18 was shifted to the left. The maximum thalweg shifting was occurred at cross-section G17, which was 7143m towards the left side during 1984 to 2000. The thalweg of the river was shifted randomly. The thalweg level for the standard BWDB cross-sections is shown in **Figure-8**. The average thalweg level in 2000 was deeper than that of 1984. An exceptional deepest point was found at cross-section G11 in 2000, which was 14.2m (please see **Figure 4**) below the PWD datum.

Variation of mean bed level (MBL)

The variation of MBL for the cross-sections over a period of 1984 to 2000 is shown in **Figure 9**. It was observed from the figure that MBL falls at all cross-sections except G1 & G15. The average MBL in 2000 is lower than that of 1984 indicating river bed erosion. The maximum MBL falls at cross-section G13 that is about 3.

Table 1: Location & shifting of thalweg measured from left bank for the standard BWDB cross-sections of the Ganges river.

C/S No.	Location of thalweg from left bank		Shifting of thalweg (m)	Direction
	1984 (m)	2000 (m)		
G1	287	2479	-2192	Right
G2	1735	1317	418	Left
G3	2187	755	1432	Left
G4	1444	431	1013	Left
G5	1552	284	1267	Left
G6	437	1455	-1018	Right
G7	1591	3904	-2313	Right
G8	4568	2564	2004	Left
G9	7600	7653	-54	Right
G10	2038	3368	-1330	Right
G11	7364	7322	42	Left
G12	3749	6348	-2599	Right
G13	4078	2894	1185	Left
G14	780	154	626	Left
G15	995	4591	-3596	Right
G16	5159	3247	1913	Left
G17	9476	2333	7143	Left
G18	4468	1586	2882	Left

Bankline Movement from Superimposed Satellite Images

Bankline movement during 1973 to 1984

In 1973 the channel of the Ganges river near the Indo-Bangladesh border in Shibganj upazila under Chapai Nawabganj district was outside Bangladesh (in India). In 1984, some downstream portion of this channel was entered into Bangladesh and proceeded by forming a sharp bend. Near Nawabganj Sadar, no significant change in channel was observed between 1973 & 1984. Near Godagari, the channel bend had become sharper in 1984 than that of 1973. Near Rajshahi City, there were two channels (left & right) by forming a char in the middle in 1973 but in 1984, there was a single channel and proceeded downstream in the southern direction. Near Charchhat, most of the channel portion passed through the Indo-Bangladesh border in 1973. But in 1984 most of the channel portion was inside Bangladesh. Upstream of Bagha, the channel was further shifted towards southern direction in 1984 relative to 1973. Near Lalpur, the channel was shifted to the northern direction in 1984 relative to 1973. Near Bheramara, the channel was divided into two channels by forming a char in the middle in 1973. But in 1984 there was a single channel only and further downstream from Bheramara, the channel was divided. Near Ishwardi, the channel was wider in 1973 relative to 1984. Near Pabna Sadar, no significant change was taken place between 1973 & 1984.

Near Sujanagar, two channels (left & right) with a char formed in the middle were combined downstream in 1973 whereas in 1984 there was a single channel only. Near Rajbari Sadar, there were two channels (left & right) with a char formed in the middle in 1973 whereas in 1984 there was a single channel only. The satellite images for the years 1973 and 1984 are superimposed and shown in **Figure-10**. The bankline movement is presented in **Table-2**.

Table 2: Bankline movement during 1973 to 1984 along section lines of the Ganges river from superimposed satellite images

Section No.	Right bank (m)	Left bank (m)
1	-410.0	+5436.0
2	0.0	-103.0
3	-1538.0	+821.0
4	-2974.0	+3056.0
5	+103.0	+205.0
6	-205.0	+3590.0
7	-718.0	+308.0
8	+1333.0	+1538.0

NB: (+) means deposition and (-) means erosion

Table-2 shows that the maximum right bank erosion & deposition is 2974m & 1333m along section-4 and section-8 respectively in 1984 with respect to 1973. The maximum left bank erosion & deposition is 103m & 5436m along section-2 and section-1 respectively in 1984 with respect to 1973.

Bankline movement during 1984 to 1993

Near Shibganj, the channel in 1993 was shifted more from Indo-Bangladesh border inside Bangladesh in the northeast direction relative to 1984. Near Nawabganj Sadar, two channels were combined into a single channel in 1993 whereas in 1984 there was a single channel only. Near Godagari, no significant change was observed between 1984 & 1993. In between Godagari & Rajshahi City, the right channel was shifted in the southwest direction. Also the width of braided portion was more in 1993 relative to 1984. Near Rajahahi City, the channel portion in the southern direction in 1984 was shifted in the east direction in 1993. Near Charghat, the two upstream channels were combined into a single channel in 1993 whereas in 1984, there was a single channel only. The channel portion along southern direction in 1984 was shifted slightly in the western direction (downstream end). Near Bagha, the river width was more in 1993 relative to 1984. Here a dominant channel was observed in 1984 at the right side but in 1993 there were two less dominant channels at the right side. Near Lalpur, in 1993 the right channel was dominant but in 1984, the left channel was dominant. Near Bheramara, the channel was shifted in the western direction in 1993 relative to 1984. Near Iswardi, the channel in 1984 was wider relative to 1993. Near Pabna Sadar, the channel in 1984 was shifted downstream in the southeast direction in 1993. In between Pabna Sadar & Sujanagar, the channel in 1984 was shifted to the southern direction in 1993. Near Sujanagar, there was a single channel in 1984 but in 1993, there were two channels.

Near Rajbari Sadar, the channel in 1984 was shifted in the southern direction in 1993. The satellite images for the years 1984 and 1993 are superimposed and shown in **Figure-11**. The bankline movement is presented in **Table-3**.

Table-3: Bankline movement during 1984-1993 along section lines of the Ganges river from superimposed satellite images

Section No.	Right bank (m)	Left bank (m)
1	+205.0	-2872.0
2	+1846.0	-287.0
3	-3385.0	-3077.0
4	-3077.0	+205.0
5	-246.0	0.0
6	-308.0	-841.0
7	0.0	-923.0
8	-1744.0	+3179.0

NB: (+) means deposition and (-) means erosion

It can be observed from **Table 3** that the maximum right bank erosion & deposition is 3385m & 1846m along section-3 and section-2 respectively in 1993 with respect to 1984. The maximum left bank erosion & deposition is 3077m & 3179m along section-3 and section-8 respectively in 1993 with respect to 1984.

Bankline movement during 1993 to 1999

Near Shibganj, the channel was shifted more in the northeast direction inside Bangladesh and formed a bend between Shibganj & Nawabganj Sadar and became close to Pagla river in 1999 relative to 1993. The confluence of two channels (in India) was shifted in the western direction in 1999 relative to 1993. Near Nawabganj Sadar, the channel was dominant in 1999 relative to 1993. Near Godagari, there was a confluence of two channels in 1999. From Godagari upto certain length downstream the channel was relatively less wider in 1999 relative to 1993. In between Godagari & Rajshahi City, the braided portion was more in 1999 relative to 1993. There were two channels in 1999 but in 1993 there was a single channel (right channel in India). Near the Rajshahi City, the channel was wider in 1999 relative to 1993. The confluence was relatively upstream in 1999. Near Charchat, at confluence three channels met in 1999 but in 1993 two channels met. The width of channel was more in 1999 relative to 1993. Near Bagha, a huge braided portion was observed both in 1993 & 1999. Near Lalpur, the width of the channel was more in 1999 relative to 1993. Near Bheramara, the channel in 1999 was wider & dominant relative to 1993. Near Iswardi, the width of channel was also more in 1999 relative to 1993. Near Pabna Sadar, the channel was bend in 1999 but in 1993 the channel was straight. Also the width of the channel was more in 1999 relative to 1993. Near Sujanagar, the channel was wider in 1999 relative to 1993. Near Rajbari Sadar, the channel was also wider in 1999 relative to 1993. The satellite images for the years 1993 and 1999 are superimposed and shown in **Figure 12**. The bankline movement is presented in **Table 4**.

Table 4: Bankline movement 1993-1999 along section lines of the Ganges river from superimposed satellite images

Section No.	Right bank (m)	Left bank (m)
1	+308.0	-2667.0
2	+226.0	0.0
3	-390.0	0.0
4	-2667.0	0.0
5	-246.0	+164.0
6	0.0	+205.0
7	-164.0	+1846.0
8	-41.0	+1518.0

NB: (+) means deposition and (-) means erosion

Table 4 shows that the maximum right bank erosion & deposition is 2667m & 308m along section-4 and section-1 respectively in 1999 with respect to 1993; the maximum left bank erosion & deposition is 2667m & 1846m along section-1 and section-7 respectively in 1999 with respect to 1993.

Conclusions

The following conclusions may be drawn on the basis of the present research study:

- Over a period from 1984 to 2000, the cross-sectional area varies randomly.
- The thalweg of the river moves from one bank to another in a random fashion.
- The mean bed level at all standard BWDB cross-sections falls in 2000 with respect to 1984 except G1 & G15, which on average indicates the channel bed degradation.
- From superimposed banklines of 1973 & 1984, 1984 & 1993 and 1993 & 1999, it is observed that various amount of shifting has been occurred at the selected locations.
- Maximum right bank erosion is 3385m along section-3 in 1993 as compared to 1984 and maximum left bank erosion is 3077m along section-3 in 1984 as compared to 1993. Maximum right bank deposition is 1846m along section-2 in 1993 as compared to 1984 and maximum left bank deposition is 3179m in 1993 along section-8 as compared to 1984. The average bank erosion & deposition rate is 156m/year & 140m/year respectively during 1973 to 1999 measured along eight representative sections.

References

- Alam, M.K. and Ahmed, S.M. (1980)**, Peak flow analysis and evaluation of sediment transport capacity of the Ganges, UGC Research Project, Department of Water Resources Engineering, BUET, Dhaka.
- Bari, M.F. (1978)**, Applicability of sediment transport formulas for the Ganges and Jamuna, M.Sc. Engg. Thesis, Department of Water Resources Engineering, BUET, Dhaka.
- BWDB (1972)**, Sediment investigation in main rivers of Bangladesh, BWDB Water Supply Paper, No. 359, Dhaka.
- BWDB (1979)**, Bankline movement for the Ganges from 1780-1973, BWDB, Vol. II.
- Dad, M.M. (1977)**, A study on the river course shifting pattern in Bangladesh, M.Sc. Engg. Thesis, Department of Water Resources Engineering, BUET, Dhaka.
- Das, S.K. (1992)**, Hydraulic geometry of the Ganges, M.Engg. Thesis, Department of Water Resources Engineering, BUET, Dhaka.
- Hossain, M.M. (1987)**, Geomorphic characteristics of the Padma upto Brahmaputra confluence, First Interim Report, R 03/87, IFCDR, BUET, Dhaka.
- Hossain, M.M. (1989)**, Geomorphic characteristics of the Padma upto Brahmaputra confluence, Final Report, R 02/89, IFCDR, BUET, Dhaka.
- Hossain, M.M. (1991)**, Total sediment load in the lower Ganges and Jamuna, paper presented at the 35th annual convention of Institute of Engineers, Bangladesh, Chittagong, March 8-11, 1991.
- Islam et al. (1999)**, Technical Journal of RRI, Vol. 06, No. 1, p. 87.
- ISPAN (1993)**, Environmental Study (FAP16) and Geomorphic Information System (FAP19), The dynamic physical and human environment of riverine charlands: Ganges and Padma, Dhaka, Bangladesh.
- Khan, A.H. and Matin, M.A. (1986)**, Morphological survey in sediment sampling in Bangladesh, Proceedings of regional workshop on erosion and sediment transport processes, UNESCO-BUET, Dhaka.
- Rahman, K.S. (1978)**, A study on the erosion of the river Padma, M.Sc. Engg. Thesis, Department of Water Resources Engineering, BUET, Dhaka.
- River Survey Project (1996)**, FA0P24, Special Report No.7, Geomorphology and Channel Dimensions.
- RRI (2003)**, A Study on River Geometry and Bankline Movement of the Ganges River in Bangladesh, Research Report, Report No. RES-1(2003).
- Sir William Halcrow and Partners Ltd (1993)**, Southwest Area Water Resources Management Project (FAP4), Morphological Studies, Vol. 3, Final Report, Dhaka, Bangladesh.
- Surface Water Simulation Modeling Program (1996)** Phase III, Final Report, Vol. II, surface water model, Dhaka.

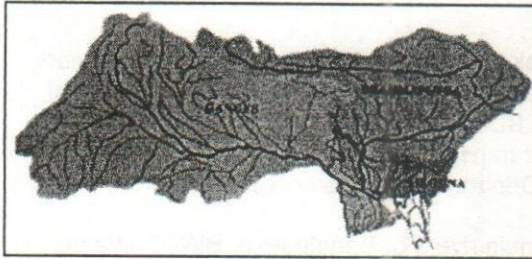


Figure 1 The Ganges river basin

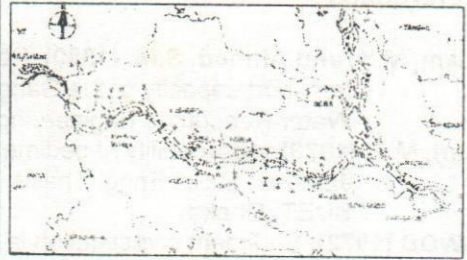


Figure-2: Standard BWDB cross-sections of the Ganges river (Das, 1992)

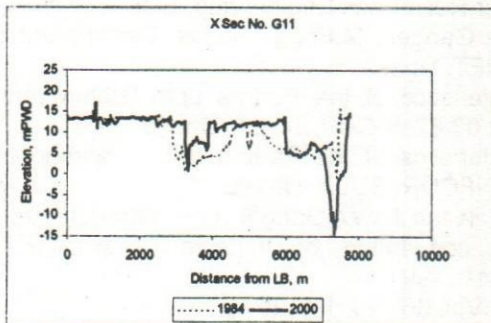


Figure 3: Superimposed cross-sectional map between 1984 and 2000 (G11)

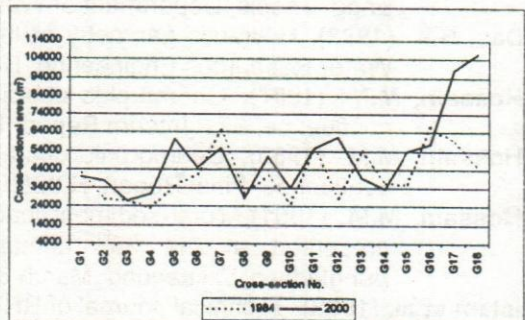


Figure 4: Variation of cross-sectional area for the standard BWDB cross-sections

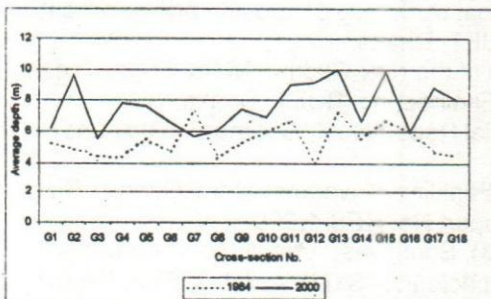


Figure 5: Variation of average depth for the standard BWDB cross-sections

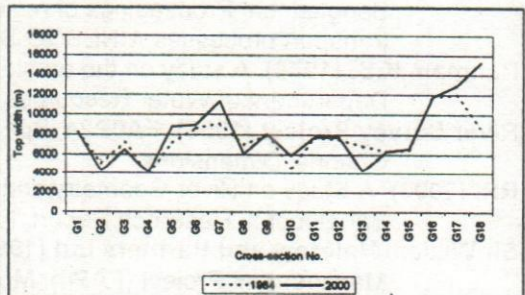


Figure 6: Variation of top width for the standard BWDB cross-sections

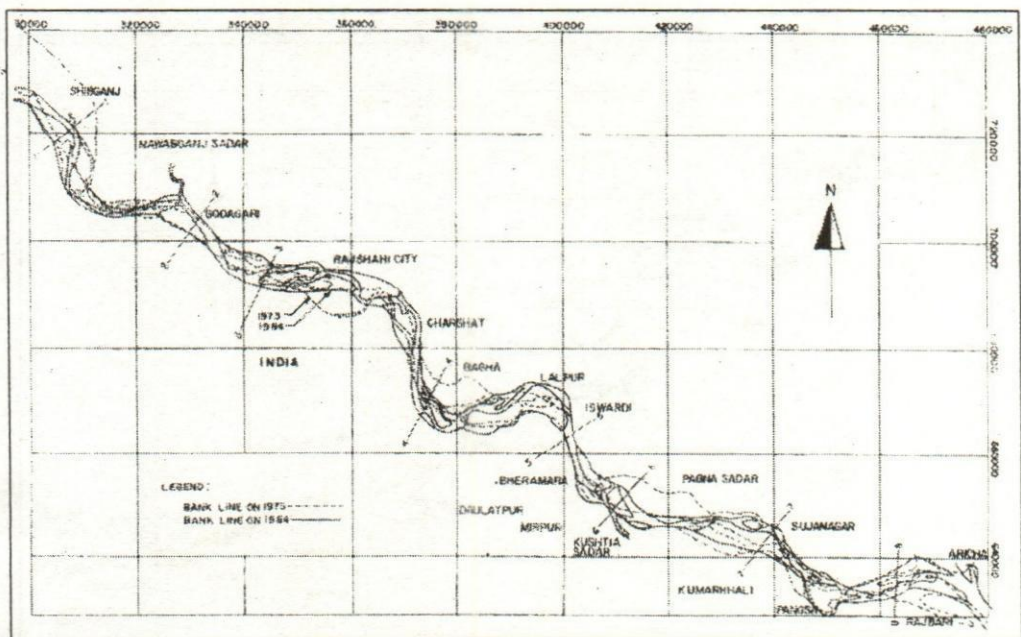


Figure 9: Superimposed bankline between 1973 and 1984

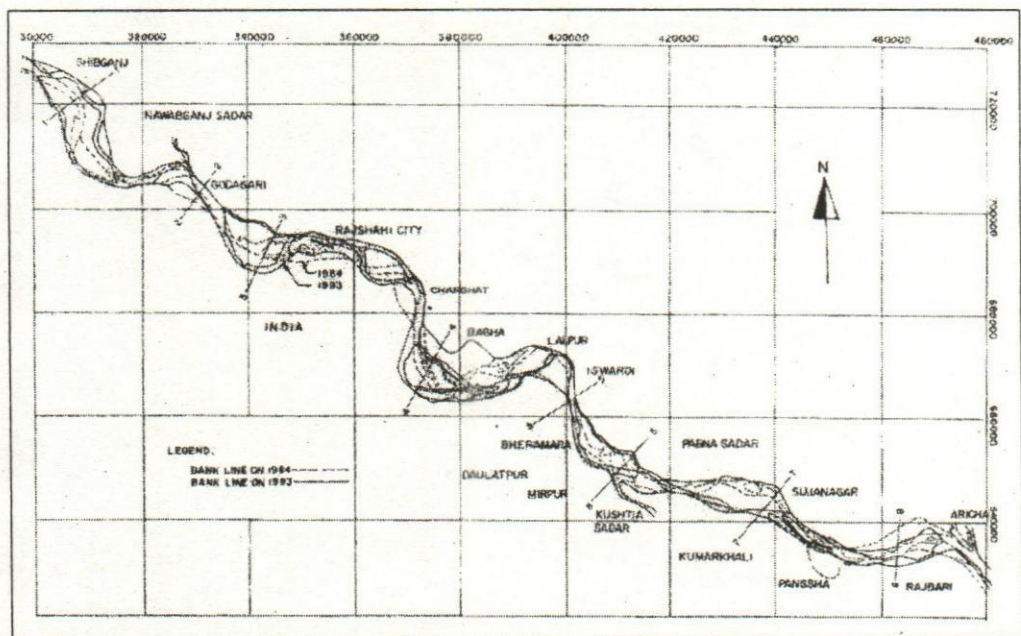


Figure 10 Superimposed bankline between 1984 and 1993

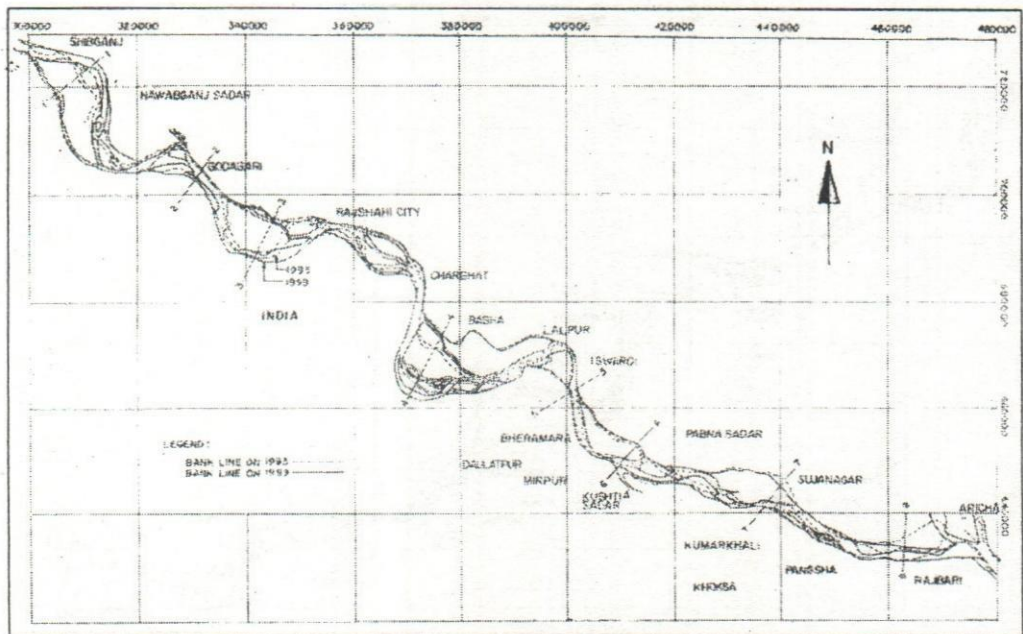


Figure 11 Superimposed bankline between 1993 and 1999

Verification of Hydraulic Jump Performances for Various Glacises

Md. Hazrat Ali¹, Binoy Kumar Paul², and Ehsan Ahmed³

Abstract

A hydraulic jump represents a wave that desires to move in upstream direction, but which it unable to do, as the flow velocity of the water is larger than the wave's celerity and is generally accompanied by large scale turbulence, dissipating most of the kinetic energy of supercritical flow. The main reason behind this study is its practical utility in hydraulic engineering and allied fields. The results of laboratory investigations on hydraulic jump performances for various channel bed patterns are presented. In the design of sluice gate involving a jump below the gate, characteristic curves show clearly the formation of jump for different gate openings under a given head. The maximum relative height is found to be 0.507 at incoming Froude number F_1 of 2.77. When F_1 increases, the jump is observed more sensitive to tail water depth. The relative energy loss is found to increase with the increase of channel slope. It is found that the value decreases with the increase of channel slope. The m_s value is found to be approximately equal to the value reported by Elevatorski (1959). The value is found to increase with the increase of channel roughness. The higher value results higher dissipation of kinetic energy, lower length of the jump, less cost of stilling basin needed. It can be concluded that the maximum jump performance is achieved for corrugated bed normal to the flow direction.

Keywords: Jump performance, bed slope, bed pattern, Froude number.

Introduction

The knowledge of open channel hydraulics is essential to water resources development. From the twine viewpoints of quantity and quality, water resources projects are of paramount importance to the maintenance and progress of civilization. Hydraulic jump is rapidly varied flow phenomenon. This type of flow is so complicated that a mere theoretical in most cases will not yield sufficient information for the purpose of practical design. Information about shear stress and turbulent characteristics enhance ones understanding of the jump phenomenon. At present, water resources play a very significant role in national development. In the planning, design and operation of water resources system, such as single and multipurpose river development projects for irrigation, flood control, power generation, etc., a basic understanding of flow in open channel is essential.

Hydraulic jump is the jump of water that takes place when a supercritical flow changes into a subcritical flow. When a stream of water moving with a high velocity and low depth strikes another stream of water moving with low velocity and high depth, a sudden rise in the surface of the former takes place. This phenomenon is called hydraulic jump.

¹ Prof. (Civil), Chittagong Univ. of Eng. & Technology, Chittagong, ² Graduate (Civil), Chittagong Univ. of Eng. & Technology, Chittagong & ³ Asst. Prof. (Civil), Chittagong Univ. of Eng. & Technology, Chittagong

Such a phenomenon may occur in a canal below regulating sluice, at the bottom of the spillway, or at a place where a steep channel slope suddenly turns flat.

When water falls over a spillway or a vertical or glacis fall, it acquires lot of momentum and velocity. Thus, high velocity, if allowed to persist shall cause large-scale erosion and scouring of downstream soil of the work and hence, it must be checked or controlled. In such situation, the phenomenon of hydraulic jump can be used with great advantage for dissipating the kinetic energy of water.

It may be noted that the depth before the jump is always less than the depth after the jump. The depth before the jump is called initial depth, after the jump is called sequent depth. In recent years, water resources projects and hydraulic engineering works have been developing rapidly throughout the world. Hydraulic jump has extensively been studied in the field of hydraulic engineering. The practical applications of hydraulic jumps are many.

The hydraulic jump was first investigated experimentally by Bidone (1920). Since then considerable research effort has gone into the study of this project. This led Belanger (1828) to distinguish between mild (subcritical) and steep slopes, since he had observed that in steep (supercritical) channels hydraulic jump is frequently produced by a barrier in originally uniform flow. Thereafter, abundant studies were made and the results were quoted by many authors. Outstanding contributions about the hydraulic jump are Ferriday (1895), Gibson (1913-14), Kennison (1916), Koch and Carstanjen (1926), Safranez (1927), Bakhmeteff and Matzke (1936), Forster and Skrinde (1950), Rouse et al. (1958), and many other authors.

There exists a little detailed information in the literature about the characteristics of hydraulic jump on corrugated surface. The main reason behind this study is its practical utility in hydraulic engineering and allied fields. Therefore, this study has been taken into consideration on the wavy surface as well as other surfaces with different bed slopes. The main aims of this study are (i) to determine the discharge and analyze the variation of hydraulic coefficients with flow geometry; (ii) to verify the types of jumps with incoming Froude number; (iii) to verify theoretical relation between Froude number and sequent to initial depth ratio; (iv) to determine the length of jump for different channel bed slopes and bed patterns; and (v) to examine the effect of tail water depths on the formation of hydraulic jump. The scope of this study is to analyze the characteristic curves of hydraulic jumps in different slopping channels and established the relation of hydraulic coefficients with flow geometry and verifies them experimentally.

Theoretical Consideration

Hydraulic jump is rapidly varied flow phenomenon and the length of jump is relatively small compared to gradually varied flow (GVF) profiles. In the analysis of hydraulic jumps in sloping channels or channels having appreciable slope, it is essential to consider the weight of water in the jump; in horizontal channels the effect of this weight is negligible. The equation of length of jumps in slopping channels will give direct determination of length of jump from known value of water head.

The equation of sequent depth will give direct determination of tail water depth knowing the values of incoming Froude number. For scour protection purposes, the analysis of effect of tail water depth on the formation of hydraulic jumps is required.

Considering all effective forces parallel to the rectangular channel bottom of unit width (Fig. 1), the momentum equation may be written as

$$\frac{Q\omega}{g}(\beta_2 V_2 - \beta_1 V_1) = P_1 - P_2 + W \sin \theta - F_f \quad (1)$$

where $Q = V_1 d_1$, $V_2 = V_1 d_1 / d_2$, $P_1 = 0.5 \omega d_1^2 \cos \theta$, $P_2 = 0.5 \omega d_2^2 \cos \theta$, W = Weight of the water contained in the control volume, F_f = total external force of friction and resistance and is considered negligible, and β_1 and β_2 = momentum coefficients and may be taken as unity.

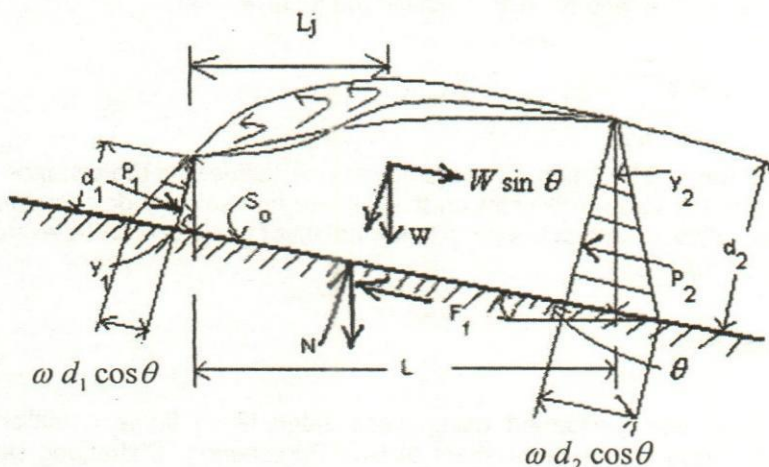


Fig. 1. Definition sketch for general momentum equation

The surface profile of the jump is a straight line; the weight of water in the jump can be computed. The discrepancy between the straight line and actual profile and the effect of slope may be corrected by a factor K . Thus,

$$W = \frac{1}{2} K \omega L (d_1 + d_2) \quad (2)$$

Substituting the value of W in Eq. (1), letting $F_1 = V_1 / \sqrt{g d_1}$, and simplifying

$$\frac{d_2}{d_1} = \frac{1}{2} (\sqrt{1 + 8G^2} - 1) = \frac{y_2}{y_1} \quad (3)$$

where $d_1 = y_1 \cos \theta$, $d_2 = y_2 \cos \theta$, and $G = \frac{F_1}{\sqrt{\cos \theta - \frac{KL \sin \theta}{d_2 - d_1}}}$, a function of F_1 and θ .

Basic Characteristics of the Jump

The basic characteristics of the jump in horizontal rectangular channels are discussed below:

Energy losses: The loss of energy after the jump is equal to the difference in specific energies before and after the jump and is expressed as

$$\Delta E = \frac{(d_2 - d_1)^3}{4d_1 d_2} \quad (4)$$

Efficiency: The ratio of the specific energy after the jump to that before the jump is defined as the efficiency of the jump. It can be expressed by

$$\frac{E_2}{E_1} = \frac{(8F_1^2 + 1)^{\frac{3}{2}} - 4F_1^2 + 1}{8F_1^2 (2 + F_1^2)} \quad (5)$$

Height of jump: The difference between the depths after and before the jump is the height of the jump. The ratio of h_j/E_1 is called the relative height.

$$\frac{h_j}{E_1} = \frac{\sqrt{1 + 8F_1^2} - 3}{F_1^2 + 2} \quad (6)$$

Length of the jump: The length of the jump may be defined as the distance measured from the front of the jump to a point on the surface immediately downstream from the roller. The ratio of the length of the jump to the height of the jump can be expressed as

$$m_s = L_j / (d_2 - d_1) \quad (7)$$

Experimental Setup

The investigation was performed using glass sided tilting flume established in the Hydraulic Laboratory of the Department of Civil Engineering, Chittagong University of Engineering and Technology. For example, the laboratory setup of wavy surface parallel and normal to the water flow, and the test run on the wavy surface parallel to the water flow are shown in **Figs. 2, 3, and 4**, respectively. The bottom surface, the slope, and the sluice gate opening of the tilting flume were the main variables in this study. The tests were performed during May-September 2003.



Fig. 2. Laboratory setup of wavy surface parallel to the water flow.

Corrugated iron sheet was placed on the channel bed parallel and across the direction of flow for various slopes. The Manning's roughness coefficient n for plain bed, corrugated surface placing perpendicular to the flow, and corrugated surface placing parallel to the flow were calculated to be 0.010, 0.021, and 0.018, respectively, indicating that n value increases with the increase of channel roughness. The higher the n value, the higher will be the dissipation of kinetic energy, resulting the lower length of the jump, and therefore saving cost of stilling basin needed to control downstream erosion of channel bed.

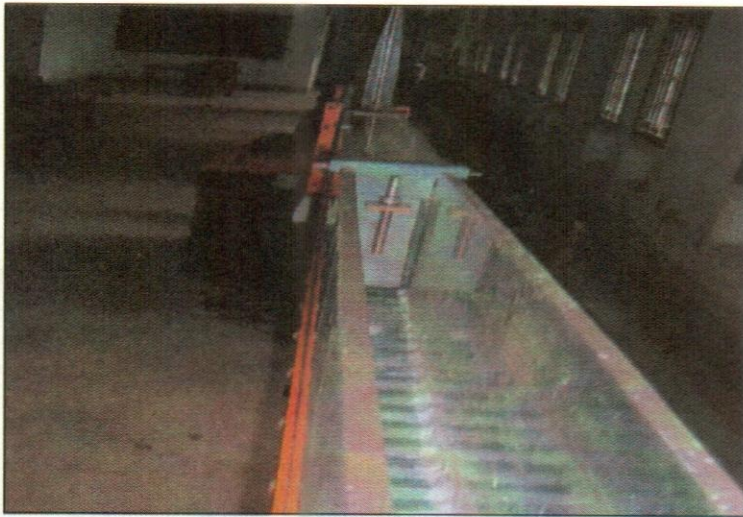


Fig. 3. Laboratory setup of wavy surface normal to the water flow.

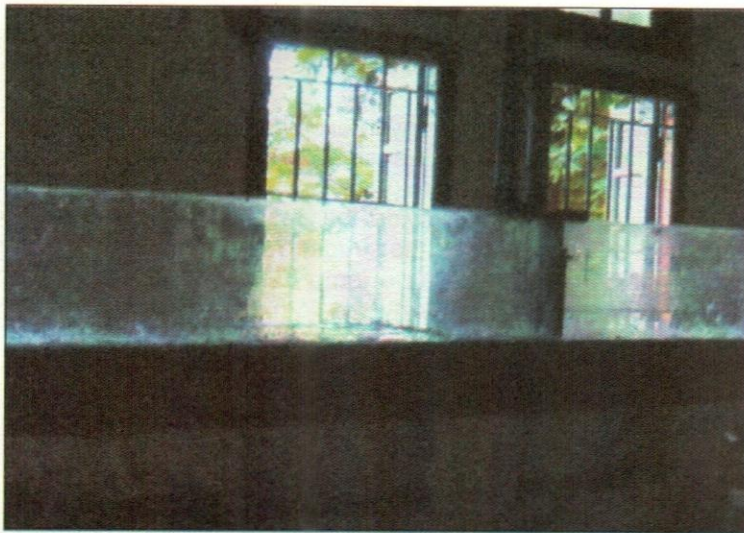


Fig. 4. Test run on the wavy surface parallel to the water flow.

Results and discussions

With reference to the experimental investigation on the hydraulic jump, the following interesting features were observed.

- As the incoming Froude number increases, the jump becomes more sensitive to tail water depth.
- The length of the jump can be determined from **Fig. 5**. **Figure 5** shows regularity over fairly flat portion for the range of well-established jumps. This curve has developed for jumps occurring in rectangular channels. In the absence of adequate data this curve may also be applied approximately to jumps formed in trapezoidal channels.
- The jump moves upstream with the increment of downstream water depth. The downstream depth is raised to such a height that the jump is drowned out in front of the sluice.
- When the tail water depth y_2' is equal to the sequent depth y_2 (**Fig. 6**), the jump occurs immediately ahead of the depth pattern so that a little difference between the actual and assumed values of the relevant hydraulic coefficients causes the jump moves downstream from the estimated portion. For scour protection purpose, this type is an ideal case.
- When the tail water depth y_2' is greater than y_2 , the jump is forced upstream and drowned out at the source, becoming a submerged jump. This is possibly the safest case in design, because the portion of the submerged jump can be most readily fixed. But for little energy dissipation, the design is not efficient.
- When the tail water depth y_2' is less than y_2 , the jump proceeds downstream. This case must, if possible, be avoided in design because the jump is repelled from the scour resisting apron.
- From the analysis of variation of hydraulic coefficient with flow geometry, it is able to determine the coefficient of discharge directly from the curve (**Fig. 7**), knowing the values of ratio of gate opening (y_g) and water head upstream of sluice gate (y_3). The characteristic curve will provide the designer with a general idea about the range of conditions under which the structure is to be operated. For instance, in the design of a sluice gate, involving a jump below the gate opening under a given head, such curve will show clearly the formation of the jump for different gate openings.

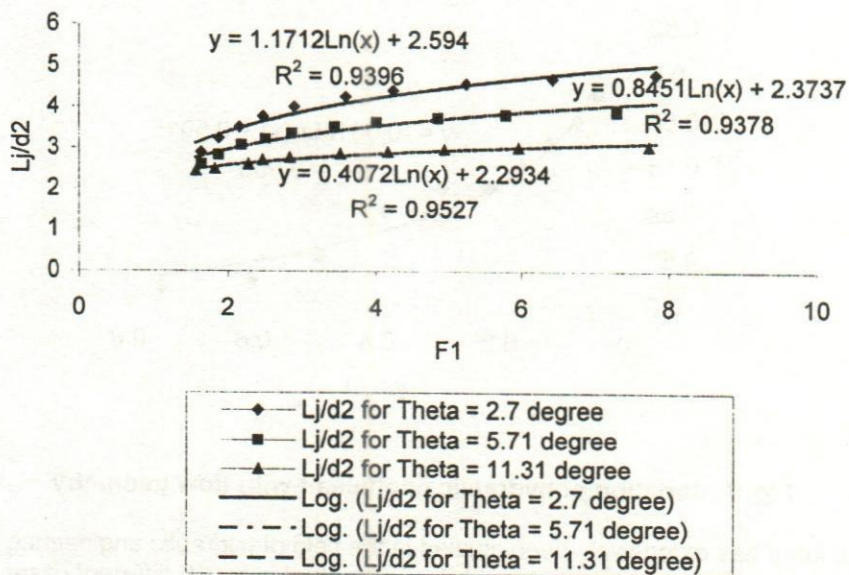


Fig. 5. Length of hydraulic jump for various slopes.

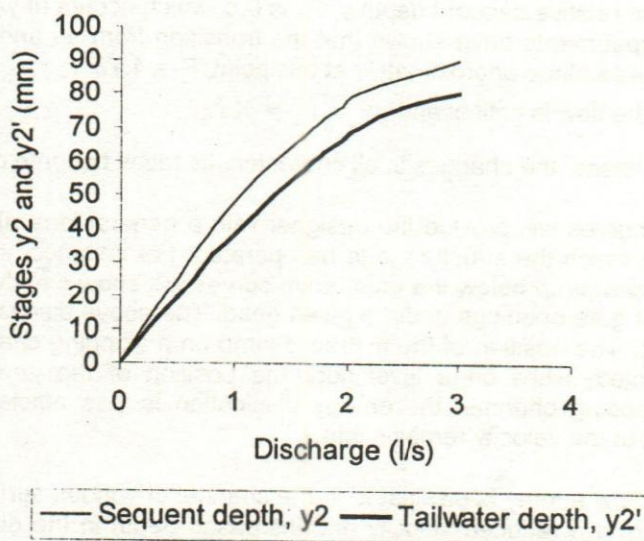


Fig. 6. Sequent depth and tail water depth for various discharges.

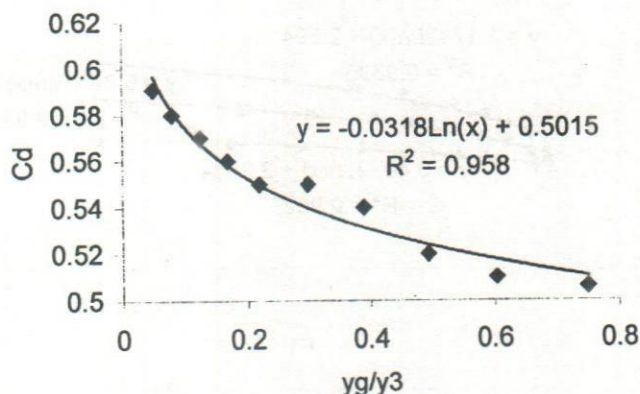


Fig. 7. Variation of hydraulic coefficient with flow geometry

Hydraulic jump has extensively been studied in the field of hydraulic engineering. In this study, the hydraulic jump performances have been studied for 10 different cases. With reference to the characteristic curves (Fig. 8) of the hydraulic jump in horizontal rectangular channels, the following interesting features may be noted.

- The maximum relative height h_f/E_1 is 0.507, which occurs at $F_1 = 2.77$.
- The maximum relative sequent depth y_2/E_1 is 0.8, which occurs at $y_1/E_1 = 0.35$ and $F_1 = 1.73$. Experiments have shown that the transition from an undular jump to a direct jump takes place approximately at this point, $F_1 = 1.73$.
- When $F_1=1$, the flow is critical and $y_1 = y_2 = \frac{2}{3} E_1$.
- When F_1 increases, the changes in all characteristic ratios become gradual.

The characteristic curves will provide the designer with a general idea about the range of conditions under which the structure is to be operated. For instance, in the design of sluice gate involving a jump below the gate, such curves will show clearly the formation of jump for different gate openings under a given head. The above discussion applies to horizontal channels. The position of the hydraulic jump on a slopping channel is definite and can be predicted, while on a level floor the position of the jump is unstable. However, on a slopping channel, the energy dissipation is less efficient because of vertical component of the velocity remains intact.

It is found that the flow energy is dissipated in the channel of various surface roughness conditions, resulting in a reduced velocity and increased depth in the direction of flow. The relative energy loss $(1 - E_2/E_1)$ is found to increase with the increase of channel slope (Fig. 8). The ratio of the length of the jump to that the height of the jump (m_s) is found to decrease with the increase of channel slopes (Fig. 9), indicating the length of the jump is decreasing, and thus, reducing the cost of stilling basin needed to control erosion. The m_s is found to be 7.2 (Fig. 9) for horizontal rectangular channel, which is approximately close to 6.9 reported by Elevatorski (1959), analyzing USBR data. Figure 9 also shows that m_s decreases with the increase of the channel slope.

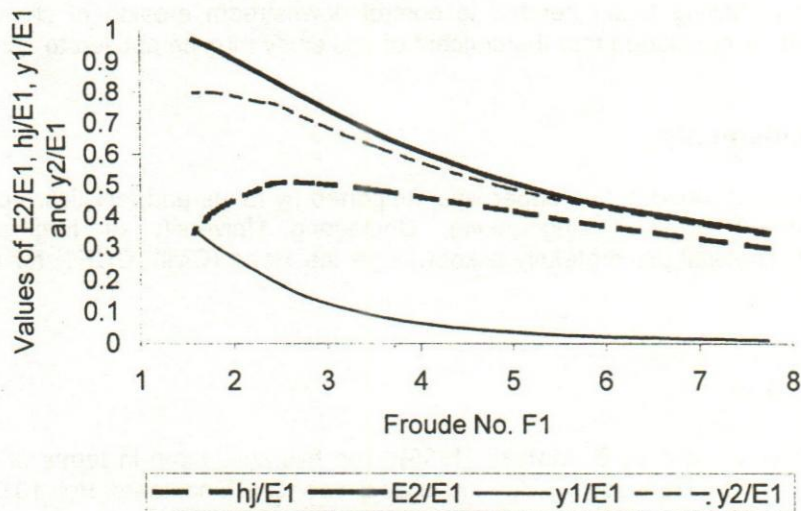


Fig. 8. Characteristic curves of hydraulic jumps in horizontal rectangular channel

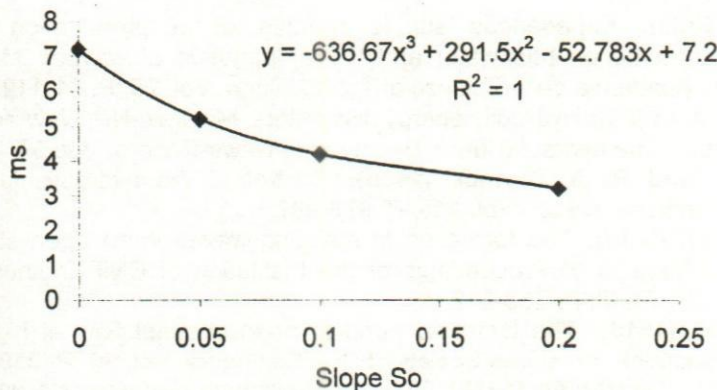


Fig. 9. Variation of mean values of m_s with the slope of the channel

Conclusions

In this study, the results of laboratory investigations on hydraulic jump performances for various channel bed patterns are verified. It is found that (i) the jump becomes more sensitive towards increased Froude number; (ii) the maximum relative height is 0.507 at F_1 of 2.77; (iii) the maximum relative sequent depth is 0.8 $y_1/E_1 = 0.35$ and $F_1 = 1.73$; (iv) the relative energy loss is found to increase with the increase of channel slope (v) the m_s value decreases with the increase of channel slope; (vi) the n value increases with

the increase of channel roughness; and (vii) the higher the n value, the higher will be the dissipation of kinetic energy, resulting the lower length of the jump, and therefore saving cost of stilling basin needed to control downstream erosion of channel bed. Finally, it can be concluded that the concept of this study may be applied to actual sized river.

Acknowledgements

The research described in this paper was supported by funds and facilities provided by the Department of Civil Engineering, Chittagong University of Engineering & Technology. The authors gratefully acknowledge the Head (Civil), CUET, for technical assistance.

References

- Bakhmeteff B. A. and A. E. Matzke (1936):** The hydraulic jump in terms of dynamic similarity. Transactions, American Society of Civil Engineers, Vol. 101, P. 630-647.
- Bélanger J. B. (1828):** Essai sur la solution numerique de quelques problemes relatifs au mouvement permanent des eaux courantes (Essay on the Numerical Solution of Some Problems Relative to the Steady Flow of Water). Carilian – Goeury, Paris.
- Bidone G. (1820):** Experiences sur le remous et la propagation des ondes (Experiments on backwater and the propagation of waves). Memorie della Reale Accademia delle Scienze di Torino, Turin, Vol. 25, P. 21-112.
- Elevatorski E. A. (1959):** Hydraulic energy dissipators. McGraw-Hill, New York.
- Ferriday R. (1895):** The hydraulic jump. Engineering News-Record, Vol. 34, No.2, P. 28.
- Forster J. W. and R. A. Skrinde (1950):** Control of the hydraulic jump by sills. Transactions, ASCE, Vol. 115, P. 973-987.
- Gibson A. H. (1913-14):** The formation of standing waves in an open stream, paper 4081. Minutes of Proceedings of the Institution of Civil Engineers, London, Vol. 197, Pt. III, P. 233-242.
- Kennison K. R. (1916):** The hydraulic jump in open channel flow at high velocities. Transactions, American Society of Civil Engineers, Vol. 80, P. 338-353.
- Koch A. and M. Carstanjen (1926):** Von der Bewegung des wassers und den dabei auftretenden Krafte (On Flow of Water and the Associated Forces). Springer-Verlag, Berlin.
- Rouse H., T.T. Siao, and S. Nagaratnam (1958):** Turbulence characteristics of the hydraulic jump, paper 1528. Proceedings, American Society of Civil Engineers, Journal Hydraulics division, Vol. 84, No. HY1, Pt. 1, P. 1-30.
- Sufranz K. (1927):** Wechselsprung und die Energievernichtung des Wassers (Hydraulic jump and energy dissipation of water). Der Bauingenieur, Berlin, Vol.8, No. 49, P. 898-905; No. 50, P. 926.

Flume Tests of Roughness Co-Efficient for a Mobile Bed Channel

Md. Lutfor Rahman¹, Md. Azizul Haque Podder² and Md. Alauddin Hossain³

Abstract

Attempts have been made to determine the roughness coefficient of a mobile bed flume in this paper under the laboratory of River Research Institute (RRI), Faridpur. In this regard nine test runs have been conducted and observatory data of this test have been analyzed and interpreted. Test runs are divided into two distinct categories to determine the effect of stage and velocity exclusively. Discharges have been varied (i) keeping velocity same and varying only water depth and (ii) keeping water depth same and varying only velocity. In this study, Chezy's roughness coefficient (C) and Manning's roughness coefficient (n) values have been determined in a mobile bed flume for different water depths keeping velocity same. It has also been determined C and n value for different velocity keeping the water depth same. It appeared that, water depth has more dominant effect on roughness than velocity. Increasing water depth showed increasing value of Manning's n under the present test scenarios.

Background and Objective of The Study

Three mighty rivers, the Padma, the Meghna and the Jamuna, flow through Bangladesh. These rivers are alluvial in nature and their combined discharge is delivered to the Bay of the Bengal. The roughness co-efficient is a dominating parameter in predicting water level and discharge. In natural rivers, flowing water erodes the bed and bank when it is under loaded with sediment and deposits sediment in the bed and bank when it is overloaded. Channel bed roughness has impact on alluvial river morphology and its sediment transport phenomena. Manning's roughness coefficient (n) and Chezy's roughness coefficient (C) are being widely used to predict roughness in drainage canals. The objective of the study is to examine variation of roughness with discharge in case of mobile bed laboratory flume and to determine the effect of changing water depth and velocity on channel roughness exclusively.

Literature Review

Methods of estimating roughness co-efficient for different flow scenarios are not still reasonably well developed. The designer has to exercise his judgment in the selection of roughness values for a particular channel. The effects of variation in flow and material size and the high turbulence in a real flood situation introduce difficulties in predicting roughness values (Raju, 1987).

Nikuradse (1932) introduced the concept of an equivalent or effective sand roughness height (Ks) to simulate the roughness of arbitrary roughness elements of the channel bottom boundary. In case of a movable bed channel consisting of sediments, the effective bed roughness (Ks) mainly consists of grain roughness (K's) generated by skin

¹ Principal Scientific Officer, ² Senior Scientific Officer & ³ Scientific Officer, River Research Institute, Faridpur

friction forces and of form roughness (K 's) generated by pressure forces acting on the bed forms (Chow, 1988). The effective bed roughness for a given bed material size is not constant but depends on the flow conditions (Rijn, 1993).

The fundamental aspect of bed roughness prediction methods is that the bed characteristics and hence the bed roughness depend on the main flow variables (depth, velocity) and sediment transport rate and sediment size. These hydraulic variables are, however, in turn strongly dependent on the bed configuration and its roughness. Another aspect is continuous variation of the discharge during rising and falling stages in rivers. Under these conditions, the bed form dimensions and hence the Chezy's coefficient are not constant but vary with the flow conditions. Uddin and Halim (1999) evaluated performance of eleven alluvial roughness predictors to determine the applicability of these roughness predictors for Gumti, Kushyara and Mohananda rivers of Bangladesh.

The values of n depends mainly on the surface roughness, amount of vegetation, channel irregularities and to a lesser degree on stage, erosion and deposition (Chaudhury, 1994). An interesting feature of the roughness coefficient has been observed in some large rivers where values of n at high stages have been found smaller than n values at lower stages (e.g. Mississippi river, Tennessee river, Irrawaddy river, etc.). No satisfactory explanation is still available for this phenomena (Subramanya, 1988). But in case of flow through circular channels, such as sewers and tile drains, largest values of n is found when the depth of flow is $0.25D$ (D is the diameter of the pipe), and the least value of n is obtained when it is completely filled with water.

Methodology and Test Scenarios

This study has been carried out in a rectangular flume with an effective mobile bed length of 21.0 meter and width of 3.00 meter and depth 1.00 m. The flume is situated at the tidal shed No.1 of the River Research Institute, Faridpur. The Flume has mobile bed and has a water re-circulation system. Some space of upstream and downstream was kept for creation the uniform flow conditions. The water level was controlled by the tailgate at the downstream. Water level has been measured with four point gauges along the length of the flume.

In the upstream side, the measuring point gauge was fitted at 3.95 m d/s from the inlet and another point gauge was fitted in the downstream side at 4.00 m u/s from the tailgate. The remaining two was fitted at the 10.00 m as well as at 14.00 m d/s of the inlet. Nine tests runs were conducted considering different scenarios. The test scenarios and test results have been given in **Table 1**. Manning's n and Chezy's C have been computed using conventional formula which is provided below:

$$n = \frac{U}{R^{2/3} S^{1/2}} \quad \text{and} \quad C = \frac{U}{\sqrt{RS}}$$

where, U = Mean velocity of flow (m/s), R = Hydraulic Radius (m), S = Energy slope.

Each test run was continued until the water level, water surface slope and the water depth had become more or less constant with time. The tailgate and flow valve have been adjusted to get a predetermined water depth and flow velocity.

Results and Discussions

The experimental results are discussed here in below. Figure 1 and Figure 2 show respectively the variation of Chezy's C and Manning's n for increasing velocity keeping the depth of water same. From **Figure 1**, it appears that, increasing velocity, keeping the depth same has no dominating influence on C. With increasing velocity, C has been decreased in case lower depth (0.15 m), while C has been increased in case of higher depth of water (0.25 m). From **Figure 2**, Manning's n shows reverse curve of C, as n is reciprocal to C. As no general trend has been obtained, it is difficult to say the impact of velocity on roughness for these test scenarios. **Figure 3** and **Figure 4** show respectively the variation of Chezy's C and Manning's n for increasing water depth keeping the velocity same. From **Figure 3**, C has been decreased and from Figure 4, Manning's n has been increased with increasing water depth. So, it appears that water depth increases roughness of the channel in case of present test scenarios.

Table 1: Test Scenarios and Test Results

Test Runs	Water depth, h (m)	Width of Flume, b (m)	Mean Velocity U, (m/s)	Water Slope, S (m/m)	Chezy's Coefficient C	Manning's Coefficient, n
T1	0.15	2.2	0.30	0.00051	35.50	0.00962
T2	0.15	2.2	0.35	0.00100	29.44	0.01158
T3	0.15	2.2	0.40	0.00136	29.40	0.01159
T4	0.20	2.2	0.30	0.00059	29.47	0.01284
T5	0.20	2.2	0.35	0.00077	28.97	0.01306
T6	0.20	2.2	0.40	0.00090	30.60	0.01237
T7	0.25	2.2	0.30	0.00047	27.54	0.01479
T8	0.25	2.2	0.35	0.00071	27.03	0.01507
T9	0.25	2.2	0.40	0.00083	28.42	0.01434

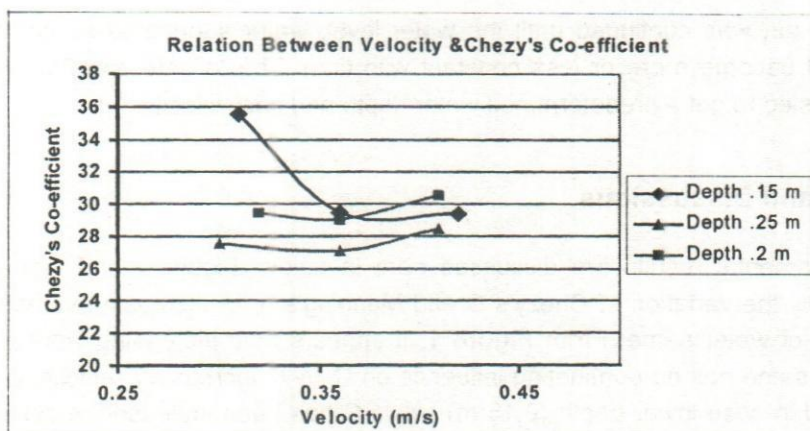


Figure 1: Variation of C with velocity at constant depth of water

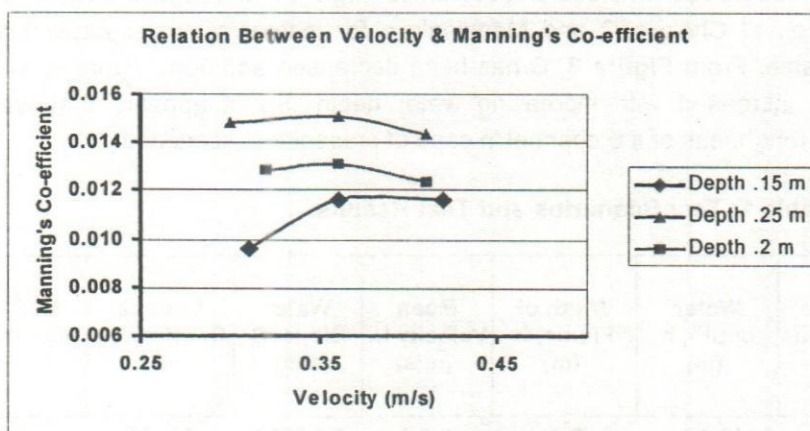


Figure 2: Variation of n with velocity at constant water depth.

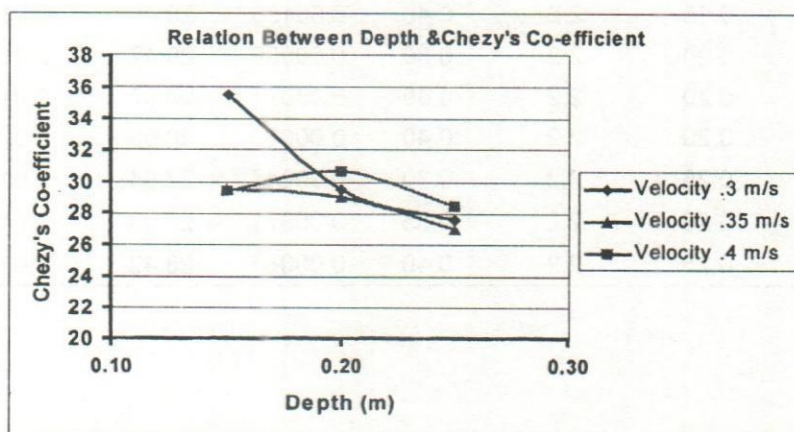


Figure 3: Variation of C with depth of water at constant velocity.

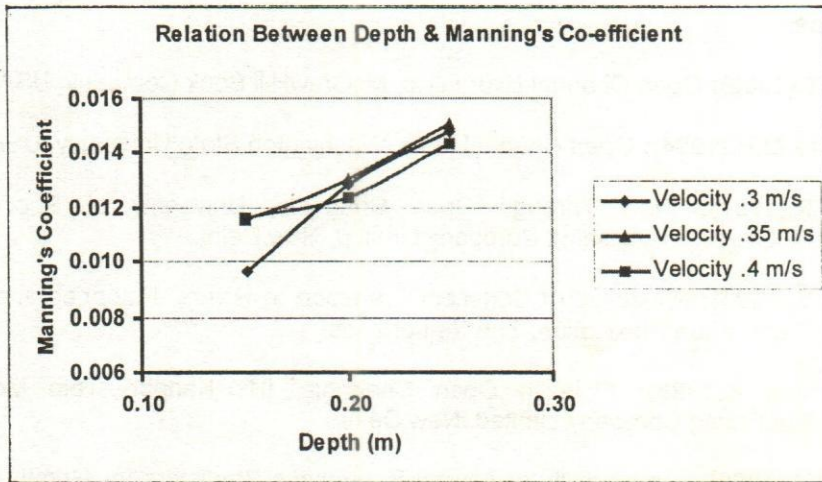


Figure 3: Variation of C with depth of water at constant velocity.

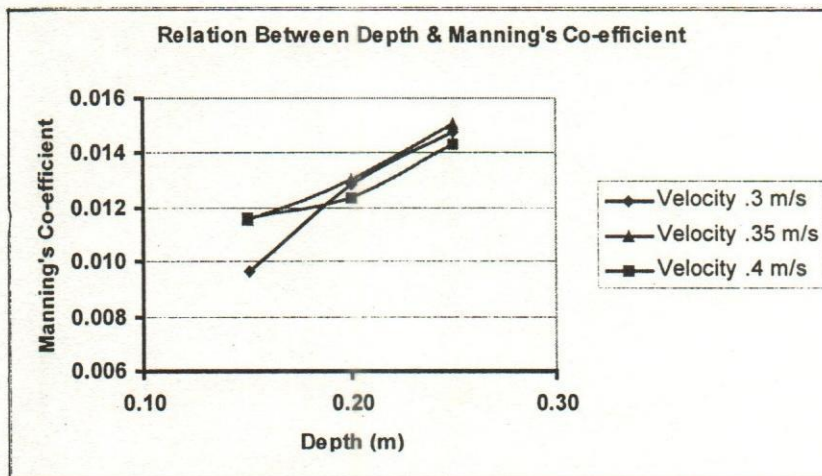


Figure 4: Variation of n with depth of water at constant velocity.

Conclusions

In this study, the Chezy's co-efficient and Manning's coefficient has been calculated from the experimental data collected for the mobile bed channel. The Chezy's co-efficient was varied between 27.03 to 35.50 $\text{m}^{1/2}\text{s}^{-1}$ and Manning's n varies from 0.01507 to 0.00962 as shown in **Table 1**. It appeared that, roughness has been increased with increasing depth of flow in these test scenarios. However, under different velocities, water level and bed materials, results may differ appreciably.

Reference

- Chow, V.T.(1988):** Open Channel Hydraulics, McGrawHill Book Company, USA.
- Chaudhury,M.H.(1994):** Open Channel Flow, Washington State Univeristy, USA.
- Raju,K,G,R,(1987):** Flow Through Open Channels, University of Roorke, Tata McGrawHill Publishing Company Limited, New Delhi.
- Rijn, L.C.V.(1993):** Principles of Sediment Transport in Rivers, Estuaries and Coastal Seas, Aqua Publication, The Netherlands.
- Subramanya, K(1988):** Flow in Open Channels, IIT, Kanpur, Tata McGrawHill Publishing Company Limited, New Delhi.
- Uddin, M.J.(1999):** "Applicability of Alluvial Roughness Predictors for Gumti, Kushyara and Mahananda River", M.Engg. Thesis, Dept. of Water Resources Engineering, BUET, Dhaka.

A Hydrological Study on The Padma River

A K M Ashrafuzzaman¹, Md. Azizul Haque Poddar¹,
Md. Alauddin Hossain² and Md. Asadul Bari²

Abstract

This paper presents the results of some hydrological study on the Padma river in terms of variation of stage & discharge, specific gauge analysis and development of non-dimensional correlation. The study shows that the annual average discharge and water level vary in sinuous pattern having some trend at different hydrometric stations when plotted with time. The specific gauge analysis based on historical data record at station Baruria Transit shows that the stage varies in sinuous pattern with slightly decreasing trend with time. Non-dimensional parameters are important in the study of alluvial river characteristics. Some non-dimensional relationships have also been developed among non-dimensional parameters at Baruria Transit.

Introduction

The combined flows of the Jamuna and Ganges rivers constitute the flow of the present Padma River. Before the avulsion of the Jamuna River, the flow was a continuation of the Ganges River only. The annual mean discharge of the Padma River is $28000\text{m}^3/\text{s}$, the bank full discharge is $75000\text{m}^3/\text{s}$ and the dominant discharge is $80000\text{m}^3/\text{s}$.

A reach of about 90km is almost straight and the platform of the river is a combination of the meandering and braiding type, indicating a wandering river. The variation of the total width of the river is quite high, ranging from 3.5km to 15km. With respect to planform, the Padma river falls in between braided and meandering river i.e. wandering river (FAP24, 1996).

The bank erosion rate studied by ISPAN (1993) shows that the rate (In the period of 1984 to 1993) is quite high, and even higher than for the Jamuna River. The braiding intensity of the river is low. There are typically only two parallel channels in the braided reach. Channel shifting processes are quite rapid.

The slope of the river is varying within a range of 8.5 to 5cm per km. The bed material sizes are also varying from 0.20 to 0.10mm.

Measurement of discharge and water level (tidal & non-tidal) is conducted by; hence the source of discharge and water level data is BWDB.

The Baruria Transit (Water level plus discharge station, Code No. 91.9L) is the immediate upstream of Goalanda Transit station on the river Padma.

The Goalanda Transit (Water level station, Code No. 91.9R) is the immediate downstream of Baruria Transit station on the river Padma.

¹ Senior Scientific Officer, ² Scientific Officer, River Research Institute, Faridpur

Bhagyakul (Water level station, Code No. 93.4L) is the downstream of Goalanda Transit on the river Padma.

Mawa (Water level plus discharge station, Code No. 93.5L) is the downstream of Bhagyakul on the river Padma.

The daily data and annual average data obtained from the aforementioned stations provide an opportunity to make a hydrological study on the Padma river. This paper presents the results of such a study based on the historical data at these stations. The Padma river within the study reach showing selected hydrometric stations is shown in Figure 1.

Specific Gauge Analysis

For the analysis of medium to long-term behavior of the river, specific gauge analysis is done to determine the trend of stage with time corresponding to a given discharge. This analysis is based on historical stage-discharge records for a gauging station with an open river section (Das, 1992).

Development of Dimensionless Groups of Variables

Dimensionless groups of variables means the variables pertinent to a physical problem are systematically organized into dimensionless groups. Such organizations effectively reduce the number of unknown quantities and generalize a problem in a way that eliminates the need for specifying any particular system of units. Flow through an alluvial stream incorporates a good number of variables and that is why dominant variables are chosen to form dimensionless parameters to describe alluvial river behavior. The variables that govern the geometry of the alluvial channel can be written functionally as follows:

$$\phi(V, D, S, \rho, g, \sigma, \rho_s, S_p, S_R, S_c, f_s, C_T) = 0 \quad (1)$$

Where,

V = Velocity, D = Depth, S = Slope of energy grade line, ρ = Density of water-sediment mixture, g = Acceleration due to gravity, σ = Measure of size distribution of bed materials, ρ_s = Density of sediment, S_p = Shape factor of the particles, S_R = Shape factor of the reach of the stream, S_c = Shape factor of the reach of the stream, f_s = Seepage force in the bed of the stream, C_T = Concentration of bed material discharge

Applying method of dimensional analysis to equation (1) and the dimensionless parameters obtained thus can be written functionally as follows:

$$\phi(VD/k, V/(gD)^{1/2}, d/D, f_s/V^2D^2, S, \sigma, \rho_s/\rho, S_p, S_R, S_c, f_s, C_T) = 0 \quad (2)$$

In equation (1) if V is replaced by Q, the discharge, and those variables, which practically govern the geometry of alluvial river, are considered then the resulting functional equation is

$$\phi(Q, W, D, d, S, g, k) = 0 \quad (3)$$

W is the width of the river and k is the kinematic viscosity.

Application of dimensional analysis to equation (3) yields,

$$\phi(D/d, D/W, S, [Q^{2/5}/(Sg)^{1/5}]/D, D/[k^{2/3}/(Sg)^{1/3}], (Q/k)/[k^{2/3}/(Sg)^{1/3}]) = 0 \quad (4)$$

These are the list of dimensionless parameters. Application of dimensionless parameters provides a basis of alternative arrangement of geometric and hydraulic properties of streams for investigations.

Hossain (1989) pointed out that when too many variables influence a phenomenon, it becomes extremely difficult to incorporate all variables into any mathematical formulation. Under such circumstances, the analysis is necessarily idealized. This type of analysis for alluvial stream is becoming potentially dependent on extensive use of different dimensionless parameters originating from theoretical considerations of more dominating variables and choosing the combinations, which yield acceptable result.

Methodology

At Baruria Transit, the annual average water level data were plotted against time for the years 1965 to 1996 to observe the variation of water level with time. The annual average discharge data were also plotted against time for the years 1966 to 1994 to observe the variation of discharge with time. The trend of water level and discharge data against time at this station was also determined. The annual average data at a station for a hydrological year has been obtained by averaging the daily data for that station. The stage-discharge relationship or rating curve was also developed using water level and discharge data at this station for the years 1966 to 1994 using daily data. The annual average tidal water level data were plotted against time for the years 1983 to 1985 to observe the variation of water level with time. The water level that undergoes tide is called tidal water level and the corresponding discharge is called tidal discharge.

At Goalanda Transit, the annual average water level data were plotted against time for the years 1964 to 1996 to observe the variation of water level with time and the trend of water level at this station was also determined.

At Bhagyakul, the annual average tidal water level data were plotted against time for the years 1968 to 1996 to observe the variation of water level with time and the trend of tidal water level was also determined.

At Mawa, the annual average tidal water level data were plotted against time for the years 1968 to 1994 to observe the variation of water level with time. The annual average tidal discharge data were also plotted against time for the years 1965 to 1994 to observe the variation of discharge with time. The trend of tidal water level and tidal discharge at this station was also determined. Rating curve was also developed using discharge & water level data for ebb tide and flood tide at the same station for the years 1968 to 1994 using daily data.

Specific gauge analysis was done at Baruria Transit using data from 1966 to 1993 based on discharge levels of 5000, 10000, 20000, 35000 & 50000m³/s. The stages

corresponding to different discharge levels mentioned above are then plotted against time. The trend of stage for each discharge level is then determined.

Non-dimensional analysis is done for the years 1981, 1983, 1984, 1988 & 1992 using rating curve at Baruria Transit. The average slope of the river is taken to be 5.0 cm/km and the value of acceleration due to gravity (g) is taken to be 9.81 m/sec². The dimensionless parameters are then calculated for the aforesaid years at Baruria Transit. In the present study the selected dimensionless parameters are W/D , $V/(gD)^{1/2}$, $Q/(kD)$, $D/[k^{2/3}/(Sg)^{1/3}]$ and $(Q/k)/[k^{2/3}/(Sg)^{1/3}]$. Non-dimensional relationships are developed between $V/(gD)^{1/2}$ & W/D , $Q/(kD)$ & W/D , $(Q/k)/[k^{2/3}/(Sg)^{1/3}]$ & W/D , $Q/(kD)$ & $V/(gD)^{1/2}$, $D/[k^{2/3}/(Sg)^{1/3}]$ & $V/(gD)^{1/2}$ and $(Q/k)/[k^{2/3}/(Sg)^{1/3}]$ & $V/(gD)^{1/2}$. The trend of each relationship is also determined.

Results and Discussion

From the separate plot of annual average discharge and water level with time, the annual average discharge has an increasing trend while the annual average water level has a decreasing trend with time at Baruria Transit as shown in **Figure 2** and **Figure 3** respectively. This indicates that river bed erosion may have occurred at Baruria Transit.

A rating curve or stage-discharge relationship has also been developed at Baruria Transit for the years 1966 to 1994, which is shown in **Figure 4**. From this figure it can be determined the water level with known discharge and vice versa at Baruria Transit.

At Goalanda Transit from the plot of annual average water level versus time it is observed that the annual average water level has a slightly decreasing trend with time as shown in **Figure 5**.

At Bhagyakul from the plot of annual average tidal water level (average value taken during ebb tide & flood tide) versus time it is observed that the annual average water level has a slightly decreasing trend with time as shown in **Figure 6**.

From the separate plot of annual average tidal water level and tidal discharge with time, both the annual average tidal water level and tidal discharge have an increasing trend with time as shown in **Figure 7** and **Figure 8** respectively.

A rating curve or stage-discharge relationship has also been developed at the same station for the years 1968 to 1994, which is shown in **Figure 9** and **Figure 10** for ebb tide and flood tide respectively. From these figures it is possible to determine the water level during ebb tide and flood tide with known discharge and vice versa at Mawa.

Specific Gauge Analysis

In the present study, the stage-discharge at Baruria Transit for the Padma has been analyzed for the years from 1966 to 1993. This analysis is based on discharge levels of 5000, 10000, 20000, 35000 and 50000 m³/s and the corresponding stages for the same period. The stages are then plotted against time to observe the variation of stage with time for different discharges mentioned above and shown in **Figure 11**. This figure explains that stages are in sinuous pattern, which is the characteristic of an alluvial river

(Das, 1992), and its trend is slightly decreasing with time. This gives an indication that river bed erosion may have occurred at Baruria Transit.

Correlation between Dimensionless Groups of Variables

Non-dimensional correlation has been developed between $V/(gD)^{1/2}$ & W/D , $Q/(kD)$ & W/D , $(Q/k)/[k^{2/3}/(Sg)^{1/3}]$ & W/D , $Q/(kD)$ & $V/(gD)^{1/2}$, $D/[k^{2/3}/(Sg)^{1/3}]$ & $V/(gD)^{1/2}$ and $(Q/k)/[k^{2/3}/(Sg)^{1/3}]$ & $V/(gD)^{1/2}$ for the period 1981, 1983, 1984, 1988 & 1992 at Baruria Transit. The plots of dimensionless parameters are shown in **Figure 12**.

Correlation between $V/(gD)^{1/2}$ and W/D

Graphical relationships showing the variation of $V/(gD)^{1/2}$ with W/D have been developed. From these plots it is observed that W/D increases with the decrease of $V/(gD)^{1/2}$ and there exists very good correlation between them.

It may be worthwhile to mention here that similar type of study was conducted by Hossain (1989) for the Ganges river in Bangladesh and found similar trend.

Correlation between $Q/(kD)$ and W/D

The graphical relationships between $Q/(kD)$ and W/D have been and it is observed that W/D increases with the decrease of $Q/(kD)$. Good correlation exists between these two parameters.

Correlation between $(Q/k)/[k^{2/3}/(Sg)^{1/3}]$ and W/D

The graphical variation of $(Q/k)/[k^{2/3}/(Sg)^{1/3}]$ against W/D is done. In this case it is observed that W/D increases with the decrease of $(Q/k)/[k^{2/3}/(Sg)^{1/3}]$ and good correlation is found between these two parameters.

Correlation between $Q/(kD)$ and $V/(gD)^{1/2}$

Graphical relationships showing the variation of $Q/(kD)$ with $V/(gD)^{1/2}$ have been done. Here it is observed that $V/(gD)^{1/2}$ increases with the increase of $Q/(kD)$ and these two parameters are well correlated.

Correlation between $D/[k^{2/3}/(Sg)^{1/3}]$ and $V/(gD)^{1/2}$

The relationships between $D/[k^{2/3}/(Sg)^{1/3}]$ and $V/(gD)^{1/2}$ in graphical form have been developed. In this case it is observed that $V/(gD)^{1/2}$ increases with the increase of $D/[k^{2/3}/(Sg)^{1/3}]$ and these two parameters are well correlated.

Correlation between $(Q/k)/[k^{2/3}/(Sg)^{1/3}]$ and $V/(gD)^{1/2}$

Graphical relationships have been developed between $(Q/k)/[k^{2/3}/(Sg)^{1/3}]$ and $V/(gD)^{1/2}$. It is observed that $V/(gD)^{1/2}$ increases with the increase of $(Q/k)/[k^{2/3}/(Sg)^{1/3}]$ and good correlation exists between these two parameters.

Conclusions

The following conclusions may be drawn on the basis of the present research study:

From the plot of annual average discharge and water level versus time, the annual average discharge has an increasing trend with time while the annual average water level has a decreasing trend with time at Baruria Transit. This indicates that river bed erosion may have occurred at Baruria Transit.

From the plot of annual average water level versus time it is observed that the annual average water level has a slightly decreasing trend with time at Goalanda Transit.

A rating curve or stage-discharge relationship is also developed at Baruria Transit during the period 1966 to 1994 for the non-tidal water level and non-tidal discharge. The general equation of rating curve obtained in the present study using data for the aforementioned period is given by:

$$WL = 2.2281 \ln(Q) - 17.221$$

From the plot of annual average tidal water level (average value taken during ebb tide & flood tide) versus time it is found that water level has a decreasing trend with time at Bhagyakul.

From the plot of annual average tidal water level (average value taken during ebb tide & flood tide) and tidal discharge versus time it is found that both the water level and discharge have an increasing trend with time at Mawa.

A rating curve or stage-discharge relationship is also developed at Mawa for the years 1968 to 1994 for ebb tide and flood tide. The general equation of rating curve obtained in the present study using data for the aforementioned period is given by:

$$WL = 1.679 \ln(Q) - 13.238 \text{ (for ebb tide)}$$

$$WL = 1.7364 \ln(Q) - 13.995 \text{ (for flood tide)}$$

At-a-station specific gauge analysis for the selected discharge levels indicated that the stages are decreasing in sinuous pattern. This means that river bed erosion may have occurred at Baruria Transit.

From the plot of dimensionless parameters between $V/(gD)^{1/2}$ & W/D , $Q/(kD)$ & W/D , and $(Q/k)/[k^{2/3}/(Sg)^{1/3}]$ & W/D , W/D increases with the decrease of $V/(gD)^{1/2}$, $Q/(kD)$ & $(Q/k)/[k^{2/3}/(Sg)^{1/3}]$ at Baruria Transit.

From the plot of dimensionless parameters between $Q/(kD)$ & $V/(gD)^{1/2}$, $D/[k^{2/3}/(Sg)^{1/3}]$ & $V/(gD)^{1/2}$ and $(Q/k)/[k^{2/3}/(Sg)^{1/3}]$ & $V/(gD)^{1/2}$, $V/(gD)^{1/2}$ increases with the increase of $Q/(kD)$, $D/[k^{2/3}/(Sg)^{1/3}]$ & $(Q/k)/[k^{2/3}/(Sg)^{1/3}]$ at Baruria Transit.

References

- Das, S.K. (1992):** Hydraulic geometry of the Ganges, M. Engg. Thesis, Department of Water Resources Engineering, BUET, Dhaka.
- Delft/DHI (1994):** River Survey Project (FAP24), Study Report 3, Morphological studies Phase 1: Available data and characteristics, Dhaka, Bangladesh.
- Hossain, M.M. (1987):** Geomorphic characteristics of the Padma up to Brahmaputra confluence, First Interim Report, R 03/87, IFCDR, BUET, Dhaka.
- Hossain, M.M. (1989):** Geomorphic characteristics of the Padma up to Brahmaputra confluence, Final Report, R 02/89, IFCDR, BUET, Dhaka.
- ISPAN (1993):** Environmental Study (FAP16) and Geomorphic Information System (FAP19), The dynamic physical and human environment of riverine charlands: Ganges and Padma, Dhaka, Bangladesh.
- RRI (2002):** A study on the geometric and bank shifting characteristics of the Padma river from Goalanda, Rajbari to Mawa, Lohajong, Munshigonj, Research Report, Report No. RES-6 (2002).
- River Survey Project (1996):** FAP24, Special Report No.3, Bathymetric Surveys.
- River Survey Project (1996):** FAP24, Special Report No.7, Geomorphology and Channel Dimensions.
- Sir William Halcrow and Partners Ltd (1993):** South-West Area Water Resources Management Project (FAP4), Morphological Studies, Vol. 3, Final Report, Dhaka, Bangladesh.
- Surface Water Simulation Modelling Program (1996):** Phase III, Final Report, Vol. II, surface water model

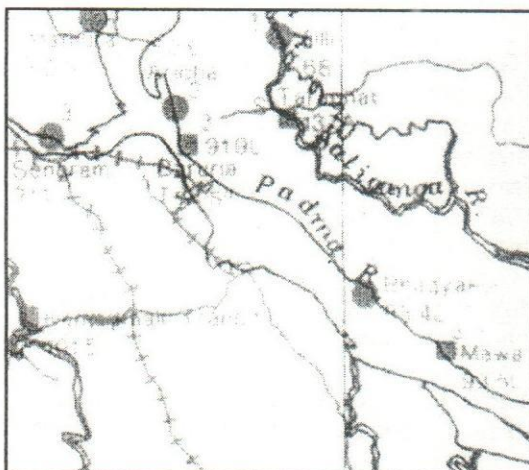


Figure 1: The Padma river within the study reach showing selected hydrometric stations (SWMC, 1996)

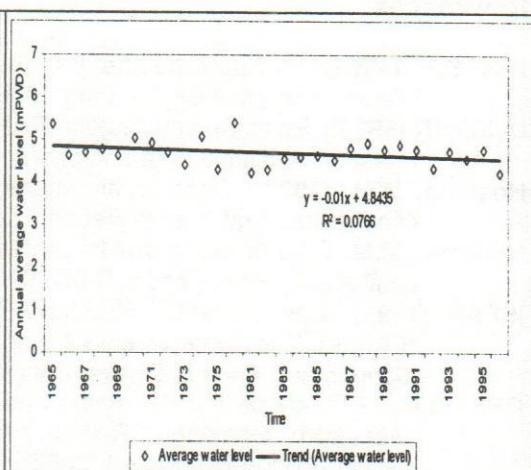


Figure 2: Variation of annual average water level at Baruria Transit

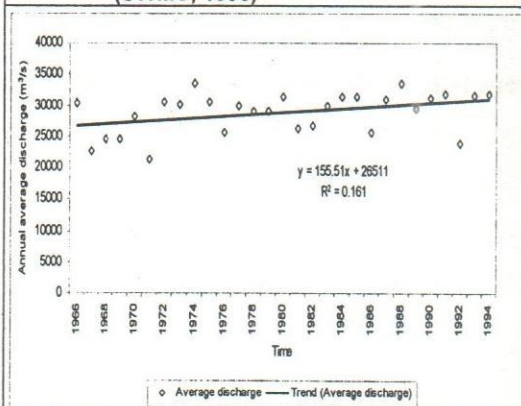


Figure 3 Variation of annual average discharge at Baruria Transit

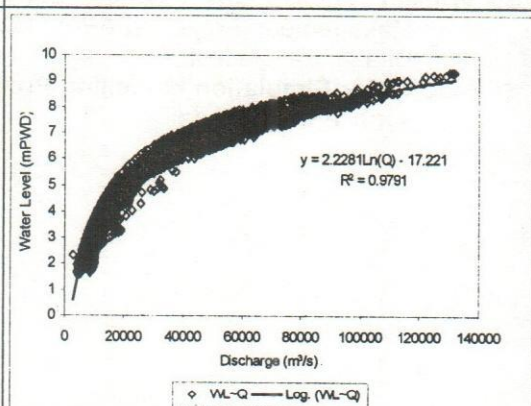


Figure 4 Rating curve at Baruria Transit

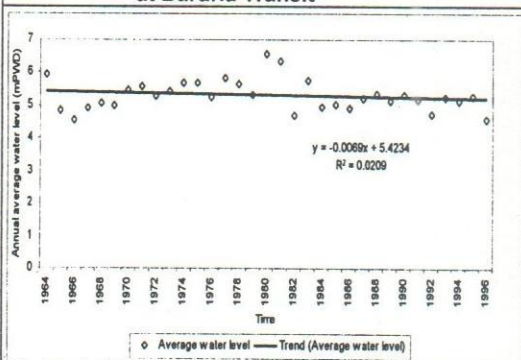


Figure 5 Variation of annual average water level at Goalanda Transit

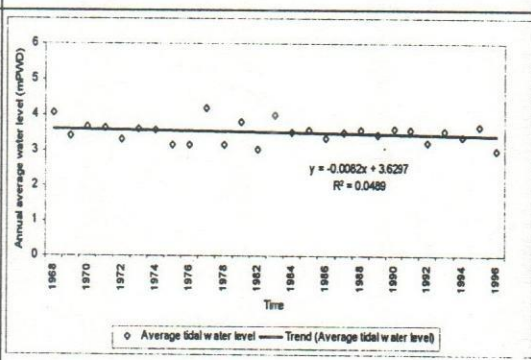


Figure 6 Variation of annual average tidal water level at Bhagyakul

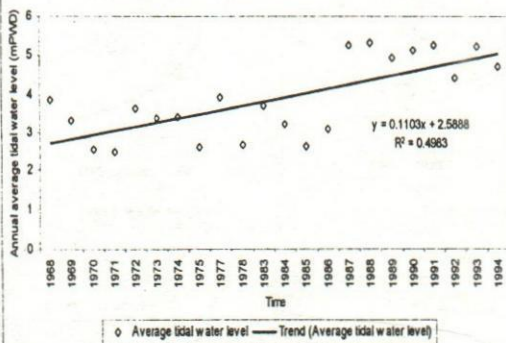


Figure 7 Variation of annual average tidal water level at Mawa

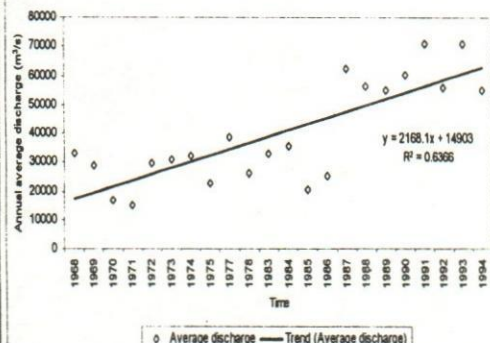


Figure 8 Variation of annual average tidal discharge at Mawa

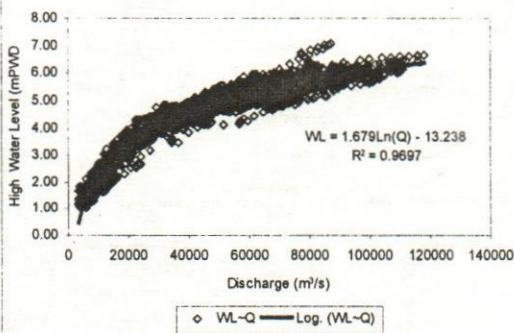


Figure 9 Rating curve at Mawa for ebb tide

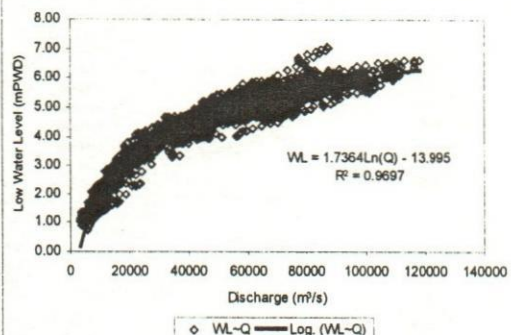


Figure 10 Rating curve at Mawa for flood tide

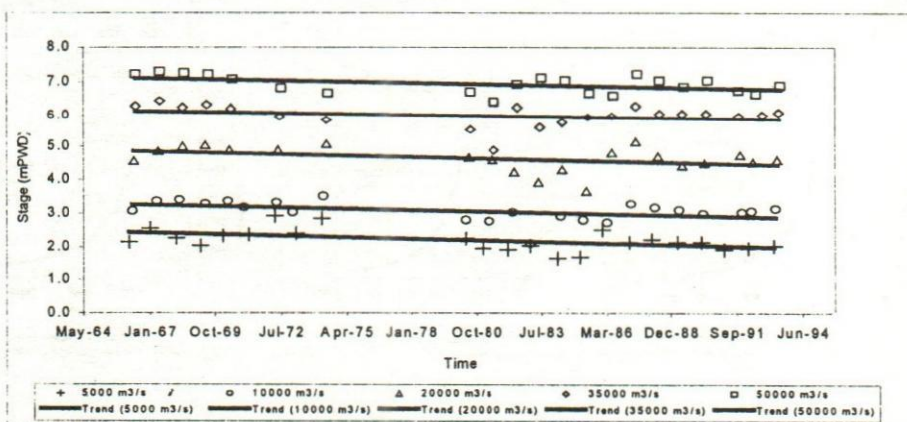


Figure 11 Variation of stage with time for different discharge levels at Baruria Transit

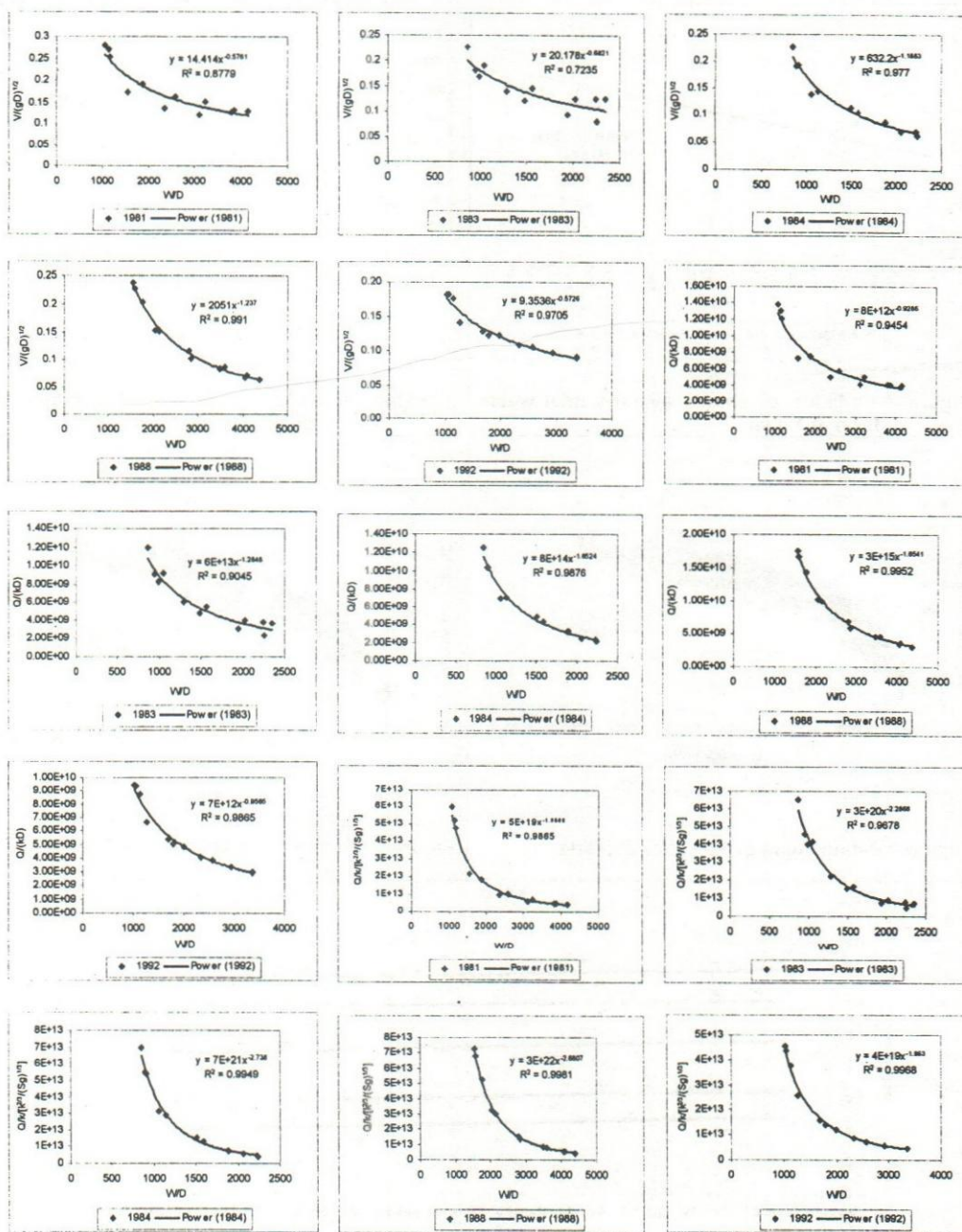
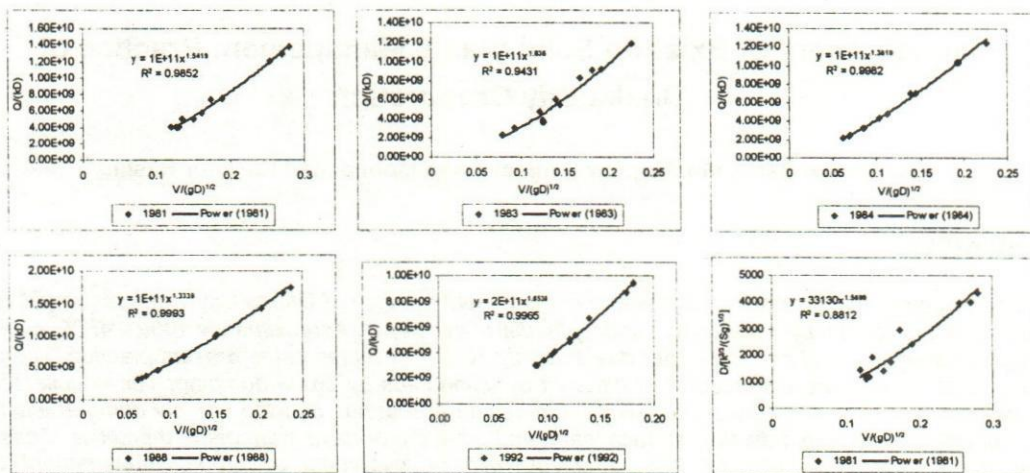


Figure 12 Non-dimensional plots of the Padma river at Baruria Transit

Figure 12 (cont.)



Improvement of Existing Solid Waste Management Practice of Dhaka City Corporation

Md. Niamul Bari¹, Md. Mujibur Rahman² and Mohammad Harunur Rashid³

Abstract

The improvement of existing solid waste management practice of Dhaka City Corporation (DCC) has been proposed by introducing sanitary landfill in this paper. Approximately 4000 – 4500 metric tons of solid waste is generated per day and only 50% is collected in the present practice. These collected wastes are disposed of at different dumping sites by crude dumping. The uncollected waste, which is accumulated into low land, roadside and drains and the crudely dumped waste contaminate soil, groundwater, surface water and air in the present management practice. These entire environmental and technical problems can be overcome by proper management of collection crews and introducing sanitary landfill for ultimate disposal without involvement of additional equipment and management cost. The unit expenditure of primary collection, secondary collection and ultimate disposal is less than the present practice. The unit expenditure (Tk.341.30/ton of waste) of entire solid waste management is also less than the present practice. From the above discussion it is obvious that the proposed management system is possible to adopt with the existing equipment and manpower facilities and without additional cost involvement.

Introduction

Solid Waste Management is the greatest problem in urban areas. Municipal government is struggling to find the best method to manage their residents' wastes. Dhaka, the capital of Bangladesh, is one of the fastest growing metropolises of the world with an annual average growth rate of population 3.72 percent (BBS, 2000). DMDP predicts the population of Dhaka to be around 15 million in the year of 2015 (Choudhury, 1998).

The major objective of this study is investigation and improvement of the existing SWM practice of Dhaka City Corporation (DCC) considering technical, economic and environmental issues. Approximately 4000 – 4500 metric tons of solid waste is generated per day with an average generation rate of 0.5 kg/cap/day from various residential, commercial and industrial activities (DCC, 2000). In addition to household, about 1000 industries of various types and capacities, 500 clinics and hospitals, 149 tanneries and construction debris contribute to daily waste generation. Only about 50% of waste is collected and dumped as crude landfill (DCC, 2000). The uncollected and crudely dumped waste contaminates soil and groundwater by percolation of leachate, surface water with addition of waste and different minerals by surface runoff and air by spreading of odor, litters and diseases. Of the total population 50% using waste enclosure or bin, 20% using roads sides, 20% drain, 10% using open ground to dispose of waste (DMDP, 1992). All of these phenomena create an alarming situation of solid waste management system of Dhaka City Corporation. In the present situation it is expected that the study will be able to solve the existing problems by finding out a better solid waste management system with the minimum utilization of resources.

¹ Senior Scientific Officer, ² Principal Scientific Officer & ³ Scientific Officer, River Research Institute, Faridpur

Methodology

The methodologies of this study in achieving the research objectives are described step by step as follows:

For the better understanding about the limitation and problems of existing solid waste management of Dhaka City Corporation, previous study and research papers are collected and studies thoroughly. Ideas have been gathered about the existing facilities and limitations and major problems are identified. To overcome these limitations and solve the problem necessary information and data are collected from different department like Conservancy Department, Transport Division, Engineering Department, and administrative zone offices of Dhaka City Corporation. Then the obtained data is analyzed to design an improved waste management system. Solid waste management system is designed considering waste generation, primary collection, secondary collection and ultimate disposal as functional element. Sanitary landfilling is considered as ultimate disposal option. Cost analysis is performed to estimate the annual expenditure as capital investment and operation and maintenance cost. Unit expenditure for each activity and also total management system is determined as Tk./ton of generated solid waste. A comparative study is performed in an effort to establish/demonstrate feasibility of the proposed solid waste management system over the present practice on the basis of unit cost. Environmental aspects are also considered. Finally a conclusion is drawn on the basis of analysis and comparative study.

Relevant Studies

Solid Waste Management Authority

The management of solid waste generated within the city is the responsibility of municipal Government. For the purpose of the administration of urban areas the Government sets up such authority under the law promulgated by the state legislature. The Municipal/City Corporations are set up under specific state enactment for major and specific cities and is bestowed with a creation of degree of independence and autonomy in mobilizing resources and providing civic services. The solid waste management related activities and associated departments are shown in **Figure 1**.

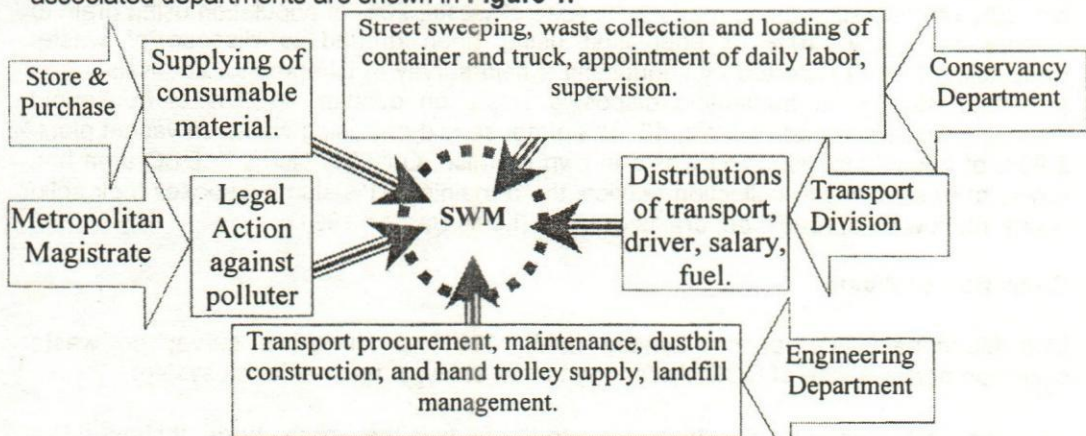


Figure 1: Solid Waste Management Related Activities and Associated Departments

Dhaka City Corporation is headed by Mayor who is an elected representative of the people and under him the chief executive officer who is deputed by Government for management of five principal areas of responsibility, which are engineering, conservancy, revenues, accounts and health.

Waste Generation in Dhaka City Corporation

Several consultants and agencies were studied the amount of solid waste generation in DCC area in the period of 1986 to 2000. In 1986 a Netherlands consulting firm (BKH) carried out a survey as a client of UNDP for solid waste management from April to July in Old Dhaka. Survey carried out in 130050 houses. They found domestic waste generated 100.96 tons/day as a rate of 0.776 kg/house. Survey result showed that wastes were generated from pucca houses 6.25 kg/week, semi pucca house 5.83 kg/week and kucha house 3.79 kg/week. BKH (1986) also carried out a survey at disposal site and found 450 tons of waste delivered in a day. This delivered waste is the total collected waste from the Dhaka City.

Recently Salam (2000) carried out a survey at "Uttara Model Town" for M.Sc. thesis. The domestic waste generation rate estimated from the survey was 0.60 kg/cap/day and 5.5 kg/household with 9.14 persons/household. In this study comparable waste density of 408 kg/m³ was obtained. The average generation rate from commercial source was found 0.56 kg/cap/day. The survey was also conducted in clinics and health center and found the waste generation rate was 1.75 kg/cap/day. In street survey, the sweeping waste was 0.36 kg/m/day for main road and 0.16 kg/m/day for internal road. In this case, DCC considered 0.1916 kg/cap/day and World Bank suggested for estimation of waste volume 0.05 to 0.2 kg/cap/day with density 500 kg/m³.

On-Site Storage

A foreign consulting organization, Mott Macdonald International Limited (MMI, 1991) reported, in Dhaka City Corporation area has 2450 C.I. sheet and 1595 RCC/masonry dustbin those are provided by DCC for storage of municipal waste. DMDP (1992) estimated the percentages of population using the existing bins and enclosures as means of disposal. The report mentioned, 50% of population using waste enclosure or bin, 20% of population using roads to dispose of waste, 20% of population using drain to dispose of waste, 10% of population using open ground to dispose of waste. Enayetullah (1994) reported by conducting a field survey in Dhanmondi and Kalabagan area that 35.17% of household disposing waste on dustbin, 41.38% of household disposing waste on road or drain, 13.10% of household disposing waste on vacant plots, 6.90% of household disposing waste in own premise. Only 9% slums in DCC area has any form of solid waste collection service, the remaining 91% slums disposes their solid waste into low land, road side, drains or khals (Louis Berger, 1991).

Collection of Waste

Mott Macdonald International Limited (MMI, 1991) conducted a survey on waste collection performance of DCC. According to that study, in an open truck system:

- The basket used to load the waste into the body is the wrong shape. It shaped like a shallow saucer.

- It should be shaped like a wide mouthed bucket. Only 42 litter of waste is loaded on to the basket.
- Body, head and shoulders of the man lifting the basket has closer direct contact with waste that is disease ridden and contaminated with urine and other animal and human excreta. This is a grave danger to his health, safety and well being.
- Both smaller and larger basket took longer; manually unloading took about 4.5 min/m³. This compares with 14.6 minutes for a five-man team to load 1 m³ of waste into a normal size truck in Dhaka and 6.8 per m³ to unload it.

Transportation of Waste

From DMDP (1992) report it is found that in 1991 DCC had a fleet of 159 trucks of 5 ton and 1.5 ton capacities during physical verification it was found 63 numbers (40%) are off road due to technical fault. At that time no demountable container was running. UNCH project no. 154 strongly recommended for the collection of waste by demountable container truck in Old Dhaka at night in 1991. Mott Macdonald International Limited (1991)-survey result shows that small truck (less than 5 ton) capacity delivered more waste at disposal site than the large truck. They recommended a 3.0-ton payload truck as the best cost effective option.

Disposal of Solid Waste

Bhide (1990) reported that DCC has waste disposal site at Mirpur with an area of 25 acres and at Jatra bari with 25 acres area. Small sites are located at Islam bagh, Hazari bag, Mukti Sarani, Dayaganj, Mughdapara, Amligula and Balu ghat. Mot. Macdonald International Limited (1991) reported that wastes were deposited in a large depression on the North of the main Dhaka- Chittagong road at Jatrabari. The empty area was about 25 acres with an average depth 5 meter. A decision was taken by DCC to develop a 50 acre (20 ha) site to South East of Dhaka of Matuail having an average depth of 5 meter. It was intended that 1.3 acres would be reserved for low cost housing whilst the reminder would be used for waste disposal. MMI estimated the life of disposal sites at Jatrabari to be 5.5 years and Matuail to be 3.2 years.

Enayetullah (1994) reported that the Jatrabari site was filled up to approximately 70%. Yousuf (1996) reported that DCC had been disposing waste at Matuail along the Dhaka-Demra road and 3 km out side the corporation jurisdiction. DCC had purchased 52 acres of land out of which 13 acres had been developed for parking/platform and rest 39 acres for landfilling. The lifetime of site was also estimated to be 4.5 years. Salam (2000) calculated the cost of present disposal of solid waste to Matuail is Tk.101.47/ton or Tk.60.60/m³.

Present Solid Waste Management Practice of DCC

On-Site Storage

Dhaka City Corporation provides concrete and C.I. sheet bins at different places mainly along the roadside. In some areas demountable containers are used for on-site storage of municipal solid waste. Presently, DCC has 410 demountable containers for on-site

storage of waste (DCC, 2000). Dhaka City Corporation does not provide any house storage article, bag, bins for homeowner's.

Collection of waste

Dhaka City Corporation does not collect waste from household. The accumulated wastes in DCC's stationary bins and demountable containers are collected by DCC. DCC has 100 demountable trucks for collection of accumulated waste from municipal dustbins at different locations. In absence of primary collection system of DCC, at present some community based organizations have taken initiative for waste collection from "house to house" by Rickshaw Van at most of the areas. They collect waste from household and unload at DCC's bins or containers.

Transportation of waste

Dhaka City Corporation has 95 open trucks with the combination of 3 tons and 5 tons payload and 100 demountable container carrying truck with 4 standby for transportation of solid waste to the disposal sites.

Table 1 show the zone wise quantity of demountable container trucks and open trucks and the round trip hauled distance of disposal site. At present DCC disposes waste at Matuail, which is located 10 km. from the city center and 30 km. from farthest boundary at Uttara and Mirpur. DCC has no transfer station for carrying waste. There is no database and no calculation to determine the number of labor, trucks and trips per vehicle per shift. Open trucks and containers are loaded manually with waste. DCC transports are scheduled as per field requirements. There is no definite route map for transportation of solid waste to the disposal site.

Table 1: List of demountable container truck and open truck of DCC

Zone	Demountable container truck			Open truck			Round trip distance
	5 Ton	3 Ton	5 Ton	3 Ton	2 Ton	1.5 Ton	
1	-	2	1	5	17	-	14 Km
2	-	18	1	9	22	1	18 Km
3	-	5	1	13	5	1	22 Km
4	1	22	2	6	5	-	18 Km
5	3	17	10	8	-	-	22 Km
6	3	8	6	9	1	-	26 Km
7	-	3	-	5	3	-	42 Km
8	-	8	7	-	1	-	44 Km
9	-	5	3	7	-	-	35 Km
10	-	1	2	-	-	-	60 Km
Total	7	89	33	62	54	2	

Reuse and Resource Recovery

DCC has no resource recovery plant for the sorting of reusable and recyclable materials. Mainly socially neglected and disadvantageous poor boys are engaged for this activity. They collect the valuable and reusable material from stationary and demountable waste collection container and from the dumping site at time of final disposal. Recently a non-government organization Waste Concern has started a

composting plant at Mirpur, Dhalpur, Green road, and Kalabagan for resource recovery. They collect wastes from community by house-to-house collection system and sorted into organic and inorganic fraction. The organic fraction of wastes is converted into compost. The plants are now running successfully with profit.

Disposal of Solid Wastes

Presently DCC disposes waste at Matuail dumping deports. The other dumping deports of DCC are Mirpur, Mugda para, Jatra bari. Jatra bari dumping sites filled up Seven years ago. Matuail landfill covers about 92 acres of low-lying agricultural land. DCC acquired 52 acres land in 1986. Waste dumping is started in the year of 1993 in it. DCC disposes wastes in a ditch and low laying land. They do not provide landfill liner as hydraulic barrier to protect the percolation of landfill leachate; cover material to control the spreading of odor, litter and diseases; permanent and temporary fences to control the spreading of litter in surrounding areas; leachate and landfill gas management system. It is only dumping of waste in a crude manner. DCC just dumps collected wastes at site and spread over the land by using bulldozer, chain dozer and compact. Due to this crude dumping of waste groundwater, surface water and also soil are contaminated in addition of leachate through percolation and surface runoff. Again spreading of odor, litter and diseases creates a great potential of environmental pollution.

Proposed Solid Waste Management Employing Sanitary Landfill

Solid waste management involves primary and secondary collection, transfer and transport, processing and ultimate disposal of wastes. Ultimate disposal of wastes is considered by conventional sanitary landfill.

Generation of Solid Waste

Waste generation is estimated for ten administrative zones of Dhaka City Corporation are presented in Table 2. Total generated waste is 3131700 m³/year (1277865 tons/year). Waste generation increment rate corresponding to population growth rate is 0.075 m³/year. Therefore, total generated waste during design period of 20 years is 67331550 m³.

Table 2: Zone wise waste generation in DCC

Zone	1	2	3	4	5	6	7	8	9	10	Total
Tons/day	444	444	230	383	457	246	446	484	280	87	3501
m ³ /day	1089	1089	562	938	1120	603	1093	1187	686	213	8580

Primary collection of waste

Primary collection involves collecting household wastes by rickshaw vans and / or by handcarts (for picking up wastes from small concrete fixed bins or C.I movable bins located at by-lanes or small pathways) and delivering them to large demountable containers or stationary dustbins located mostly at roadsides. Usually rickshaw vans is used for this collection work. The standard volume of rickshaw vans is 1m³. Generally a waste collector can collect 10 trips/day. The required number of rickshaw vans and

collectors is shown in **Table 3**.

Table 3: Requirement of rickshaw vans and collector

Zone	1	2	3	4	5	6	7	8	9	10	Total
Rickshaw vans	109	109	56	94	112	60	109	119	69	21	858
Collector	109	109	56	94	112	60	109	119	69	21	858

Secondary Collection of wastes

Secondary collection involves picking up large demountable containers on to container truck from container location and transporting them to disposal sites. The number of trips for demountable container truck is estimated. The volume of demountable container is considered 12.25 m³, which is generally used in DCC. There are two collectors involves with every collection vehicle. Secondary collection can be operated in two shifts to reduce the requirement of collection vehicle. The requirement of secondary collection is estimated and shown in **Table 4**. Number of trip/vehicle/day can be estimated by using equation 1.

$$\text{No. of trip/vehicle/day, } N_d = (1 - w) H / (P_{hcs} + s + a + bx) \quad (1)$$

$$N_d = (1 - 0.15) 8 / (0.067 + 0.25 + 0.05 + 0.04x) = 6.8 / (0.367 + 0.04x) \quad (2)$$

Where,

N_d = Number of trip per day

w = Off route = 0.15 hr/trip (Tchobanoglous et.al., 1993)

H = Work hour = 8 hr/day

P_{hcs} = Pick up time required per trip = 0.067 hr/trip (Tchobanoglous et.al., 1993)

s = At-site time = 0.25 hr/trip

a = Empirical constant depends on speed limit = 0.05 hr/trip (Tchobanoglous et.al., 1993)

b = Empirical constant depends on speed limit = 0.04 hr/km (Tchobanoglous et.al., 1993)

x = Round trip distance

Table 4: Requirement of transport for secondary collection

Zone	1	2	3	4	5	6	7	8	9	10	Total
Container No.	89	89	46	77	91	49	89	97	56	17	700
Trips/day, N_d	7	6	6	6	6	5	3	3	4	3	---
Vehicle	7	7	4	6	8	5	13	16	7	4	77
Collector	26	30	16	24	32	20	52	64	28	14	306

Design of Sanitary Landfill

The design of sanitary landfill involves preparation of site, design of trench, estimating cell dimensions, lying of bottom liner, spreading of waste, spreading of cover material, compaction of waste, control of landfill leachate, and management of landfill gas. A landfill site consists a platform scale, office building and equipment shade, unloading area, sorting recycling area, space for special wastes and storage area for cover material are located in one end in the compound.

Design of Trench

The depth of borrow pit varies from 3m to 9m (Davis and Cornwell, 1998). The depth of borrow pit is considered 7m and the ratio of waste to cover material is 4:1. Actual thickness of filled waste is 5.6 m. The effective area for landfill trench is 962 ha. The side slopes typically range from 1.5:1 to 2:1 (Davis and Cornwell, 1998).

Construction of Bottom Liner

A bottom liner is an engineering system to contain and control the pollution of the land and water environments surrounding the land disposal operation. Usually clay is used as a bottom liner. A clay liner is usually constructed of 0.3m to 1m thicknesses. Assume thickness of bottom liner is 0.75m. Total required volume of liner is equal to the effective landfill area multiplied by the thickness of liner is equal to 7214095 m^3 . A typical conventional sanitary landfill is shown in Figure 2.

Landfill Cover

The recommended ratio of cover material and solid wastes is 1:4. So, the total volume of cover material is one fifth of the total volume of waste. Total volume of cover material is 13466310 m^3 . At the end of each day's operation, a 200 mm layer of cover material is placed over the compacted fill.

Design of Cell of Landfill

Thickness of the layer of spreading solid waste is 0.6m. Useful fill area will be 50% to 80% of gross area (Davis and Cornwell, 1998). Useful area is considered as 70% of gross area. Daily filling height of cell is considered as 3.5m (50% of total depth) and cell width is 4.0m. For 0.6m wastes spreading thickness, the compaction layer is 6 for full depth.

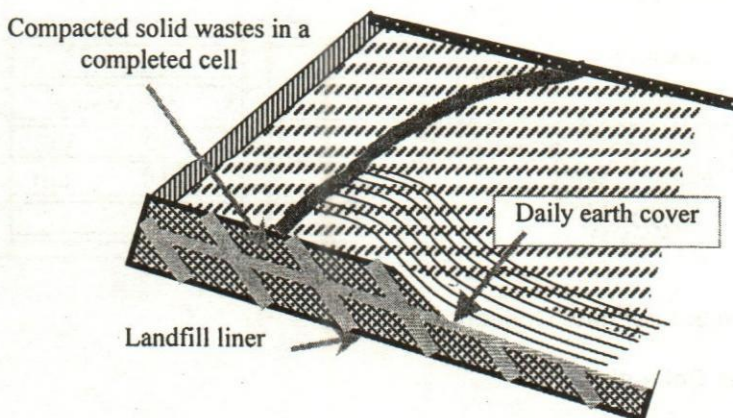


Figure 2: Typical Conventional Sanitary Landfill

Compacting of Solid Wastes

The density of the compacted fill is somewhat dependent on the equipment used at the landfill site and the moisture content of the waste. Compacted solid waste density varies

from 300 to 700 kg/m³. Here design density of compacted wastes is considered 600 kg/m³. For complete compaction required 4 (four) passes by single equipment (Davis and Cornwell, 1998). Working hour per day is 8.0 and working efficiency is 80%. Width of equipment is 2.0 m and over lapping is 33%. Total requirement of land, bottom liner, cover material and no. of dozer for waste spreading and compaction shown in **Table 5**.

Table 5: Total requirement of land, bottom liner, cover material and dozer

Effective area (ha)	Total area (ha)	Liner (m ³)	Cover (m ³)	Dozer (No.)	Excavator (No.)
962	1374	7214095	13466310	7	2

Design of the leachate collection system

There are numbers of leachate collection systems. The more common system is the piped bottom system. The collection channels typically include perforated collection pipes in a bed of packed gravel with slopes in the range of 1% to 5%. This degree of inclination promotes migration of the leachate in the direction of collection pipes or channels. The gravel should have a size in the range of 3.5 cm to 5 cm (Diaz, et.al, 1996). The cross section of schematic pipe collection system is shown in **Figure 2.20**. The leachate collection pipes usually have a diameter of 10cm, and the perforation usually cover about 50% of the pipe circumference. The collection pipes are placed about 5 to 6m apart. The layer of sand is about 60cm thick and is placed on top of the collection pipes a few weeks before the first load of waste is discharged on the cell (Diaz, et.al, 1996). The of leachate collection is shown in **Figure 3**. erforated pipe of 10cm is laid parallel to the length of the landfill site. To discharge the collected leachate into the perforated collection pipe a network is made by using solid pipe in transverse direction of the collection pipe of 15cm diameter with 100m spacing. A delivery pump is fitted at center of 400 sq.m. of the network. Then total requirement for leachate collection is estimated and is shown in **Table 6**.

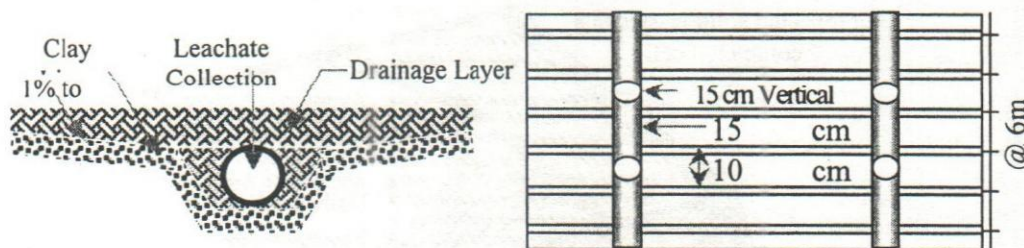


Figure 3: Leachate Collection System

Design of Gas Collection

If the landfill has been properly operated during its lifetime, gas can be recovered from a landfill not originally designed for that purpose by way of drilling a number of boreholes into the landfill at selected gas collection points. The boreholes should be 0.66 to 1m in diameter. Their depth should be from 50% to 90% of the refuse depth. The boreholes are fitted in the same manner as collection wells used in fills designed for gas recovery. The wells are built by progressively backfilling gravel around the gas collection pipe.

Detail design of landfill gas collection is described in **Figure 4** and the requirement of landfill gas collection is shown in **Table 6**.

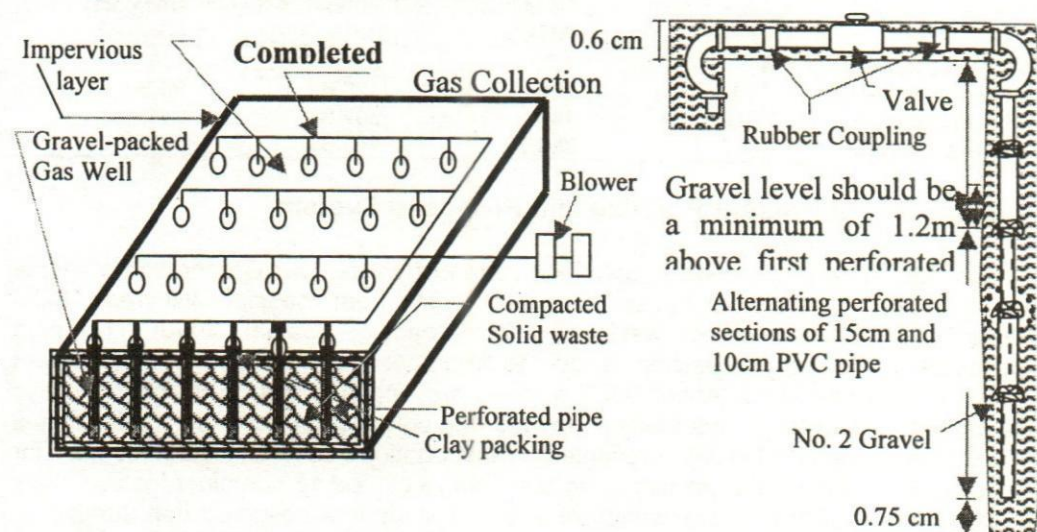


Figure 4: Well System Used for the Recovery of Gases from Landfill (Peavy, et.al, 1985)

Table 6: Requirement of leachate and landfill gas collection

Operation Item	Perforated pipe (Km)		Blind pipe (Km)		Pump (Nos.)
	10cm	15cm	10cm	15cm	
Leachate collection	748	---	---	46.93	105
Gas collection	0.929	0.464	0.698	38.70	1

Analysis of cost involvement

Cost involves in every activity in form of capital cost and operation-maintenance cost. Operation and maintenance cost is estimated for one year and capital cost is considered for total design period. Design period is considered 20 years. Annual expenditure is estimated considering the depreciation and salvation of assets by using equation 2. Finally unit cost of waste management is estimated as Tk/ton of waste. **Table 7** represent the annual cost and unit cost of major activities and also of total waste management system.

$$\text{Annual Cost} = \text{Capital Cost} \times \text{CRF} + \text{Annual O\&M Cost} - \text{Salvage value} \times \text{SF} \quad (3)$$

$$\text{Where, CRF (Capital Recovery Factor)} = \frac{i(1+i)^n}{(1+i)^n - 1}$$

$$= \frac{0.1(1+0.1)^{20}}{(1+0.1)^{20} - 1} = 0.1175$$

$$\text{SF (Sinking Fund)} = \frac{i}{(1+i)^n - 1} = \frac{0.1}{(1+0.1)^{20} - 1} = 0.0174$$

$$i = \text{Discount Rate} = 10\%$$

$$n = \text{Design Period} = 20 \text{ years}$$

$$\text{Salvage Value} = 1\% \text{ of capital cost}$$

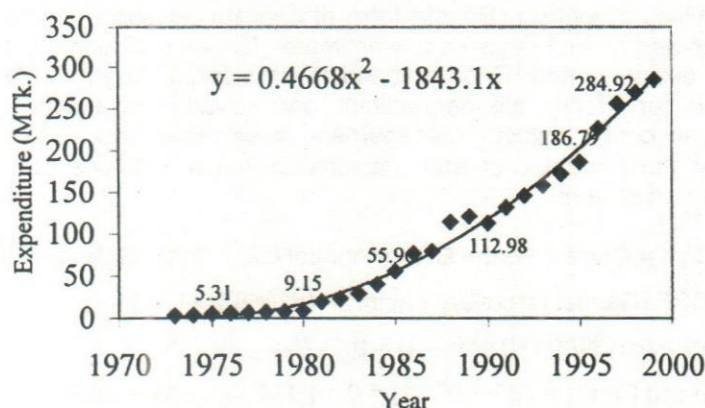
$$\therefore \text{Annual Cost} = 0.1175\text{CC} + \text{O\&M} - 0.000174\text{CC}$$

Table 7: Cost Involvement in solid waste management

Activities of SWM	Capital cost (MTk.)	O&M cost (MTk.)	Annual cost (MTk.)	Unit cost (Tk./ton)
Primary collection	4	1.72	2.19	1.70
Secondary collection	149	109	126.5	98.60
Ultimate Disposal	1355	149	307.84	241
Total expenditure	1622	259.72	449.88	341.30

Comparisons of Present Practice and Proposed System

Unit cost for primary collection is only Tk.1.70/ton of waste. City Corporation authority does not collect waste from house but collect waste from roadside. Whereas, DCC spends Tk.1152/ton to collect waste only from roadside (Salam, 2000). This high expenditure for primary collection is due to improper management of incompetent excessive collection crew. About 6000 workers are engaged with 2080 hand trolleys from primary collection. In this study it is found that unit cost for secondary collection is Tk.98.60/ton. Yousuf (1996) presented transportation cost of Tk.68.60/ton for demountable container system assuming one vehicle carried 16 containers in two shifts per day. From DCC's transport schedule and this study it is observed that number of container to be transported by one vehicle per shift is varied from 3 to 7 from zone to zone with respect to distance of disposal site. Salam (2000) has shown the unit cost of secondary collection for Gulshan and Uttara area is Tk.346.10/ton and Tk.387.25/ton respectively. Again DCC already has 100 (4 standby) demountable container truck and 410 waste collection container. Out of 100 only 77 trucks can be used in proposed system and remaining can be used as standby. DCC only have to purchase about 300 waste collection containers. Again unit cost for ultimate disposal of waste is Tk.241/ton of waste. Dhaka Metropolitan Area Integrated Urban Development Project Report Volume – 3 in 1981 reported that disposal cost only considering bulldozer and pay loader cost is Tk.24/ton. In this report, site preparation and development, land cost, employee cost and other operational cost are not considered.

**Figure 5: Operation and Maintenance Cost of Waste Management of DCC**

Finally unit expenditure for total solid waste management is Tk.341.30/ton of waste. DCC shows the total operation and maintenance expenditure of solid waste management from 1973 to 1999 which is presented in **Figure 5**. The figure shows the

trend of expenditure is increasing which is very sharp from 1990. The expenditure in the year 1999 is MTk.284.92. Therefore unit cost for operation and maintenance of solid waste management is Tk.216.15/ton, however in the proposed system unit cost for operation and maintenance is Tk.197/ton.

Again considering the environmental aspects, present solid waste management practice of DCC creates great treat on environment by contaminating soil, groundwater and surface water and spreading of odor, litter and diseases. However, proposed waste management system does not create any environmental problem.

Conclusion

The following conclusions are drawn on the basis of above discussion and results obtained from this study considering technical, economic and environmental aspects.

Only 50% of the generated solid waste is collected and dumped as crude landfilling. The remaining uncollected waste, which is accumulated into low land, roadside and drains and the crudely dumped waste contaminate soil, groundwater, surface water and air in the present management practice.

Total generated wastes are to be collected and disposed of by sanitary landfilling. Therefore there is no possibility of contamination of soil, groundwater, surface water and air in the proposed management system.

Unit expenditure of every functional element of solid waste management i.e., primary collection, secondary collection and ultimate disposal is less in the proposed management system with respect to present practice.

The proposed management system is possible to adopt with the existing equipment and manpower facilities and without additional cost involvement.

References

- BBS (2000):** Statistical Pocket Book of Bangladesh 2000, Statistic Division, Ministry of Planning, Dhaka, Bangladesh.
- Bhide, A.D. (1990):** Solid Waste Management at Dhaka, Khulna & Natore, WHO project Assignment report: BANCWSOOL July - August.
- BKH, (1986):** Solid Waste Management, Housing Development Project, UNDP/UNCHS (Habitat), Bangladesh.
- Choudhury, J.R. (1998):** A Review of Problems of Dhaka Metropolis and Their Suggested Solution. *Problems of Dhaka Metropolis and Integrated Approach towards Solution*, IEB, Bangladesh.
- Davis, M.L & Cornwell, D.A, (1998):** 'Introduction to Environmental Engineering' Third edition, Mc Graw-Hill publications company.
- DCC (2000):** Solid Waste Management of Dhaka City, Published by Dhaka City Corporation, Dhaka.

- Diaz, L.F, Savage, G.M, Eggerth, L.L & Golueke, C.G. (1996):** *'Solid Waste Management for Economically Developing Countries.'* McGraw-Hill publication company.
- DMDP (1992):** Dhaka Metropolitan Development Planning Waste Management Report, Presented by Mott. Macdonald International limited, Engineering and planning consultant GOB, RAJUK.
- Enayetullah (1994):** A Study of Solid Waste Management for Environmental Improvement of Dhaka City, MURP-Thesis, Department of URP, Bangladesh University of Engineering and Technology, Dhaka.
- George Tchobanoglous, Hilary Theisen and Samuel Vigil (1993):** Integrated Solid Waste Management – Engineering Principles and Management Issues, International Editions, McGraw-Hill, Inc. Publication.
- Louis Berger, (1991):** Dhaka Integrated Flood Protection Project (FAP-8B), ADB, Dhaka.
- MMI (1991):** Mott. Macdonald International Ltd. and Culpin Planning Ltd. of UK, Draft Technical Manual No. 10 for Solid Waste Management, Support for Urban Management and Municipal Services Program, UNDP/UNCHS (Habitat), Bangladesh.
- Peavy, H.S, Rowe, D.R. and Tchobanoglous, G.(1985):** *'Environmental Engineering'* McGraw-Hill publication company.
- Salam M. A. (2000):** Analysis and Design of Solid Waste Management System for a Residential area of Dhaka City, M.Sc. Thesis, Bangladesh University of Engineering and Technology, Dhaka.
- Yousuf T. B. (1996):** Sustainability of solid waste management system of Dhaka City Corporation, M.Engg. Thesis, Bangladesh University of Engineering and Technology, Dhaka.

Geotechnical Investigation of South Western Zone of Bangladesh and Correlation between Some Index Properties

Uma Saha¹, Fatima Rukshana², Md. Matiar Rahman Mondol¹ and Shailen Kumer Ghosh²

Abstract

Geotechnical investigation is an important aspect and needs for any physical structure of construction. Geotechnical investigation is basically a combination of number of investigations such as, field investigation and laboratory investigation. In this geotechnical investigation, field data has been collected through Bangladesh Water Development Board (BWDB) and laboratory investigation i.e. analysis has been carried out at River Research Institute (RRI). Laboratory analysis has been conducted after receiving the soil sample from BWDB. Both field investigation and the laboratory analysis data are available in RRI. So, several numbers of data of different years of south western zone has been collected from Soil Mechanics Division of RRI.

In this paper, geotechnical investigation has been done to the structures of construction, which are involved to manage water, control water etc. and other physical infrastructure of developing areas. Here correlation has been developed between compression index (cc) and water content (WN), liquid limit (WL), plasticity index (PI), initial void ratio (e₀) of soil. Another correlation has been established between unconfined compressive strength (qu) & penetration resistance (N) of soil and between the ratio of undrain cohesion intercept and effective overburden pressure (Cu/σ) & plasticity index. Established equations ensure that cc increases with WN, WL, PI, e₀ and qu increases with N and Cu/σ increases with PI. These equations are reasonably accurate compared to the other recognized equations. Some unknown parameters will have to determine by knowing one parameter through these established co-relation.

Introduction

Bangladesh is a riverine country and having most complex river system in the world. Due to complexity of the river and their tributaries, distributaries and other regions, Bangladesh is inundated almost every year. Flood hit the several water control structure and physical infrastructure. So, to manage flood and built and rebuilt the structures, it becomes essential to construct various physical infrastructures and water control structures.

To do the design of structure of construction, at first needed to know its engineering properties. As the design criteria entirely depends on its geo-technical criteria and engineering properties of soil, so, it is very much essential to know these properties. To considering these things, it has been attempted to discuss about geo-technical investigation and its determining properties. As one parameter of soil is determined by knowing another parameter, so, an attempt has also been made to establish correlation between different engineering parameters of soil.

In connection of this paper, south western zone of Bangladesh has been considered. As Bangladesh is a developing country and flood hit all over the region of Bangladesh, so government has undertaken numbers of projects for its development. South western zone is one of the zones wherever numbers of projects are completed and running. That's why it has been considered a zone like south western zone of Bangladesh.

¹ Principal Scientific Officer, ² Senior Scientific Officer & ³ Scientific Officer, River Research Institute, Faridpur

RRI is involved all the water control structures and physical infrastructures of BWDB through analysis of soil. In that case, it is easy to collect soil data of south western zone. These data's actually has been taken from different areas of south western zone of Bangladesh which are available in RRI.

In the connection of the paper, several numbers of data has been collected from the different project of south eastern zone of Bangladesh wherever so many numbers of water control structures like regulator, bridge, culvert, embankment, dyke, drainage outlet, bypass channel etc. has been built up for manage flood, water logging, drainage congestion and proper maintaining of main channel of irrigation has been built up. The data has been collected from other infrastructures also.

Bangladesh soil deposits contents silts, silty clays and clays of low to medium plasticity occur predominantly in the upper layers. South western zone contents the raised alluvial terrace deposits, the alluvial flood plain deposits and tidal plain deposits.

The main objective of the study is to establish equation between some parameters of soil from which some unknown parameter is to calculate by knowing other parameter of soil.

Literature Review

Geological Features of Soil of Bangladesh

Most of Bangladesh is an extremely flat delta area which consists of a large alluvial basin floored primarily with Quaternary sediments deposited by the Ganges-Padma, the Brahmaputra-Jamuna and the Meghna river systems and their numerous tributaries and distributaries. The north eastern and eastern boundaries of Bangladesh follow the mountainous areas in India and Burma. Rocks underlying the border areas consist mainly of poorly consolidated shale's and silty sand stones and conglomerates. The alluvial deposits of the country have varying characteristics ranging from piedmont deposits near the mountains to swamp and deltaic deposits near the southern sea – shore (Morgan and McIntire, 1959).

The three main physiographic divisions namely (i) Tertiary and Pleistocene hill formations, (ii) Uplifted Pleistocene Alluvial Terraces, and (iii) Recent Flood plain and Piedmont Alluvium of the country including the greater administrative districts are shown in **Figure.-1**. Hunt (1976) has mentioned that the recent flood plain and piedmont alluvium occupies roughly seventy percent of the land area of the country. Safiullah (1991) has mentioned that the raised alluvial terrace deposits, the alluvial flood plain deposits and tidal flood plain deposits constitute about more than eighty percent of land surface of Bangladesh. The hilly region on the northeast, east, and southeastern borders of the country constitutes only about fifteen percent of the area.

General Soil Condition and Earlier Studies

Hunt (1976) has grouped Bangladesh soil deposits into six units and from the brief soil descriptions of the six units it is observed that silts, silty clays and clays of low to medium plasticity occur predominantly in the upper layers and he has suggested 3 to 6 percent CBR values for deposits of (1) estuarine and tidal flood plain ,(2) raised alluvial

terraces, (3) alluvial flood plain and (4) alluvial flood plain but including depressions; and 10 percent for (5) Himalayan piedmont deposits and (6) hill soils.

Serajuddin and Ahmed (1982) have indicated from their study of the soils of different project areas of Bangladesh occurring up to the depths of about 6 to 7m that silt and clay materials of low to medium plasticity occur predominantly in many areas in the upper soils strata in Bangladesh.

Previous Established Empirical Equation

Some authors have been made co-relations on different types of soil of Bangladesh through investigation of soil.

Md. Serajuddin (1964) has been established a co-relation for Khulna clay

$$C_c = 0.50 (e_0 - 0.50), \text{ Where, } C_c = \text{compression index, } e_0 = \text{initial void ratio}$$

Md. Serajuddin and Md. Alimuddin (1967) two empirical equations for East Pakistan clays-

$$C_c = 0.0078 (L_w - 14), \text{ Where, } C_c = \text{compression index, } L_w = \text{Liquid limit, and}$$

$$C_c = 0.44 (e_0 - 0.30), \text{ Where, } C_c = \text{compression index, } e_0 = \text{initial void ratio}$$

K.R. Arora (1992) expressed his book that the unconfined compressive strength can be determined from the following equation

$$q_u = 12.5 N, \text{ Where, } q_u = \text{Unconfined compressive strength,}$$

$$N = \text{Standard penetration resistance}$$

Sanglerat (1972) proposes the following relationship between N and q_u for different soil types with the values of k ranging from 13.33 to 25.

$$\text{For clay, } q_u = 25 \text{ N kPa}$$

$$\text{For silty clay, } q_u = 20 \text{ N kPa}$$

$$\text{For silty sandy soil, } q_u = 13.33 \text{ N kPa}$$

Murthy (1993) investigated the relationship between N and q_u for the preconsolidated silty clay encountered at Farakka in west Bengal, India and suggested the equation as follows,

$$q_u = N/7.5 \text{ kg/cm}^2 = 13.33 \text{ N kPa}$$

Where, q_u = Unconfined compressive strength

$$N = \text{Standard penetration resistance}$$

Md. Serajuddin (1969) found that for coastal embankment soils that the comparison between static Dutch Cone penetrometer cone resistance and unconfined compression strength of the undisturbed Shelby tube samples are

$$q_u = 1.5N, \text{ Where, } q_u = \text{Unconfined compressive strength}$$

$$N = \text{Standard penetration resistance, and}$$

$C_c = 0.50 (e_0 - 0.50)$, Where, C_c = compression index, e_0 = initial void ratio

$C_c = 0.135 (w - 20)$, Where, C_c = compression index, w = natural water content

Md Serajuddin et. al (2001) has given a list of empirical equation of different authors including him

$C_c = 0.009 (w_L - 20)$ -----Terzaghi and Peck (1967)

Where, C_c = compression index, w_L = liquid limit

$C_c = 0.0078 (w_L - 14)$ -----Serajuddin and Ahmed (1967)

Where, C_c = compression index, w_L = liquid limit

$C_c = 0.009 w_N + 0.005 w_L$ -----Kappula (1968)

Where, C_c = compression index, w_N = natural water content, w_L = liquid limit

$C_c = 0.0097 + 0.009 w_L + 0.0014 I_p + 0.0036 w_N + 0.1165 e_0 + 0.0025 C_p$ --Kappula (1981)

Where, w_L = liquid limit, I_p = Plasticity index, w_N = natural water content

e_0 = initial void ratio, C_p = percent finer than 2 micron at %

$C_c = 0.37 (e_0 + 0.003 w_L + 0.0004 w_N - 0.34)$ -----Azzouz et. al (1976)

Where, e_0 = initial void ratio, w_L = liquid limit, w_N = natural water content

$C_c = 0.156 + 0.041 e_0 + 0.00058 w_L$ -----A-khafaj & Andersland (1992)

Where, e_0 = initial void ratio, w_L = liquid limit

$C_c = 0.30 (e_0 - 0.27)$ -----Azzouz et. al (1976)

Where, C_c = compression index, e_0 = initial void ratio

$C_c = 0.44 (e_0 - 0.30)$ -----Serajuddin & Ahmed (1967)

Where, C_c = compression index, e_0 = initial void ratio

$C_c = 0.4049 (e_0 - 0.3216)$ -----Serajuddin (1987)

Where, C_c = compression index, e_0 = initial void ratio

$C_c = 0.2765 [G_s (1 - e_0) / G_s] - 0.5171$ Serajuddin (1987)

Where, C_c = compression index, G_s = specific gravity

K.R. Arora (1987) explained his book that the compression index is related to the in-situ void ratio e_0 or water content (w_0) as below

$C_c = 0.54 (e_0 - 0.35)$

$C_c = 0.0054 (2.6 w_0 - 35)$

The co-efficient of compressibility a_v may be calculated from the compression index as under

$$a_v = 0.435 C_c / \sigma_a$$

Where, σ_a is the average pressure for the increment.

Skempton (1957) expressed the relationship $C_u / \sigma = 0.11 + 0.0057 PI$

Where, C_u = Undrained cohesion intercept

σ = effective overburden pressure, PI = Plasticity index (%)

Methodology

For establishing equation between some parameters of soil, south- western zone of Bangladesh has been considered. As south-western zone is one of the developing area and so many structure of construction is involved in this development. For design of construction of structure, BWDB has collected soil samples. The drilling was explored in south west region such as Khulna, Jessore, Magura, Sathkhira, Faridpur, Gopalganj, Madaripur, Shariatpur of Bangladesh which has been shown by legend in the map in **Figure-1 & 2**. The depth of the exploration was more or less 72' and undisturbed soil sample has been collected from (15'-17'), (20'-22'), (25'-27') and (30'-32') and occasionally it is (40'-42').

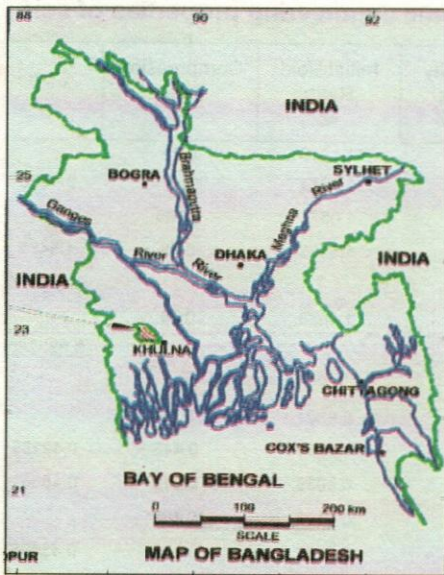


Fig-1: Map of Bangladesh

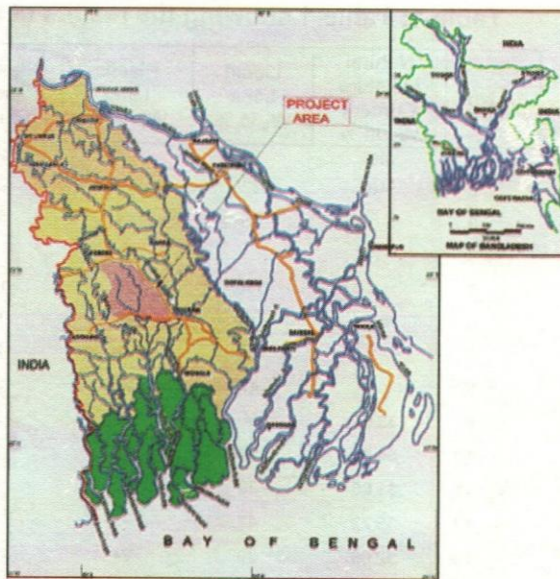


Fig-2: South Western zone of Bangladesh

After collection of soil samples, BWDB has sent both disturbed and undisturbed samples at RRI for analysis of soil. RRI has conducted soil test and analysis. So, RRI is involved with all the project of south western zone of Bangladesh. RRI has huge

numbers of data of south western zone of Bangladesh. In this paper, all the data's of undisturbed soil samples has been collected from soil mechanics division of RRI.

Soil test has been performed by skill soil technicians through the supervision of concern officer. Data preparation and interpretation has been completed by authors through the conventional equations of soil mechanics. Subsequent analysis has also been performed by authors.

Data Analysis and Results

Data has been analyzed in the conventional way and shown in tabular form in Table-1 and Table-2. Liquid limit, plastic limit and plasticity index has been analyzed from Atterberg's limit test. Compression index has been calculated from the virgin compression line of void ratio and log-pressure curve according to Terzaghi and Peck. For determining shear strength, cohesion and angle of internal friction has been determined from Mohr's Circle diagram on unconsolidated undrained triaxial shear test. Effective overburden pressure has been calculated from the supplied boring log.

Standard penetration resistance has been determined using equation,

$$q_u = 12.5 N$$

Where, q_u = unconfined compressive strength in kN/m^2

N = standard penetration resistance

Table-1: Table-1 showing the results of some engineering properties of soil.

Sl. No.	Natural Moisture Content W_N in %	Liquid Limit W_L in %	Plastic Limit W_p in %	Plasticity Index PI in %	Initial Void Ratio e_0	Compression Index C_c	C_u/σ
1.	46	24		22	1.1216	0.29	
2.	46	22		24	1.1814	0.3	0.4023
3.		45	21	24	1.0371	0.265	
4.					1.5465	0.43	1.5465
5.		180	70	110			0.463478
6.	79.38	102	45	57	1.6076	0.74	
7.		48	26	22			0.383285
8.		47	25	22			
9.	33.61	50	26	24	0.9301	0.28	
10.	54.54	57	30	27	1.4851	0.446	0.42289
11.	31.66	39	62	13	0.9039	0.212	0.48551
12.	35.72	42	72	15	0.9197	0.182	
13.	32.06	39	24	15	0.9131	0.199	0.43695
14.		38	28	10			0.56356
15.	33.22	41	24	17	0.8369	0.173	0.46863
16.	61.23	117	68	49	1.0982	0.307	0.41615
17.	35.35	57	25	32	0.9066	0.227	0.37009
18.	42.79	62	28	34	1.1436	0.43	0.40278
19.	39.16	52	25	27	1.1487	0.37	0.34903
20.	26.62	50	24	26	0.6839	0.185	

Sl. No.	Natural Moisture Content W_N in %	Liquid Limit W_L in %	Plastic Limit W_p in %	Plasticity Index PI in %	Initial Void Ratio e_0	Compression Index C_c	C_u/σ
21.		56	26	30			
22.	61.12	85	40	45	1.1294	0.67	0.26107
23.	31.2	45	22	20	1.006	0.277	0.44986
24.	39.14	45	24	21	1.2324	0.327	0.278019
25.	40.86	46	24	22	1.1976	0.33	0.29142
26.		151	62	89	2.4991	1.135	
27.	24.98	48	18	30	0.5911	0.178	
28.	30.24	54	27	27	0.94742	0.292	
29.	21.93	42	17	25	0.621	0.16	
30.	41.62	68	32	36	1.2178	0.449	0.2626
31.	40.04	48	27	21	0.9566	0.265	0.37911
32.	42.51	62	29	33	1.1048	0.232	0.28464
33.	57.76	68	38	30	1.7144	0.545	0.35433
34.	32.29	46	27	19	1.0048	0.2245	0.48153
35.	31.31	42	26	16	0.9312	0.168	0.43098
36.	54.53	62	31	31	1.31	0.347	0.36498
37.	29.86	45	24	21	0.8961	0.216	0.458517
38.	32.12	45	25	20	0.9732	0.23	0.461363
39.	42.05	55	28	27	1.2321	0.406	0.384555
40.	30.54	46	26	20	0.9581	0.359	0.47433
41.	43.93	43	26	17	1.2253	0.315	0.322406
42.	33.32	34	25	9	1.2752	0.434	0.374503
43.	28.71	46	27	19	1.0068	0.216	0.485807
44.	35	54	27	27	1.0471	0.263	0.463639
45.	43.65	55	25	30	1.2252	0.31	0.482044
46.	65.23	77	37	40	1.3294	0.375	
47.	46.11	59	28	31	1.4052	0.335	0.359777
48.	35.92	55	26	29	1.1422	0.301	0.23107
49.	41.42	46	24	26	1.1216	0.29	
50.	42.15	46	22	24	1.1844	0.3	0.4023
51.	35.11	45	21	24	1.0371	0.265	

Table-2 : Table-2 showing the results of standard penetration resistance and unconfined compressive strength

Sl. No.	Standard Penetration Resistance (SPT)	Unconfined Compressive Strength (q_u) in kN/m^2	Sl. No.	Standard Penetration Resistance (SPT)	Unconfined Compressive Strength (q_u) in kN/m^2
1.	1	7.85	20	3	36.29
2.	1	8.56	21	3	41.38
3.	1	10.2	22	4	49.98
4.	1	12.21	23	4	50.66

Sl. No.	Standard Penetration Resistance (SPT)	Unconfined Compressive Strength (q_u) in kN/m^2	Sl. No.	Standard Penetration Resistance (SPT)	Unconfined Compressive Strength (q_u) in kN/m^2
5.	1	14.31	24	4	52.5
6.	1	17.49	25	4	54.78
7.	2	20.85	26	5	55.9
8.	2	21.28	27	5	58.43
9.	2	22.65	28	5	61.31
10.	2	24.44	29	6	73
11.	2	27.28	30	6	79.81
12.	2	27.69	31	7	88.82
13.	2	30	32	8	94.39
14.	2	30.16	33	8	100.04
15.	3	32.59	34	8	106.01
16.	3	32.63	35	8	106.02
17.	3	34.1	36	11	138.21
18.	3	34.62	37	13	159.57
19.	3	35.68			

Compression index vs. natural water content w_N , liquid limit w_L , plasticity index PI and initial void ratio e_0 graph has been plotted and shown in **Figure- 3**, **Figure-4**, **Figure-5** and **Figure-6** respectively.

Unconfined compressive strength q_u and standard penetration resistance (SPT) N has been plotted in the graph and shown in **Figure-7**.

The ratio of undrain cohesion intercept and effective overburden pressure (C_u/σ) vs. plasticity index PI graph has been plotted and shown in **Figure-8**.

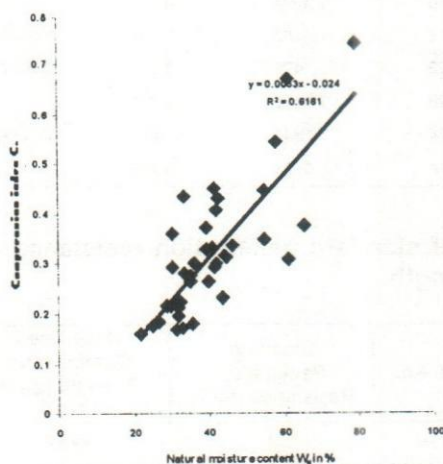


Fig-3: Relationship between compression index and natural moisture content

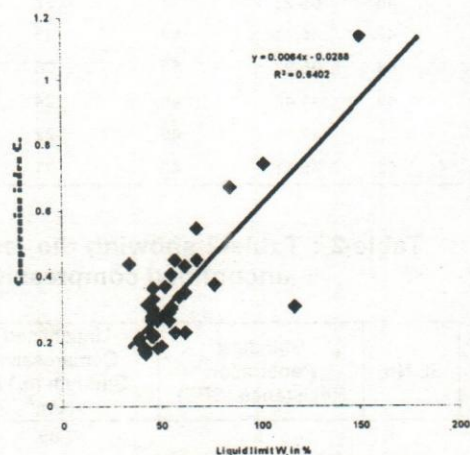


Fig-4: Relationship between compression index and liquid limit

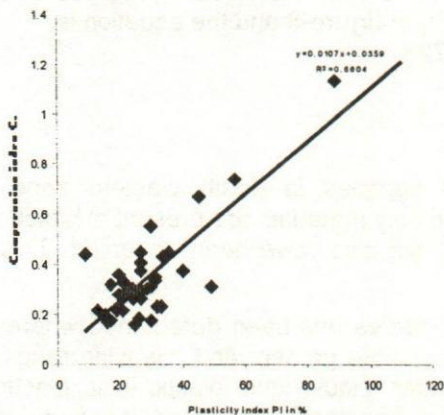


Fig-5: Relationship between compression index and plasticity index

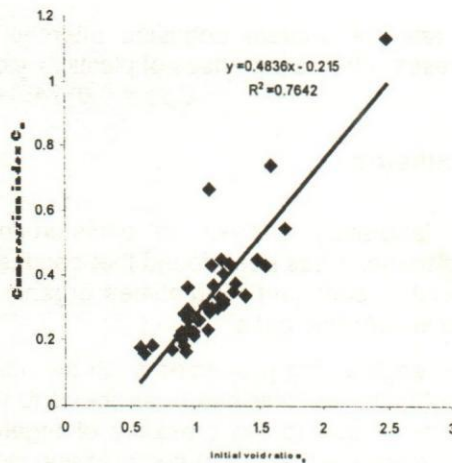


Fig-6: Relationship between compression index and initial void ratio

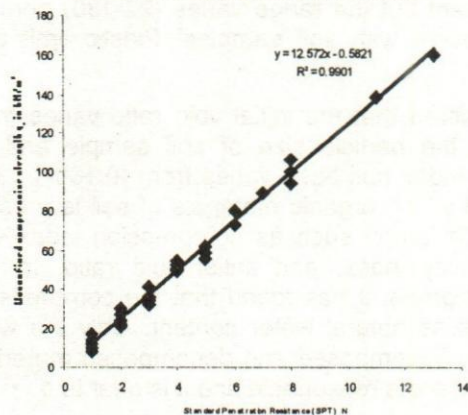


Fig-7: Relationship between unconfined compressive strength and standard penetration resistance

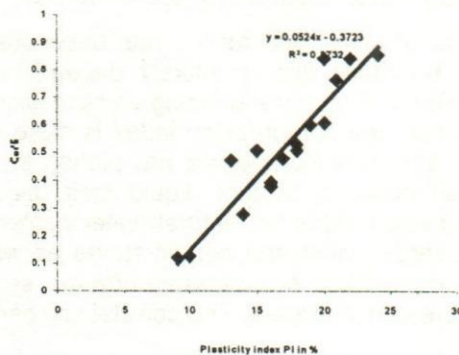


Fig-8: Relationship between the ratio of undrain cohesion intercept to effective overburden pressure and plasticity index

From **figure-3**, it is found that compression index (C_c) increases with the increases of natural water content (W_N) and the established equation become,

$$C_c = 0.0083W_N - 0.024$$

From **figure-4**, it is observed that compression index (C_c) increases with the increases of liquid limit (W_L) and the established equation is,

$$C_c = 0.0064W_L - 0.0288$$

In **figure-5**, it is shown that compression index (C_c) increases with the increases of plasticity index (PI) and the established equation is,

$$C_c = 0.0107PI + 0.0359$$

From **figure-6**, it is found that compression index (C_c) increases with the increases of initial void ratio and the established equation become,

$$C_c = 0.4836e_0 - 0.215$$

Unconfined compressive strength (q_u) increases with the increases of standard penetration resistance (N) in **figure-7** and the equation is,

$$q_u = 12.57N - 0.5821$$

The ratio of undrain cohesion intercept and effective overburden pressure (C_u/σ) increases with the increases of plasticity index (PI) in **figure-8** and the equation is,
$$C_u/\sigma = 0.0524PI - 0.3723$$

Discussion

After laboratory analysis of undisturbed soil samples in south western zone of Bangladesh, it has been found that sand, silt and clay materials are present at which silt material is dominant. Sometimes organic materials also have been observed. This is found in very little case.

Some engineering properties such as index properties has been determined wherever natural water content has been found to varies (20-65) percent and this wide range of variation is due to the presence of organic matter. Liquid limit, plastic limit, plasticity index, initial void ratio and compression index has also been determined. It is found that liquid limit varies normally from (22-50) percent but the range varies (22-180) percent when the organic material and peat is present with soil samples. Plastic limit and plasticity index varies as the same manner.

In case of initial void ratio it has been observed that the initial void ratio varies from (0.5911-1.7144) this is entirely depend on the particle size of soil sample and its ingredients. The corresponding compression index has been varies from (0.160-1.135). Of course, the compression index is more at which organic materials of soil is present more. The index properties are plotted in the graph such as compression index vs., natural moisture content, liquid limit, plasticity index, and initial void ratio. In the compression index vs. natural water content graph, it has found that the compression index varies within the certain range as well as natural water content. Only the wide range of variation occurs when organic, semi decomposed and decomposed materials were present in the soil. The correlation coefficient is reasonable and it is near to 1.

It has been found from the compression index and liquid limit graph that compression index increases gradually as well as liquid limit. Some deviation also has been found. It is due to ingredients of soil particles i, e, occasionally organic materials are present and sometime silt content varies and sometime clay and sand particles vary. The correlation coefficient is more or less near about 1.

In the compression index vs. plasticity index graph it has been found that compression increases linearly whereas the plasticity increases in the limited range. Only the compression index increases rapidly when ingredients vary. In this graph some deviation occurs. The correlation coefficient is very near to 1.

In the compression index vs. initial void ratio graph, it has been found that the compression index increases slowly as well as initial void ratio. The correlation coefficient is near to 1.

It has been observed from the C_u/σ vs. PI graph that C_u/σ varies as well as PI varies. This observation has been carried out in case of only silt soil. The correlation coefficient is near about 1.

In the unconfined compressive strength vs. standard penetration resistance graph, it has been found that unconfined compressive strength increases as well as standard penetration resistance increases. The correlation co-efficient is approximately 1.

Conclusions

In this paper some correlations have been established between some index properties such as compression index (c_c), water content (W_N), liquid limit (W_L), plasticity index (PI), initial void ratio (e_0) of soil. Another correlation has been established between unconfined compressive strength (q_u) & penetration resistance (N) of soil and between the ratio of undrain cohesion intercept and effective overburden pressure (C_u/σ) & plasticity index of soil. The established equations are,

Established Equations	Correlation Co-efficient (R^2)
$C_c = 0.0083W_N - 0.024$	0.6161
$C_c = 0.0064W_L - 0.0288$	0.6402
$C_c = 0.0107PI + 0.0359$	0.6604
$C_c = 0.4836e_0 - 0.215$	0.7642
$q_u = 12.57N - 0.5821$	0.9901
$C_u/\sigma = 0.0524PI - 0.3723$	0.9732

These established correlations are reasonably accurate compared to the other recognized equation. Some deviation has been occurred due to some disturbance and presence of disturbing ingredients. From the established correlation one parameter will have to be calculated by knowing another parameter.

Acknowledgement

The authors gratefully acknowledge to the technicians who were involved in the soil testing works in the laboratory.

References

- Arora K.R.(1992) " Soil Mechanics and Foundation ", Standard Publishers Distributors, Delhi, India, P 1218.
- Serajuddin Md.(1964), "Correlation of some Engineering Properties of subsurface soils occurring in the coastal Embankment Project area of Khulna District" Geotechnical Studies on Bangladesh Soils, December 2002, PP (13-30).
- Serajuddin Md.and Ahmed (1967) "Studies on Engineering properties of East Pakistan Soils"" Geotechnical Studies on Bangladesh Soils, December 2002, PP(53-66).
- Serajuddin Md. (1969) " A Study of the Engineering Aspects of Soils of Coastal Embankment Project Area in East Pakistan "Geotechnical Studies on Bangladesh Soils, December 2002, PP(99-116).
- Serajuddin Md. et.al (2001) " Characterization of Uplifted Pleistocene Deposits in Dhaka Clay "Geotechnical Studies on Bangladesh Soils, December 2002, PP (253-272).
- Serajuddin Md. and M.A. Alim Chowdhury (1996) " Correlation Between Standard Penetration Resistance and Unconfined Compressive Strength of Bangladesh Cohesive Deposits", Journal of Civil Engineering, The Institution of Engineers, Bangladesh , Vol.CE, No. 1, June 1996 , PP(69-83).
- Soil Testing Report, River Research Institute of South Western Zone of Bangladesh.

Triaxial Extension Test and Nonlinear Model Parameters of Barind Soil

Syed Abdul Mofiz¹

Abstract

An experimental investigation of the tensile behavior of Barind (expansive) soil was carried out using a computer control GDS triaxial apparatus. Testing program concentrated on the study of normally consolidated drained triaxial CTE, TE and RTE extension stress path tests on sample of size 50 mm diameter and 100 mm high soil specimen. Testing was carried out at effective consolidation pressures ranging between 100-500 kPa by using a stress controlled triaxial apparatus. The unload-reloading tests were done at effective confining pressure 200 kPa for the determination of unload-reload model constants. The non-linear (hyperbolic) elastic model parameters for the compacted barind soil were determined from the test results. An attempt is made to verify the model parameters by comparing numerical predictions with the experimental test results. Numerical analysis using hyperbolic model parameters indicated good agreement with the experimental results.

Introduction

In semi-tropical and tropical areas, compacted soil have been employed as a standard practice in geotechnical construction works to improve the settlement characteristics of foundation, stability of slope, and embankments as well as seepage control in the dam cores. Most of the research work that exists in the literature aimed at setting guidelines to ensure the satisfactory performance of the soil materials under compression and shear. The practice of neglecting the tensile strength of soils in most stability analysis has led to an almost absence of the test data on the behavior of soils in the negative effective stress range. Geotechnical engineers commonly adopted conventional triaxial compression tests data in design practices in dealing with the slope stability and embankment problems on compacted soil, but most of them ignore tension test of such soil. However, tensile stress regimes are encountered in many geotechnical structures such as rigid and flexible layer pavements, in the upper part of the natural and compacted slopes, and in the dam cores. In the Barind tract of Bangladesh a large number of civil engineering structures were built on highly Plastic (expansive) soils before the 1980s are now showing signs of deterioration. This deterioration which is make known by swelling and cracking of the superstructure, due to shrinkage which was no considered during construction work. The performance and integrity of the structures may be endangered when the generated tensile stresses in such systems exceed the ultimate tensile capacity of the soil. This paper describes the detailed description of the use of hydraulic triaxial test apparatus for the evaluation of tensile stress-strain properties of compacted barind soil. The non-linear model has been used for the model prediction of tensile stress-strain behavior of the barind soil.

¹ Prof., Dept. of Civil Engineering, Rajshahi University of Engineering & Technology, Rajshahi

Literature Review

Barind soil can be found in major parts of the northern region of Bangladesh and has been used as a low cost construction material for many years. Its availability at and around construction sites and the resulting reduction in transportation costs are the primary practical factors. A review of the previous work indicated that most tension tests on soils have been to determine tensile strength rather than stress-strain characteristics. Conlon (1966) first reported tension test on soils in the triaxial equipment. Bishop and Graga (1969) explained the feasibility of performing tension tests in triaxial equipment by employing specimens with reduced central sections. Parry and Nadarajah (1974) reported tension tests under undrained conditions with pore water measurement. Ajaz and Parry (1975) reported that the soil under tensile stress fields exhibit non-linear behavior. Al-Hussaini (1981) also performed tests using triaxial set up in which the failure mechanism was achieved under a stress system with one of the principal stresses being tensile in character. Berdie (1991) carried out tension test of non-uniform cross-section test specimens and investigated the tensile stress-strain behavior of kaolin within the framework of established constitutive relations under an axi-symmetric (conventional) stress system.

This paper will focus on the tensile stress-strain properties of barind (expansive) soil and to determine the non-linear model parameters. These model parameters play important roles in predicting tensile forces in tension governing pavement and foundation problems on barind soil.

Stress Path and Applications

In the field soil element undergoes different stress paths depending upon the loading conditions. Current practice is to use relationships to interpolate the shear strength values for slope failure with tension crack as shown in **Figure 1(a)**, shallow foundation failure surface using either the triaxial compression, direct shear or triaxial extension tests as shown in **Figure 1(b)**, and for excavation problems shown in **Figure 1(c)**. Considering the geometry of the potential failure surface, weighting factors may be applied to derive the appropriate strength to use in the limiting equilibrium analysis for a given field stress path.

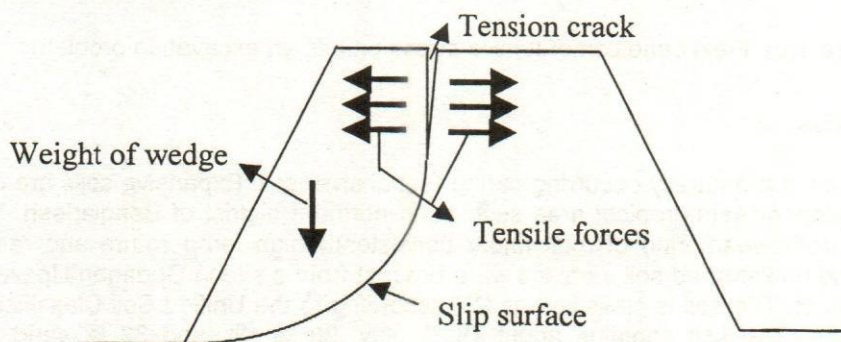


Figure 1(a). Tensile crack in a embankment slope

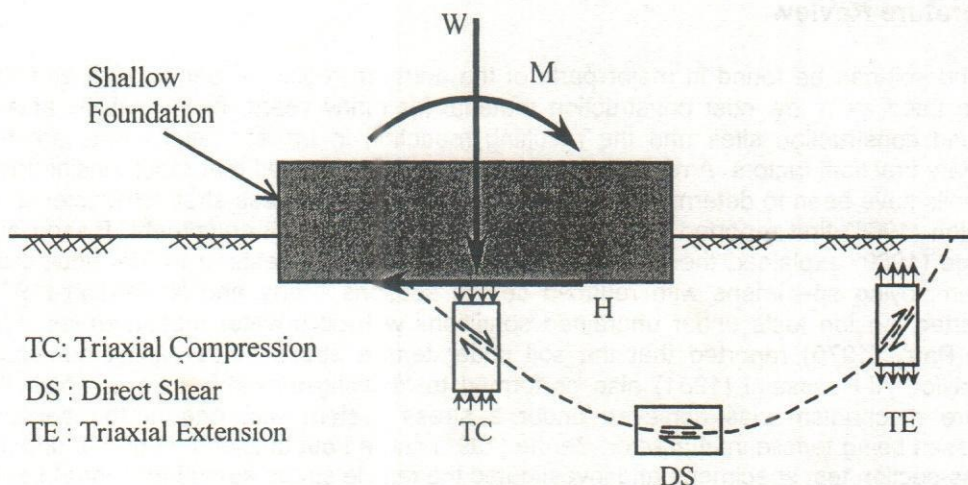


Figure 1(b). Failure surface of different field stress paths in a shallow foundation problem

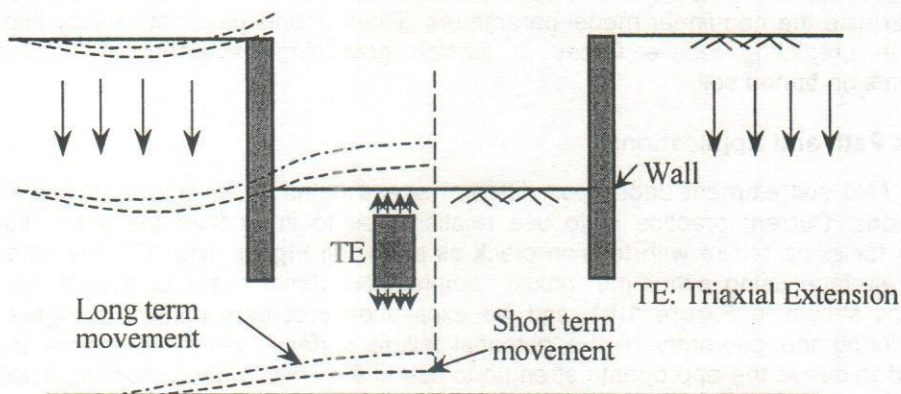


Figure 1(c). Field condition of tensile stress path in an excavation problem

Soil Properties

The soil tested is a naturally occurring barind (expansive) soil. Expansive soils are often found in tropical or semi-tropical area such as in northern district of Bangladesh. They are formed from weathering of rock under consistently high temperature and rainfall. Disturbed and undisturbed soil samples were brought from a site in Godagari Upazilla of Rajshahi district. The soil is classified as CH according to the Unified Soil Classification (USC) System. The soil contains about 48 % clay, 20 % silt, and 32 % sand. The maximum dry density from the standard Proctor test was 16.64 kN/m^3 and the optimum moisture content was about 25.10%. The geotechnical properties of the barind soils are presented in **Table 1**.

Table 1. Geotechnical properties of barind soil

Description of Soil Properties	Value
Specific Gravity, G_s	2.61
Liquid Limit, w_L (%)	75
Plastic Limit, w_p (%)	42
Plasticity Index, I_p (%)	33
Linear Shrinkage, L_s (%)	16.48
Maximum Dry Density, ρ_d (kN/m^3)	16.64
Optimum Moisture Content, w_{opt} (%)	25.10
Activity, A	0.76
pH	4.6

Non-Linear Elastic Model

The stress-strain behavior of soil becomes nonlinear particularly as failure conditions are approached (**Figure 2**). Duncan and Chang (1970) developed the non-linear elastic model or better known as the hyperbolic model. The frictional shear resistance and axial displacement relationship at any confining pressure is expressed as

$$(\sigma_1 - \sigma_3) = \sigma_d = \frac{\varepsilon_a}{\frac{1}{E_{is}} + \frac{\varepsilon_a}{(\sigma_1 - \sigma_3)_{ult}}} \quad (1)$$

where σ_d is the frictional shear resistance, ε_a is the axial shear strain, E_{is} is the initial shear tangent stiffness, and $(\sigma_1 - \sigma_3)_{ult}$ is the asymptotic value of shear at infinite displacement of the hyperbolic curve.

When a soil is subjected to zero shear stress (i.e. $(\sigma_1 - \sigma_3) = 0$), its stress strain behavior is modeled using the initial modulus E_{is} . The variation of the initial tangent shear modulus with confining consolidation pressure is represented by an empirical equation suggested by Janbu (1963)

$$E_{is} = K P_a \left(\frac{\sigma_3}{P_a} \right)^n \quad (2)$$

where K is the shear stiffness number, n is the shear stiffness exponent number, and P_a is the atmospheric pressure. The different constants in above equation are obtained by conducting triaxial tests on residual soil at varying consolidation pressures. The values of K and n are determined by plotting the experimental data of E_{is}/P_a and σ_3/P_a on a log-log scale.

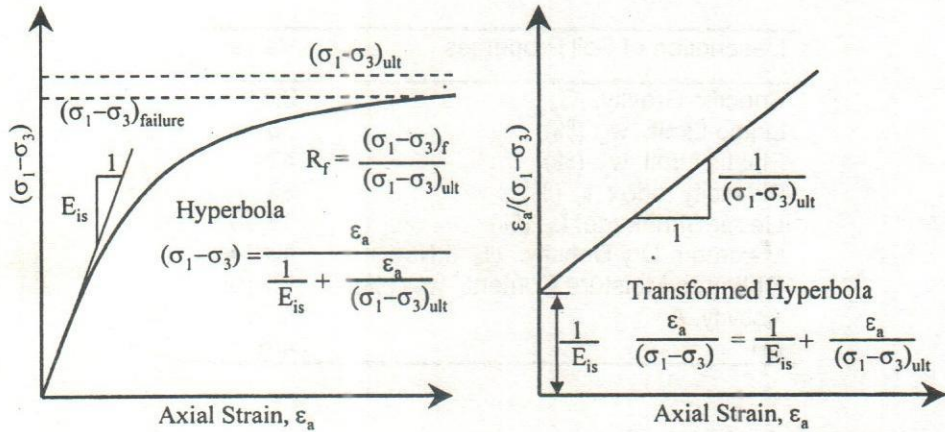


Figure 2. Schematic and numerical representation of hyperbolic model (nonlinear)

The variation of ultimate deviator stress with σ_3 is accounted for by relating $(\sigma_1 - \sigma_3)_{ult}$ to the stress difference at failure, $(\sigma_1 - \sigma_3)_f$, and using the Mohr-Coulomb strength equation to relate $(\sigma_1 - \sigma_3)_f$ to σ_3 . The criteria to define $(\sigma_1 - \sigma_3)_f$ is the maximum deviator stress which results in the best approximation of the actual stress-strain curve. The values of $(\sigma_1 - \sigma_3)_{ult}$ and $(\sigma_1 - \sigma_3)_f$ are related and can be expressed as

$$R_f = \frac{(\sigma_1 - \sigma_3)_f}{(\sigma_1 - \sigma_3)_{ult}} \quad (3)$$

where R_f is the failure stress ratio as shown in Figure 2. The value of R_f is always less than or equal to 1.0 and varies from 0.5 to 1.0 for most soils. The variation of $(\sigma_1 - \sigma_3)_f$ with σ_3 is related through the Mohr-Coulomb strength equation and can be expressed as

$$(\sigma_1 - \sigma_3)_f = \frac{2c \cos \phi + 2\sigma_3 \sin \phi}{1 - \sin \phi} \quad (4)$$

where c is the cohesion intercept and ϕ is the angle of internal friction.

Differentiating the equation of hyperbola shown in Figure 2 with respect to ϵ_a and then substituting the expression into Equations 1, 3, and 4, an expression for the tangent shear modulus can be obtained

$$E_{ts} = \frac{d\sigma}{d\epsilon_a} = \left[1 - \frac{R_f(1 - \sin \phi)(\sigma_1 - \sigma_3)}{2c \cos \phi + 2\sigma_3 \sin \phi} \right]^2 E_{is} \quad (5)$$

This relationship can be used to calculate the value of tangent shear modulus for any stress conditions if the values of the parameters K , n , c , ϕ and R_f are known.

The hyperbolic stress-strain model accounts for the non-linear volume change behavior of soils by assuming that the bulk modulus of the soil varies with the consolidating confining pressure and is independent of the percentage of mobilized strength (Duncan et al. 1980). The variation of bulk modulus B , with confining pressure is estimated by the following equation

$$B = \frac{(\sigma_1 + \sigma_2 + \sigma_3)}{3\varepsilon_v} \quad (6)$$

where $\sigma_1, \sigma_2, \sigma_3$ are the principal stresses, and ε_v is the volumetric strain corresponding to the stress condition. Also, the bulk modulus may be found by an empirical equation if the same soil is tested at various confining pressures, as follows:

$$B = K_b P_a \left(\frac{\sigma_3}{P_a} \right)^m \quad (7)$$

where K_b is the bulk modulus number, and m is the bulk modulus exponent. The variation of B is linear when the logarithm of (B/P_a) and (σ_3/P_a) are plotted against each other. The bulk modulus number equals (B/P_a) at a value of (σ_3/P_a) equal to one and m is the slope of the resulting line.

In the non-linear stress-strain relationships, the average value of unload-reload elasticity modulus, E_{ur} is used for both the unloading and reloading test conditions. The value of E_{ur} is related to the confining pressure and can be expressed as

$$E_{ur} = K_{ur} P_a \left(\frac{\sigma_3}{P_a} \right)^n \quad (8)$$

where K_{ur} is the unload - reload modulus number. The value of K_{ur} is always larger than the value of K and may be 20% greater than K for stiff soils and dense sands. For soft soils and loose sands, K_{ur} may be three times as large as K . The value of the exponent n is assumed to be equal to the primary loading exponent.

Sample Preparation and Testing

A disturbed sample of the barind soil with 68 percent silt and clay fraction was used in this investigation. The soil was first dried under laboratory air-dry conditions, then ground and passed through 2 mm sieve. The dry powder was carefully wetted with a spray gun to the standard optimum moisture content. The moist soil was then stored in several sealed plastic bags in moist room for about a week before use. In order to get the best possible standard homogeneity, compaction was performed in three layers in a 50 mm diameter and 100 mm high special type of splitting cylindrical mold. A rate of 0.15 mm/min for compression on a triaxial press was adopted, and each layer was compacted following the approach (Cui and Delage, 1996) to ensure Proctor maximum density and moisture content with a double piston system.

Triaxial Apparatus

The triaxial extension cell is based on the design of Bishop and Wesley's (1975) hydraulic

triaxial apparatus for controlled stress path testing developed at Imperial College of Science and Technology, London. As shown in the schematic diagram in **Figure 3**, axial force is exerted on the test specimen by means of a piston fixed to the movable base pedestal. The top cap of the test specimen is fixed in position by an adjustable rod passing through the top of the cell. The piston moves vertically up and down in a linear guide comprising a cage of ball bearings housed in a turret joining the cell to the base. The piston is actuated hydraulically from an integral lower chamber in the base of the cell which contains deaerated water. The piston is sealed into the upper cell and the lower chamber by matched Bellofram rolling diaphragms, which sweep equal volumes of water. The extension device is fitted to the triaxial cells in place of the redundant load cell. The object of the extension device is to allow axial stress to be reduced below radial stress. In conventional triaxial cells this normally not possible because the radial stress or cell pressure acts vertically on the top cap. The photographic view of the hydraulic triaxial apparatus with extension test arrangement is shown in **Figure 4**. Fixed the bottom of the rod is a truncated conical fitting which mates with the plane top cap of the triaxial test specimens. The top cap is fitted with a bell mounted surgical PVC dip molded sleeve. The cell is filled with water, with air being purged out through the hollow reaction rod. The reaction rod is then adjusted to dock the plane and conical parts together. Lightly smearing the angled surfaces with soft silicone grease ensure good contact. A small suction can then be applied to the top of the hollow reaction rod to cause the sleeve to seal the interface. Cell pressure is then applied. As the top cap is now sealed to the fixed reaction rod, cell pressure does not act vertically on the test specimen.

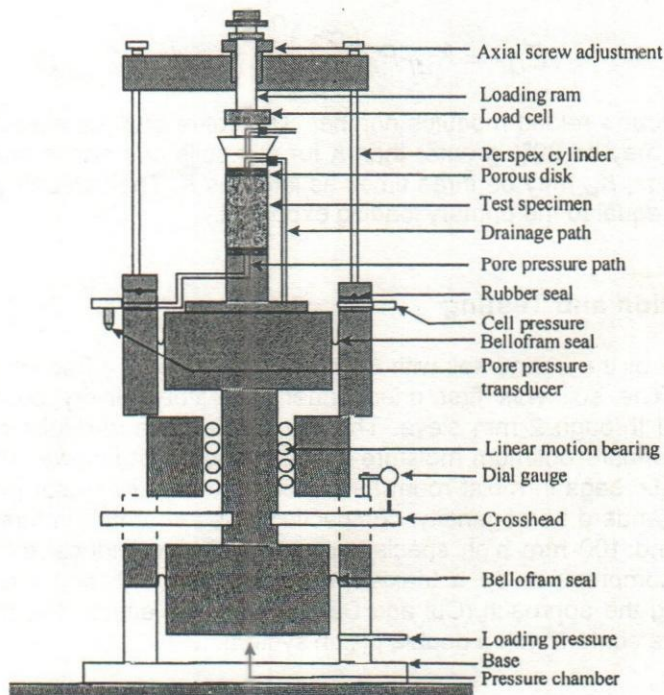


Figure 3. Diagrammatic layout of the hydraulic triaxial extension apparatus (Mofiz 2000)

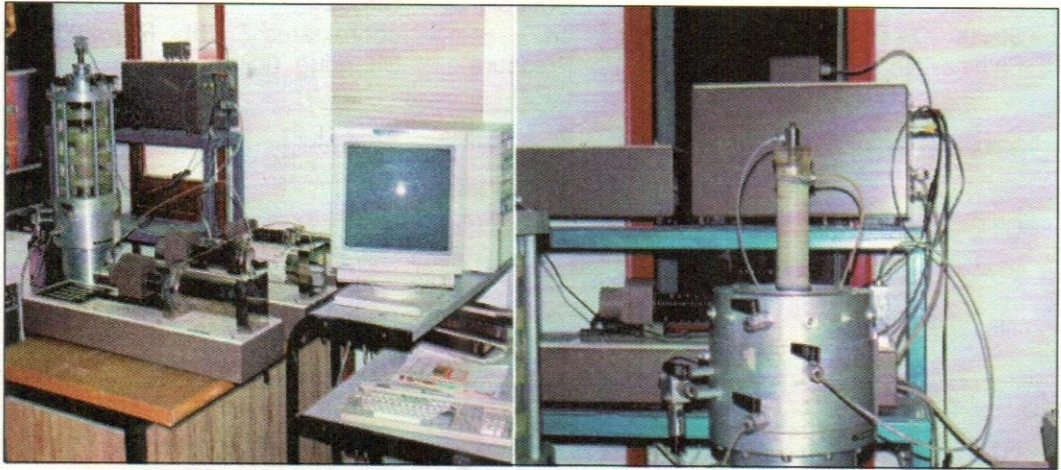


Figure 4. Photographic views of GDS triaxial testing system and setting arrangement of triaxial extension test specimen

Testing Program

The triaxial testing programs for compacted barind soil are divided into three stress paths. The stress paths used in the drained triaxial testing are Conventional Triaxial Extension, CTE; Reduced Triaxial Extension, RTE; and Triaxial Extension, TE. All of these stress paths lie on a triaxial plane and are shown in **Figure 5**. Details of extension stress paths testing program for barind soil are presented in **Table 2**. The experimental program was conducted in a series of drained triaxial extension test using a 50 mm diameter and 100 mm high sample. All the tests were carried out at effective consolidating pressure varying from 100-500 kPa.

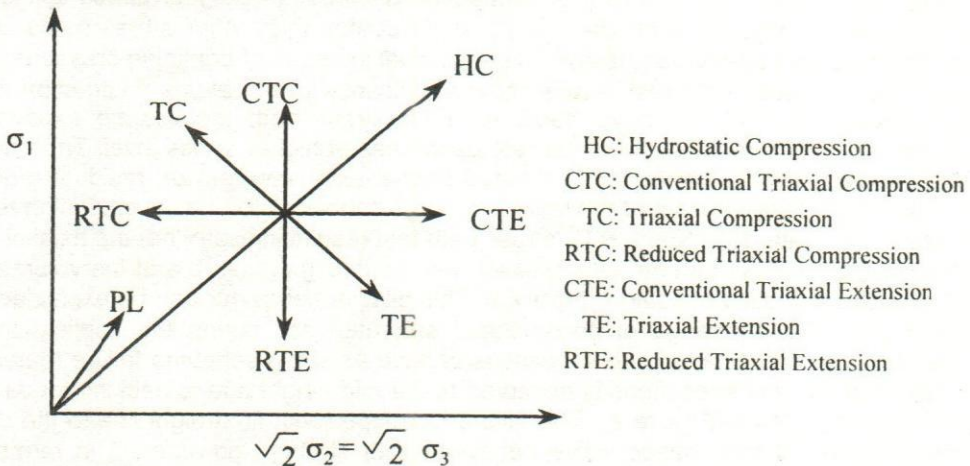


Figure 5. Schematic representations of different stress paths

Table 2 Testing programs of triaxial extension stress paths

Stress Paths	Test No.	Water Content (%)	Soil Density (kN/m ³)	Consolidati on Pressure (kPa)	Stress coordinates Shearing (kPa)			Remarks	
		w	γ _d	σ _c	B _p	σ ₁	σ ₃		B _p
CTE	1	24.95	16.48	150	50	850	150	50	Stress Control
	2	24.98	16.53	250	50	1050	250	50	
	3	25.01	16.44	350	50	1250	350	50	
	4	25.08	16.43	450	50	1450	450	50	
TE	1	24.97	16.36	150	50	50	200	50	Stress Control
	2	24.95	16.51	250	50	50	350	50	
	3	25.01	16.37	350	50	50	500	50	
	4	25.04	16.43	450	50	50	650	50	
RTE	5	25.06	16.39	550	50	50	800	50	Stress Control
	1	24.91	16.42	150	50	50	150	50	
	2	24.96	16.41	250	50	50	250	50	
	3	24.97	16.40	350	50	50	350	50	
	4	24.93	16.39	450	50	50	450	50	
	5	25.04	16.41	550	50	50	550	50	

Results and Discussion

In this investigation, three triaxial extension stress path tests, i.e. CTE, TE and RTE were conducted. The shear stress versus axial strain and volumetric strain versus axial strain for the various stress paths at consolidation pressures (σ_c) between 100 kPa to 500 kPa are shown in **Figure 6** to **Figure 8**. As in the case of compression loadings, the stress-strain relationships are non-linear and the failure strains increases with the increase in confining pressure for all the stress paths. Similarly, the σ - ϵ curves do not produce any distinct peak points. The volume change characteristics for the conventional triaxial extension (CTE) paths exhibit contraction volume change behaviour at lower stress levels and the rate of contraction decreases at higher stress levels. In these cases, the volume contraction is more noticeable than other stress paths. The main reason of this behaviour may be due to gradual increase of confining pressure until failure. The TE stress path test results show significantly lower volume contraction than CTE stress paths. On the other hand, for RTE stress path the volume expansion increases at lower stress level and the rate decreases at higher stress level. Taha et al. (1999) reported similar behaviour in drained triaxial extension test on residual granite soil. Thus, the failure stress and the volume change behaviour for triaxial extension tests are also stress path dependent. RTE stress path test results indicate that the axial strain corresponding to maximum stress increases with confining pressure and the volumetric strain exhibits a dilative behaviour **Figure 8**. This dilative behaviour can be explained, in part, by the volume change of consolidated saturated soil during the application of tensile stress. In most cases, the specimens behave as strain softening failure material. The failure of the test specimens is observed at the mid height due to necking for all the triaxial extension tests (**Figure 9**). The failure envelope (best-fit straight line to the data points) indicates a frictional-cohesive behaviour with strength parameters in terms of effective stresses in which $\phi = 27^\circ$ and $c' = 23$ kPa.

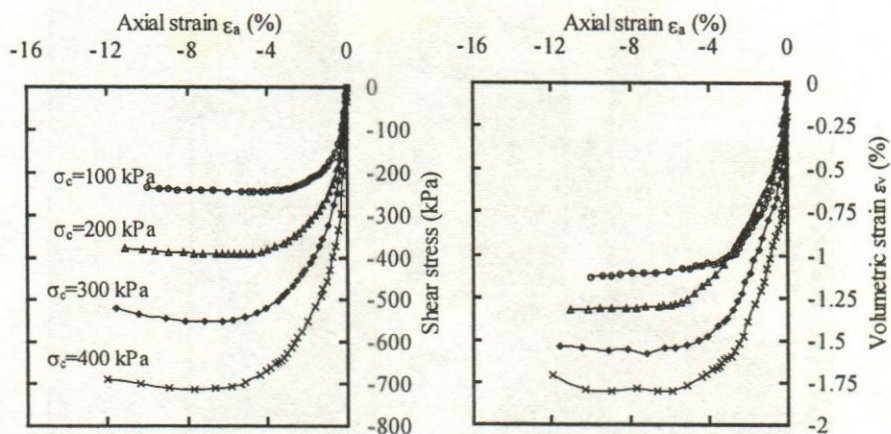


Figure 6. Stress-strain and volume change behavior of barind soil for CTE stress path

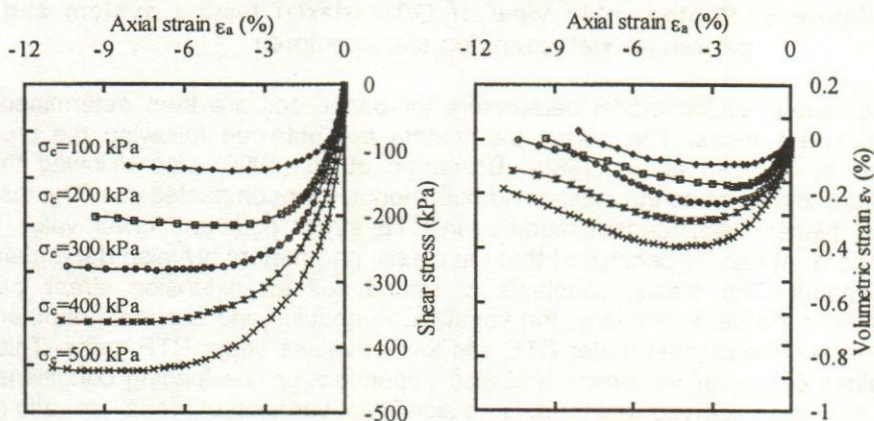


Figure 7. Stress-strain and volume change behavior of barind soil for TE stress path

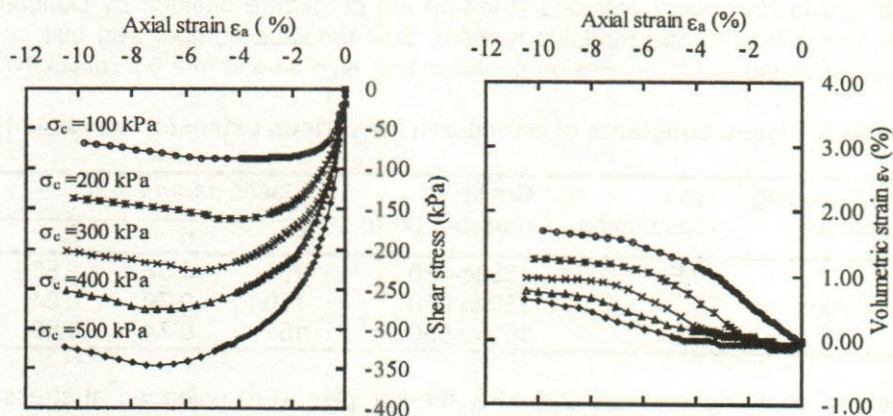


Figure 8. Stress-strain and volume change behavior of barind soil for RTE stress path



Figure 9. Photographic view of GDS triaxial testing system and failure pattern triaxial extension test specimen

The non-linear elastic model parameters for barind soil are then determined for the various stress paths. The elastic parameters are obtained following the procedures outlined by Duncan et al. (1980). Boscardin et al. (1990) also followed the same procedure to determine the elastic and bulk modulus for compacted soil. The test results showed higher initial tangent modulus in CTE stress path and lower value for RTE stress path. It can be concluded that the elastic parameters are also dependent on the stress paths. The elastic constants of barind soil for extension stress paths are presented in **Table 3**. Similarly, the variation of modulus and exponent number is such that it shows the highest under CTE and lowest values under RTE paths. This follows the values of the failure strains and also dependent on the loading conditions (stress path). It is also observed that there is no significant variation of the failure ratio (R_f). The non-linear elastic model parameters for compacted barind soil fill material were then determined from these tests. The effective stress hyperbolic and Mohr-Coulomb strength parameters were obtained following the procedure outlined by Duncan et al. (1980). The unload-reload modulus number, bulk modulus number and bulk modulus exponent of barind soil for extension are $K_{ur} = 198$, $K_b = 93$ and $m = 0.5$ respectively.

Table 3. Elastic constants of barind soil for various extension stress paths

Test loading condition	Type of stress paths	Confining pressure (kPa)	Elastic parameters		
			K	n	R_f
Extension	CTE	150 to 450	250	0.97	0.85
	TE	150 to 550	170	0.79	0.84
	RTE	150 to 550	151	0.74	0.85

For tests at confining pressure 200 kPa, the samples were unloaded at stress levels (ratio of maximum deviator stress to unloading stress) of 0.90 and 0.96 for drained test. The results of multiple unloading and reloading tests for barind soil is shown in **Figure 10**. It is observed that for cycles of unloading-reloading, the barind soil maintains a small amount of hysteresis. Furthermore, the modulus for both cycles of unloading-reloading

are the same, even though they occur at different strains and stress levels. On the basis of these observations, it seems reasonable to believe that the stress-strain behaviour of barind soil on unloading and reloading may be approximated with a high degree of accuracy as being linear and elastic. Because this linear behaviour is independent of the value of stress difference, the representative modulus value is dependent only upon the confining pressure.

The E_{ur} were obtained from the best-fit straight line at the stress-strain plot (**Figure 10**). The values of K_{ur} were then calculated using Equation (8). Analysis was made to verify the model parameters by comparing numerical predictions with the experimental triaxial extension test results. The measured and predicted stress-strain curve for drained triaxial extension tests is shown in **Figure 10**. In addition, the stress-strain prediction for test without unloading cycle is shown in **Figure 11**. In order to check the sensitivity of the model parameters, the modulus number and modulus exponent were varied up to $\pm 5\%$. Within this range, the results exhibit that there is no significance difference in the predicted response. On the other hand, if this tolerance is more than $\pm 5\%$, then the predicted behavior deviated from the measured values. Thus, it is important that these parameters be obtained as accurate as possible since deviation of 5% or more can lead to deviation in the predicted behavior. Increasing the stress ratio, R_f , (maximum of 1.0) also provided a better estimate of the triaxial stress-strain relationships.

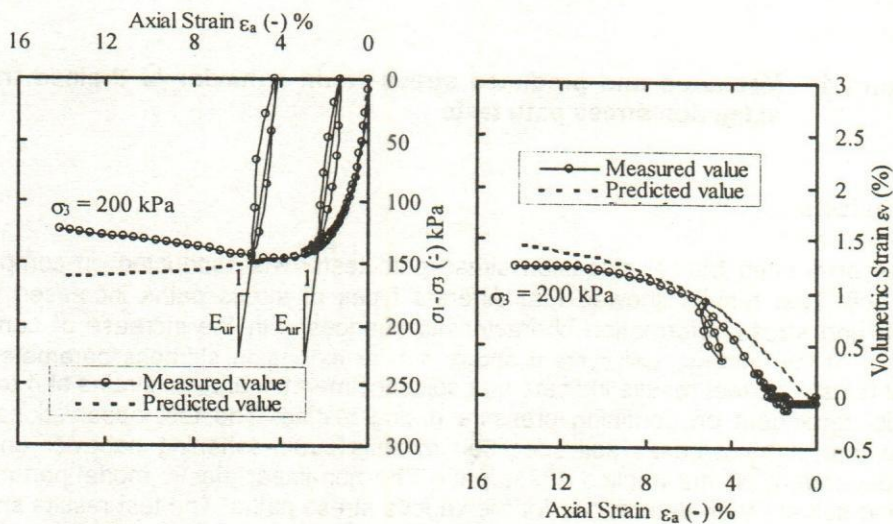


Figure 10. Stress-strain and volume change behavior of unload-reload drained triaxial extension test

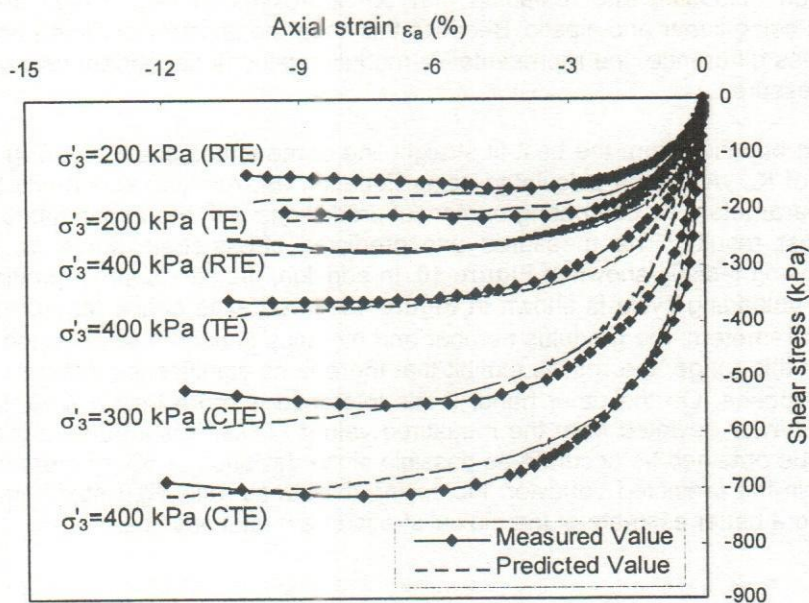


Figure 11. Measured and predicted stress-strain behavior of drained triaxial extension stress path tests

Conclusions

A series of drained triaxial extension stress path tests was conducted on compacted barind soil. Test results showed that different types of stress paths increased shear strength and stress-deformation characteristic changes with the increase of confining pressure. At low strains, soil system shows similar extension stiffness parameters for drained tests. The test results indicate that soil specimen fail at axial strains at 4 to 8 %, which is dependent on confining pressure during testing. The test observations also indicate that in most cases soil specimen exhibits strain-softening behavior and are highly dependent on the applied stress path. The non-linear elastic model parameters for barind soil are then determined for the various stress paths. The test results showed higher initial tangent modulus in CTE stress path and lower value for RTE stress path. This is due to fact that the lower value of failure strain was found for CTE path in comparison to the RTE path. It can be concluded that the elastic parameters are also dependent on the stress paths. During testing the specimens exhibit dilatants behavior but the degree of dilation being dependent on the confining cell pressure. The unload-reload elastic parameters such as modulus number, bulk modulus number and bulk modulus exponent of barind soil are determined. Theoretical analysis using the hyperbolic model indicates good agreement with the experimental results.

Acknowledgements

This investigation was carried out in the Geotechnical Engineering Laboratory of Rajshahi University of Engineering & Technology, Rajshahi, Bangladesh. The author thanks the Ministry of Science & Technology, Government of People's Republic of Bangladesh for providing the necessary financial support.

References

- Ajaz, A., and Parry, R.H.G. (1975): Stress-strain behavior of two compacted clays in tension and compression, *Geotechnique*, vol. 25(3), pp. 495-512
- Al-Hussaini, M.M. (1981): Tensile Properties of Compacted Soils in Laboratory Shear Strength of Soils, ASTM STP 740, R.N. YONG and F.C.TOWNSEND(Editors), pp. 207-225.
- Berdie, E.K. (1991): Triaxial Tension Tests on Compacted Kaolin, *Journal of Geotechnical Engineering*, vol. 22, pp. 121-141.
- Bishop, A.W. and Garga, V. K. (1969): Drained Tension Tests on London Clay, *Geotechnique*, vol.19, pp. 309-313.
- Bishop, A.W. and Wesley, L.D. (1975): A Hydraulic Triaxial Apparatus for Controlled Stress Path Testing, *Geotechnique*, vol. 25(4), pp. 657-670.
- Boscardin, M.D., Selig, E.T., Lin, R.S. & Yang, G.R. (1990): Hyperbolic parameters for compacted soils. *Journal of Geotechnical Engineering*, ASCE, vol. 116(1), pp. 89-103.
- Conlon, R.J. (1966): Landslide on the Toulmoustou River, Quebec, *Canadian Geotechnical Journal*, vol. 3(3), pp. 113-144.
- Cui, Y.J. and Delage, P. (1996): Yielding and plastic behavior of an unsaturated compacted silt, *Geotechnique*, vol.46(2), pp. 291-311.
- Duncan, J.M., and Chang, C.Y. (1970): Non-linear analysis of stress and strain in soils, *Journal of Geotechnical Engineering*, ASCE, vol. 96(5), pp. 1629-1653.
- Duncan, J.M., Byrne, P., Wong, K.S., and Mabry, P. (1980): Strength, stress-strain and bulk modulus parameters for finite element analysis of stresses and movements in soil, *Geotechnical Engineering Research Report: UCB/GT/80-01*, Department of Civil Engineering, University of California, Berkeley.
- Janbu, N. (1963): Soil compressibility as determined by oedometer and triaxial tests, *Proceedings European Conference on soil Mechanics and Foundation Engineering*, Wssbaden, Germany, vol. 1, pp. 19-25.
- Mofiz, S.A. (2000): Behaviour of unreinforced and reinforced residual granite soil, PhD Thesis, Universiti Kebangsaan Malaysia, pp.315.
- Parry, R.H.G. and Nadarajah, V. (1974): Anisotropy in a natural soft clayey silt, *Engineering Geology*, vol. 8, pp. 287-309.
- Taha, M.R, Mofiz, S.A., Hossain, M.K. & Asmirza, M.S. (1999): Model simulation of residual soil in triaxial extension tests. *Proceedings of the Fifth Geotechnical Engineering Conference, Geotropika-99*, pp.105-114.

Effectiveness of Revetment using Physical Modeling: A Case Study of Arial Khan Roadway Bridge

**Md. Abdus Samad¹, A K M Ashrafuzzaman², Md. Rafiqul Alam³,
Swapan Kumar Das³ and Md. Azizul Haque Poddar²**

Abstract

An undistorted physical model study has been carried out to determine the effectiveness and design parameters of the optimized revetment at the upstream of West Guide Bund (WGB) of a roadway bridge over the Arial Khan river. The study includes observing flow patterns and flow concentration around the structure. The revetment has been placed to combat river bank erosion, which is subjected to different angle of flow attack. The study reveals that 1.01km revetment having side slope 1:2 and launching apron with length 20m & average thickness 1.6m appears to work satisfactory for bank protection. The maximum value of the design parameters in terms of scour & velocity at the end of the launching apron of revetment is found to be 6.16m and 3.23m/s respectively.

Introduction

The Arial Khan is one of the main distributaries of the river Padma. It is a very dynamic and morphologically active river. A roadway bridge is presently under construction on the river Arial Khan. Due to the morphological changes of the river upstream of the bridge, it is apprehended that the bridge itself might be in danger due to erosion at the upstream of the WGB. Under these circumstances, River Research Institute (RRI) was commissioned to conduct a physical model study to identify the extent of bank erosion at the upstream of WGB and to find out the probable measure to address the problem. Accordingly a distorted overall physical model study has been conducted by which the extent of bank erosion was identified as well as the optimized length of revetment was determined. The effectiveness and design parameters such as velocity, scour etc of the optimized revetment have been checked by carrying out an undistorted physical model for the finalization of the design of revetment.

Model Design

An undistorted physical model is constructed considering horizontal and vertical scale of 1:80. The model is designed fulfilling the Froude's model law in such a way that sufficient sediment transport is ensured. The vertical scale should be selected in such a way that sufficient water depth can be ensured in the model for velocity measurement and the length scale should allow the model to be accommodated into the open-air model bed of RRI. Reynolds number should be high enough to ensure rough turbulent flow in the model.

The scour velocity is selected in such a way that the model is expected to reach the dynamic equilibrium condition by running the model for about 15-18 hours.

The annual maximum water level and discharge data at Chawdhury Char (Water level & discharge station) on Arial Khan river have been analyzed using Gumbel distribution

¹Director (Hydraulic Research), ² Senior Scientific Officer,³ Principal Scientific Officer, River Research Institute, Faridpur

and the estimated hundred-year return period discharge and water level are 6605m³/s and 8.65mPWD respectively. However the Client (JOCL-BCL) considers the design discharge for the bridge is 6900m³/s and the design water level at the bridge site is 7.9mPWD that are selected for model investigation.

The basic design parameters and the corresponding scales have been derived as shown in **Table 1**.

Table 1 Hydraulic and morphological parameters required for model study

Description	Unit	Prototype	Model	Scale
Length (L)	m	4200	53	80
Width (W)	m	500	6.25	80
Average water depth (h)	m	8.0	0.100	80
Slope (i)	-	0.00005	0.00005	1.0
Average velocity (u)	m/s	1.38	0.15429	8.94
Average cross sectional area (A)	m ²	5000	0.781	6400
Critical velocity (u _{cr})	-	0.395	0.246	1.61
Shields parameter (θ)	-	2.020	0.019	106.67
Discharge (Q)	m ³ /s	6900	0.121	57243
Discharge for scour simulation (Q _s)	-	-	0.197	-
Median particle diameter (D ₅₀)	m	0.00012	0.00016	0.75
Dimensionless particle diameter (D _*)	-	2.688	3.58	0.75
Critical Shields parameter (θ _{cr})	-	0.089	0.067	1.33
Chezy roughness co-efficient (C)	m ^{1/2} /s	70	30	2.33
Froude's number (F _r)	-	0.156	0.156	1.0
Shear velocity (u _*)	m/s	0.063	0.007	8.9
Critical shear velocity (u _{*cr})	m/s	0.0132	0.0132	1.0
Particle Reynolds number (R _{e*})	-	6.264	0.934	6.71
Reynolds number (R _e)	-	9200000	12857.39	715.54

An open-air model bed having size 80mx20 m has been used for setting up the model. The area reproduced in the model is about 4.2km of the river reach from 3.6km upstream and 0.6km downstream of the Arial Khan Roadway Bridge. The model set-up is shown in **Figure 1**. The boundary of this model is taken from the distorted overall model.

Model Test Scenarios

During model study one calibration test and three application test runs with revetment along the upstream of the WGB have been conducted. Test T0 contributed to the calibration of the model. The application tests T1 to T3 are carried out with a view to observe the performance of the revetment as a bank protection structure to prevent riverbank erosion at the upstream of the WGB of the Arial Khan roadway bridge. The test scenarios that were considered during model study are described in **Table 2**.

Table 2 Test scenarios of the model

Test	Objective	Test Scenarios
T0	Calibration of the model	April 2004 bathymetry with existing structures i.e. bridge components
T1	To observe the effectiveness of the proposed revetment and to determine the design parameters	Same as T0 plus 1.01km revetment upstream of WGB
T2	To observe the performance of the proposed revetment placed upstream of the WGB through guiding the flow by Right Guide Wall (RGW) & Left Guide Wall (LGW)	Same as T0 plus 1.01km revetment upstream of WGB. The approach flow has an angle of 30 degree with the revetment
T3	To observe the performance of the proposed revetment placed upstream of the WGB through guiding the flow by Right Guide Wall (RGW)	Same as T0 plus 1.01km revetment upstream of WGB plus 100m cut Ferry Ghat brick road. In this test the approach flow has an angle of 45 degree with the revetment

Model Calibration

Calibration is done for matching the model with the prototype condition. The velocity distribution at the upstream section is simulated at the upstream boundary of the model. The velocity distribution at the calibration section (CS-29) is measured in the model and compared with the prototype value as shown in **Figure 2**. From this figure it is evident that the measured values found in the model are very close to the prototype values.

Analysis and Interpretation of the Test Results

Calibration Test

Calibration test i.e. test T0 is done to simulate the model with the prototype i.e. existing condition. The bathymetry of April 2004 with existing structures is reproduced in the model.

In the calibration test, bank erosion is observed in three reaches: at the left bank starting from CS25 towards upstream; at the right bank from CS20 to CS16 upstream of WGB and at the left bank from CS11 to CS8 downstream of East Guide Bund (EGB). The qualitative bank erosion is shown in **Figure 3**. The bank erosion at upstream of WGB is found to be very severe and a threat for the bridge. The near bank velocities upstream of WGB are in the range of 1.45 to 2.32m/s within the reach between CS20 & CS16 indicating the magnitude of near bank velocities was higher than the erodable velocity.

The flow lines recorded by float tracking are shown in **Figure 4**. The flow lines are concentrated near the eroded bank upstream of EGB. The measured near bank velocities and flow lines indicate that river training structure is essential between CS20 & CS16 to combat bank erosion upstream of WGB for the safety of the Arial Khan bridge.

The velocities in the model from right bank up to 160m for CS20 to CS16 are also measured and are shown in **Table 3**.

Table 3 Flow velocity (m/s) in test T0

CS no.	Velocity (m/s)				
	Distance from right bank (m)				
	0.00	40.00	80.00	120.00	160.00
20	1.45	2.04	1.88	1.82	1.70
19	2.01	2.13	1.76	1.58	1.82
18	2.00	2.38	1.88	1.82	1.70
17	2.21	2.20	1.83	1.89	1.59
16	2.32	2.14	2.02	2.14	1.77

Application Tests

The application tests *i.e.* test T1, T2 & T3 are carried out with 1.01km-optimized revetment along the right bank line upstream of WGB under different angle of flow attack.

In revetment, various sizes of CC blocks are used in the bank slope and launching apron. Block of size 50cm×50cm×50cm (1-layer) is used in the sloping portion; block of sizes 50cm×50cm×50cm, 40cm×40cm×30cm & 30cm×30cm×30cm (3, 4 & 5-layers) is used with different proportions in the launching apron portion. The percentage of different sizes of CC block used in the bank slope and launching apron of revetment can be seen in **Table 4**.

Table 4 Proportion of various sizes of CC blocks in the slope and launching apron

Bank slope		Launching apron	
Block size	Percentage	Block size	Percentage
50cm×50cm×50cm	100%	50cm×50cm×50cm	55%
-	-	40cm×40cm×30cm	30%
-	-	30cm×30cm×30cm	15%

It is noted that the conceptual design of revetment is done by RRI and that can be finalized after considering the design parameters. The plan & section of revetment can be seen in **Figure 5**. The test results of the application tests are given below.

Test T1

In this test, 1.01km revetment upstream of WGB is reproduced in the model. From the flow lines as shown in **Figure 6**, it is observed that under this condition the flow lines are parallel to the revetment indicating less scour along the revetment. Also the flow lines are concentrated downstream of EGB.

The velocities in the model from right bank up to 160m for CS20 to CS16 are also measured and are shown in **Table 5**.

Table 5 Flow velocity (m/s) in test T1

CS no.	Velocity (m/s)				
	Distance from right bank (m)				
	0.00	40.00	80.00	120.00	160.00
20	0.00	2.02	2.08	2.08	2.08
19	0.00	2.44	2.44	2.13	2.31
18	0.00	2.74	2.56	2.31	2.07
17	0.00	3.05	2.44	2.25	1.82
16	0.00	1.04	1.79	2.62	2.13

The velocities and equilibrium scour depths are measured at some 23 points along the end of the launching apron of revetment. The maximum velocity and maximum scour are found to be 3.05m/s and 4.48m respectively.

Test T2

In this test 1.01km revetment upstream of the WGB is reproduced in the model with an approach flow of angle 30 degree with the revetment. The flow is guided by RGW & LGW upstream of the constructed revetment to make approach flow angle 30 degree with the revetment in order to attack the revetment under such condition.

From the flow lines as shown in Figure 7, it is observed that under this condition the flow lines are parallel to the revetment indicating less scour along the revetment. Also the flow lines are concentrated downstream of EGB.

The velocities in the model from right bank up to 160m for CS20 to CS16 are also measured and are shown in Table 6.

Table 6 Flow velocity (m/s) in test T2

CS no.	Velocity (m/s)				
	Distance from right bank (m)				
	0.00	40.00	80.00	120.00	160.00
20	0.00	1.58	1.51	2.13	1.94
19	0.00	1.99	2.31	2.38	1.70
18	0.00	2.74	2.44	2.19	2.19
17	0.00	3.17	2.62	1.94	1.70
16	0.00	2.44	3.05	2.38	1.88

The velocities and equilibrium scour depths are measured at the same 23 points along the end of the launching apron of revetment as shown in **Figure 8**. The maximum velocity and maximum scour is found 3.23m/s and 6.16m respectively.

The development of scour with time around revetment can be seen in **Figure 9**. From this figure it is evident that after a certain time interval scour has reached a certain value and scour is no longer occurring with time. In other words, equilibrium condition has been reached in the model.

Test T3

In test T3, 1.01km revetment upstream of the WGB along with cutting of 100m Ferry Ghat brick road has been reproduced in the model. The flow is guided by RGW upstream of revetment to make the approach flow angle 45 degree with revetment in order to attack the revetment under severe condition. From the flow lines as shown in **Figure 10**, it is observed that under this condition the flow lines are parallel to the revetment indicating less scour along the revetment. Also the flow lines are concentrated downstream of EGB.

The velocities in the model from right bank up to 160m for CS20 to CS16 are also measured and are shown in **Table 7**.

Table 7 Flow velocity (m/s) in test T3

CS no.	Velocity (m/s)				
	Distance from right bank (m)				
	0.00	40.00	80.00	120.00	160.00
20	0.00	1.51	1.76	1.70	1.94
19	0.00	2.07	1.94	1.82	1.79
18	0.00	2.44	2.07	1.91	1.94
17	0.00	2.99	2.59	2.13	1.82
16	0.00	2.25	2.38	2.31	2.13

The velocities and equilibrium scour depths are measured at the same 23 points along the end of the launching apron of revetment. The maximum velocity and maximum scour is found 2.86m/s and 3.68m respectively.

Conclusions

- It is observed from the flow lines and near bank velocities that river training structure is necessary between CS20 & CS16 to combat river bank erosion upstream of WGB.
- The tested revetment is found to work effectively.
- The maximum velocity along the end of the launching apron of revetment is found 3.23m/s.
- The maximum scour along the end of the launching apron of revetment is found 6.16m.

Recommendations

- Total 1010m revetment is recommended to construct in the field to combat right bank erosion at upstream of WGB.
- Some CC blocks have been displaced near CS-17 from the launching apron of revetment as observed in the model test. In that case, CC blocks should be kept ready for emergency dumping if necessary.
- The model is tested with the conceptual design made by RRI as shown in **Figure 5**. The final design is to be made by the client considering the design parameters obtained from the model study.

Acknowledgement

The authors are grateful to the Roads and Highways Department (RHD), Japan Overseas Consultant Co Ltd (JOCL) and Bangladesh Consultants Ltd (BCL) for their valuable suggestion during model study at RRI.

References

- Globe Survey Company (2004):** Report on Bathymetric and Topographic Survey and Hydraulic Data Collection of Arial Khan River for Physical Model Study.
- River Survey Project (1996):** FAP24, Final Report, Main Vol, No.1.
- River Survey Project (1996):** FAP24, Special Report No.3, Bathymetric Surveys.
- River Survey Project (1996):** FAP24, Special Report No.7, Geomorphology and Channel Dimensions.
- RRI (2004):** Physical Model Study of Arial Khan Roadway Bridge, Draft Final Report, September.
- RRI (2004):** Physical Model Study of Arial Khan Roadway Bridge, Final Report, November.
- Satellite Imageries** of Arial Khan River, CEGIS, Dhaka.
- SWMC (2001):** Hydraulic Mathematical Modeling Study of Arial Khan Roadway Bridge, Volume I, Main Report, February.
- SWMC (2001):** Hydraulic Mathematical Modelling Study of Arial Khan Roadway Bridge, Volume II, Appendices, February.
- Van Rijn C. (1984):** Bed Forms and Alluvial Roughness, Sediment Transport, Part-III, ASCE Journal of Hydraulic Engineering, Vol. 110, No. 12.

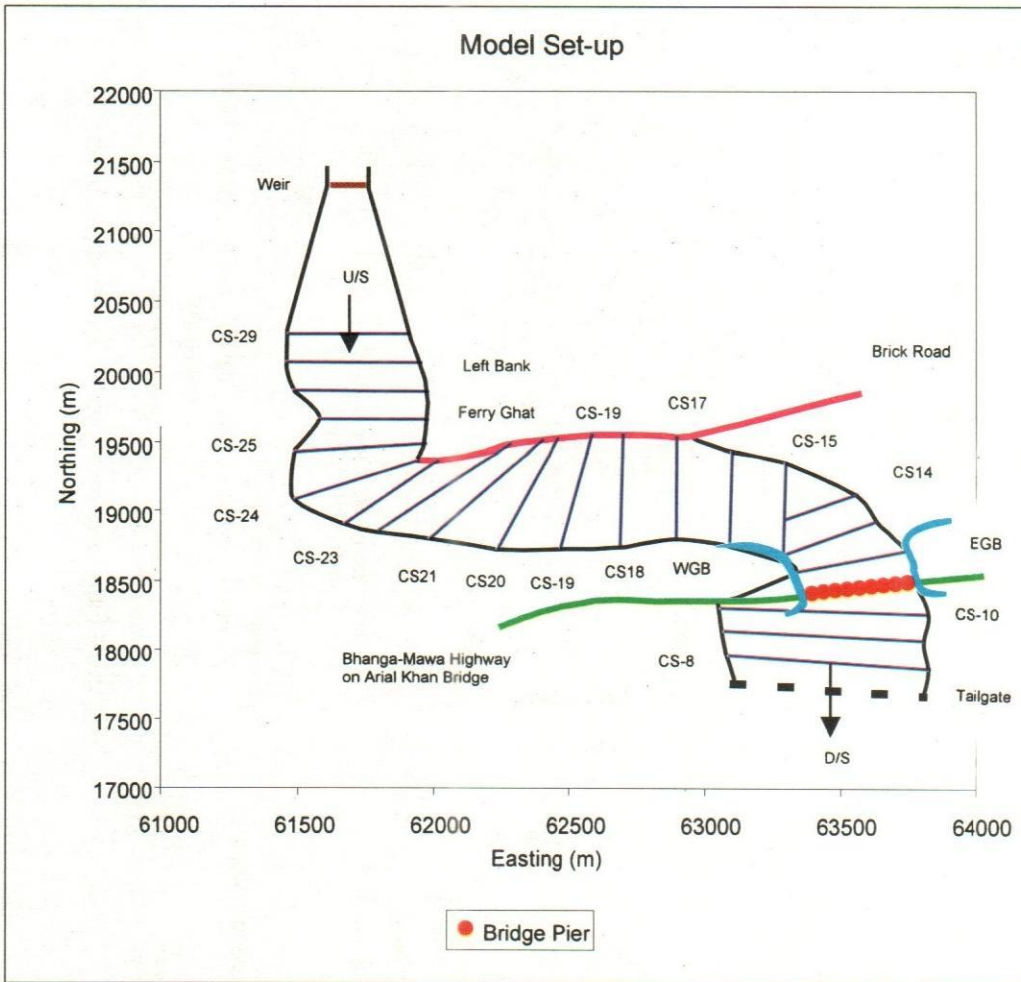


Figure 1 Model set-up

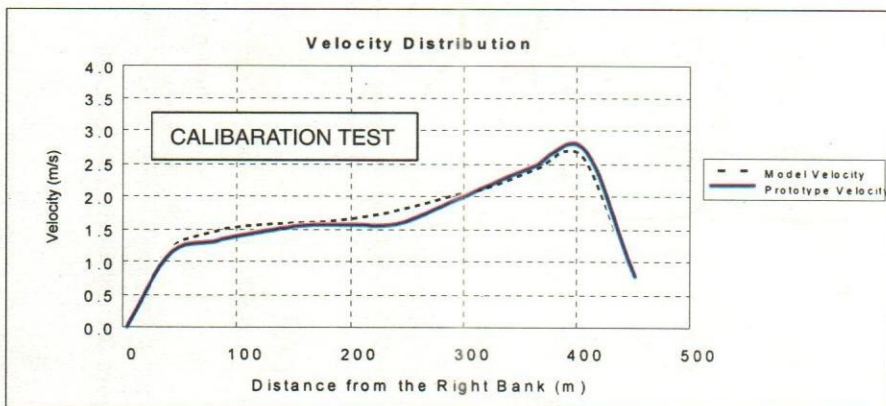


Figure 2 Comparison between prototype and model velocity at CS-29

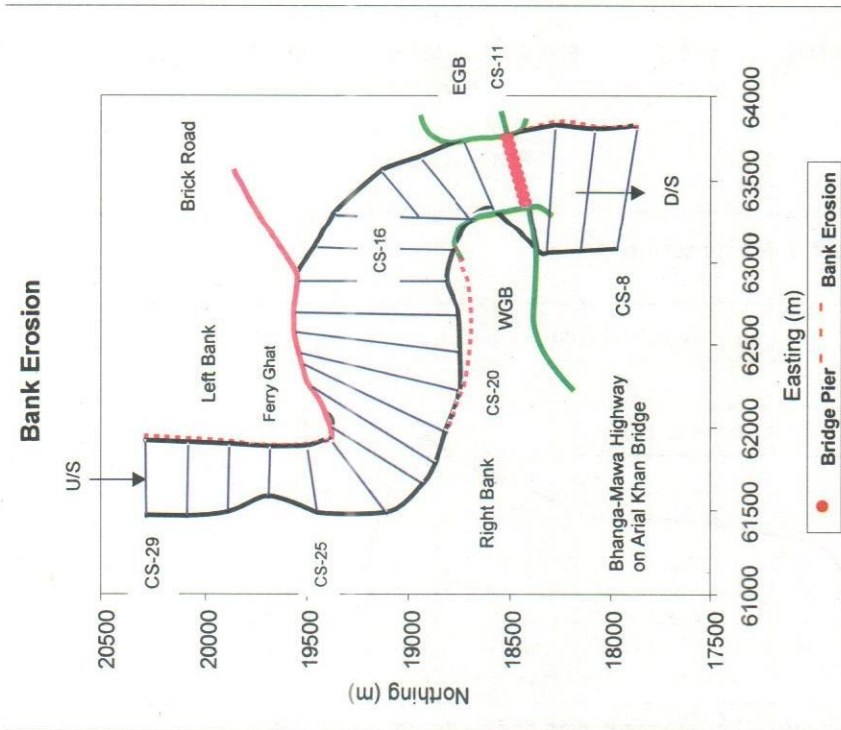


Figure 3 Qualitative bank erosion

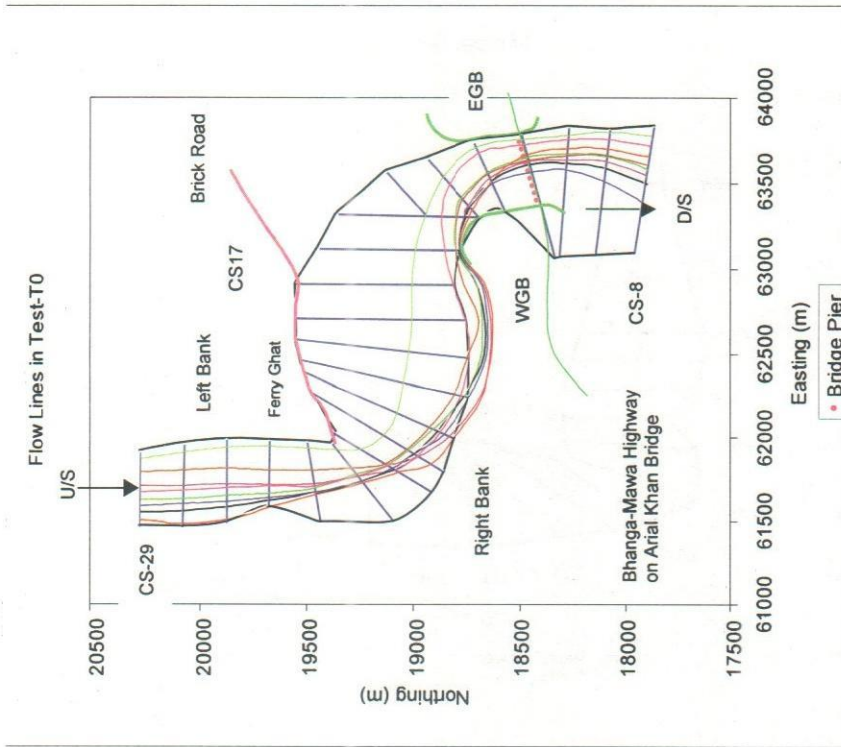


Figure 4 Flow lines recorded by float tracking in test T0

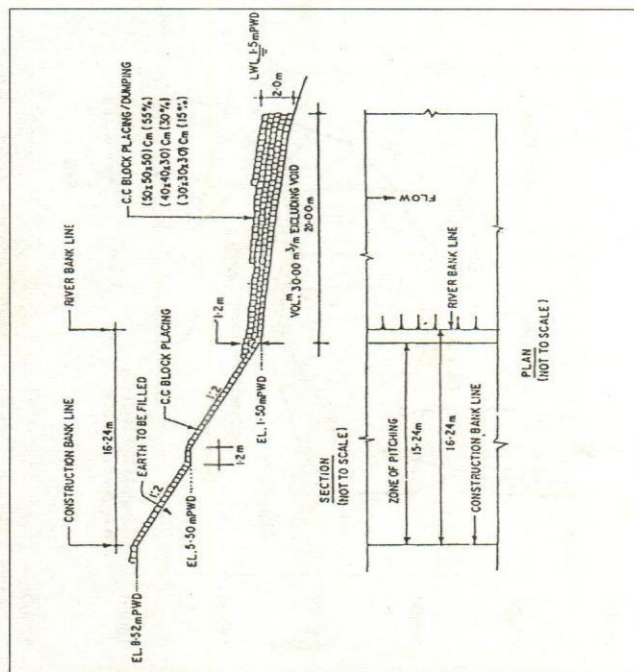


Figure 5 Plan & section of revetment

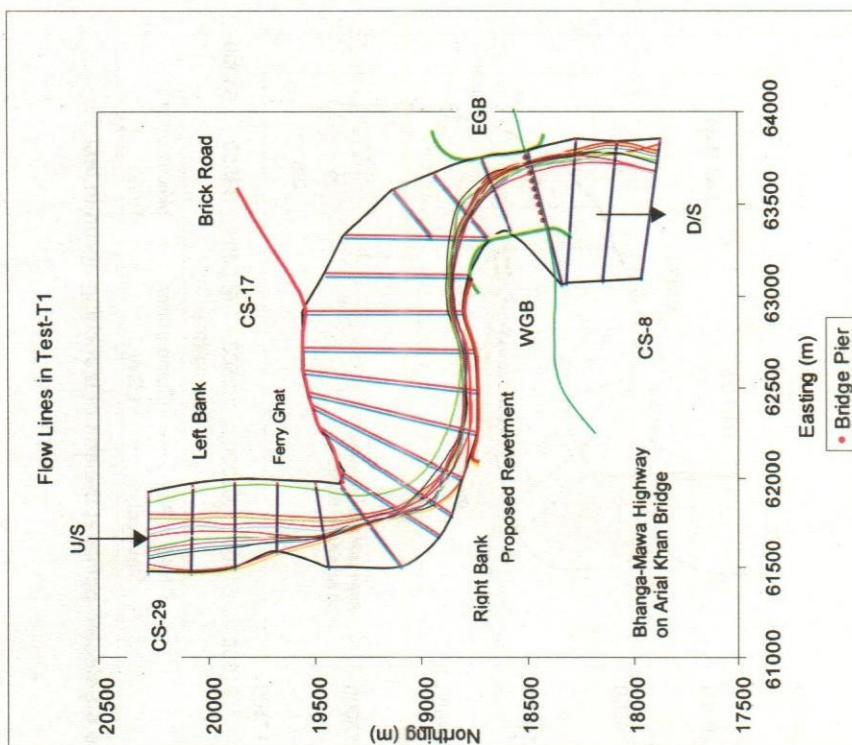


Figure 6 Flow lines recorded by float tracking in test T1

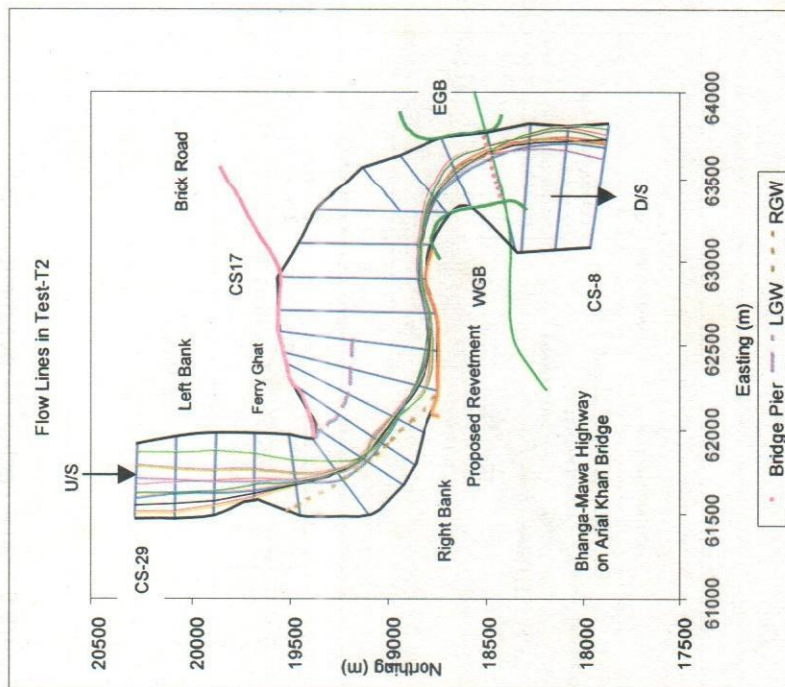


Figure 7 Flow lines recorded by float tracking in test T2

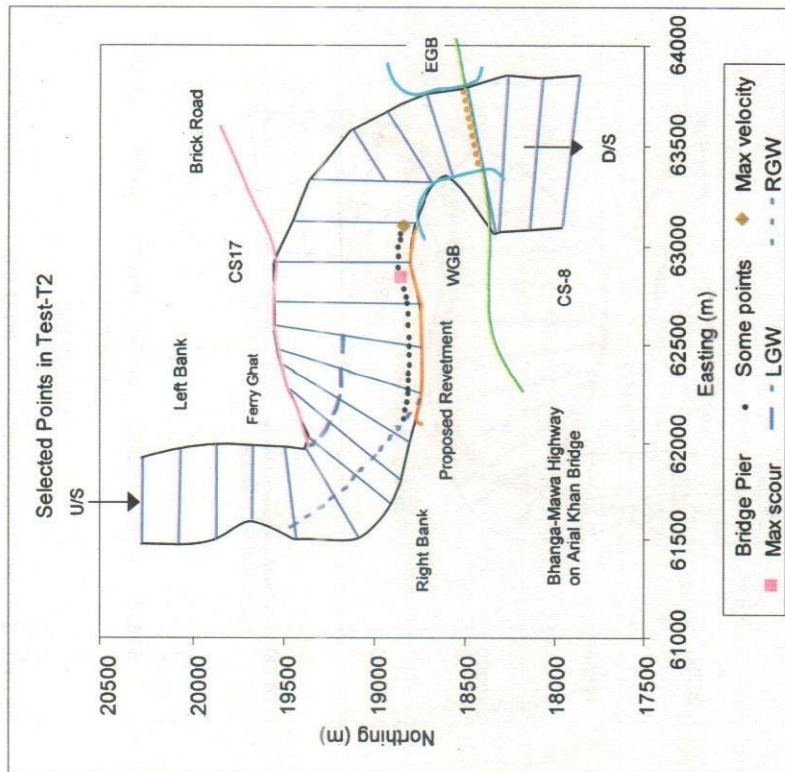


Figure 8 Selected points at the end of launching apron in test T2

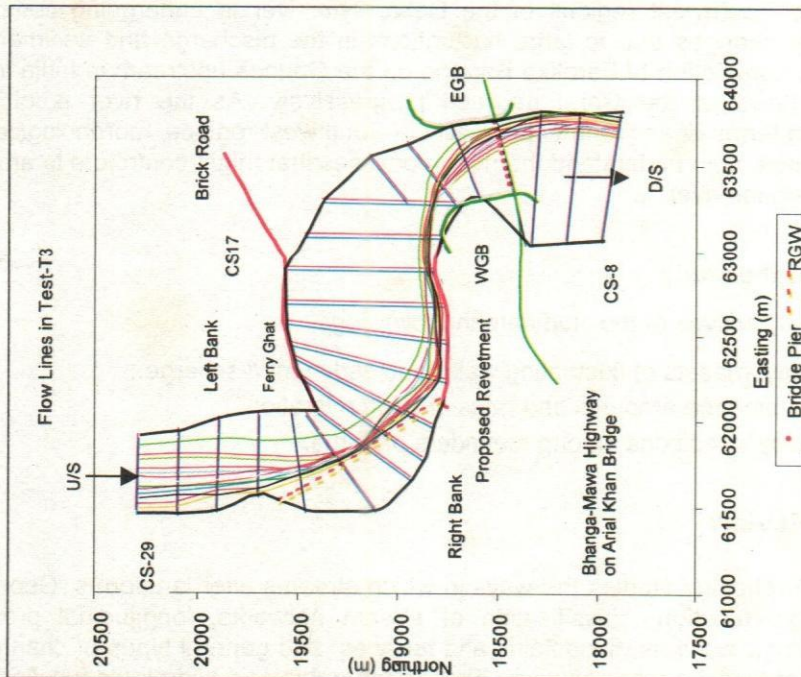


Figure 9 Flow lines recorded by float tracking in test T3

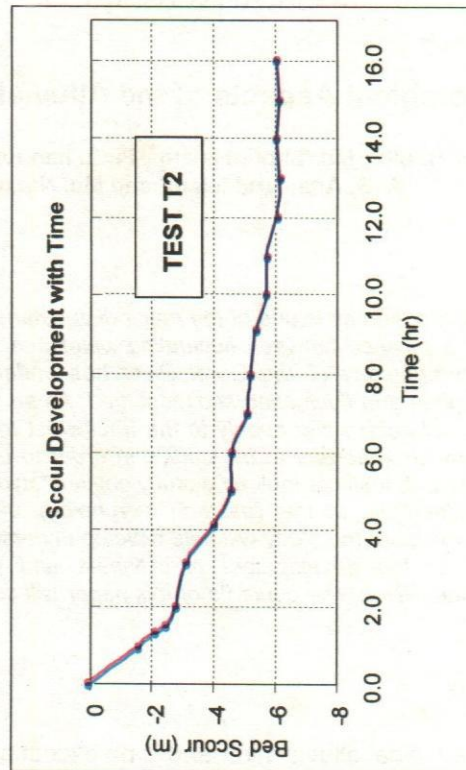


Figure 10 Development of scour with time around the revetment in test T2

Morphological Aspects of the Alluvial River Gorai-Madhumati

Md. Kayser Habib¹, Md. Shofiul Islam¹, Pintu kannungoe², Syed Md. Anwaruzzaman³
A. S. Anawarul Islam² and Md. Nazrul Islam Siddique⁴

Abstract

The river Gorai-Madhumati is one of the major distributaries of the river Ganges. The morphology of this river is a balance between fluctuating water and sediment discharge. Over the last few decades the morphology of the Gorai River has undergone changes due to change in the hydrological regime and fluctuating sediment load. As an important distributor of the Ganges and only the source of fresh water supply to the Southwest region, the morphological aspects of this river are very much important to be studied in order to understand the river behavior. With this view River Research Institute took up a study entitled "Hydraulic and Morphological aspects of the river Gorai-Madhumati". In this research morphology of the river Gorai-Madhumati has been studied. The findings of the study will help develop understanding of the river conditions and draw the attentions of the development practitioners and policy planners to this issue of the Gorai_Madhumati River. The contents of this paper will also be helpful for future research in this field.

Introduction

The Gorai is a typical alluvial river and is no exception of other rivers of Bangladesh. It is one of the largest distributaries of the Ganges and is a major source of fresh water supply to the Southwest regions of the Delta. The river is undergoing complicated morphological changes due to large fluctuations in the discharge and sediment load. Following the completion of Farakka Barrage on the Ganges upstream in India in 1975, dry season flows of the Gorai declined progressively. As the river is of utmost significance in terms of environmental quality of Southwest regions, morphological study of the river would help understand the river processes that might contribute to any future action restoring the river.

Objectives of the study

The principal objectives of the study are the following:

- To identify impacts of fluctuating water and sediment discharge.
- To determine the amounts and rates of bend migration.
- To develop conditions among meanders patterns.

Literature Review

Fluvial geomorphology studies the ways in which streams alter landforms. Geomorphic and hydrologic function, classification of stream networks, longitudinal profiles of streams, geologic controls, floodplains and terraces, and general types of channels are components of fluvial geomorphology. First, geomorphic and hydrologic functions need to be understood. The processes of erosion, transportation, and deposition of sediments

¹ Scientific Officer, ² Principal Scientific Officer (Addl. Charge), ³ Senior Scientific Officer, & ⁴ Chief Scientific Officer (Current Charge), River Research Institute, Faridpur

are most relevant in fluvial geomorphology. Stream systems generally erode material in the steeper upper reaches. This material is transported via stream channels and eventually deposited in the lower reaches of a stream system, and ultimately into oceans. Whether given streams reach is erosional, transportational, or depositional depends on several hydraulic characteristics. Classification of stream networks is based on stream orders and on hierarchical classification. Stream order is a measure of the number of tributaries feeding any given fluvial system. Hierarchical classification considers stream network patterns, stream reach, and stream channel units. A single, small channel with no tributaries is classified as a first order stream (Strahler, 1946). A second order stream is formed by the juncture of two first order streams. Two-second order streams combine to form a third order stream, and so on. Hierarchical classification includes the stream networks overall patterns and the characteristics of the stream reach. Contiguous sections of channel with similar overall characteristics are defined as stream reaches. Upper stream reaches are generally steeper with higher gravitational potential than lower stream reaches. An important concept in stream hydrology is that of a constrained versus an unconstrained stream. Where bedrock, colluviums, alluvium, or other deposited weathered bedrock prevents the lateral migration of a stream, that stream is said to be constrained.

Methodology

Bend migration amounts and rates:

Down valley migration rates

Down valley migrations of river bends are found to be a dominant process of the river Gorai-Madhumati in the tidal lower course. The river bend can simultaneously migrate both laterally and down valley. Sometimes down valley migrations are associated with inner bank erosion and outer bank build up. During this study the amounts and rates of such down valley migrations have been determined from the available information and for the time span considered. **Table 1** presents the rates of down valley migrations over three different time periods with respect to year 1985. It can be seen from the table that during first three years the average annual migration rate is 145.8. However, when considered over a period of seven years the average annual rate is seen to have decreased (113.8). It means down valley migration slowed down during last four years of the considered time period.

Table 1: Down valley migration rates over different time periods

Time span	Range of variation of annual migration rates (m/y)	Average annual rate (m/y)	Standard deviation	Co-efficient of variation
1985-88	0 to 292	145.8	66.7	59.5
1985-92	0 to 196.5	113.8	40.8	35.8
1985-95	0 to 195	139.7	37.4	26.8

above mentioned reality. The peak discharges and high flows in the river Gorai generally occur in the month of August-September. The discharge data supplied by WARPO provides following information as to peak discharges in the years from 1985 to 1995 (Table 2).

Table 2: Peak discharges in the years from 1985 to 1995

Year	Peak discharge (m ³ /s)
1985	6290
1986	5230
1987	7500
1988	8400
1989	4460
1990	5380
1991	7020
1992	4160
1993	8880
1994	7560
1995	4260

The magnitude of peak discharges shown in the above table helps explain why down valley migration rates were higher in the time period 1985-88 and 1992-95 than in the time period 1988-92.

Inner bank erosion

In the tidal lower course of the river it is found that erosion at the inner bend and build up at the outer bend can take place in any river bend over a certain time period. It is revealed from the examination of the data as flow increases, the flow tends to cut across the convex bar to be concentrated against the concave bank below the apex of the bend. Because of this process, meanders tend to move in the down valley direction, and the zone of maximum erosion is usually in the downstream portion of the bend due to the flow impingement at the higher flows. The material eroded from the outer bank is transported downstream and is generally deposited in the next crossing or point bar. This process also results in the deposition of sediment along the upper portion of the concave bank. From this study the following observations have been made as to inner bank erosion (Table 3).

Table 3: Observed maximum and minimum inner bank erosion over different time period

Time period	Maximum inner bank erosion (m)	Minimum inner bank erosion (m)
1985-88	500	350
1988-92	130	0
1992-95	600	400

The information presented in the above table bears testimony of the fact stated in the previous section i.e. the higher the magnitude of peak discharge the higher the amounts of inner bank erosion.

Outer bank migration rates

Over the period from 1985 to 1995 the river bends of the lower course of the Gorai are found to be very much active in terms of lateral migration (outer bank erosion). In order to analyze the lateral migration rates three time periods of 3, 7 and 10 years have been considered beginning from 1985. The information as to range of variation of the yearly erosion rates, average annual erosion rates, standard deviation and co-efficient of variation for three time periods appears in the **Table 4**. It is noticeable from the information presented in the table that average annual erosion rate is 91 m for the first three years and 67.2 m when considered for seven years from the beginning. It means annual average erosion rates are lower in the period 1988-92 than in the period 1985-88. In fact it is seen that during the period 1988-92 the annual average erosion rate is 60.8 m.

Table 4: Outer bank migration rates over different time periods

Time span	Range of variation of annual migration rates (m/y)	Average annual rate (m/y)	Standard deviation	Co-efficient of variation
1985-88	0 to 167	91	61	67
1985-92	0 to 133	67.2	44.3	66
1985-95	0 to 135	66.2	37	56

When considered for the time period 1985-88 it can be seen that average annual erosion rate is 66.2 m. It indicates erosion rate is higher in the period 1992-95 than in the period 1988-92. The similar trend is observed in case of down valley migration rates. It can, therefore, be concluded that both down valley and lateral migration rates are dependent on the magnitude of discharge.

The rates of outer bank migration depend on bank resistance, flow characteristics and sediment transport. According to Nanson and Hickin the yearly bank erosion rate M (m) can be expressed as:

$$M = f(C, Y_b, W, r_m / W)$$

Where, M = yearly erosion rate (m), C = Chezy co-efficient ($m^{0.5}/s$), W = channel width (m), Y_b = the opposing force per unit boundary area resisting migration and r_m = bend radius (m). If it is assumed that the parameters C and Y_b do not vary along the river the equation reduces to:

$$M = f(W, r_m / W)$$

The measurements of channel width, radius of bend curvature and the rate of bank erosion are used to verify the above relationship for the river Gorai. The measured parameters have been divided into classes and numbers of observations for each class have been determined. The observed erosion rates versus the number of observations appear in **Figure 1**. In **Figure 2** observed relative radius of curvature versus the number of observations has been shown.

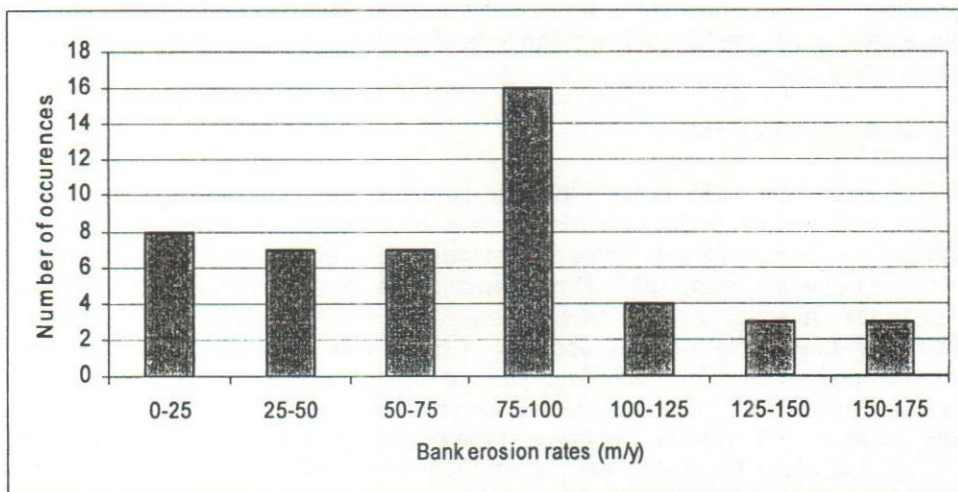


Figure 1: Observed bank erosion rates versus number of occurrences

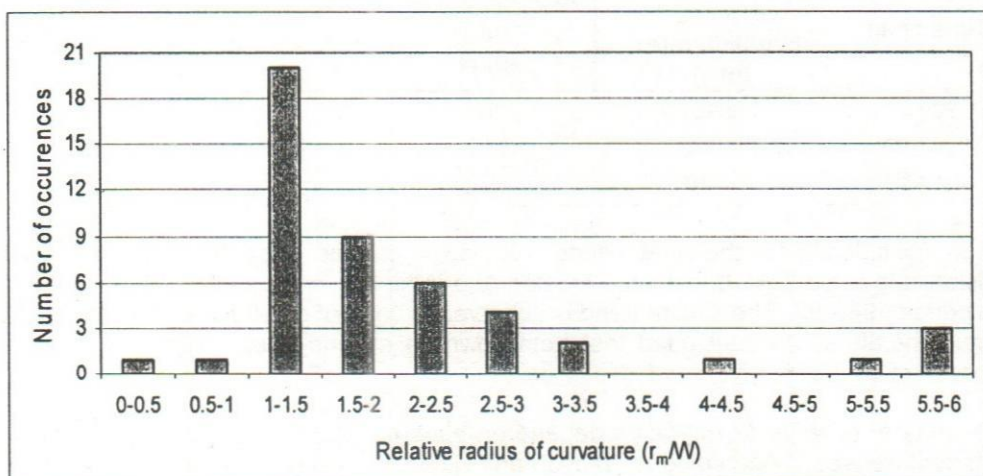


Figure 2: Observed bank erosion rates versus number of occurrences

A plot showing the relationship between relative radius of curvature (r_m/W) of curvature and yearly bend migration rate is presented in **Figure 3**. Despite lots of scatter in the plot a two degree polynomial trend line is still indicative of the fact that bend migration rates are controlled by bend curvature. It is noticeable from the trend line that maximum migration rates occur in the domain $2 < r_m/W < 3$. The relationship between dimensionless relative migration rate and bend curvature has been plotted and shown in the **Figure 4**.

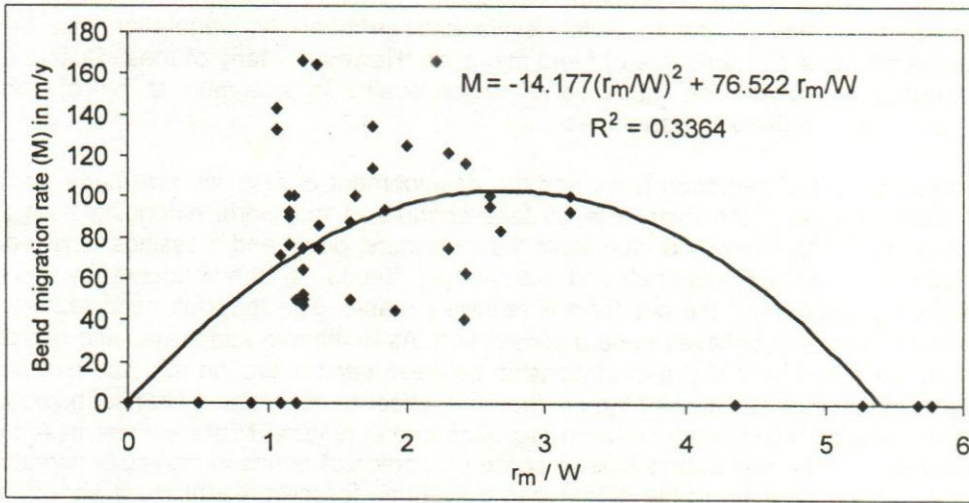


Figure 3: The relation between bend migration rate (M) and relative bend curvature

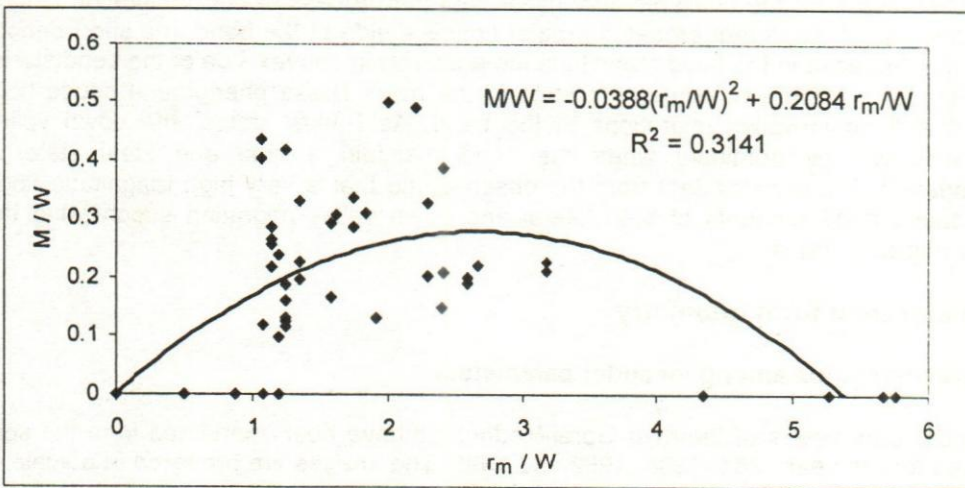


Figure 4: The relation between dimensionless relative bend migration rate (M) and bend curvature

It can be seen from the plot that here also a two degree polynomial trend line confirms the contention that maximum bend migration rates occur at $2 < r_m/W < 3$. Some very low values of M and M/W indicate that a number of bends migrated a little or did not migrate at all. It might have happened due to the fact that erosion rates have been obtained images of a long interval yielded very low values of yearly erosion rates. The equation of the two polynomial trendlines is given below:

$$M = -14.177(r_m/W)^2 + 76.522 (r_m/W)$$

$$M/W = -0.0388(r_m/W)^2 + 0.2084 (r_m/W)$$

Apart from the influence of relative radius of curvature on bend migration rates as revealed from the study there are several other factors such as bank material weight

and texture, physicochemical properties, shear and cohesive strength, bank heights and cross-sectional shape, ground water levels and permeability, vegetation etc. have influence on rates and amounts of bend migration. However, many of these factors are approximately known. The influence of water quality is assumed to be of minor importance for the rivers in Bangladesh.

The assessment of migration rates and the development of rate law are made for the tidal lower course of the river. The off take channel of the Gorai extending from the mouth to the Gorai Railway Bridge lacks the meanders, pools and crossings. The reach between the off take channel and Kamarkhali Bends is characterized by strong meandering pattern but the planform is relatively stable. The tortuous bend feature at Kamarkhali bends is believed to be a constriction. As to the migration rates and rate law it should be noted here that the relationship between bank migration rate and river size is difficult to isolate because of the confounding effect of intermittent channel migration and the complex relationship between migration and curvature. Migration rate based on simple mean of the raw data is biased by the proportion of bends in particular curvature classes. An examination of the determined curvatures for the present study shows that such problem does not arise.

It is observed from the available information that the process of bend migration begins with a seasonal flood that erodes the outer concave side of the bend in a short period. With the decrease in the flood magnitude the accretion in convex side of the bend starts. This tends to reform an equilibrium state in the river. These phenomena cause both lateral and down valley migrations at the bend. As Parker stated, the down valley migration will be dominant when the bend maintain a final and ideal state of meandering. It is also evident from the observations that a very high magnitude flood can cause large amounts of both lateral and down valley migration suppressing the usual migration rates.

Meander plan form geometry

Interrelationships among meander parameters

Meander parameters of the river Gorai-Modhumati have been measured from the spot images for the year 1985, 1988, 1992 and 1995. The images are prepared at a scale of 1: 1,00, 000. Since the upper course of the river is more or less stable despite being sinuous, the active lower tidal lower course has been selected for developing relationships. All active bends of this reach have been taken into account for analysis. The measurements of meander wavelength (M_L) and channel width (W) provide following average relationships for different years:

$M_L = 11.2 W^{1.01}$	in 1985
$M_L = 11.8 W^{1.01}$	in 1988
$M_L = 11.4 W^{1.01}$	in 1992
$M_L = 11.8 W^{1.01}$	in 1995

The general relationship between meander wavelength (M_L) and channel width (W) for the entire period has been established (Figure 5) and seen to be as:

$$M_L = 6.2615 W^{0.4095} \text{ where both } M_L \text{ and } W \text{ are in km.}$$

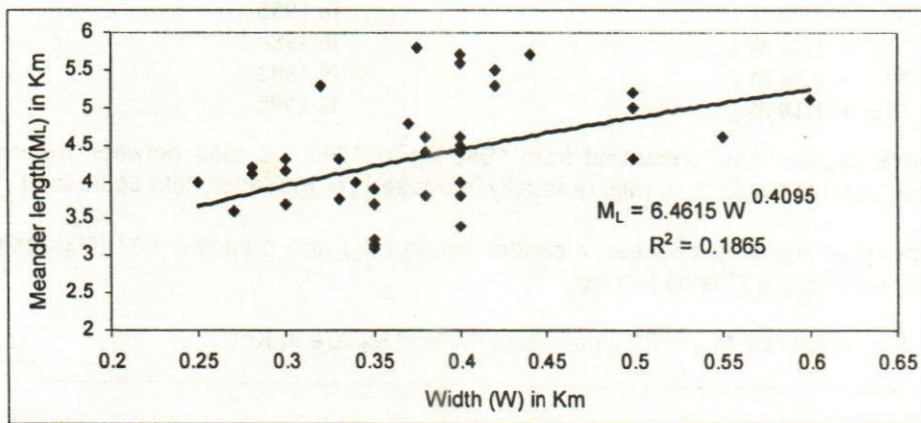


Figure 5: Relationship between meander length (M_L) and channel width (W)

Relationships between meander belt (M_B) and channel width (W) have been developed for different years and shown hereunder:

$M_B = 9.75 W = 5.35 W^{1.10}$	in 1985
$M_B = 10.52 W = 5.81 W^{1.10}$	in 1988
$M_B = 10.02 W = 5.52 W^{1.10}$	in 1992
$M_B = 9.99 W = 5.51 W^{1.10}$	in 1995

The general relationship between meander belt (M_B) and channel width (W) for the entire period has been developed (**Figure 6**) and found to be as:

$M_B = 3.0854 W^{-0.1967}$ where both M_B and W are in Km.

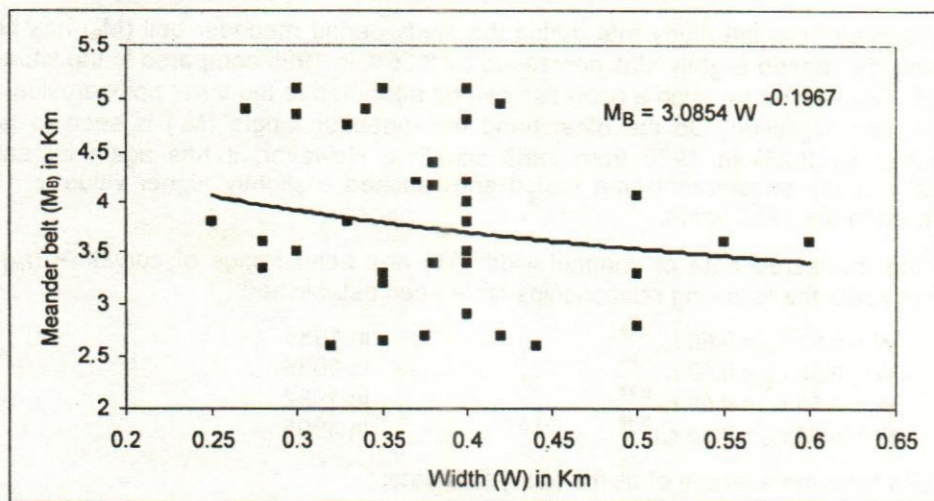


Figure 6: Relationship between meander belt (M_B) and channel width (W)

The relationship between meander belt (M_B) and meander length (M_L) for different years as found from the study has been shown below:

$$M_L = 1.15 M_B$$

in 1985

$$M_L = 1.12 M_B$$

in 1988

$$M_L = 1.14 M_B$$

in 1992

$$M_L = 1.18 M_B$$

in 1995

The above relationships show that from 1988 up to 1995 the ratio between meander length (M_L) and meander belt (M_B) gradually increased i.e. meander ratio decreased.

The general relationship between meander length (M_L) and meander belt (M_B) for the entire period (**Figure 7**) is as follows:

$$M_L = 5.1707 M_B^{-0.1365} \text{ where both } M_L \text{ and } M_B \text{ are in Km}$$

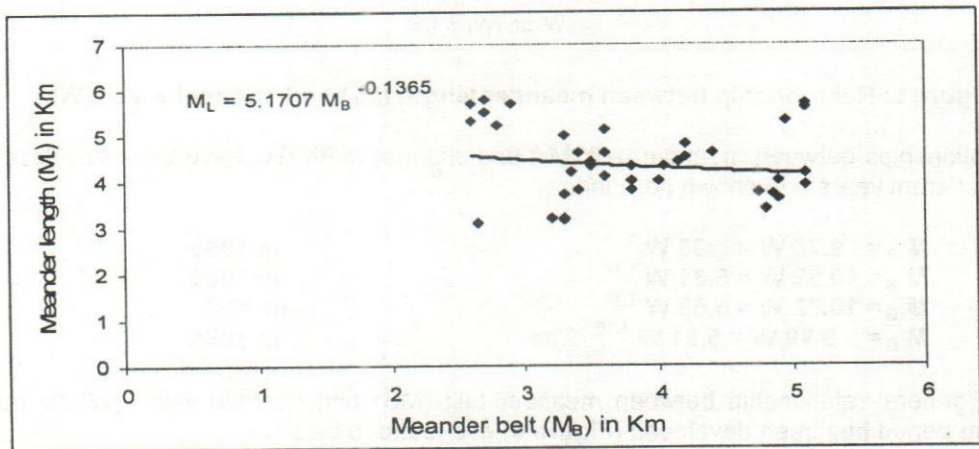


Figure 7: Relationship between meander length (M_L) and meander belt (M_B)

It is observed from the study that during the study period meander belt (M_B) has been gradually decreased slightly. It is decreased by 3.35% in 1995 compared to the situation in 1985. The reason for such a decrease can be attributed to the inner bank erosion and down valley migration. On the other hand the meander length (M_L) is seen to have decreased by 3.2% in 1988 from 1985 situation. However, it has again increased gradually in the subsequent time period and reached a slightly higher value in 1995 compared to the 1985 value.

From the measured data of channel width (W) and bend radius of curvature (r_m) for different years the following relationships have been established:

$$W = 0.62 r_m = 0.66 r_m^{0.99}$$

in 1985

$$W = 0.56 r_m = 0.60 r_m^{0.99}$$

in 1988

$$W = 0.56 r_m = 0.60 r_m^{0.99}$$

in 1992

$$W = 0.53 r_m = 0.56 r_m^{0.99}$$

in 1995

It is seen from the average of all the four years data:

$$W = 0.57 r_m = 0.604 r_m^{0.99} \text{ where both } W \text{ and } r_m \text{ are in meter}$$

Leopold et al. (1964) proposed the following relationship between W and r_m :

$$W = 0.71 r_m^{0.99} \text{ where all dimensions are in meter}$$

The deviation of the established relationship from that proposed by Leopold et al. is not at all unreasonable. The relationship largely depends on the considered flow width. In the present study channel width corresponds to low flow width.

The general relationship between W and r_m for the entire period is established (Figure-8) that appears below:

$$W = 0.3753 r_m^{0.0093} \text{ where both } W \text{ and } r_m \text{ are in Km}$$

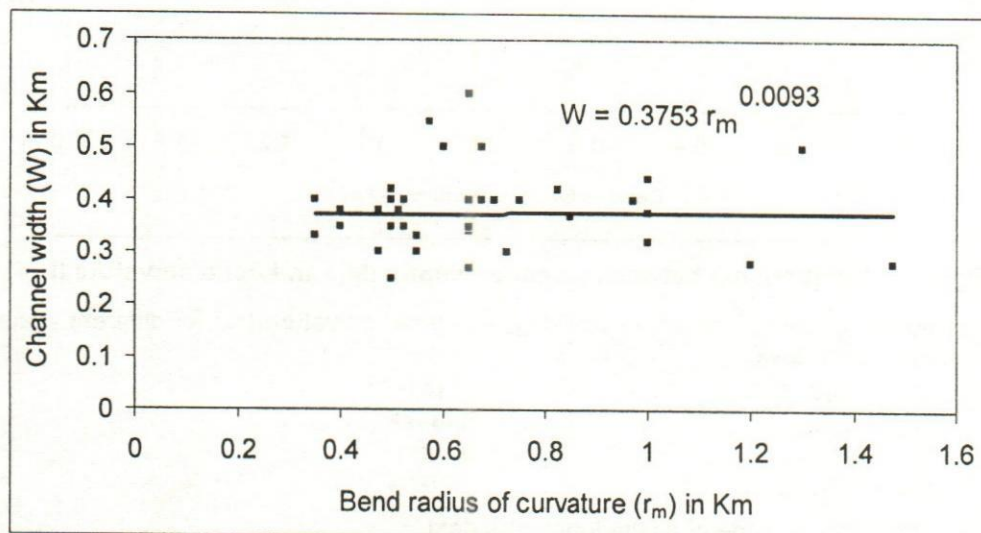


Figure 8: Relationship between channel width (W) and bend curvature (r_m)

The relationship between meander length (M_L) and bend curvature (r_m) for different years appears below:

$M_L = 6.92 r_m = 7.88 r_m^{0.98}$	in 1985
$M_L = 6.65 r_m = 7.57 r_m^{0.98}$	in 1988
$M_L = 6.38 r_m = 7.28 r_m^{0.98}$	in 1992
$M_L = 6.20 r_m = 7.08 r_m^{0.98}$	in 1995

It is seen from the average of all the four years data:

$$M_L = 7.43 r_m^{0.98} \text{ where both } M_L \text{ and } r_m \text{ are in meter}$$

Leopold et al. (1964) proposed the following relationship between M_L and r_m :

$$M_L = 4.7 r_m^{0.98} \text{ where all dimensions are in meter.}$$

The variation of the established equation from the proposed equation can be attributed to the fact that different channel width are used for developing the equations and proposed equation may not be valid everywhere.

The general relationship between M_L and r_m for the entire period has been established (Figure 9) and the relationship is: $M_L = 4.6917 r_m^{0.1812}$ where all dimensions are in Km.

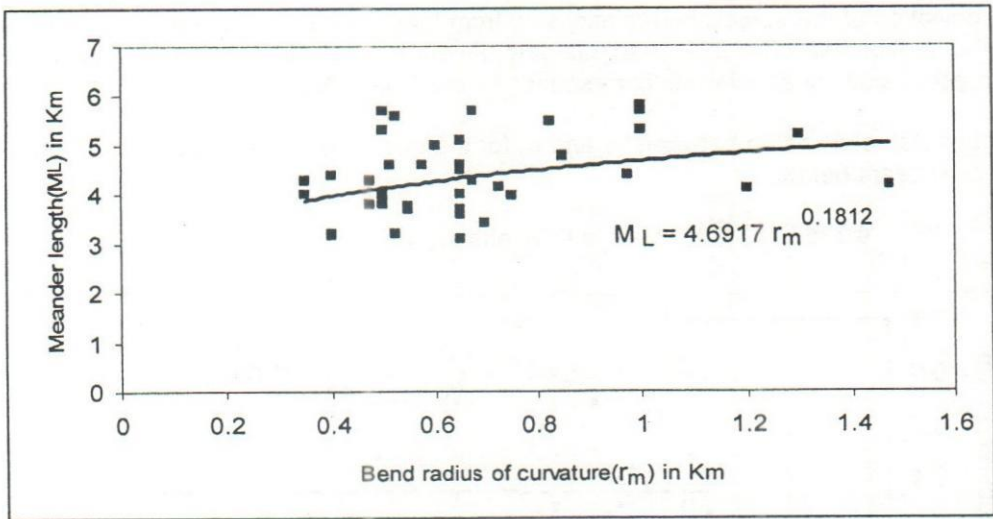


Figure 9: Relationship between meander length (M_L) and bend curvature (r_m)

The relationship between meander belt (M_B) and bend curvature (r_m) for different years is found to be as follows:

$M_B = 6.04 r_m$	in 1985
$M_B = 5.94 r_m$	in 1988
$M_B = 5.60 r_m$	in 1992
$M_B = 5.24 r_m$	in 1995

It is seen from the average of all the four years data:

$$M_B = 5.69 r_m \text{ where both } M_B \text{ and } r_m \text{ are in meter.}$$

The general relationship between M_B and r_m for the entire period has been established (Figure 10) and the relationship is:

$$M_B = 3.3689 r_m^{-0.2306} \text{ where all dimensions are in Km}$$

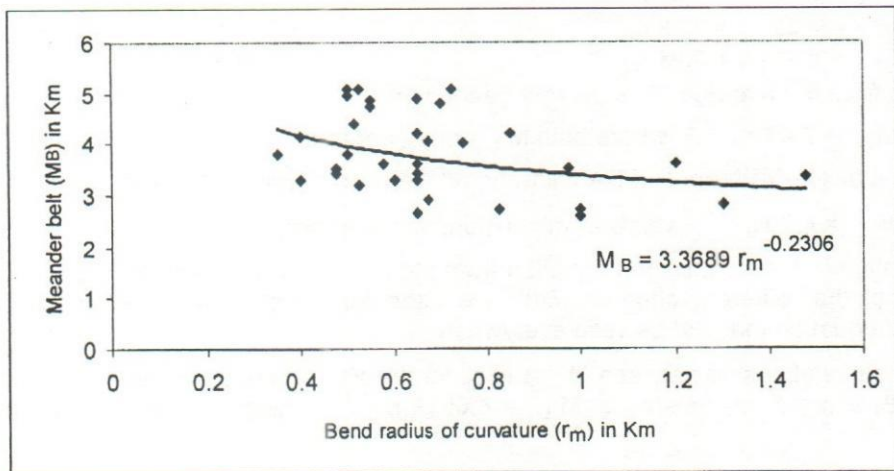


Figure 10: Relationship between meander belt (M_B) and bend curvature (r_m)

In natural rivers, discharge magnitudes determine the meander parameters. An attempt is made to relate the maximum discharge (Q_{max}) and annual mean discharge (Q_{ma}) with meander belt (M_B) and meander length (M_L). The following general relationships have been found:

$$M_L = 58.6 Q_{max}^{0.5} \quad \& \quad M_L = 116.7 Q_{ma}^{0.5}$$

$$M_B = 51.1 Q_{max}^{0.5} \quad \& \quad M_B = 101.8 Q_{ma}^{0.5}$$

An attempt is also made to develop general relationships between channel width (W) and maximum discharge (Q_{max}) and channel width (W) and annual mean discharge (Q_{ma}). The relationships are as follows:

$$W = 5.87 Q_{max}^{0.5} \quad \& \quad W = 9.45 Q_{ma}^{0.5}$$

Where channel width (W) stands for low flow width, width is in meter and discharge is in m^3/s . Sinuosity (S_r) is defined as the ratio of the length along the channel to meander length. Sinuosity is an important parameter that defines meander geometry and determines the shape of meanders. The satellite images for planform developments of the Gorai show that the upper course of the river was stable. The average sinuosity of the lower tidal course has been determined for the years 1985, 1988, 1992 and 1995. The variation in the average sinuosity of the upper and lower course of the river Gorai for different time periods and years was determined under FAP-4 (1993). The variation in the average sinuosity of the lower course of the Gorai is shown in Table 5.

Table 5: Variation in average sinuosity of the Gorai lower course

Year	Average sinuosity	Comments
1904-24	2.20	Source: FAP-4 (1993)
1985	2.10	
1988	2.13	
1989	2.3	Source: FAP-4 (1993)
1992	2.08	
1995	2.04	

It can be seen from the table that the sinuosity of the lower course of the Gorai-Madhumati was greater than 2 for all the considered years. It confirms that the lower course of the river was highly sinuous. FAP-4 (1993) studies revealed that the upper course of the river was historically less sinuous than the lower course.

Conclusions and recommendations

Conclusions

The following conclusions have been drawn from the study:

- The upper course of the river Gorai-Madhumati is characterized by strong meandering pattern but relatively stable
- The characteristic features of the bend migration processes of the lower tidal course of the river Gorai-Madhumati has been identified as outer bank migration (lateral), down valley migration and inner bank erosion
- Down valley migration rates and amounts are positively correlated with the peak discharge magnitudes

- During the period from 1985 to 1988 annual downvalley migration rates varied from 0 to 292 m with an average of 145.8 m and standard deviation 66.7
- During the period 1985-92 and 1985-95 the annual average downvalley migration rates were 113.8 m and 139.7 m respectively
- Maximum inner bank erosion of 600 m occurred in the period 1992-95
- Inner bank erosion amounts are positively correlated with the magnitude of peak discharges
- Over the time period 1985-88, 1985-92 and 1985-95 the annual average outer bank migration rates were 91 m, 67.2 m and 66.2 m respectively
- At a few bends the river are seen to have migrated a little and also amounts of bend migration are different at different locations for a certain time span. It implies that the migration rates depend on many factors
- The outer bank migration rates depend on the relative bend curvature. The maximum migration rate occurs with the relative bend curvature at $2 < r_m/W < 3$
- Average meander wave length and meander belt show a correlation with the average channel width. The general relationship between meander wave length and channel width and meander belt and channel width indicates that meander wave length is positively and meander belt is negatively correlated with the channel width
- Meander wave length (M_L) is negatively correlated with meander belt (M_B)
- Average channel width (W) is strongly correlated with bend curvature (r_m) and channel width (W) is positively correlated with bend curvature (r_m)
- Mean wave length (M_L) is positively and meander belt (M_B) is negatively correlated with bend curvature (r_m)
- The sinuosity (S_r) of the tidal lower course of the river was found to be greater than 2 (two). It means the river is highly sinuous there
- The lower tidal course is more sinuous than the upper course

Recommendations

In view of the limitations cited in the previous section, the following recommendations are made for the future study:

- The study should be conducted taking a long time-span into account and more continuous series of data should be collected
- Frequent and detailed field investigations are required for the study
- The cross-sectional data should be collected frequently and correctly and with regular intervals
- There should have more discharge and water level gauging stations and recording should be done correctly by improving the data collection system
- Budget provision should be adequate

Reference

- FAP 4 (1993)**, River survey project, delft hydraulics & others, study Report-1, Selection of study topics for phase 2, govt. of Bangladesh
- Leopold, L.B., Wolman, M.G., Miller, J.P., 1964.** Fluvial Processes in Geomorphology. Freeman, San Francisco, 522 pp.
- Leopold, L.B., and Wolman, M.G. (1957).** River channel patterns: braided, meandering and straight. U.S. Geol. Surv. Prof. Paper 282-B, Washington, DC.
- Stahler, S.A. (1946)** Sinuosity of alluvial rivers in the great planes. Bull. Geol. Soc. Am., 74, pp. 1089-1100

Interpretation of Geoelectric Soundings in Deciphering Aquifer in Kushtia Municipality

M. Shahinuzzaman¹ and M. Nozibul Haque²,

Abstract

This paper deals with the results of the resistivity survey in Kushtia Municipality in order to study the subsurface geological sequences as well as to locate the groundwater saturated permeable beds. Six Schlumberger soundings have been made by the authors in this investigation in the last week of May, 2004. The data has been interpreted as a multilayer step function resistivity model by an automatic iterative process proposed by Zohdy, 1989. An equivalent model of minimum layers has been constructed for each location. The transverse and longitudinal resistivities as well as the co-efficients of anisotropy have been studied. The values of the co-efficient of anisotropy are ranging from 1 to 1.94. From the knowledge of geology, hydrogeology and co-efficients of anisotropy, the results of the Vertical Electrical Soundings (VES) have been interpreted for deciphering the aquifer. The lateral variation of Water Table has been prepared. The geoelectrical resistivity results have been compared with the available nearest borehole lithological information and the depth to the water table has been directly measured from the surface to compare with the detected depth to the water table which show encouraging relations.

Introduction

The electrical properties of the subsurface can be explored either electrically or electromagnetically. Electrical resistivity methods are normally less costly than other subsurface investigation methods. The vertical electrical sounding is generally made to investigate the change of the formation resistivity with depth. To attain this purpose, it is necessary to arrange the measurements in such a manner that, at different measurements, the value of the measured potential difference is affected by the formation resistivity of different depth ranges. The degree to which it is affected depends on the size, shape, location and electrical resistivity of the subsurface layers or bodies. It is therefore possible to obtain information about the subsurface from potential measurements made at the surface. This method finds many applications in the field of engineering geology and hydrogeology. More particularly in unconsolidated formations, the survey may be used to search for water bearing strata, in which case the properties of the formation materials as well as their geometry are important. Clean sands and gravels, having high porosities, make good aquifers. When saturated with fresh water they have medium resistivities and can easily be differentiated from lower resistive impermeable clay and from bedrock which is usually of much higher resistivity.

Groundwater resource, although replenishable, is not inexhaustible. With the phenomenal increase in the use of groundwater in Kushtia Municipality in recent years, the need has arisen for the better understanding and functioning of groundwater reservoirs in response to natural and man made conditions. In the extreme dry weather

¹ M.Sc Student & ² Associate Prof. Dept. of Electronics & Applied Physics, Islamic University, Kushtia-7003, Bangladesh.

condition, water abstraction rate of the tube wells decreases due to the falling of groundwater level in some places of this area. The wide and uneven distribution of groundwater thus necessitates detailed study in specific areas for obtaining information about water table for judicious use and the conservation of this groundwater resource. The development of groundwater system required the knowledge about the behaviour of the hydro geological system due to various stresses. Although several methods can be enumerated under the geophysical heading, only the electrical resistivity and seismic refraction method have more than limited application to groundwater investigation. In the Kushtia Municipality, the Geoelectrical Resistivity method has not yet been employed for hydrogeological investigation. So the Geoelectrical Resistivity method has been used in the present study to interpret subsurface geoelectrical parameters in deciphering the aquifer of the area.

General Features of the Study Area

Geography

The study area, the Kushtia Municipality, is located on the bank of the river Gorai, one of the tributaries of the Ganges (longitude 89°06' E - 89°12' E and latitude 23°54' N - 23°57' N) as shown in **Figure.1**. The Ganges delta includes several district of Kushtia, Jessore, Khulna and western part of the districts of Faridpur and Barishal (Khan, 1991). The area is almost plain. The Gorai is sustaining the environmental balance and socio-economic development of the area. The alluvium is composed of mostly clay, silt and fine sand which are gray and brown in color.

Climatic Conditions

The study area, like the rest part of Bangladesh, enjoys monsoon climate with seasonal wind reversal. Based on rainfall, temperature and pressure, a yearlong cycle can be broken down into the four seasons: winter (December to February), summer or pre-monsoon (March to June), monsoon (July to September) and autumn or post monsoon (October to November). The annual average rainfall varies between 1500 mm to 1750 mm. The average wind speed of the area is 7.25 miles per hour. The area has high relative humidity. The mean annual relative humidity is of 77 percent. The lowest and highest temperatures are 6°C and 43°C respectively (BWDB, 2000).

Hydrogeology

A hydrogeological system is recognizable in the southwest region of Bangladesh, of which the study area constitutes a very small part. The sub-surface geology and the aquifer system of the study area and their corresponding hydrogeological characteristics, in general, can be described as follows (BWDB 2000):

- (i) An upper surface layer made up of primarily clay is moderately thick.
- (ii) An intermediate layer made up primarily of fine sand. This unit is characterized by moderate porosity and permeability. In most places, the system is exploited to produce water through hand tube wells and other manually operated pumping units for domestic purpose.

- (iii) A deeper layer is comprised mainly of sand, ranging from medium to coarse in size and known as the main aquifer. This aquifer is characterized by high porosity and moderate to high permeability. This system is capable of providing large quantity of groundwater.

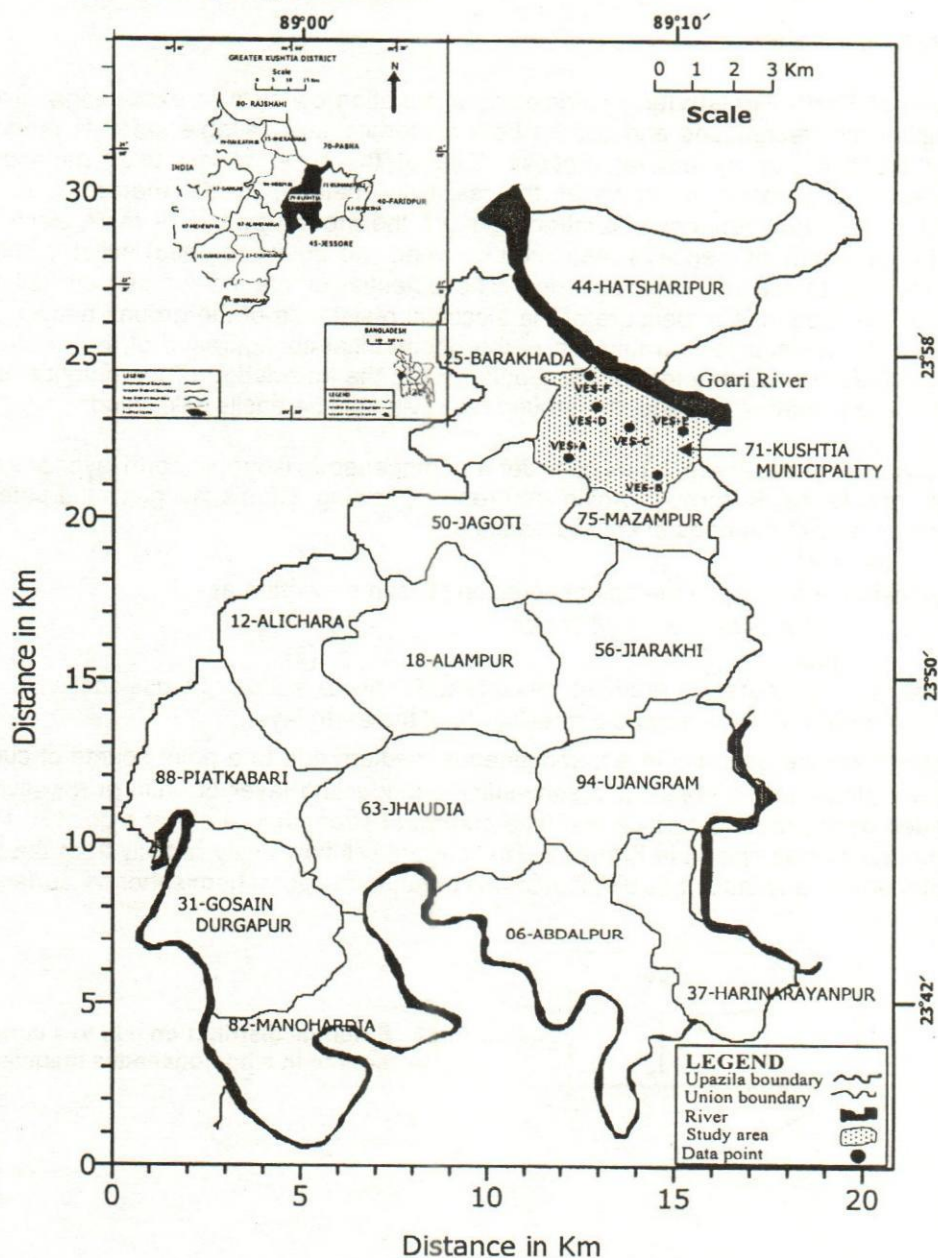


Fig.1: Location map showing study area and data points.

The aquifer is recharged mainly by the average rainfall of 1600 mm/year infiltrating into ground. Additional recharge occurs from the river channels of the Gorai as well as some other surface

water bodies in wet months. The major discharge occurs due to abstraction for domestic purpose and irrigation in some parts. The groundwater reservoir also loses its storage by the river channels in dry months (Islam, 2001). Groundwater levels generally ranges from 0 m to about 8 m from ground surface (BWDB, 2000).

Literature Review

Theory of Earth Resistivity – Geoelectric exploration consists of exceedingly diverse principles and techniques and utilizes both stationary and variable currents produced either artificially or by natural process. One of the most widely used methods of geoelectric exploration is known as the resistivity method. In this method, a current (direct or very low frequency) is introduced into the ground by two or more electrodes and the potential difference is measured between two points (probes) suitably chosen with respect to the current electrodes. The potential difference for unit current sent through the ground is a measure of the electrical resistance of the ground between the probes. The resistance is a function of the geometrical configuration of the electrodes and the electrical parameters of the ground. From the knowledge of the potential drop, current and electrode spacing, the ground resistivity can be easily calculated.

For quantitative treatment, let us consider a homogeneous isotropic earth layer of length l and resistance R through which a current I is flowing. Ohm's law gives the potential difference across the ends of the resistance as-

$$\Delta V = RI \quad (1)$$

By definition, $R = \rho l/A$, so the above equation (1) can be written as-

$$\Delta V = \rho l I / A, \text{ or, } \Delta V / I = \rho l / A$$

$$\text{or, } \text{grad } V = \rho j \quad (2)$$

where, $\text{grad } V$ = potential gradient, j = current density, A = area of cross-section, l = length of the layer and ρ = resistivity of the earth layer.

To determine the potential in a homogeneous medium due to a point source of current on the surface, let us consider a semi-infinite conducting layer of uniform resistivity ρ , bounded by the ground surface and let a current of strength $+I$ enter at a point A on the ground surface as shown in **Figure.2**. This current will flow away radially from the point of entry and at any instant its distribution will be uniform over a hemispherical surface.

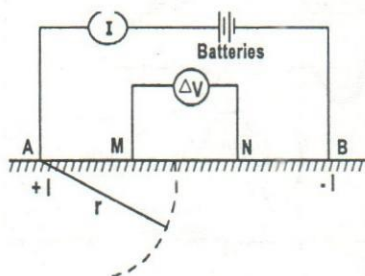


Fig.2 : Potential distribution due to a current source in a homogeneous medium.

At a distance r , away from the current source, the current density j , would be-

$$j = I / 2\pi r^2 \quad (3)$$

The potential gradient $-\delta V / \delta r$ associated with the current is given by equation (2) which when using equation (3) can be written as:

$$-\delta V / \delta r = \rho j = \rho I / 2\pi r^2 \quad (4)$$

The negative sign indicates that the potential increases in the opposite direction to the current flow. Integrating equation (4), we get,

$$V = I\rho / 2\pi r \quad (5)$$

This is the basic equation, which enables the calculation of the potential distribution in a homogeneous conducting semi-infinite medium.

Resistivity Measurement – During the resistivity measurement over the earth surface the target is energized by current and the potential difference between two points are measured. The potential difference between points M and N (**Figure.2**) caused by current +I at the "source" (entry point A) is

$$V = (I\rho / 2\pi) \cdot (1/AM - 1/AN) \quad (6)$$

In the same manner, the potential difference between M and N caused by -I current at the "sink" (exit point B) is

$$V = (-I\rho / 2\pi) \cdot (1/BM - 1/BN) \quad (7)$$

The total potential difference between M and N is, therefore given by the sum of the right hand side of equation (6) and (7) and is

$$V = (I\rho / 2\pi) \cdot (1/AM - 1/BM - 1/AN + 1/BN)$$

$$\text{or } \rho = (2\pi V / I) \cdot \{1/ (1/AM - 1/BM - 1/AN + 1/BN)\} \quad (8)$$

$$\text{or } \rho = (2\pi V / I) \cdot K \quad (9)$$

where, $K = \{1/ (1/AM - 1/BM - 1/AN + 1/BN)\}$ and it denotes the geometric factor of an electrode configuration.

Determination of anisotropy: The steps taken in the process of interpretation of geo-electric resistivity data are based upon the assumption that the geo-electric layers are isotropic. However, in reality all geological formations are appeared to be anisotropic. This phenomenon is quite common in clay or shale reach formations. In such condition the electrical resistivity is the same in all directions along a layer and has different value in the direction perpendicular to the stratification. The ratio between the resistivity in the perpendicular direction and that in the direction of the stratification is termed as co-efficient of anisotropy.

Thus the co-efficient of anisotropy may be defined by taking the square root of the ratio of resistivities measured in the two principal directions. Let the transverse (ρ_t) and longitudinal (ρ_l) resistivities are the resistivities of the formation across and along the bedding plane respectively. The formula used to determine the co-efficient of anisotropy is as follows –

$$\lambda = \sqrt{\frac{\rho_t}{\rho_l}} \quad (10)$$

$$\text{where, } \rho_t = \frac{T}{H} = \frac{\sum_{i=1}^n \rho_i h_i}{\sum_{i=1}^n h_i} \quad \text{and} \quad \rho_l = \frac{H}{S} = \frac{\sum_{i=1}^n h_i}{\sum_{i=1}^n \frac{h_i}{\rho_i}}$$

where T = transverse resistance, S = longitudinal conductance, ρ_i = resistivity of the i^{th} layer and h_i = thickness of the i^{th} layer.

Deciphering of Aquifer: The electrical resistivity of formations depends on the porosity, total dissolved solids of the pore fluid, linearity or tortuosity of interconnected pore spaces, presence of conducting minerals such as clays and temperature. Clays and silts normally rich in water soluble minerals have low resistivity. The conductivity of sands and gravels, on the other hand, is mainly due to presence of water in the pore spaces as they are composed mostly of electrically non-conducting minerals and they show a significant variation in conductivity between their dry and saturated states. Sands occurring above the groundwater level, generally show high resistivity values and below the water table the values depend on the nature of the pore water. Sand may show resistivity in the range of clays when the pore water is saline and shows higher resistivities in the case of fresh or brackish water (Woobaidullah, 1999).

The resistivity of clay varies from 5-35 $\Omega\text{-m}$ whereas the range of resistivity for finesand-clay saturated with moderately fresh water is 35-80 $\Omega\text{-m}$. The value of resistivity for medium-coarse sand is more than 80 $\Omega\text{-m}$ (Norwroozi, 1999; Shahid, 2000; Woobaidullah, 1999).

Methodology

Data Collection

In resistivity measurements, the instrument is usually simple. In this work, the Digital Multimeters (Model: GWM 351) supplied by the Department of Electronic and Applied Physics, Islamic University, Kushtia, have been used in measuring the current supplied by the current electrodes and potential difference between potential electrodes. The present resistivity survey was carried out in the Kushtia Municipality by the authors themselves in the last week of May, 2004. Vertical Electrical Soundings (VES) employing Schlumberger Configurations were conducted at different locations. To determine the resistivity using Schlumberger Configuration, the current through the current electrodes and potential between potential electrodes are measured shifting the electrodes outward centering a point maintaining $AB \geq 5MN$ (Figure.3). A total of six locations were selected for resistivity measurements as shown in Figure.1. Each location is treated as a separate VES number, such as VES-A, B, C, D, E and F. The field works were made with the maximum current electrode spacing (AB) of 200 m.

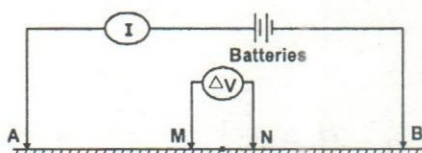


Fig.3 : Schlumberger Configuration to measure the earth resistivity.

The measured parameter the apparent resistivity, ρ_a , which is the product of a geometrical factor (K), 2π and the quotient of the measured potential difference (ΔV), and the source current I . The apparent resistivity is plotted vs. $AB/2$ on bilogarithmic

paper, resulting Vertical Electrical Sounding curve. The VES curves show the change of resistivity with depth, since the effective penetration increases with increasing current electrode spacing.

Interpretation – Several methods have been developed for direct interpretation of VES curves over horizontally stratified media. These methods may be divided into two groups. The first group does the transformation of a VES curve into its corresponding resistivity transform curve using forward filters (Ghosh, 1971 and Koefoed, 1979). This resistivity transform curve is then interpreted using methods based on Pekeris (1940). But there are many drawbacks of this technique. The second group of interpreting methods relies on inverting the sounding curves itself without first transforming it to its resistivity transform curve (Zohdy, 1989). In the present study, a fast iterative method for the automatic interpretation of Schlumberger sounding curves based on Zohdy (1989) has been used to determine the layer parameters of horizontally stratified subsurface media to propose a multi-layer model in the sounding locations. This method does not require a preliminary guess for the number of layers, their resistivities and thickness, and it does not require extrapolation of first and last branches of the sounding curve to their respective asymptotes. The number of layer is equal to the number of digitized points and the layer boundaries are spaced uniformly on a logarithmic scale. This method provides a theoretical curve that fits the observed field curve as closely as possible and gives a corresponding well-behaved layering model eliminating the extremely thin layers. In the present investigation this technique has been adopted for the interpretation of VES data.

Initial Data Preparation: In general a sounding curve is the composition of several overlapping segments. This segmented field curve is processed and reduced to a continuous curve prior to its interpretation in terms of horizontal stratified model. A sampling interval of six points per logarithmic cycles is considered optimal for defining the form of a sounding curve. The iterative process depends on the following initial assumptions :

- The number of layers in the model equals the number of digitized points on the observed curve. This assumption remains unchanged throughout the iterative process.
- The depths of the model layers are equals to the digitized electrode spacing, which are equal on a logarithmic scale.
- The true resistivities of the model equal the apparent resistivities. In practice, the true resistivity-depth curve is unknown. Having calculated a theoretical curve using shifted depths and apparent resistivities, a better fit between the observed and calculated sounding curves is obtained by adjusting the amplitudes of layer parameters as shown in **Figure.4**.

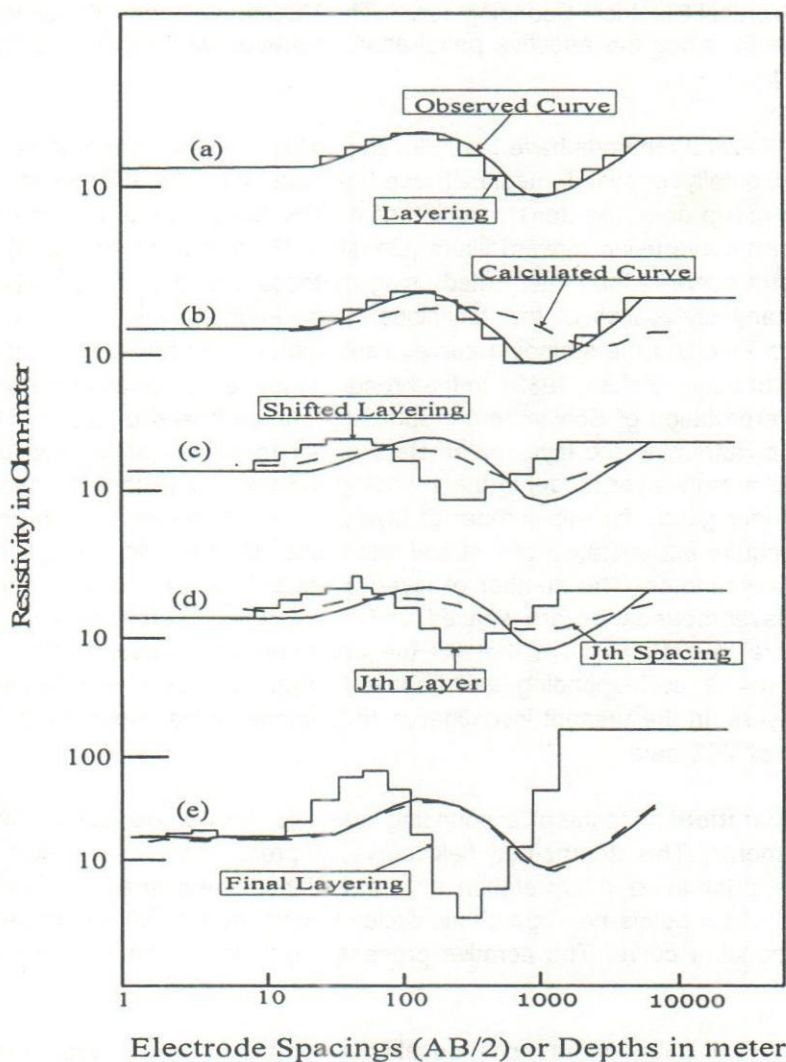


Fig.4 : Graph showing iterative process of interpreting a sounding curve of unknown layers (Zohdy, 1989).

The iterative process is terminated when one of the following conditions is met-

1. Less than 2 rms percent of deviation of field data which is calculated by the formula-

$$rms\% = \sqrt{\frac{\sum_{j=1}^N \left(\frac{\rho_{oj} - \rho_{cj}}{\rho_{oj}} \right)^2}{N}} \times 100 \dots \dots \dots (11)$$

where, ρ_{oj} = jth "observed" apparent resistivity, ρ_{cj} = jth calculated apparent resistivity,
 N = number of digitized apparent resistivity points (with $j = 1$ to N)

2. Less than 5 percent fit i.e., fitting tolerance is less than 5%, or
3. Maximum of 30 iterations is reached. However, an average of 10 iterations is considered.

The automatic interpretation of Schlumberger sounding curves based on Zohdy (1989) has been used to determine the layer parameters for VES-A to propose a multilayer model in detailed.

VES-A (Bus Terminal): This sounding station is located in the south-west corner of the study area. The ground surface is almost plain. Twelve layers have been identified within the depth of 25 m. These layers have been used in reducing this multilayer model to a five-layer model. The thin layers have been merged and a model is prepared to best fitting with the digitized curve. The results show the fitting tolerance of 0.53 percent with the field curve. The automatic interpreted curves and reduced multilayer model of VES-A has been shown in **Figure.5(a)**, **Figure.5(b)** and **Figure.5(c)**. The layer parameters are presented in **Table-1**. The geoelectric parameters of this VES have been compared with the nearest (approximately 1 km away) borehole lithology as shown in **Figure. 5(c)**.

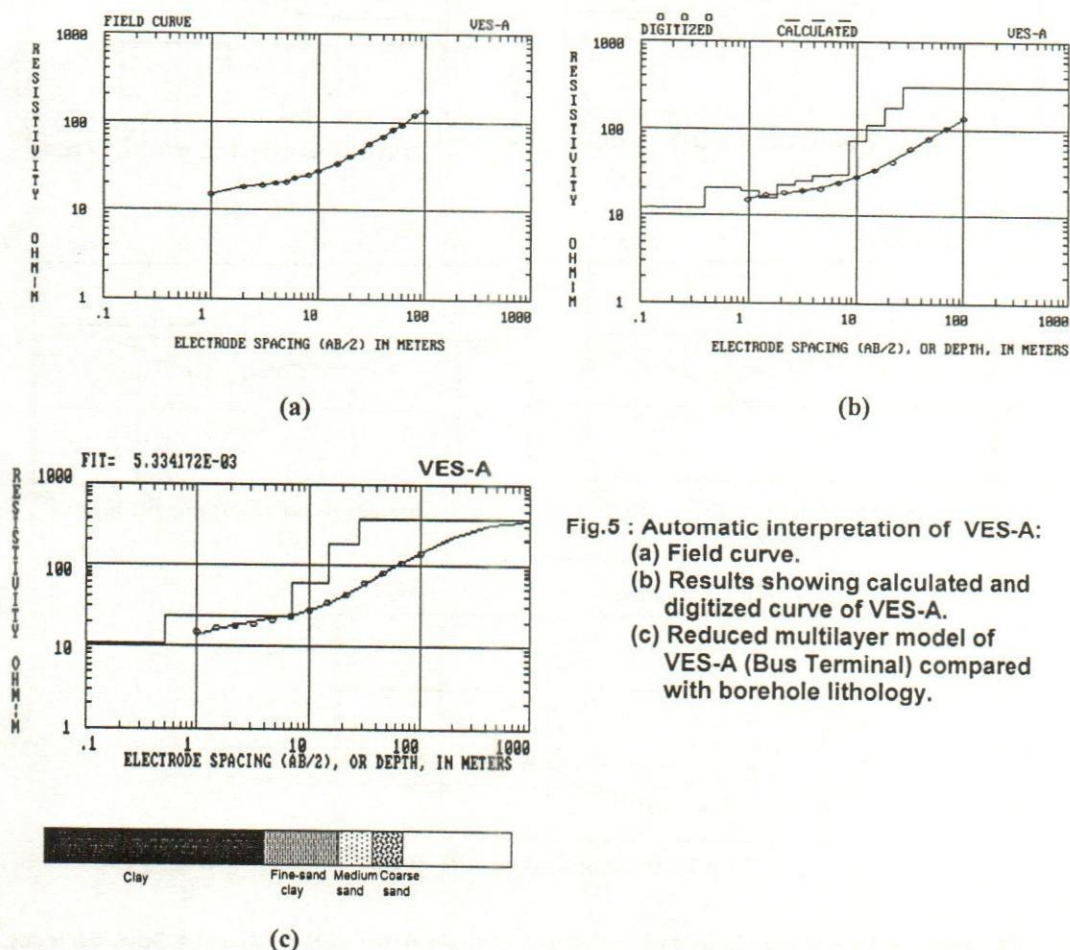


Fig.5 : Automatic interpretation of VES-A:
 (a) Field curve.
 (b) Results showing calculated and digitized curve of VES-A.
 (c) Reduced multilayer model of VES-A (Bus Terminal) compared with borehole lithology.

Table-1 : The layer parameters of VES-A (Bus Terminal).

Layer No.	Depth to the layer (m)	Thickness of the layer (m)	Resistivity of the layer ($\Omega\text{-m}$)
1	0.0	0.5	10.5
2	0.5	6.5	23
3	7	8	60
4	15	13	180
5	28	∞	400

∞ Means undetermined

Following the same procedure, all other VES data have been interpreted and presented in **Figure.6(a)**, **Figure. 6(b)**, **Figure.6(c)**, **Figure.6(d)** and **Figure.6(e)**. The interpreted layer parameters have been tabulated in **Table-2**.

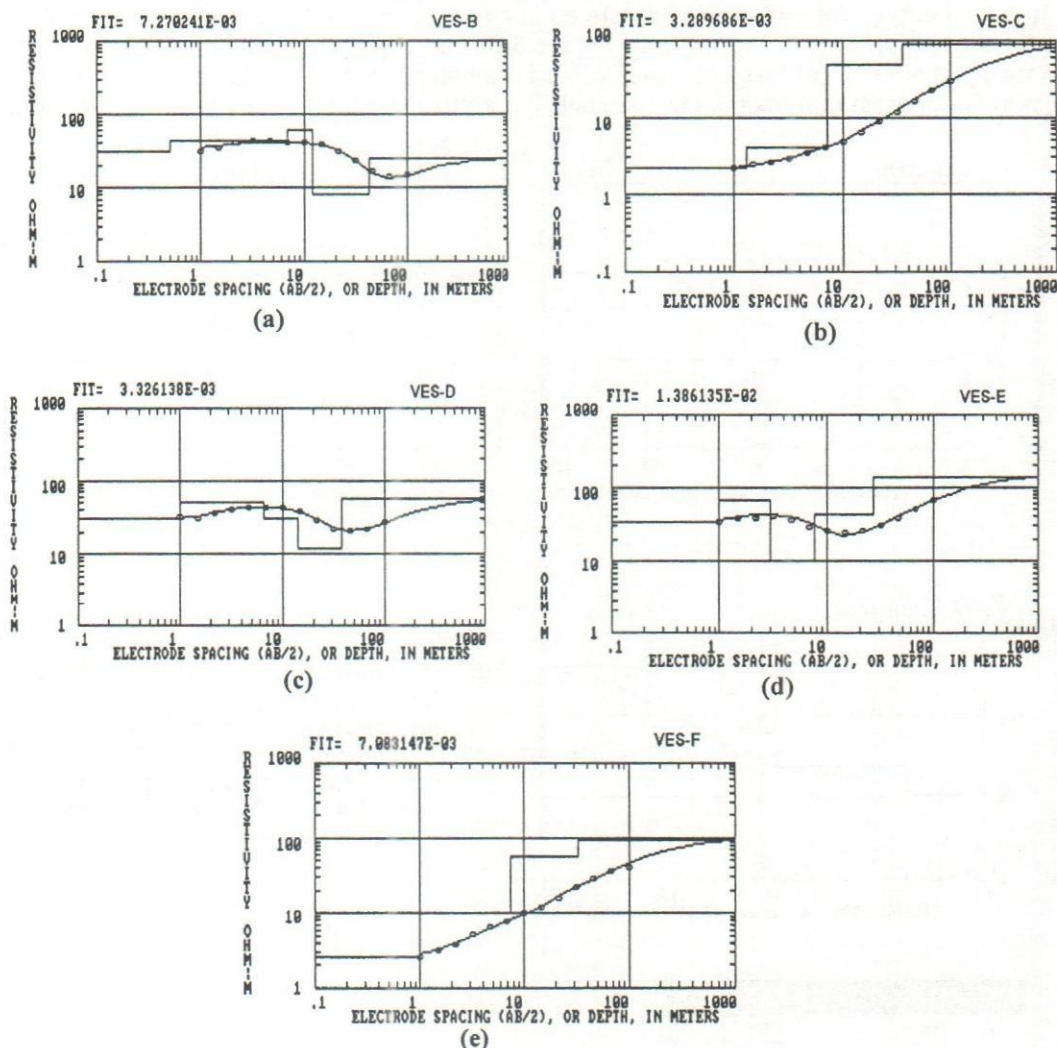


Fig.6 : Reduced multilayer model of (a) VES-B (Housing), (b) VES-C (Kushtia Govt. College), (c) VES-D (Zila School), (d) VES-E (Adarsha College) and (e) VES-F (Police Line).

Table-2 : The interpreted results of VES-A, B, C, D, E and F. Resistivity in ohm-meter

VES No.	Resistivity in ohm-meter					Thickness in meter				
	ρ_1	ρ_2	ρ_3	ρ_4	ρ_5	h_1	h_2	h_3	h_4	h_5
VES-A	10.5	23	60	180	400	0.5	6.5	8	13	∞
VES-B	30	42	60	8	25	0.5	6.4	5.1	31	∞
VES-C	2.2	4	50	90		1.3	5.9	27.8	∞	
VES-D	30	50	30	12	55	1	5.5	7.5	24	∞
VES-E	35	65	10	42	140	1	2	4.6	19.4	∞
VES-F	2.5	10	58	95		1	6.5	25.5	∞	

∞ Means undetermined

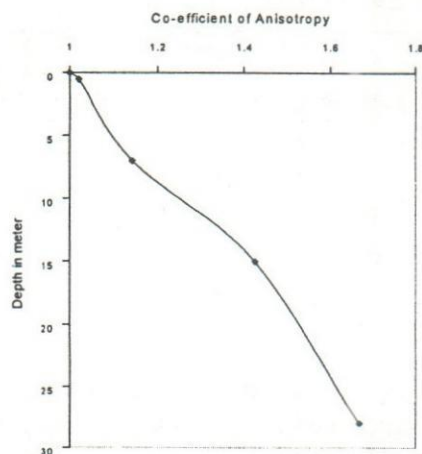
Co-efficient of Anisotropy – In the present work, the co-efficients of anisotropy of different formations at different depths have been calculated at six locations as shown in **Figure.1**. The layer parameters for the best fit model have been taken into consideration in calculating the co-efficient of anisotropy of different layer combinations. The variation of anisotropy to the depth ranging from 27 m to 43 m has been shown in **Figure.7** and tabulated in **Table-3**. The values of the co-efficients of anisotropy are ranging from 1 to 1.94.

The critical analysis of values of the co-efficients of anisotropy (**Figure.7**) in each sounding (except VES-B) indicates that the depths of 7 m, 7.9 m, 7.2 m, 6.5 m, and 7.5 m of VES-A, C, D, E and F respectively at which the co-efficients of anisotropy have a remarkable change of its value might possibly be indicated as the water table. For the confirmation, the depth to the water table from the surface at four locations covering the area has been measured directly during the study, which ranges from 6 m to 7.5 m.

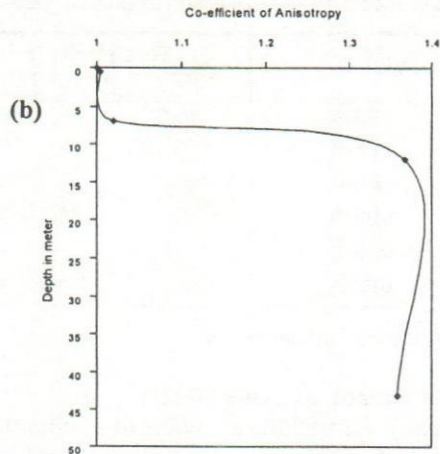
The depths to the water table depict the inequalities in the position of water table with respect to the ground surface and are useful in delineating recharge and discharge areas, locating sites for wells and dealing with drainage, artificial recharge or other problems in which the depth of the water table is critical. The detected water saturated zone with its resistivity and depth at six sounding locations of the investigated area have been identified and presented by shades in **Table-3**. **Figure.8** shows the lateral variation of water table of the area studied. From this figure it is seen that the depth to the water table in the north and east sides show a maximum value of 7.55 m, whereas in the south-east corner this value is less than 6.95 m. Although there is an upward folding of water table in the north-west corner, but the average slope is directed toward the north and east sides from the south-west corner of the area.

From the knowledge of the geology, hydrogeology and anisotropy, the results of the geoelectric soundings have been studied in deciphering the water saturated zones of the area investigated.

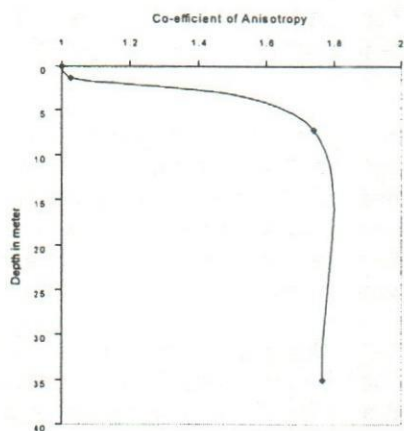
VES-A (Bus Terminal): The interpretation of the sounding curve of this VES gives five layer section. The top layer consists of wet clayey soil of resistivity 10.5 Ω -m with 0.5 m thick. The second layer might be composed of clayey of resistivity 23 Ω -m having thickness of 6.5 m whereas the third layer starting from the depth of 7 m from the surface showing resistivity of 60 Ω -m and seems to be composed of finesand-clay saturated with moderately fresh water. The next layer with resistivity of 180 Ω -m



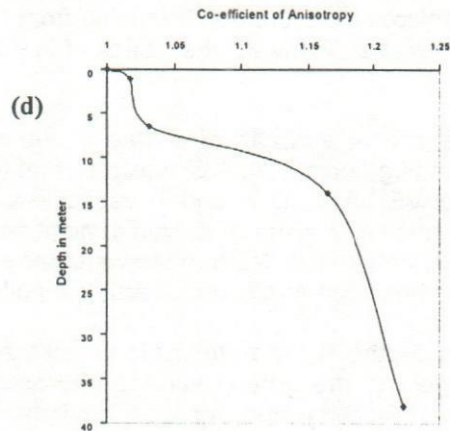
(a)



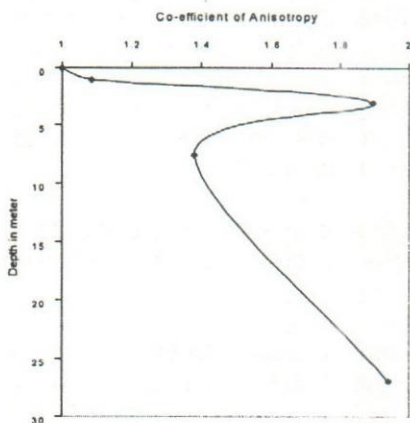
(b)



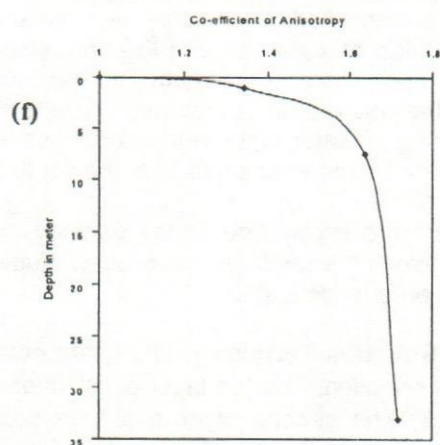
(c)



(d)



(e)



(f)

Figure.7 : The change of the co-efficients of anisotropy with depth at (a) VES-A, (b) VES-B, (c) VES-C, (d) VES-D, (e) VES-E and (f) VES-F.

Table-3: Calculated layer parameters of the investigated area.

VES-No.	Interpreted resistivity model parameters			Transverse Resistivity $\rho_t = \sum \rho_i h_i / \sum h$ (Ω -m)	Longitudinal Resistivity $\rho_l = \sum h_i / \sum h_i \rho_i$ (Ω -m)	Co-efficient of anisotropy $\lambda = \sqrt{\rho_l / \rho_t}$
	Depth to layer (m)	Layer thickness (m)	Resistivity (Ω -m)			
VES-A	0.0	0.50	10.5	10.500	10.500	1.0000
	0.5	6.50	23.0	22.107	21.198	1.0211
	7.0	8.00	60.0	42.316	32.380	1.1430
	15	13.0	180	106.24	52.265	1.4250
	28	17.0	400	217.21	77.827	1.6700
VES-B	0.0	0.50	30.0	30.000	30.000	1.0000
	0.5	6.40	42.0	41.130	40.833	1.0036
	6.9	5.10	60.0	49.150	47.262	1.0197
	12	31.0	8.00	19.483	10.414	1.3677
	43	2.00	25.0	19.728	10.691	1.3583
VES-C	0.0	1.30	2.20	2.2000	2.2000	1.0000
	1.3	5.90	4.00	3.6750	3.4860	1.0266
	7.2	27.8	50.0	40.470	13.353	1.7400
	35	10.0	90.0	51.476	16.470	1.7670
	0.0	1.00	30.0	30.000	30.000	1.0000
VES-D	1.0	5.50	50.0	46.923	45.359	1.0170
	6.5	7.50	30.0	37.857	35.596	1.0313
	14	24.0	12.0	21.526	15.877	1.1640
	33	7.00	55.0	26.733	17.853	1.2230
	0.0	1.00	35.0	35.000	35.000	1.0000
VES-E	1.0	2.00	65.0	55.000	50.675	1.0853
	3.0	4.60	10.0	27.763	14.637	1.8967
	7.6	19.4	42.0	37.992	27.520	1.3800
	27	18.0	140	78.795	40.577	1.9410
	0.0	1.00	2.50	2.5000	2.5000	1
VES-F	1.0	6.50	10.0	9.3330	5.1720	1.343
	7.5	25.5	58.0	46.863	17.469	1.637
	33	12.0	95.0	59.700	20.265	1.7163

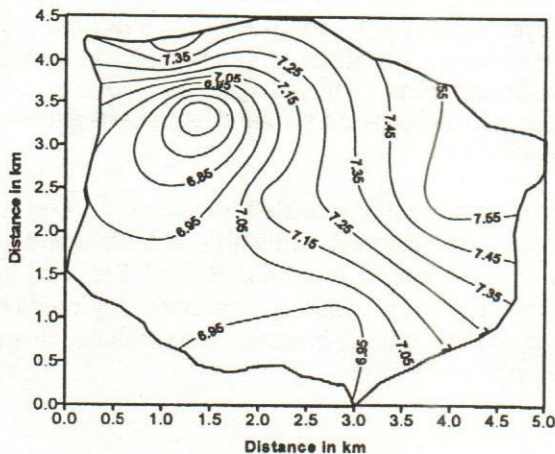


Fig.8 : The lateral variation of Water-Table (interval 0.1m).

indicates the sandy layer saturated with fresh water followed by a medium-coarse sandy layer of 400 Ω -m saturated good quality fresh water which may be treated as aquifer.

The lithology of the nearest borehole to the VES-A has been compared with the interpreted results as shown in **Figure.5(c)**.

VES-B (Housing) : The interpretation of sounding curve of VES-B gives four layer section. The first layer consists of dry top soil of resistivity 30 Ω -m with thickness of 0.5m. The resistivity of 42 Ω -m of the second layer indicates the composition of dry clay having thickness of 6.4 m. The third layer shows resistivity of 60 Ω -m and seems to be composed of finesand-clay containing moderately fresh water. The depth to the top of the water saturated zone from ground surface for this location is 6.9 m. Low resistivities of the next two layers indicate that the formations may be of clay/ sandy clay saturated with poor quality water.

VES-C (Kushtia Govt. College) : The sounding point located at Kushtia Govt. College is a wet land. At this site the top soil of 1.3 m thick shows resistivity of 2.2 Ω -m and is followed by a thin clay layer of 4 Ω -m with thickness of about 6 m. The depth to the top of the moderately fresh water saturated finesand-clay layer is 7.2 m having resistivity of 50 Ω -m. The resistivity of the estimated last layer at depth 35 m indicates a medium-coarse sandy formation with fresh water which may be used for groundwater abstraction.

VES-D (Zila School) : The interpretation of sounding curve of VES-D gives five layer section. The top layer consists of soil of resistivity 30 Ω -m with thickness 1 m. The second layer may be composed of sandy clay of resistivity 50 Ω -m having thickness 5.5 m. The resistivity of first and second layers are comparatively higher than those of the VES-A, VES-C and VES-F because of dry formations. The third layer shows resistivity of 30 Ω -m and seems to be composed of finesand-clay containing moderately fresh water. The depth to the top of the saturated zone from ground surface for this location is 6.5 m. Low resistivities of the next two layers might be due to the poor quality groundwater.

VES-E (Adarsha College) : At this location the top soil is more resistive showing the resistivity of 35 Ω -m reflecting the soil as dry and is followed by 2 m thick dry clay of resistivity 65 Ω -m. Below the second layer there is a 4.6 m thick clay of resistivity 10 Ω -m. The fourth layer consists of sandy clay having resistivity of 42 Ω -m with 19.4 m thick indicates a moderately fresh water saturated zone. The resistivity of 140 Ω -m of the obtained last layer might be composed of medium-coarse sand saturated with fresh water which may be treated as main aquifer.

VES-F (Police Line) : The first layer of this location consists of wet soil mixed with conducting particles of resistivity 2.5 Ω -m with thickness 1 m whereas the second layer is composed of wet clay of resistivity 10 Ω -m having thickness 6.5 m. The third layer shows resistivity of 58 Ω -m which seems to be composed of finesand- clay containing moderately fresh water. The last layer resistivity of 95 Ω -m falls in the resistivity range of medium-coarse grained sand saturated with fresh water.

Conclusion

The interpretation of vertical electrical sounding survey consists of expressing the information given by the field data in geologic features. With regard to the distribution of the electrical resistivity in the subsurface the interpretation is normally based upon the assumption that the subsurface consists of a finite number of distinct layers that are separated from each other by horizontal boundary planes. The best fit model parameters at every VES locations of the area investigated show a wide range of resistivity variation with depth and the presence of a very thick layer at the bottom.

Geoelectrical resistivity soundings carried out at different locations within the Kushtia Municipality showed that the soundings results were in good conformity with the geological and hydrogeological information of the area and provide useful data about the depth of the aquifer. The presence of water table at shallow depth in the dry season and an aquifer of medium-coarse grained materials within useable depth tending to support the area hydrogeologically favorable.

References

- BWDB (2000)** : Environmental Baseline of Gorai River Restoration Project, EGIS II, Dhaka Bangladesh.
- Ghosh D. P. (1971)**: The application of linear filter theory to the direct interpretation of geoelectrical resistivity sounding measurements, *Geophys.Prosp.*, vol.19, p.192-217.
- Islam M. S., Haque M. N. & Hasan M. A. F. M. R. (2001)** : Hydrogeological conditions in the northern part of Kushtia Sadar Upazila of Bangladesh, *The Journal of Geo-Environmental, Dept. of Geography and Environmental Studies, Rajshahi University, Bangladesh*, vol.1, p. 79-88.
- Khan F. H. (1991)** : The Geology of Bangladesh, Wiley Eastern Ltd., India, p. 207.
- Koefoed O. (1979)**: *Goesounding Principles 1, Resistivity sounding Measurements*, Elsevier Scientific Publishing company, Oxford.
- Nowroozi A. A., Horrocks S.B and Henderson P. (1999)** : Saltwater intrusion in the freshwater aquifer in the eastern shore of Virginia: a reconnaissance electrical resistivity survey, *Journal of Applied Geophysics*, vol.42, p. 1-22.
- Pekeris C. L. (1940)** : Direct method of interpretation in resistivity prospecting, *Geophysics*, vol. 5, p. 31-42.
- Shahid S. (2000)** : Groundwater potential modeling in a soft –rock area using GIS based integrated Geophysical approach, Ph.D. thesis, Dept. of Geology and Geophysics, IIT, Kharagpur, India, p. 239.
- Woobaidullah A. S. M., Rahman M, Hossain M. T. & Khaleque M. A, (1998)** : Results of geoelectric survey in deciphering the aquifer in around Dhaka city, *Dhaka University of Journal of Science*, .vol. 47(1), p. 93-101.
- Zohdy, A. A. R. (1989)** : A new method for the automatic interpretation of Schlumberger and Wenner sounding curves, *Geophysics.*, vol.54, No.2, p. 245-253.

Compaction Characteristics of Embankment Soils of Jamalpur Priority Project: A Case Study

Md. Rafiqul Alam¹, and A.S. Anwarul Islam²

Abstract

Bangladesh is a river-influenced land. Jamalpur district of Bangladesh is situated in the flood plain of the Jamuna and the Old Brahmaputra and is subjected to regular flooding every year causing extensive damages to lives, properties and standing crops. To protect this district from devastating flood embankment construction and maintenance is necessary. This paper deals with the evaluation of compaction of embankment soils of Jamalpur Priority Project, Jamalpur. Some officers and staff of River Research Institute and consultant of the project conducted field investigation in the study area. All the samples collected from the study area were tested and analyzed in the soil mechanics laboratory of River Research Institute in 1992. Authors obtained these data of Jamalpur priority project during their investigation at Soil Mechanics Laboratory of River Research Institute. The aim of the study was to evaluate the amount of compaction, embankment derives from natural causes and hence to correlate the findings with type of embankment materials. The salient results obtained from the study of the soil samples of the project are found as follows. For silty fine sand compaction range is 74.31% to 96.93%. For sandy silt compaction range is 64.06% to 91.79% and for sandy clay compaction range is 78.97% to 89.94%. This paper presents the results of field and laboratory investigation done on soil samples of some selected reaches along with the embankments and the conclusion thereof.

Introduction

Bangladesh Water Development Board is engaged in the development of the Vast and challenging water resources of Bangladesh. Several thousand kilometers of earth embankments were constructed over a number of years in the different parts of the country for river training and flood control, for irrigation and drainage purposes and for the protection of coastal areas from saline water during spate and cyclones. The earth embankments were generally constructed by placing of soils in different layers by head basket manually without compaction. Road embankments were also generally constructed without compaction.

The rate of construction was significantly slow; consequently much of the settlement took place before the "running surface" was laid. In order to construct an embankment it is essential to use material that can be both placed satisfactorily and compacted sufficiently so that it can form a long term stable fill which will not settle significantly.

So, for sufficient compaction equipment or movement of heavy machinery was allowed to undergo compaction naturally.

¹ Principal Senior Scientific Officer, ² Principal Scientific Officer (Addl. Charge), River Research Institute, Faridpur

Jamalpur district lies in the flood plain of the mighty Jamuna River and the Old Brahmaputra River and composed of alluvial soil deposits. Alluvial deposits range from flood sand to over bank silt and ponded silt and ponded clay. Most areas of the district are flooded annually (Alam, 1990). The problem in the area arises from flooding, which occurs from different sources such as local rainfall and over bank flow from rivers.

To protect the localities situated nearby the river Jamuna from its devastating flood, an earth embankment over a length of about 80 km was constructed on a priority basis. Starting from Bahadurabad, the embankment passes through Islampur and Madargonj Upazilla and ends at Jagannathgonj via Mulbari of Sharishabari upazilla. The consultant of the Jamalpur priority project came to River Research Institute and requested for collecting and testing the sample for evaluation of compaction. Accordingly River Research Institute collected the soil samples. Field density tests were performed in some selected locations of the earth embankment at Jamalpur constructed by head basket placing of materials. The embankment was old and it was used as village road but it was not compacted. The objective of the investigation was to study the amount of compaction that the embankment might have derived from natural causes. The importance of the study is to improve the engineering properties and qualities of soils used as sub grade of embankment. Compaction generally increases shear strength of the soil and hence the stability and bearing capacity. It is also useful in reducing the compressibility and permeability of soil.

Literature Review

Compaction of soil is the process by which the solid soil particles are placed more closely together by mechanical means, thus increasing the dry density (Wick, 1944). It is achieved through the reduction of air voids in the soil, with little or no reduction in the water content. The air voids cannot be eliminated altogether by compaction, but with proper control they can be reduced to a minimum. The bearing capacity of a earth dam or man-made fill can be very large if it is properly designed and compacted. Qualitatively speaking, compaction increases the shear strength and decreases the compressibility of the soil (Teng, 1981).

The compactness of a given compacted soil is expressed in terms of percentage of compaction. Representative samples of the soil are tested in the laboratory to determine its maximum dry density under a specific compaction. The maximum dry density, say 110 kN/m^3 is used as a basis for compaction. If the same soil is compacted in the field to a dry density of say, 100 kN/m^3 then the percentage of compaction said to be $100/110=91$ percent, or the soil is compacted to 91% of maximum density. Generally 95%-100% compaction is specified for fills supporting foundations. In areas where settlement is of less importance such as landscaped areas 90% compaction may be sufficient (Teng, 1981).

According to Knight (1966), compaction may accomplish the following objectives:

- It allows using practically any area, with any type of foundation materials, for construction of a useable facility.
- It reduces, or controls to a safe maximum, the detrimental stresses or deformation imposed on foundation soils due to the variable loads involved.

- It provides a rapid means of obtaining a relatively consolidated or stabilized foundation, using the available materials to allow economical construction of a facility designed for the site.

There are several methods by which the density of a soil can be increased either in the laboratory or in the field. Compaction is the term used to refer to the more or less rapid reduction in voids deliberately by mechanical means during the construction process in the field or during the preparation of a sample in the laboratory. Usually no water is expelled from the voids during compaction (Murthy, 1993). Natural compaction of an embankment can result from the following two causes:

- Consolidation to over burden pressure of the embankment.
- Seepage forces acting downstream through embankment causing adjustment of soil grains.

Compaction may be accomplished in the following ways:

- Reduction of voids or increase of density produced during the construction of an earthen embankment or dam.
- Reduction in voids produced in a layer of sub grade by roller during construction.

The purpose of compaction is to improve the qualities of the soil used either as a sub-grade material for roads, Highways, runways, canal embankments and in the fills of dams. According to Murthy (1993), the properties of the material that are important in the construction are as follows:

- High shear strength.
- Low permeability and water absorption.
- Little tendency to settle under repeated loading.

Compaction of a soil measured in terms of the dry density of the soil, which is the weight of soil solids per unit volume of the soil bulk. The dry density may be expressed as the mass of solids in gm/cm³ or kg/m³. If ρ_t is the bulk density and w is the moisture content, the dry density ρ_d may be expressed as:

$$\rho_d = \rho_t / (1+w)$$

The percent compaction is defined as,

$$\begin{aligned} \% \text{ Compaction} &= (\text{dry density}/\text{maximum dry density}) \times 100 \\ &= (\rho_d / \rho_{t \text{ max}}) \times 100. \end{aligned}$$

Good compaction is the result of the proper combinations of many variables. The process of compaction depends primarily of the following components:

- Specifications: A clear list of particulars as to the methods or the amount of compaction required by the designer.
- Moisture control: The specified range of moisture that is compatible with the soil type and the desired density.

- Compactive efforts: The number of coverage and type and size of equipment to be used.
- Depth of soil layer: a specification normally referred to as the lift thickness, which, when used with the conditions mentioned in item 2 and 3, will give the desired end result mentioned in item 1 (Knight, 1966).

Moisture control is the one variable that is the most sensitive slight changes and is different for each type of soil. A few of the additional variables that also affect the degree of compaction obtained are:

- Types and gradation of the material (granular, cohesive, swelling etc).
- Adequacy of blending of moisture operations on the fill or in the borrow area.
- Weather conditions at time of compaction (sunny, cloudy, windy, temperature etc.)
- Firmness of foundation beneath the fill (knight, 1966)

When considering all the variables that enter into the process of obtaining good compaction, it becomes quite evident that considerable experience and a thorough knowledge of soils and equipment are essential.

Methodology

Selection of Study Area

The study area was selected depending on the soil characteristics of different locations of three upazilla namely Islampur, Madargonj and Sharishabari through which the embankment passes.

Data Collection

Both the consultant and River Research Institute personnel investigated the study area thoroughly and agreed to collect samples for field and laboratory investigation. By selecting sites frequently the samples were collected randomly by ring method for field test and other samples were randomly collected by hand boring and packed in polythene bags for laboratory test. Then all the samples were taken to River Research Institute, Faridpur. All the data were collected from Soil Mechanics Laboratory of River Research Institute, Faridpur and from field test.

Data Preparation

For compaction, there are only two broad tests such as field test and laboratory test. Brief description of these two methods is given below. The two methods were used for analyzing the samples and data preparation.

Field Test

A total 24 field density tests were conducted in different locations of the project by ring method. The soil samples were collected by ring method and preserved in double polythene bags as per different location. Then the samples were brought in the laboratory. The mass of the samples and polythene bags and only polythene bags were taken. Then the mass of the soil was determined. The volume of the ring was also

determined. The wet density of the soils were determined by the relation, $\rho_t = M/V$ where M = mass of soil, V = volume of the ring. The field dry density was determined by $\rho_d = \rho_t / (1+w)$, where w = water content of the soil. Liquid limit, plastic limit, natural moisture content, unified soil classifications and grain size distribution tests were performed. The results were shown in Table-1.

Table-1: The test result of soil samples of field test in connection with Jamalpur Priority Project Study, Jamalpur

Bore hole No.	Location	Depth in (m)	Classification of materials	L.L (%)	P.L (%)	P.I (%)	N.M.C (%)	Field dry density by ring method kg/m ³
R ₂ . C ₅	Panchpaula	1	clay, little fine sand	45	25	20	27.52	1470
BHE-12	Mazcebari		fine sand, little silt	-	-	-	13.07	1264
BHE-15&16	Digalkandi	0.8-Borrow pit	silt, little fine sand	-	-	-	9	1286
BHE-16A	Char Telakpur	0.8-Borrow Pit	fine sand and silt	-	-	-	4.83	1418
CHE-12	Mohisbaton	1-Crest	fine sand, some silt	-	-	-	6.04	1238
BHE-10	Gubindi	0.75-Crest	silt, little fine sand	39	27	12	10.09	1496
CHAT-E-3	Kandapara	1.85-Crest	fine sand and silt	-	-	-	9.32	1206
RW-E-1 (ring)	Hasen Jawar	1.25-Crest	silt, little fine sand	43	25	18	26.94	1308
BHE-18-400M	Char Khaligapur	1.3-Crest	silt, some fine sand	-	-	-	19.44	114
BHE-49	Pogal digha	2.0-Crest	silt and fine sand	-	-	-	18.63	1663
R ₂ -C ₁	Sadupur	0.8-Crest	silt, trace fine sand	-	-	-	14.69	1340
BHE-7	Tokerchar	1.5-Crest	silt, trace fine sand	40	22	18	14.78	1480
BHE-27A	-	1-Crest	silt, little fine sand	-	-	-	13.35	1331
CHE-15	Mahmudpur	1.5-Crest	silt, little fine sand	-	-	-	3033	1282
BHE-25	Kulkandichar	1-Crest	silt, trace fine sand	-	-	-	14.80	1333
BHE-20	Kazipur	1.3-Crest	silt, some fine sand	-	-	-	17.36	1407
R ₃ -C ₂	Dalipur	1-Crest	clay, trace fine sand	53	27	26	31.00	1298
R ₂ . C ₁	Sadupur	1.8-Borrow Pit	silt, trace fine sand	37	27	10	18.39	1464
BHE-47	Mul Bari	1-Crest	clay, little fine sand	43	4	19	42.34	1111
RWSE-2	Baushi	0.9-R.L.	silt, little fine sand	39	27	12	20.20	1360
JAMAL-2	Pingal haty	1-Crest	clay, trace fine sand	48	25	23	21.19	1412
BHE-29	Karitayar	1-Crest	clay, trace fine sand	39	25	14	13.35	1331
BHE-22	Chakaria	2-Crest	clay, trace fine sand	42	25	17	26.67	1349
CHE-6	Chardudigacha	1-Crest	clay, trace fine sand	-	-	-	22.65	1181

Note: (-) indicates nil.

In the Table-1, liquid limit (L.L) of the soil samples is the water content at which the soil changes from the liquid state to the plastic state of the soil, which is determined in the laboratory by Casagrande's apparatus. Plastic limit (P.L) of the soil is the water content below which the soil stops behaving as a plastic material. It is determined in the laboratory by rolling the soil into a thread of approximately 3 mm diameter without crumbling. Plasticity Index (P.I) = Liquid limit (L.L) - Plastic limit (P.L) i.e. the difference between the liquid limit and the plastic limit of the soil. The natural moisture content (N.M.C) of the soil = M_w/M_s , where M_w = mass of wet soil and M_s = mass of dry soil. $N.M.C = (M_2 - M_3) / (M_3 - M_1) * 100$ where M_1 = mass of container with lid, M_2 = mass of container, lid and wet soil, M_3 = mass of container, lid and dry soil.

Laboratory Tests

A small amount about 3 kg of soil from each of the samples whose field density tests were performed brought to the laboratory for natural moisture content, grain size distribution, Atterberg Limit tests. For laboratory standard proctor test about 20 kg of soil from other locations were also brought to the laboratory. Liquid limit, plastic limit, N.M.C, gradation curve and unified soil classification tests were performed on the disturbed soil and ring samples also. To show relationship with Casagrande's A-line the results of limit tests were plotted and shown in **Figure-1**.

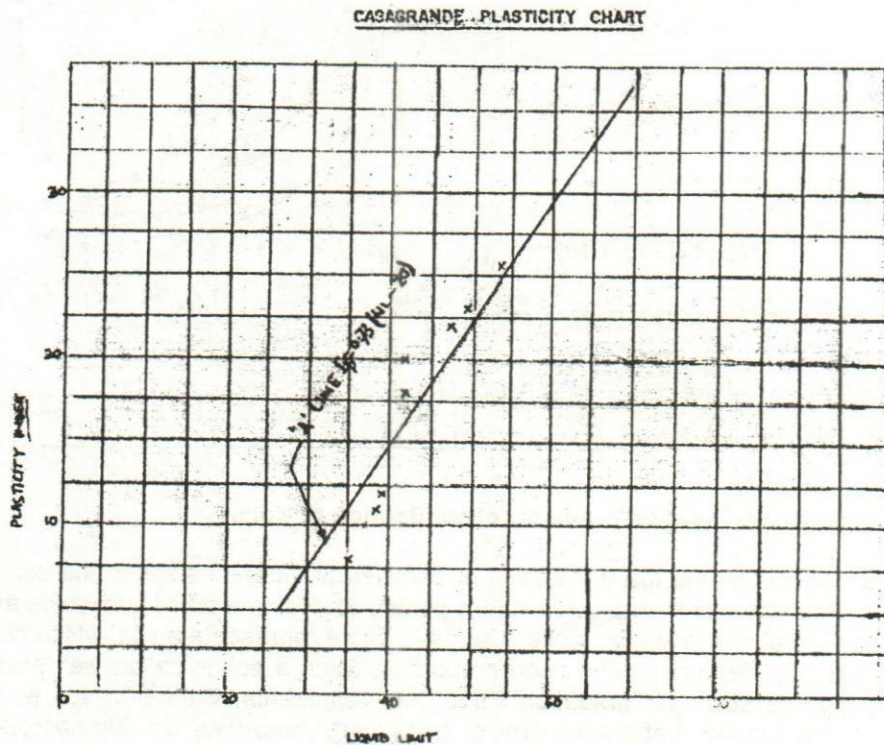


Figure-1: Casagrande's plasticity chart.

In **Figure-1**, the Casagrande's A-line has the equation $I_p = 0.73(W_p - 20)$. It separates clay materials from silt materials. The exact type of the soil is determined from the plasticity chart. The grain size distribution of selected samples is shown in **Figure-2**.

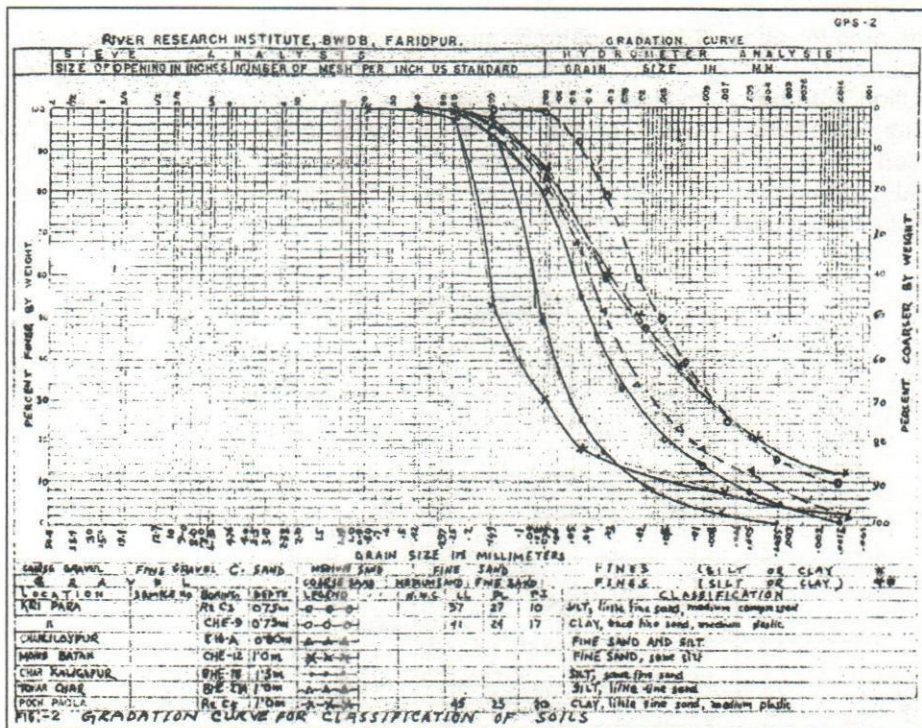


Figure-2: Gradation curve for classification of soils.

The **Figure-2** represents the distribution of particles of different sizes in the soil mass. The percentage finer N than a given size is plotted as ordinate on natural scale and the particle size as abscissa on log scale. The flat S curve represents a soil, which contains the particles of different sizes in good proportion. Such a soil is called well graded or uniformly graded soil. The gradation curve also represents whether a soil is coarse graded or fine graded. Laboratory proctor tests were performed on ring samples and other disturbed soil samples. To assess the amount of compaction and the water content required in the field compaction tests were done in the same soil in the laboratory. The tests provided a relationship between the water content and the dry density. The water content at which the maximum dry density is obtained from the relationships provided by the tests. Proctor used standard mould of 10.16 cm internal diameter and an effective height of 11.68 cm with a capacity of .00094 m³. The mould had a detachable base plate and a removable collar of 5.08 cm height at its top. About 3 kg of air dried pulverized soil passing 4.75 mm sieve was taken. Water was added to the soil to bring its water content to about 4% if the soil was coarse grained and to about 8% if it was fine grained. The water content should be much less than the expected water content. The soil was mixed thoroughly and covered with a wet cloth and left for maturing for about 15 to 30 minutes. The mould was cleaned, dried and greased lightly. The mass of the empty mould with base plate, but without collar was taken. The collar was then fitted to the mould. The mould was placed on solid base and full with fully matured soil to about one third of its height. The soil is compacted by 25 blows of rammer, with a free

fall of 310 mm. The blows are evenly distributed over the surface. The soil surface was scratched with a spatula before the second layer was placed. The mould was filled to about two thirds height with the soil and compacted again by 25 blows. Like wise the third layer was placed and compacted. The mass of the mould, base plate and compacted soil was taken and the mass of the compacted soil was determined. The bulk density of the soil was computed from the mass of the compacted soil and the volume of the mould. Representative soil samples were taken from the bottom, middle and top of mould for determining water content. The dry density was computed from the bulk density and the water content. The bulk density $\rho_t = M/V$ gm/ml, where M = mass of compacted soil in gm and V = volume of the mould in ml. Dry density $\rho_d = \rho_t / (1+w)$, w is the water content. The soil removed from the mould was broken with hand, more water was added to the soil so as to increase the water content by 2 to 3%. It was thoroughly mixed and allowed to mature. The test was repeated and the dry density and the water content were determined. Compaction curves were plotted between the water content as abscissa and the corresponding dry density as ordinate. It was observed that the dry density increases with an increase in water content till the maximum dry density attained. With further increase in water content, the dry density decreases. The water content corresponding to the maximum dry density is known as the optimum water content O.W.C or the optimum moisture content O.M.C. From the compaction curves made on the proctor test, the optimum moisture content and corresponding maximum dry density were determined.

The data for the compaction curves fits polynomial equations and R^2 values vary from 0.571 to 1. These figures are shown in the **Figure-3 to 6**.

The results of the liquid limit and plasticity index, natural moisture content and unified soil classifications, field dry density, maximum dry density, optimum moisture content and compactions were shown in **Table-2**.

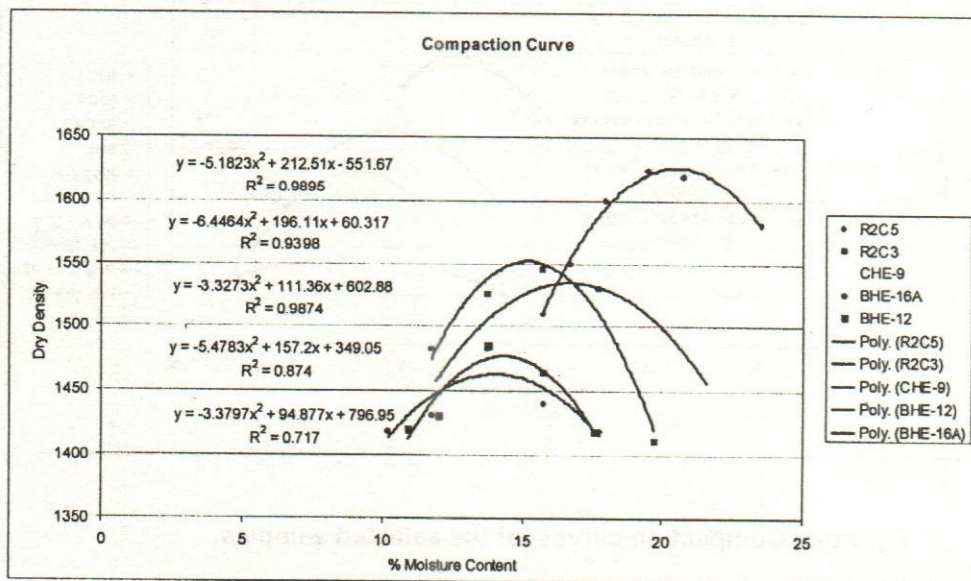


Figure-3: Compaction curves for the selected samples.

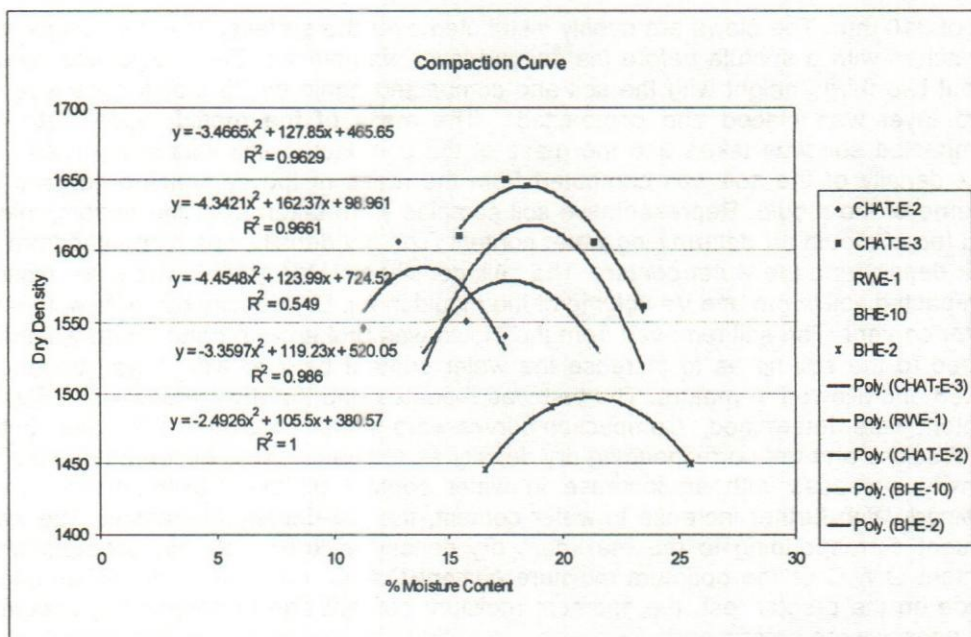


Figure-4: Compaction curves for the selected samples.

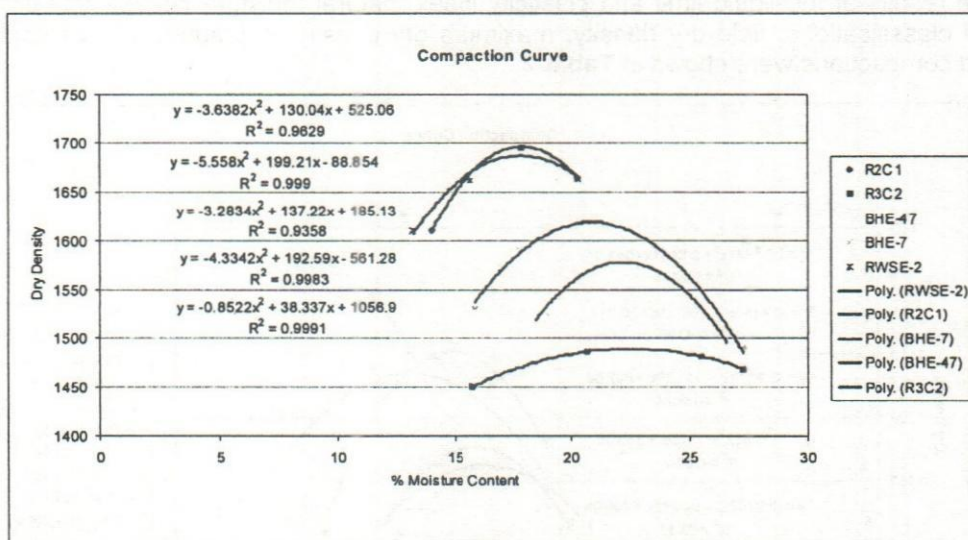


Figure-5: Compaction curves for the selected samples.

Table-2: The test result of soil samples laboratory proctor test in connection with Jamalpur Priority Project

Bore hole No.	Location	Depth in (m)	Classification of materials	L.L (%)	P.L (%)	P.I (%)	N.M.C (%)	Field dry density kg/m ³	Max. dry density kg/m ³	Optimum Moisture content (%)	Compaction (%)
BHE-17A	Khurma para	0.5-G.L.	fine sand, trace silt	-	-	-	7.53	-	1512	16	-
R ₂ : C ₃	Panchpaula	1	clay, little fine sand	45	25	20	27.52	1470	1635	20.5	89.93
R ₂ : C ₃	Kazipara	0.5-Crest	silt, little fine sand	37	27	10	20.40	-	1548	16	84.51
BHE-14	Kazihata	0.5-Borrow pit	silt, trace fine sand	35	27	8	40.37	-	1523	16.65	-
CHE-9	-	0.75	clay, trace fine sand	41	24	17	28.57	-	1544	16.93	78.97
BHE-12	Mazcebari	-	fine sand, little silt	-	-	-	13.07	1264	1493	14.70	84.68
BHE-32	-	0.8-Borrow pit	silt and fine sand	-	-	-	12.09	-	1467	14.75	-
BHE-15&16	Digalkandi	0.8-Borrow pit	silt, little fine sand	-	-	-	9	1286	1444	15.20	-
BHE-16A	Char Telakpur	0.8-Borrow Pit	fine sand and silt	-	-	-	4.83	1418	1464	14.90	96.93
CHE-12	Mohisbaton	1-Crest	fine sand, some silt	-	-	-	6.04	1238	1566	18.90	74.31
CHAT-E-2	Barnaria	0.8-Borrow Pit	silt, some fine sand	-	-	-	16.09	-	1623	13.40	64.06
BHE-10	Gubindi	0.75-Crest	silt, little fine sand	39	27	12	10.09	1496	1649	17.30	90.70
BHE-19	Caligapur	0.90-G.L.	fine sand, trace silt	-	-	-	14.07	-	1473	19.50	-
CHAT-E-3	Kandapara	1.85-Crest	fine sand and silt	-	-	-	9.32	1206	1581	18	76.30
BHE-11	Kolabudha	1-Borrow Pit	silt, some, fine sand	-	-	-	17.01	-	1649	18.45	-
BH-JAMAL-E1	Binandipara	1.2-Crest	fine sand, some silt	-	-	-	19.53	-	1530	17.00	-
BHE-23	Harindhara	1.3-Borrow Pit	silt, some fine sand	-	-	-	30.41	-	1479	18.92	-
RW-E-1 (ring)	Hasen Jawar	1.25-Crest	silt, little fine sand	43	25	18	26.94	1308	1623	18.35	87.26
BHE-18-400M	Char	1.3-Crest	silt, some fine sand	-	-	-	19.44	114	1468	20.00	77.92
BHE-49	Khaligapur Pogal digha	2.0-Crest	silt and fine sand	-	-	-	18.63	1663	1508	21.20	77.14

Bore hole No.	Location	Depth in (m)	Classification of materials	L.T (%)	P.L (%)	P.I (%)	N.M.C (%)	Field dry density kg/m ³	Max. dry density kg/m ³	Optimum Moisture content (%)	Compaction (%)
BHE-13	Islampur	0.8-Crest	silt and fine sand	-	-	-	18	-	1410	12.20	-
R ₂ -C ₁	Sadupur	0.8-Crest	silt, trace fine sand	-	-	-	14.69	1340	1710	18.00	91.79
BHE-7	Tokerchar	1.5-Crest	silt, trace fine sand	40	22	18	14.78	1480	1628	19.70	90.90
BHE-27A	-	1-Crest	silt, little fine sand	-	-	-	13.35	1331	1627	16.50	81.80
CHE-15	Mahmudpur	1.5-Crest	silt, little fine sand	-	-	-	30.33	1282	1537	22.50	83.42
BHE-25	Kulkandichar	1-Crest	silt, trace fine sand	-	-	-	14.80	1333	1583	18.20	84.18
BHE-20	Kazipur	1.3-Crest	silt, some fine sand	-	-	-	17.36	1407	1634	19.00	86.10
R ₃ -C ₂	Dalipur	1-Crest	clay, trace fine sand	53	27	26	31.00	1298	1491	24.00	87.07
BHE-1	Hasem	1.25	clay, trace fine sand	43	25	18	30.20	-	1593	23.50	-
R ₂ -C ₁	Sadupur	1.8-Borrow Pit	silt, trace fine sand	37	27	10	18.39	1464	1595	21.60	-
BHE-27	Gujumary	1-Borrow Pit	clay, little fine sand	42	22	20	26.22	-	1570	22.80	-
BHE-47	Mul Bari	1-Crest	clay, little fine sand	43	4	19	42.34	1111	1582	23.20	70.22
RWSE-2	Baushi	0.9-R.L.	silt, little fine sand	39	27	12	20.20	1360	170815 97	12.75	86.87
BHE-46	Baghmara	1.2-Borrow Pit	silt, some fine sand	-	-	-	14.50	-	1566	15	-
RWSE-2	Baushi	0.67-G.L.	silt, some fine sand	38	27	11	19.97	-	1628	20	-
JAMAL-2	Pingal haty	1-Crest	clay, trace fine sand	48	25	23	21.19	1412	1590	23.65	86.73
BHE-29	Karitayar	1-Crest	clay, trace fine sand	39	25	14	13.35	1331	1563	11.20	89.94
R ₁ -PS ₃	Chatal	-	fine sand, some silt	-	-	-	4.34	-	1545	16.40	-
BHE-33	Bridge	1-Borrow Pit	silt, trace fine sand	-	-	-	6.39	-	1685	21.50	-
R ₃ -C ₁	-	0.65-Borrow Pit	silt, trace fine sand	-	-	-	26.56	-	1604	17.50	-
BHE-22	Chakaria	2-Crest	clay, trace fine sand	42	25	17	26.67	1349	1590	22.80	84.12
BHE-41	Karia	1-Borrow Pit	silt, little fine sand	36	26	10	6.61	-	1545	13.90	-
BHE-34	kaila Kandi	-Borrow Pit	silt, trace fine sand	-	-	-	14.00	-	1557	20.50	-
BHE-43	Chunjiapatal	-Borrow Pit	silt, trace fine sand	-	-	-	14.00	-	1594	18.80	-
R ₁ -PS ₄	-	-Borrow Pit	clay, trace fine sand	47	25	22	16.00	-	1614	22.80	-
CHE-6	Chardudigacha	1-Crest	clay, trace fine sand	-	-	-	22.65	1181	1724	17.90	73.17

Bore hole No.	Location	Depth in (m)	Classification of materials	L.L. (%)	P.L. (%)	P.I. (%)	N.M.C. (%)	Field dry density kg/m ³	Max. dry density kg/m ³	Optimum Moisture content (%)	Compaction (%)
BHE-8	Shajadpur	0.75 G.L.	silt, trace fine sand	38	27	11	10.12	-	1736	19.30	-
BHE-35	Char Pakerdah	-Borrow Pit	fine sand, some silt	-	-	-	10.00	-	1772	14.50	-
BHE-36	Char Chandpur	Borrow Pit	clay, trace fine sand	42	24	18	12.00	-	1754	18.40	-
BHE-38	Tartapara	1.5-Borrow Pit	clay, trace fine sand	44	25	19	17.00	-	1700	20.40	-
BHE-39	Khilkati	Borrow Pit	silt, little fine sand	-	-	-	14.00	-	1620	16.40	-
BHE-44	Suakor	Borrow Pit	silt, little fine sand	-	-	-	13.00	-	1768	16.80	-
CHE-9	-	0.75-Crest	clay, trace fine sand	-	-	-	19.00	-	1616	23.50	89.06
BHE-16	Bhaddra	1- Crest	silt, some fine sand	-	-	-	-	-	16.20	16.20	-

Note: (-) indicates nil.

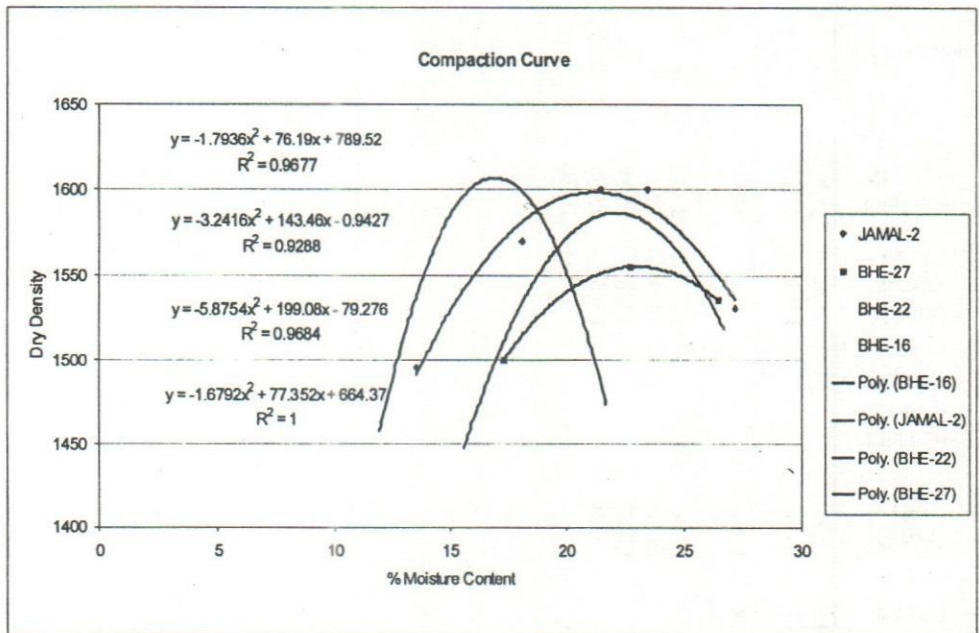


Figure-6: Compaction curves for the selected samples.

Results and Discussions

From the tested result it is observed that the materials of the study area consist of silty fine sand, sandy clay and sandy silt. It is evident that the soil of the earth embankment is cohesionless in most of the locations and cohesive in some locations. It is also found that the compaction range of the materials varies from 64% to 92%. In this case, only the natural watering was supplied. So the degree of compaction was not satisfactory. But it is observed that only one soil sample of the embankment at Telapukur exceptionally indicated 96.93% compaction which was satisfactory. It is also found that water contents of the soil samples varied from 4.34% to 42.34%.

Conclusions and Recommendations

For sandy clay and sandy silt materials under conditions to the tested embankment 4.34%-42.34% moisture content and 70%-97% compaction, the following conclusions regarding natural compaction are derived from this study:

- An increase in compaction of the embankment is necessary.
- Water content in soil of some areas of the study is very high. So, it is necessary to reduce moisture content by applying proper compaction according to material.

For silty fine sand materials slight increase in compaction is observed. This increase is probably due to the much permeability and cohesion less characteristics of the material which used washing of fines down through the embankment.

There is an apparent increase in density due to seepage forces of downward percolating water. In conclusion the following be mentioned:

- In fine sand where seepage is greater and forces are stronger only a slight density increase is observed.
- Densities in newly placed materials are lower than the materials in old embankment.
- In most cases it is found that moisture content increases with depth.

Most rainwater runoff of the embankment and small amount that percolated into the embankment seeps at such a slow rate and is discontinuous in nature that no influential forces are developed.

Acknowledgement

The authors are grateful to Md. Osman Gani Biswas, S.T.-C, Md. Mojibur Rahman, S.T.-B and other officers and staff of Geotechnical Research Directorate of River Research Institute those who were associated with field and laboratory works. The authors are thankful to the consultants of Jamalpur Priority Project study, Jamalpur for planning the study.

References

- Alam, M.K.H., Shahidul, A.K.M., & Khan, M.R.(1990), " Geological Map of Bangladesh" Geological Survey of Bangladesh.
- Das, B.M. (1987), " Advanced Soil Mechanics", 2nd edition. McGraw-Hill Book Company.
- Knight, D.K. (1966), " Compacted Fills", Proceedings of the Montana Conference on soil mechanics, Foundation Engineering, Helena, Montana. USA.
- Mrs Wick A.H.D (1944), "The Basic Principle of Soil Compaction & their Application" International Civil Engineering
- Murthy, V.N.S. (1993), " A Test Book of Soil Mechanics & Foundation Engineering" Fourth Edition, Delhi, India.
- Teng, W.C. (1981), " Foundation Design", 8th Edition, Practice-Hall of India Private Limited, New Delhi.
- Terzaghi, K. (1949), "Soil Mechanics in Engineering Practice", 3rd Edition, John Wiley & Sons, Inc. New York.

Abbreviations

p_d	=	Dry density
p_t	=	Wet density
$p_{d\max}$	=	Maximum dry density
N.M.C	=	Natural moisture content
L.L.	=	Liquid Limit.
P.L.	=	Plastic Limit
P.I.	=	Plasticity Index.

Rainwater Harvesting in Bangladesh: A Sustainable Source of Safe Water

Md. Alauddin Hossain¹, and A.K.M. Ashrafuzzaman²

Abstract

Groundwater is the main source of water supply in urban and rural areas of Bangladesh. Though groundwater is available in Bangladesh, but the availability of groundwater for drinking purposes has become a problem for the arsenic and excessive dissolved iron in groundwater. On the other hand, surface water polluted by point as well as non-point sources and in dry season the country is facing acute shortage of both surface and groundwater for their daily life. Under these circumstances, an alternative source of drinking water is a crying need for the country. Rainwater harvesting can be considered as a viable source as it is the purest among the water sources. The existing house-roof could be used as catchment surface for sufficient rainwater harvesting. The storage tank represents the largest investment in rainwater harvesting system. The study showed that for full utilization of rainwater potential for average family in the rural areas of Bangladesh, a storage tank of capacity 4.4m³ is required for an uninterrupted water supply and at a constant rate throughout the year and 4.4m³ tank could be affordable by the rural dwellers.

Introduction

The sources of water in Bangladesh are surface water, groundwater and rainwater. The availability of water in terms of quantity and quality, present situation and problems associated with the sources have been discussed below:

Surface Water Availability and Problems

Surface water is abundant in the wet season in Bangladesh. An estimated 795,000 million cubic meter (Mm³) of surface water is discharged per year through the Ganges-Brahmaputra system, in the downstream of the confluence of the Ganges and the Brahmaputra. This is equivalent to 5.52m deep water over a land area of 144,000 km². There are other rivers discharging surface water into the Bay of Bengal. In dry season country suffers due to shortage of water both surface and groundwater (BUET, 2004)

Traditionally, before and during the early stages of tubewells installation by UNICEF, that is in 1970 decade rural water supply was largely based on protected ponds (surface water). People used surface water (ponds, dug well and river water) for domestic purposes. There are about 1,288,222 ponds in Bangladesh having an area of 0.114 ha per pond and 21.5 pond per mauza. About 17% of these ponds are derelict and probably dry up in the dry season. But surface waters receive pollutants from agricultural, industrial, domestic and municipal sources. The bacteriological quality of water in these ponds is extremely poor due to unhygienic sanitary practices and absence of any sanitary protection. Many of these ponds are chemically and bio-

¹ Senior Scientific Officer & ² Scientific Officer, River Research Institute, Faridpur

chemically contaminated for fish culture.

The faecal coliform concentration in most surface water sources lies in the range of 500 to several thousand per 100ml. As a result water-borne diseases due to ingesting water that contains bacteria/viruses would affect peoples. Water-borne diseases include typhoid, cholera, dysentery and diarrhoeal diseases (BBS, 1997).

Groundwater Availability and Problems

Groundwater is the main source of water supply in urban and rural areas of Bangladesh. Except for few hilly regions Bangladesh is entirely underlain by water bearing aquifers at depths varying from zero to 20m below ground surface. Groundwater in Bangladesh is available in adequate quantity, but the availability of groundwater for drinking purposes has become a problem for the following reasons (BUET, 2004):

- Arsenic in groundwater;
- Excessive dissolved iron;
- Salinity in the shallow aquifers in the coastal areas;
- Lowering of groundwater level;
- Rock/stony layers in hilly areas.

So, it may be said that in spite of heavy rainfall, readily accessible groundwater and large river systems in this country, at present water scarcity for drinking purpose is the major problem in Bangladesh due to arsenic contamination in groundwater and surface water pollution by point sources and non-point sources. Under these circumstances, an alternative source of drinking water is a crying need for the country. This source needs also to be safe, cost-effective, available, sustainable and acceptable. Rainwater harvesting may be the solution for drinking water supply for the rural people in Bangladesh.

Methodology

The methodology of this study is as follows:

- To review literature on the rainwater harvesting system.
- To collect data and information for the calculation of the storage infrastructure.
- To assess the capacity of the storage tank for an average family size.
- To assess its (storage tank) affordability.

Literature Review

Concept of Rainwater Harvesting System

Rainwater harvesting is the collection of raindrops. In most cases, a roof is used for this purpose. The rainwater then flows through the gutters, into a collection tank.

Rainwater harvesting technologies are simple to install and operate. No specialized skill is necessary to operate the system. It does not require any pumping device to abstract

the water. The system also requires little maintenance work. Local people can be easily trained to implement such technologies and construction materials are also readily available. Rainwater harvesting is convenient in the sense that it provides water at the point of consumption, and family members have full control of their own systems, which greatly reduces operation and maintenance problems. Running costs, also, are almost negligible. Water collected from roof catchments usually is of acceptable quality for domestic purposes. It offers immense convenience equal to piped water supply. The major advantage of the rooftop rainwater harvesting system (RWHS) is that the system is independent and suitable for scattered settlements.

The quantity of water that can be harvested is determined by the amount of rainfall and the size of catchment (or roof) area. Now, it is obvious to know how much rainfall and what size of roof surface can harvest what quantity of water. In principle 1 liter of water can be harvested from 1mm rainfall on 1 square meter effective area. Though there is some losses in this system due to lost by evaporation and for washing the catchment area using first flush rain that produces inferior quality rainwater, but for the simplification here it is assumed zero.

Generally rainwater is clean and fresh enough to drink. There is no problem collecting rainwater from corrugated iron sheet roof or tiles roof. If the system remains clean and properly flushes the first foul rainwater, then the quality of stored water conform to the WHO standard except the limit of pH value. pH value is a little bit higher than the WHO guideline value. To minimize pH value of the stored water one should apply a thick cement paste layer inside the tank during construction (NGO Forum for drinking Water Supply and Sanitation, 2001).

Studies in Thailand, India, and Sri Lanka, show that properly stored rainwater is safe from bacteria and can be stored for many months. Also, research in Bangladesh by the International Center for Diarrhoeal Disease Research, Bangladesh, (ICDDR) confirms that rainwater can be a safe drinking water source.

Components of Rainwater Harvesting System (RWHS)

Rainwater Catchments (Roofing Materials & Size in Bangladesh)

The catchment area for rainwater collection is usually the roof, which is connected with a gutter system to lead rainwater to the storage tank. Different types of roofing materials are used in Bangladesh. These include cement concrete, tiles, corrugated iron (C.I.)/metal sheet, straw with and without polythene covering, bamboo with polythene covering. According to the Bangladesh Bureau of Statistics (1995), about 48% households in the rural area have tiles, C.I./metal sheet as roofing materials. These roofing materials are suitable for rainwater catchment. However, others can be used with some modifications such as use of polythene covering for straw roofing. A thatched roof can also be used as catchment area by covering it with polyethylene but it requires good skills to guide water to the storage tank. In coastal areas of Bangladesh, cloths fixed at four corners with a pitcher underneath are used during rainfall for rainwater collection.

There is no data availability on roof size in Bangladesh. However, a limited field survey was carried out in Chuadanga, one of the arsenic affected districts (Ferdausi, 1999).

Only the household having metal sheet as roof materials were considered and the data is given in **Table 1**.

Table 1: Roofing size and no. of household in a typical rural area

Roofing size	<20m ²	20-40m ²	40-60m ²	60-80m ²	>80m ²
No. of household	21	18	36	14	11

(Source: Ferdausi, 1999)

The data was collected from 100 households by random selection. This data may not be applicable in all rural conditions in Bangladesh. However, it provides an idea about the available catchment area.

Gutters and Down-Pipes

These are the component that catch the rainwater from the roof catchment surface and transports it to the cisterns (storage tank) and flush foul water. The gutters need to be well supported so that it does not sag or be pulled away from its supports due to its weight when loaded with water. In addition, it needs an adequate slope for its entire flow length so that stagnant pools, which could provide breeding places for mosquitoes, are avoided. The gutters and down-pipes are made of different kinds of locally available materials. Different materials can be used as gutters and down-pipes and material requirements depend on the roof size. Some are fabricated from corrugated iron (C.I.) sheet, galvanized iron (G.I.) pipes and PVC pipes. Others are of bamboo, betel nut trees, palm trees or even the bark of banana plants made by the households themselves.

Storage Tanks (Cistern)

Storage tank is that system or structure where the collected rainwater is stored. There are different kinds of storage tanks in Bangladesh. The available storage tanks are Motka (earth-made), ferrocement tanks, plastics buckets both cylindrical and rectangular shape, galvanized iron sheet tanks, RCC ring tanks, brickwork tanks of different volumes according to the sizes of the families. The capacities of tanks are determined by the requirement of water for the users or householders depending upon the types of uses of it and also of the annual rainfall availability and the size of the roof. The average life expectancy of a storage tank is considered about 10-15 years. There are both above ground tank and underground tank in Bangladesh. For underground storage tanks, there is required the use of a pump to draw water to the surface.

Technical Feasibility Study

Rainwater Availability

A 10-year rainfall pattern based on the mean rainfall intensity recorded in 28 stations from the period 1987 to 1996 is shown in **Figure 1**. It appears that the average yearly rainfall in the country during 1987 to 1996 varies from 2000-2800mm, that is, 2.0 to 2.80m³ of rainwater is available per m² of catchment area each year for the

development of a rainwater based water supply system. However there are some losses in the collection system. The available rainwater can be estimated using the following equation (Ahmed, 1999 and Hossain, 2004):

$$Q = C I A \quad (1)$$

Where, Q = Total quantity of rainwater available in m^3 /year, C = Coefficient of available runoff, I = Rainfall in m /year and A = Catchment area in m^2

From equation (1), it can be said that the quantity of water that can be harvested is determined by the amount of rainfall, size of catchment (or roof) area and runoff coefficient. For this calculation, if we assume for rural area of Bangladesh as the following:

A = Average effective house roof area = $3m \times 4m = 12m^2$

I = Yearly lowest rainfall = 1200mm (1.2m)

$C = 0.75$, then $Q = 10.8m^3 = 10,800$ litre

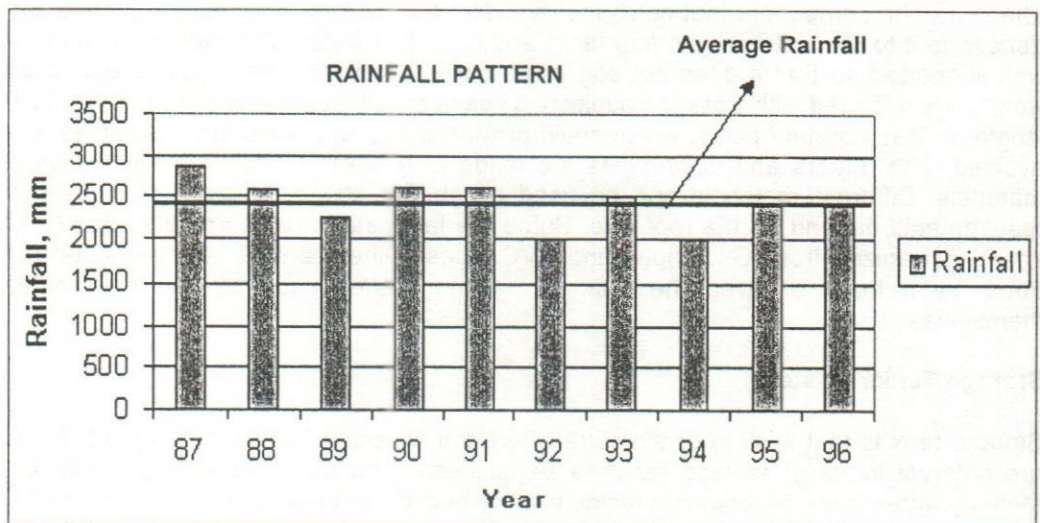


Figure 1: Variations of annual rainfall in Bangladesh (Source: Ahmed, 1999)

If we assume I = average rainfall = 2500mm (2.5m), then $Q = 22.5m^3 = 22,500$ litre. About 25 per cent of the rainwater may be assumed to be lost by evaporation and for washing the catchment area using first rain that produces inferior quality rainwater. For this reason $C = 0.75$ has been considered

On the other hand, According to the Bangladesh Bureau of Statistics (1995), the average household size is 5.48 persons and 57% population having household size between 4 to 7. The average household size is taken as 6 for the calculation and the daily water consumption assumed for drinking and cooking purposes is 5 liter per capita per day (lpcd). So, water required for the average family/household size for whole year is $Q = 5 \times 6 \times 31 \times 12 = 11,160$ litre. Therefore, it has been seen that the existing house roof could be used as catchment surface for sufficient rainwater harvesting. However, annual rainfall of Bangladesh varies from 1200mm to 5500mm (NGO Forum for Drinking Water

Supply and Sanitation, 2001) that indicates a significant potential for harvesting rainwater and thus it can be a sustainable water source for the coming future.

Rainwater Catchment (Roofing Size) Calculation

Rainwater can be collected from any types of roof but concrete, tiles and metal roofs give cleanest water. The minimum catchment area A, can be derived for a family from Equation (1) as follows (Ahmed, 1999 and Hossain, 2004):

$$A = 0.365qN/CI \quad (2)$$

Where, A = Catchment area in m^2 , q= Required water per capita per day in litre (lpcd)
N= Number of people for the family, C= Runoff co-efficient, I= Rainfall in m/year

The Equation (2) can be written for an average annual rainfall, I= 2.4 m/yr as indicated in **Figure 1** and a co-efficient of runoff C= 0.75 in the following form:

$$A = 0.203qN \quad (3)$$

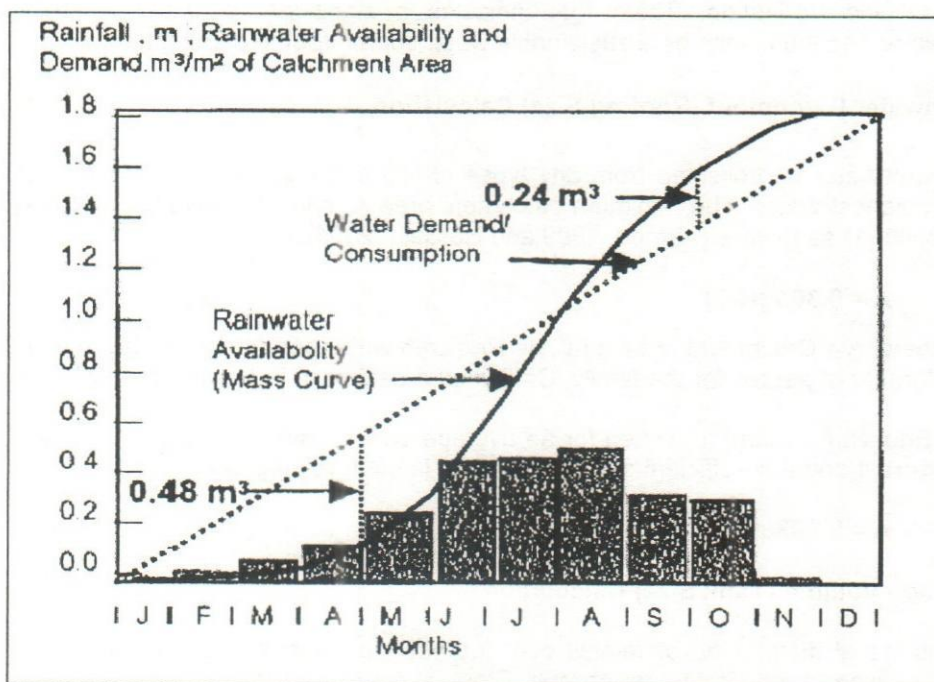
Storage Volume (Tank Size) Calculation

The unequal distribution of rainfall over the year requires storage of rainwater during rainy season for use in the dry season. Storage volumes of rainwater for the year round use are calculated by using mass curve method. Household size is one of the important parameter in designing a rainwater harvesting system specifically by using the mass curve analysis method. It is related to the total water demand, storage volume and catchment area. The minimum volume of the storage tank V, required for rainwater harvesting can be computed by the equation (Ahmed, 1999 and Hossain, 2004) as follows:

$$V = 0.365fqN \quad (4)$$

Where, V= Volume of storage tank in m^3 , f = the fraction of total available rainwater to be stored for consumption at a constant rate throughout the year, q= Required water per capita per day in litre (lpcd), N= Number of people for the family.

The total annual rainfall in 1996 as shown in **Figure 1** is approximately equal to the average annual rainfall of the last 10 years. The monthly distribution of average rainfall in 1996 shown in **Figure 2** and it is assumed to represent the average condition. The rainwater availability mass curve assumption and cumulative consumption/demand of total available rainwater at constant rate is also shown in **Figure 2**.



(Source: Ahmed, 1999)

Figure 2: Rainfall intensity, cumulative rainfall availability and demand

The mass curve has been prepared considering the fact that 75 per cent of the rainwater would be available. It may be observed that there is a shortfall of 0.48 m^3 in the dry periods and an excess of 0.24 m^3 during rainy season. For full utilization of rainwater potential, a storage tank of capacity 0.72 m^3 that is 40 percent of the available rainwater is required for uninterrupted water supply at a constant rate throughout the year. However, if only drinking and cooking water is harvested, the sizes of the storage tank and catchment area would be smaller and within an affordable range of a family. Substituting $f = 0.4$ in Equation (4) for representative rainfall distribution of 1996, the minimum volume of the storage tank required for rainwater becomes:

$$V = 0.146qN \quad (5)$$

The average household size is $N=6$ and the daily water consumption for drinking and cooking purposes is $q=5$ liter per capita per day (lpcd). Substituting these value in equation (5), we get minimum volume of the storage tank, $V=4.38 \text{ m}^3=4.4 \text{ m}^3$, that is 4400 liter.

The size of tank for a typical family varies between 2.92 and 4.4 m^3 based on family size 4 and 6 respectively. There is a regional variation of rainfall and rural poor people has limited catchment area. For a particular family required water can be collected from different size of catchment area based on availability of rainwater which is shown in Figure 3 below as follows.

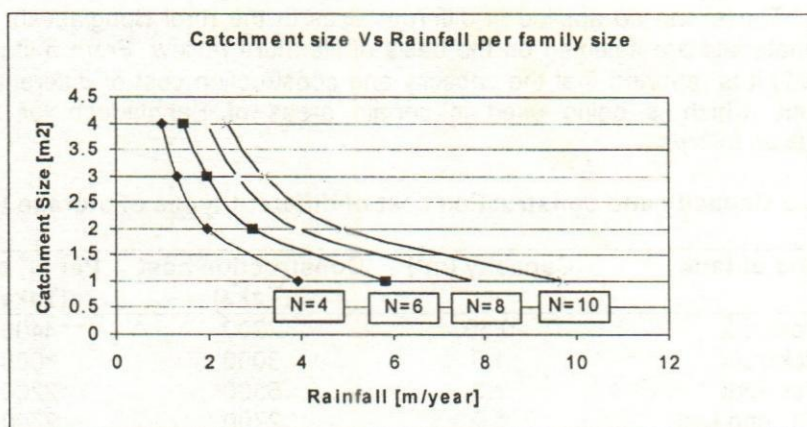


Figure 3 Required catchments size and rainfall for a typical family (Source: Hossain, 2004)

Affordability Study

The storage tank represents the largest investment in a rainwater harvesting system. One advantage for the household in collecting rainwater from its roof is that the roof has already been paid for and so additional investments are limited to tanks and gutters.

Materials and Costing of Gutters and Down-Pipes

Different materials can be used as gutters and down-pipes and material requirements depend on the roof size. From a study by Ferdausi (1999) in Bangladesh, it is noted that the bamboo made gutters and down-pipes have short life span. It normally works properly only one season. Again, leakage is a major concern in case of bamboo and wood made gutters and down-pipes. The cost of G.I. pipes is very high compared to other materials. PVC pipes are low-cost and readily available at the rural areas of Bangladesh. The PVC pipes are suitable materials for gutters and down-pipes. **Table 2** gives the costing of gutters and down-pipes. The cost includes about 8 meter guttering and down-pipe with accessories and labor cost.

Table 2 Costing of gutters and down-pipes

Materials	Total cost (Taka)
Bamboo made	220
Wood made	640
PVC pipes	740
G.I. pipes	2240

(Source: Ferdausi, 1999)

Materials and Costing of Storage Tanks

A storage tank is the most expensive component of a rainwater harvesting system. The storage tanks are constructed from different materials depending on local situation. Some potential materials for storage tank have been selected after reviewing different

documents. These can be applied in different sizes in the rural Bangladesh. No fixed design or materials are selected on the basis of literature review. From a study (NGO Forum, 2001) it is reported that the capacity and construction cost of different types of storage tank, which is being used in certain areas of Bangladesh for rainwater harvesting is as follows:

Table 3 Capacity and construction cost of different types of storage tank

Sl. No.	Type of tank	Capacity (m ³)	Construction cost (Taka)	Per m ³ cost (Taka)
1	Brickwork	0.50	2200	4400
2	Brickwork	1.0	3000	3000
3	Brickwork	2.5	5500	2200
4	RCC ring tank	1.0	2700	2700
5	RCC ring tank	2.5	4000	1600
6	Ferrocement jar	0.5	2900	5800
7	Ferrocement jar	1.0	3500	3500
8	Ferrocement jar	2.5	4500	1800
9	Ferrocement tank	2.5	4100	1640
10	Ferrocement tank	3.2	5500	1719
11	Motka (earth-made)	0.5	350	700
12	Motka (earth-made)	1.0	600	600

(Source: NGO Forum for drinking water supply and sanitation, 2001).

From the above table, it may be said that the cost of a rainwater harvesting system depends on the type of system, i.e. capacity of the tank and the construction materials used. The cost per unit volume of the tank decreases with increase in tank size. As seen from Table 3, the cost of earthen jars (Motka) is cheaper than other tank materials. The estimated cost of RCC ring tank and ferrocement tank (cement reinforced with iron mesh or wires) is found to be relatively cheaper than other tank materials, because of its thinner size.

However, the capital cost of the designed system (4.4m³) in Bangladesh using RCC ring materials will cost about 6500Taka, while if Ferrocement tank materials is considered, the cost will be about 7000Taka. Comparing the two, the use of RCC ring tank material could be better. The main advantage of the RCC tank is the familiarity of the construction process with the local people. This is true because, RCC ring tanks are used and constructed widely in the rural areas of Bangladesh for sanitary latrine construction.

Under the affordability assessment, information from the office of Bangladesh Bureau of Statistics (1997) shows that the average annual income of the rural dwellers is about 36,000Taka. This amount is seen to be greater than the amount required to own the designed 4.4m³ storage tank under the two types of construction materials considered above. The implication of this is that, the 4.4m³ storage tank could be affordable by the rural dwellers in Bangladesh.

Conclusions and Recommendations

Conclusions

The rainwater harvesting system is found to be technically feasible on the basis of the prevailing rainfall pattern and it can be a good source of water supply in the coastal, in the hilly, and in the acute arsenic affected areas in Bangladesh. For full utilization of rainwater potential for average family in the rural areas in Bangladesh, a storage tank of capacity 4.4m^3 is required for an uninterrupted water supply and at a constant rate throughout the year. Affordability assessment shows that the 4.4m^3 tank could be affordable by the rural dwellers.

Recommendations

Though, the designed system is seen to be affordable when compared with the average annual income, but this may not be true for those earning below the poverty line. In this regard, there is need to extend financial assistance to this category of people, which could be in the form of micro-credit system, grants from Government, grants from NGOs and donors.

References

- Ahmed MF (1999):** Rainwater Harvesting Potentials in Bangladesh, Proceedings of the 25th WEDC Conference on Integrated Development for Water Supply and Sanitation, Addis Ababa, Ethiopia, 363-365.
- Bangladesh Bureau of Statistics (1997):** Statistical Year Book of Bangladesh, Ministry of Planning, Govt. of People's Republic of Bangladesh.
- Bangladesh Bureau of Statistics (1995):** Statistical Year Book of Bangladesh, Ministry of Planning, Govt. of People's Republic of Bangladesh.
- BUET (2004) :** Water Supply Situation Analysis, [online] http://www.buet.ac.bd/itn/publications/as_mitigation/as_mitigation_part4_2.pdf [2004, August 30].
- Ferdausi SA (1999):** Study of Low-Cost Arsenic Mitigation Technologies for Application in Rural Bangladesh. M.Sc. Thesis SEE 087, Department of Sanitary and Environmental Engineering, IHE, Delft, The Netherlands.
- Hossain MA (2004):** Rainwater Harvesting in Bangladesh: A Sustainable Source of Safe Water. Individual Study Report for M. Engg in Water Resources Management, UNESCO-IHE, Delft, The Netherlands.
- NGO Forum for Drinking Water Supply and Sanitation (2001):** Rainwater Harvesting System. NGO Forum for Drinking Water Supply and Sanitation, Bangladesh.

Optimising the Planning and Engineering Design of Hydraulic Structures for Shrimp Culture in Bangladesh

Faruq Ahmed Mohiuddin¹, and Wahiduzzaman¹

Abstract

The coastal polders in the districts of Cox's Bazar, Khulna, Satkhira and Bagerhat in Bangladesh are very suitable for shrimp cultivation. Rapid development of shrimp farming in the extensive coastal and brackish water areas in southern part of Bangladesh has made a very significant contribution to the national export earnings. But unplanned shrimp farming development has led to decrease of shrimp production rate, degradation of agricultural land and have negatively affected the livelihoods of local people. The Fourth Fisheries Project (FFP) has been taken up by the Government of Bangladesh with the objectives of increasing production of shrimp by rehabilitating the Third Fisheries Project (TFP) polders (4 nos.) and conducting Feasibility Study of Polder No. 15 in the South West Region. The project area is located in the district of Khulna and Satkhira. Specialized services were provided by IWM for shrimp culture management to the Consultants of the Feasibility Study of Polder no. 15 and rehabilitation assessment of TFP Polders (5, 23, 31 and 32) by optimising the engineering plan and design of hydraulic structures with the aid of mathematical models and assist in proper water management in the polders. One-dimensional hydrodynamic mathematical modelling technique has been applied to assess water level and discharge at the un-gauged locations inside the polders and in its periphery. The engineering plan and design of the hydraulic structures have been optimised by the selection of dimensions and vantage of the structures by assessing the performance of the structures fulfilling the required design depth (0.6m to 0.9m) of the shrimp culture pond (block by block) with exchange of minimum 50% to 200% of water within a fortnight. The proposed exchange rate of water is an indicator of required water quality of shrimp culture.

Keywords: Coastal, Polder, Shrimp, Engineering Plan, Design, Mathematical Model, Water Management, Shrimp Culture, Vantage

Introduction

Bangladesh experiences colossal damages frequently due to disastrous floods and cyclones. To mitigate flood damage embankments have been constructed over the years along riverbanks. These engineering works and developments have been beneficial in reducing damages of properties and intensification of agricultural food production but gave rise to adverse impacts on the environment, such as (i) reduction of flood plain area, (ii) consequent increase in flood flow and water level within the embanked flood channel, (iii) change in sediment movement regime because of changed channel hydraulics, (iv) drainage congestion etc. Computer based mathematical models are being increasingly used by engineers and planners in the

¹ Senior Specialist, Institute of Water Modelling, Dhaka

country for water resources system planning, management and design, as well as to study the impact of various existing and proposed projects.

This paper deals with the development, calibration and application of a one-dimensional simulation model to study the impact on hydraulic condition of a river system with and without project situation. The present study concerns with optimising the planning and engineering design of hydraulic structures for Shrimp Culture in Bangladesh.

The estuarine areas have been developed under the Coastal Embankment Project (CEP) of Bangladesh Water Development Board (BWDB). The coastal polders in the districts of Cox's Bazar, Khulna, Satkhira and Bagerhat are very suitable for shrimp cultivation. Rapid development of shrimp farming in the extensive coastal and brackish water areas in southern part of Bangladesh has made a very significant contribution to the national export earnings. But unplanned shrimp farming development has led to degradation of agricultural land and have negatively affected the livelihoods of local people. The FFP aims at increasing production of shrimp by rehabilitating the 4 nos. polders in Khulna and Satkhira districts, which were implemented under the TFP. The project area has also included a new polder no. 15 in the district of Satkhira for detailed feasibility study.

One-dimensional hydrodynamic mathematical modelling technique has been applied to assess the water level and discharge at the un-gauged locations inside the project and in its periphery. Assessing the water management of the shrimp block with the aid of mathematical models has optimised the engineering design of hydraulic structures.

Problems and Issues

BWDB took up Coastal Embankment Project (CEP) in early 1960's to protect the poldered areas against salinity intrusion by constructing different types of embankments and sluices and this was proved to be a great success in respect of paddy cultivation. In recent years, shrimp culture activities have been developed in many polder areas in an intensive manner. All the polders are generally saucer – shaped flood plains with higher elevation along the peripheral CEP dykes, gradually sloping towards the centre of the polder.

The TFP ideologies and objectives could not be achieved satisfactorily due to unimplemented project components, which includes construction of channels and construction of appropriate separate structures for flushing and drainage purpose. Inappropriate structure design and use of structures for both flushing and drainage of water contribute substantial damage to shrimp farming activities.

Main source of income of the inhabitants residing inside the polder is related to shrimp culture. Shrimp producers are the wealthy and powerful people but the poor is involved in collecting shrimp fry from open water and also in wage labouring in shrimp *Ghers* and agriculture.

Since the start of shrimp cultivation, there has been a great change in terms of access to and use of water resources in all the polders. Previously, the people had free access to rivers, canals, beels and they could catch fish, irrigate water for growing crops and

navigate freely as common property resources. But after introduction of shrimp culture, the access to the water resources has been restricted which shrimp Gher owner presently controls.

In the process of shrimp cultivation technology and method, the shrimps are cultivated in Ghers following improved traditional/extensive method including gher preparation, collection of shrimp Post Larvas both from natural systems and hatcheries, exchanging water of the gher at fortnightly intervals etc. But there is some weakness in the practice and inappropriate planning and design of structures for which the rates of shrimp production have not been satisfactory.

Required Hydraulic Criteria for Shrimp Culture

Main parameters

- The system must be capable of supplying design water requirement and maintain the flood protection of the existing Polder embankment;
- The system should be capable of draining all the polluted water from shrimp block (or pond) to the river during the low tide;

Planning Criteria

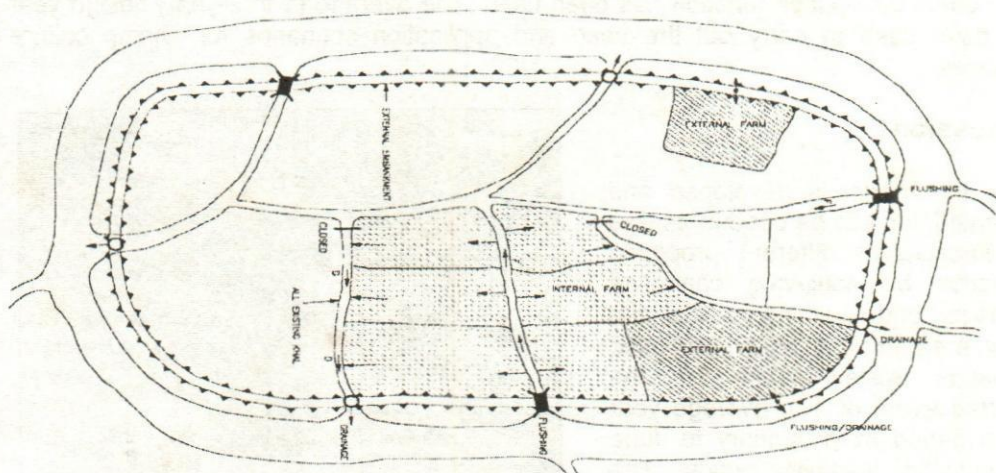
- The design depth of pond is 0.91m or greater. The minimum depth of pond is 0.60m can be accepted for the critical period;
- To maintain the water quality of pond, exchange of water of minimum 50% to 200% of water within a fortnight by maintaining design depth is required;

Schematic Concept of Shrimp Plan

In a shrimp project the following types of infrastructures are normally required:

- Embankment - a) peripheral and b) internal dykes;
- Sluices - a) peripheral - Flushing sluices
 - Drainage sluices
 - Flushing cum drainage sluices
- b) internal - Flushing sluices
 - Drainage sluices
 - Flushing cum drainage sluices
- Channel System - a) Flushing channel, b) Drainage channel and c) Flushing cum drainage channel

Figure 1 shows a schematic concept of the general plan where location of embankment, channels, shrimp farms, sluices etc. are shown.



Approach and Methodology:

Modelling Approach

In the normal process mathematical modelling starts with the collection and processing of historical and recent data. Then the development and calibration of a base model takes place in different steps. For the present study the model developed by Institute of Water Modelling (IWM) for river systems of South West Region of Bangladesh has been applied to generate boundaries for the study area model.

Methodology

MIKE11 mathematical modelling technique developed in the Danish Hydraulic Institute (DHI) has been used in the study. The MIKE11 software is based on an implicit finite difference scheme solution of the Saint Venant equations [1]. For hydrodynamic model the following equations are used;

$$\frac{dQ}{dt} + \frac{d}{dx} \left(\beta \frac{Q^2}{A} \right) + gA \frac{dh}{dx} + \frac{gn^2 |Q^2|}{AR^{3/4}} = 0$$

$$b \frac{dh}{dt} + \frac{dQ}{dx} = q$$

here A is the flow area, b is the width of channel, h is the stage, Q is the discharge, R is the hydraulic radius, n is the roughness coefficient, β is the momentum distribution coefficient, q is the lateral inflow rate per unit length.

Selection of Design Year

Frequency analysis has been carried out based on historical rainfall data and water level data in and around the study area for selection of design year for different return period.

Log-normal distribution function has been used. The average (1 in 2-year) design year has been used to carry out the base and application scenarios for shrimp culture purposes.

Discussions

Once the model is developed and calibrated, it could be used to assess the impacts of different proposed scenarios by achieving controlled drainage and flushing inside the study area. In this study proposed scenarios were tested for the selected event of 1 in average year return period from January to June for detailed feasibility study. The model has been developed including the flushing and drainage khals with the area elevation function of the shrimp block as an additional storage area. The study area model including shrimp block, flushing and drainage sluices of the Polder-15 are shown in Figure 2. The developed model has been used to see the performance of the structures for shrimp culture and to assist in proper water management in the polders. The simulation results has been interpreted to select the shrimp culture requirement in terms of design depth of pond (managed block by block) inside the polder, and



Figure 2: The Study Area of Polder-15

required exchange of pond water within fortnight (neap to neap tide) to maintain the water quality inside the pond.


The selected structures (no. of Vent and Size) have been included in the model set-up to assess the performance of the flushing and drainage sluices. This simulation is considered as option simulation, where existing features are demonstrated as flushing khal, drainage khal and area-elevation for storage of the shrimp block area. The block area has been described as additional storage area in the model set-up. For instance, optimisation of structures for shrimp block – E are illustrated below:

Table 1 Proposed Ventage of Flushing and Drainage Sluices for different simulation

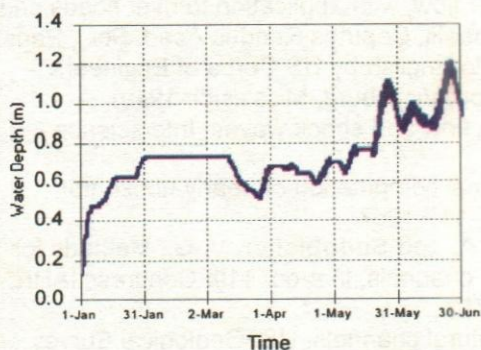
Block	Flushing Sluice No	Number of Flushing Sluices Vent Size: 0.9m x 1.2m				Drainage Sluice No	Number of Drainage Sluices Vent Size: 0.9m x 0.9m			
		Sim-1	Sim-2	Sim-3	Sim-4		Sim-1	Sim-2	Sim-3	Sim-4
E	F7	3	3	4	4	D6	1	2	2	4
	F8	4	4	5	5					3

Table 2: Estimated Pond Water Depth and Water Exchange Rate for Alternative Simulation

Month	Sim-1			Sim-2			Sim-3			Sim-4		
	Estimated Pond Water Depth		Estimated Exchange Rate	Estimated Pond Water Depth		Estimated Exchange Rate	Estimated Pond Water Depth		Estimated Exchange Rate	Estimated Pond Water Depth		Estimated Exchange Rate
	Max	Avg	%	Max	Avg	%	Max	Avg	%	Max	Avg	
Jan-1	0.64	0.57	0.0	0.64	0.57	0.0	0.66	0.59	0.0	0.64	0.57	0.0
Jan-2	0.75	0.69	0.0	0.75	0.69	0.0	0.76	0.71	0.0	0.75	0.69	0.0
Feb-1	0.75	0.75	0.0	0.75	0.75	0.0	0.76	0.76	0.0	0.75	0.75	0.0
Feb-2	0.75	0.75	0.0	0.75	0.75	0.0	0.76	0.76	0.0	0.75	0.75	0.0
Mar-1	0.75	0.70	114.3	0.75	0.69	118.0	0.76	0.69	121.7	0.75	0.68	120.4
Mar-2	0.71	0.60	48.8	0.70	0.58	51.8	0.71	0.59	50.3	0.69	0.57	53.2
Apr-1	0.73	0.71	117.0	0.71	0.69	121.1	0.73	0.70	122.6	0.69	0.67	124.0
Apr-2	0.76	0.70	75.7	0.74	0.67	78.3	0.76	0.69	77.6	0.72	0.65	80.0
May-1	0.82	0.77	76.2	0.80	0.74	79.8	0.82	0.76	80.1	0.77	0.72	81.8
May-2	1.17	0.98	77.4	1.12	0.94	84.9	1.16	0.97	85.2	1.08	0.91	89.1
Jun-1	1.06	0.99	109.7	1.01	0.93	105.5	1.04	0.96	105.1	0.98	0.89	101.9
Jun-2	1.28	1.10	86.2	1.22	1.04	89.0	1.27	1.07	89.7	1.18	1.00	91.5

 No water has been drained during this fortnight, only flushing is considered to raise the initial pond water depth

Estimated Pond Water Depth
Block - E



Estimated Pond Water Exchange Rate
Block - E

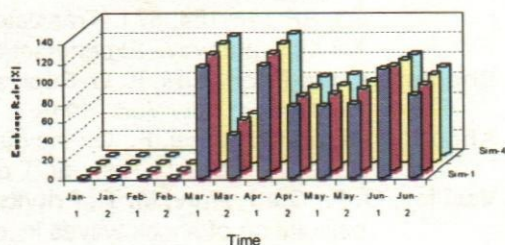


Figure 2: Estimated Pond Water Depth and Exchange Rate

Interpretation of model simulated results:

- The model results have been presented in terms of pond water depth of individual blocks of shrimp culture inside the polder and percentage of exchanged water within a fortnight from January to June.

- The hydrographs indicate the pond water depth inside the polder area, while the tabular form of model data provided quantitative assessment of design depth and required exchange of flow.

During simulation gate operation were logged to maintain the following criteria:

- no drainage has been allowed from January to March to raise the initial pond water depth and for initiation of shrimp cultivation;
- flushing and drainage gate operation is required during the monsoon to maintain the required pond water depth inside the shrimp block;

From the analysis of alternate plans, suitable plans would be selected based on required hydraulic and planning criteria.

Conclusion

The study has been devoted to assist in proper water management for shrimp culture inside the polder. Models for detailed Feasibility Study of the Shrimp Culture has been conceived to understand the complex flushing and drainage system of the polder area. The model considers the flushing and drainage system of the study area in a comprehensive way to simulate water level, discharge at the un-gauged locations inside the polder due to internal rainfall and inflow from external sources. The impact on any structural interventions on flushing and drainage system in terms of designed pond water depth and required exchange of water within a fortnight could easily be evaluated from the model results.

References

- Saint-Venant, B. De.** Theory of unsteady water flow, with application to river floods and propagation of tides in river channels, *Coputes Rendus Acad. Sci.*, Paris, 73, PP 148-154, 871 (Translated into English by US Corps of Engineers, No.49 Waterways Experiment Station, Vicksburg, Mississippi, 1949).
- Courant, R. and Friedrichs, K. O.** Supersonic flow and shock waves, Interscience Publishers, New York, 1948
- Abbott, M. B. and Ionescu, F.,** On the numerical computation of nearly horizontal flows, *J. Hydraulic Res.*, 5(2), pp 97-117, 1967.
- Vasiliev, O. F., Gladyshev, M. T., Pritvits, N. A. and Sudobicher, V. G.,** Methods for calculation of shock waves in open channels, in proc. 11th Congress IAHR, Leningrad, USSR, paper 3.44, 1975
- Barnes, H. H.** Roughness characteristics of natural channels, US Geological Survey Water Supply Paper 1849, 1967.
- Engelund F. and Hansen, E. A.,** Monograph on sediment transport in alluvial streams, Teknisk Forlag, Copenhagen, Denmark, 1967.
- MIKE11 user's guide,** Horsholm, Danish Hydraulic Institute, Denmark 1988
- BETS, AQUA, and SWMC (2001)** – Final Report, Feasibility Study (Phase-I) of Shrimp and Coastal Aquaculture Component, Fourth Fisheries Project, Bangladesh Engineering & Technological Services (BETS) Ltd, AQUA Consultant & Associates Ltd, Surface Water Modelling Centre (SWMC), November 2001.

Determination of the uplift pressure of Teesta Barrage by electric analogy method

A.S Anwarul Islam¹, Md Rafiqul Alam² and Dibakar Chakma³

Abstract

This paper deals with the determination of the uplift force and safety factor against the piping for both barrage and under sluice sections of Teesta barrage. Teesta barrage was constructed on a reinforced concrete structure. There was a probability of percolating some water underneath the structure. For this purpose electric analogy method was used to establish equipotential lines and flow lines to construct flow nets. The result and key findings of this paper is the resultant of vertical forces in the downstream face of barrage and its under sluices from gate at crest to the toe of glacis would act in upward direction. The exit gradient is more than sufficient for both cases. The result obtained from the study indicates that the sheet pile of under sluice at the toe is more than sufficient and there is no room to reduce the length of the sheet pile at the toe similar to that of barrage.

Introduction

Bangladesh Water Development Board has constructed a barrage across the Teesta river near Dalia, in the district of Nilphamari. This barrage was designed by the directorate of design, Teesta head works. River Research Institute took up study to determine uplift pressure and the seepage by electric analogy method under the barrage section as per request of design directorate, Teesta head works. Teesta barrage is a concrete structure resting on a permeable foundation of more or less fine sand. The objectives of this paper is the determination of uplift force and the factor of safety against piping for the Teesta barrage section and its under sluice. The problem of the Teesta barrage section was undermining of apron by scour, the other problem was to determine the head water elevation for barrage section & its under sluices. The expectation of result is that the resultant of vertical forces would act in downward direction all through out the barrage section and whether the given design of the sheet piles of barrage and under sluices are sufficient or not.

Basic Principle of flow through porous medium

The quantity of water flowing through a saturated soil mass as well as the distribution of water pressure can be estimated by the theory of flow of fluids through porous medium. While computing these quantities with the help of theoretical analysis the following assumptions are made (punmia,B,C,1994).

- Both water and saturated porous medium are incompressible. The size of the pore spaces does not change with time regardless of pressure.
- The seeping water flows under a hydraulic gradient which is due to gravity head loss or Darcy's law for flow through porous medium is valid.
- There is no change in the degree of saturation in the zone of soil through which water seeps and the quantity of water flowing into any element of volume is equal

¹ Principal Scientific Officer, ² Principal Scientific Officer (Addl. charge) & ³ Scientific Officer, River Research Institute, Faridpur

to the quantity which flows out in the same length of time.

- The hydraulic boundary conditions at entry and exit are known. According to the assumption (3) we can write the equation of continuity (Punmia,B,C,1994 & Transactions of the ASCE) as

$$\delta u / \delta x + \delta v / \delta y = 0 \quad (1)$$

$$\text{where, } u = k dp/dx \text{ and } v = kdp/dy \quad (2)$$

These are Darcy's law of flow, where u and v are the two components of the discharge per unit gross area in the directions x and y respectively; and k is a permeability coefficient which includes the effect of viscosity.

Substituting the equation (2) in (1) we can obtain the general differential formula for the steady flow of water through homogeneous materials for two dimensional flow has the form of Laplace equation.

$$\delta^2 p / \delta x^2 + \delta^2 p / \delta y^2 = 0 \quad (3)$$

where , p is the pressure

Again ,if the component of the current are i_x and i_y in the x –direction and y direction respectively, the equation of continuity is given by

$$\delta i_x / \delta x + \delta i_y / \delta y = 0 \quad (4)$$

But , according to the ohm's law, we have

$$i_x = C \delta E / \delta x \text{ and } i_y = C \delta E / \delta y \quad (5)$$

where , C is a co- efficient of $\delta E / \delta x$ and $\delta E / \delta y$ are the components of voltage gradient in the x - direction and y direction..

Now, substituting the equation (5) in the equation (4) we have form of Laplace equation

$$\delta^2 E / \delta x^2 + \delta^2 E / \delta y^2 = 0 \quad (6)$$

The similarity of equation (3) and (6) is the basic principle by which the electric Analogy method is applied. Equation (3) represents two families of curves, intersecting at right angles which are usually referred to as the flow lines and equ potential lines. It is to be mentioned that four methods are in common use for the construction of flow nets or for the solution of equation (3) , They are namely.

- Analytical or Mathematical derivation method
- Scale model method
- Graphical method
- Electrical analogy method

The Electric Analogy:

The Darcy's law governing the flow of water through soil is analogous to ohm's law governing the flow of electric current through conductors. Darcy's law $V = K i$ and ohm Law $I = (1/R)E$ are linear and of the same form, Where V is the velocity of flow, K is the permeability coefficient and i is the hydraulic gradient (RRI Report no. 76,1983). The problem at hand was to set up to a model scale with conductivity paper as the porous media and using electrodes to represent the active boundaries and non-conducting surface for inactive boundaries. The gradients of electrical potential was then measured between the two electrodes which were connected with a source of electrical energy.

Features of Teesta Barrage and Undersluice

The Teesta barrage is a reinforced concrete structure resting on a permeable foundation of more or less fine sand. The principal features of sections of the barrage and under sluice are:

- Length of the section – 58.22m
- Crest elevation – 48.77m R.L
- Up stream floor elevation – 47.55 m R.L
- Down stream elevation – 15.11m R.L & 14.50m R.L (under sluice)
- Pond level – 51.82m R.L
- Length of the section – 58.2m (after modification)

Four rows of sheet piling have been proposed; One row at the beginning of the structure, a second row located under the toe of upstream slope. A third row at the toe of down stream glacis and the fourth row at the downstream end of the structure. It is notable that the profile of Barrage (weir) section and that of under sluice section were subsequently modified. Thus the modified length of piles from upstream sections of barrage and under sluice are.

Barrage Section

D1 – 6.1m
D2 – 6.1m
D3 – 6.1m
D4 – 7.62m

Under sluice section

D1 – 7.62m
D2 – 6.2m
D3 – 7.62m
D4 – 9.14m

(0.61m of pile length are inside of the structure).

Methodology

The model of the section of Teesta barrage was constructed to 1: 100 scale and the equi potential line across the section with piling was determined. Next, the position of conductors and non conductors making up the side boundaries of the conducting paper was reversed and a second family of lines was determined. The second set is known as the flow lines which defines the direction of seepage flow through porous media and would be normal to the equi potential lines determined in the first experiment. The flow lines are super- imposed over the equi potential lines previously obtained and the combined form is known as a Flow Net. (**figure-1**). The flow net is graphical representation of the direction of flow and the magnitude of the pressure head in the porous media. From the flow net the following factors can be analyzed.

- Uplift pressure
- Factor of safety against piping.

Uplift pressure (For barrage section)

The potential gradient/hydraulic gradient across the base of barrage with respect to the horizontal distance from the upstream face of barrage is plotted and is shown in **fig –1**. This indicates the potential gradient / hydraulic gradient across the barrage section and seepage line. The uplift pressure acting under the barrage is the product of the effective head on the barrage and the potential gradient at any point which is the difference between head water and tail water elevation. For the Teesta barrage, the maximum head water with gates fully closed has been taken at 51.82m R.L (pond level) and the lowest tail water elevation is taken as downstream apron elevation of 45.11m R.L. This would give as effective head of $(51.82\text{m} - 45.11\text{m}) = 6.71\text{m}$. The flow net of modified barrage structure is shown in **Figure-2**.

The computation of uplift force and the downward acting (opposite) force has been done and is given in **table-1** and plotted in **Figure-3** along with potential gradient across the base of barrage. In calculating downward force acting by the barrage section, the density of concrete is assumed to be 1.4 under water. However, the weight of the piers, gates, road bridge blocks has not included in the computation.

Uplift pressure (for Under sluice section)

Electric analogy experiment was also done with the section of Teesta under sluice to determine the uplift pressure and the exit gradient. The flow nets are drawn for this section and is given in **Figure- 4**. In this case the maximum head water with gates fully closed has been taken as 51.82m R.L.(pond level) and the lowest tail water elevation is taken as apron elevation of under sluice which is 44.50m R.L. This would give effective head of 7.32m. The computation of uplift force and the downward acting force which is the depth of water on the under sluice plus the thickness of concrete structure has been done and is given in **table-2** and plotted in Fig-6 along with the potential gradient across the base of under sluice from the upstream end. The flow net of modified structure of under sluice is shown in **Figure-5**

In calculating downward force acting on under sluice section the density of concrete is assumed to be 1.4 under water. The weight of gates, piers, road bridge and block has not been included in the computation.

Factor of safety against piping (for barrage section)

The factor of safety against piping is the ratio of the floatation gradient to the exit gradient.

$$F_s = G_f / G_e$$

where G_f - Floatation gradient, G_e - exit gradient

From flow net **Fig-1**, The hydraulic gradient at exit; $G_e = D_h / a_s$

Where, $D_h = h/n$ and h = effective head = 6.71m, a_s = Length of the side near / exit or 3.05m, n = No. of squares between two adjacent flow lines = 20.

Hence, $G_e = h/n * a_s = 6.71/20 * 3.05 = 0.11$, and $G_f = (1-p) (s-1)$

where, p = porosity = 35%, s = Sp. gr. of material = 2.7

so, $G_f = (1-0.35) (2.7-1) = 0.65 * 1.7 = 1.10$

Therefore $F_s = G_f / G_e = 1.10/0.11 = 10$.

Computation of Factor of safety against piping from electric analogy experiment (for under sluice section)

Factor of safety F_s against piping is given by $F_s = G_f / G_e$

Where $G_e = D_h / a_s$, $D_h = h/n$

Here, h = effective head = 51.82 - 44.50 = 7.32m

so, $G_e = h / a_s * n = 7.32 / 3.05 * 20 = 0.12$

and $G_f = (1-p) (s-1) = (1-0.35) (2.7-1) = 1.10$

There fore, $F_s = G_f / G_e = 1.10/0.12 = 9.1$

In both cases a factor of safety of 5 to 7 may be accepted for sand of Teesta river near barrage site at Doani

Seepage Flow

If the properties of the material composing the porous medium are known, It is possible with flow net to compute the quantity of seepage flow to expect within a fair degree of accuracy. The discharge through a flow tube is from Darcy's law.

$$q = av = aki = ak\Delta h/a \text{ (Hydraulic Research Laboratory Report no.3, 1961)}$$

where i = hydraulic gradient and a = length of side of smallest complete square at exit
since $\Delta h = h/n_1$

where h =effective head and n_1 =No.of squares between the two adjacent flow lines=20

$$q = kh/n_1; \text{ and } Q = qn_2 = khn_2/n_1$$

where n_2 = no. of squares between the two adjacent equi potential lines = 9 & 10 for barrage & under sluice respectively. The coefficient k depends not only on permeability of porous medium but also on the physical properties of the fluid flowing such as viscosity and specific weight can be expressed as

$$K = cd^2w / \mu$$

where c = constant for material in medium, d = mean grain size, w = sp. wt of fluid,
 μ = dynamic viscosity of the fluid.

The following values have been chosen

$$\text{porosity} = 35\%$$

$$\text{Uniformity coefficient} = d_{60}/d_{10} = 0.16/0.09 = 0.18$$

$$d_{50} = 0.15\text{mm and } C = 0.5 \text{ cm/sec}$$

$$\text{The permeability coefficient for the above condition is } K = 0.5 \cdot 0.015 \cdot 0.015 / 0.010 \\ = 0.0112 \text{ cm/sec}$$

The seepage flow (for barrage section) will then be

$$Q = Khn_2/n_1 = 0.000112 \cdot 6.71 \cdot 9/20 = 3.4 \times 10^{-4} \text{ cumec/m}$$

That is 3.4×10^{-4} cumec per meter width of Barrage.

$$\text{The seepage flow for under sluice section will be } Q = Khn_2/n_1 = 1.12 \times 10^{-4} \cdot 7.32 \cdot 10/20 \\ = 4.1 \times 10^{-4} \text{ cumec per meter width of under sluice.}$$

The upper limit of d_{60} , of most of the soil samples are in the fine sand range i.e. from 0.4mm to 0.074mm (soil report of Doani barrage site, Report no.45 (81). 1981.RRI).

Results & Discussion:

Flow nets were constructed for original & modified design of Teesta Barrage section & its under sluice by electric analogy method.

For Barrage:

- The result of experiment indicated that the resultant of vertical forces would act in downward direction all through out the Barrage section with head difference 6.71m except in the portion of downstream glacis between the toe of gate and the third row of sheet pile. The structure would be a reinforced concrete and the unbalanced uplift force has been taken into account in the design of structure.
- The result, however, indicates that the weak point in the section where the uplift force would act when the gates would remain closed and with maximum head difference.
- There would be practically no change of exit gradient.

For Under sluice

- The result of experiment indicated that the resultant vertical force would act in downward direction for the under sluice section for head difference of 7.32m except in the portion of downstream glacis between the toe of gate near the crest and the third row of sheet pile,
- However, the result indicated that the location of unbalanced uplift force which should be considered for the safety of structure.
- There would be practically no change of exit gradient.

Conclusions:

The following conclusions are drawn on the basis of the study.

- The invert of the stilling basin of the barrage section is 45.11m R.L. while that of under sluice is 44.50m R.L.
- The depth of cut-off wall at the toe of stilling basin of barrage section is 7.62m and that of under sluice is 9.14m
- The cut-off wall goes up to 35.35m R.L. in the case of barrage and 33.22m R.L. in the case of under sluice section.
- The result indicated that the sheet pile of under sluice at the toe is more than sufficient and there is no room to reduce the length of the sheet pile at the toe similar to that of barrage.

Acknowledgment:

The authors are highly grateful to late Mr. A. Rahman, Ex. Director of Hydraulic Research Laboratory, Dhaka and Ex model Adviser, R.R.I and Mr. T. Hussain, Ex. Director (H.R.), RRI for their kind suggestions. The authors are also thankful to Mr. Idrichur Rahman, Ex. Sr. Research officer and Mr. Abdul Kader, A.S.O, RRI for their co-operation to study this experiment. The Authors are also thankful to Golam Kibria, Draftsman and Md. Enayetur Rahman Khan, Data Entry operator, Biplob L. Das, computer operator for their co-operation.

References:

- American Society of civil Engineers (1947):** Transaction of American Society of civil Engineers, Volume -112, New York, published by the Society.
- Hydraulic Research Laboratory (1961):** Electric analogy study of uplift pressure-Teesta barrage, Teesta project, report number - 3.
- Hydraulic Research Laboratory (1983):** Electric analogy study of Teesta barrage and under sluice, Teesta Project, Report number - 76
- Murthy prof. V.N.S.(1993):** A text book of Soil Mechanics & Foundation Engineering, 4th Edition.
- Punmia, Dr B.C Jain A.K (1994):** Soil Mechanics & Foundation 13th Edition.
- River Research Institute (1981):** Soil Report of Doani barrage site, report no 45.

Table -1: Computation of uplift Pressure & downward force of barrage section

Uplift Pressure				Downward Force				
Horizontal distance in (m) from U.S.	Piling Point	Potential %	Uplift force (m) in water	Horizontal distance in (m)	Thickness of concrete in (m)	wt. of concrete (m) in water	wt. of water (m)	Downward force (m) water
(0)		100	6.70	0	1.83	2.56	4.27	6.83
0.91		90	6.04	0.91 (Φ1)	1.83	2.56	4.27	6.83
0.91		80	5.36	4.88	0.91	1.28	4.27	5.55
0.91	Φ1	75	5.30	9.14	0.91	1.28	4.27	5.55
1.22		70	4.70	14.02	1.83	2.56	4.27	6.83
14.02		65	4.36	14.63 (Φ2)	1.83	2.56	4.27	6.83
14.63	Φ2	60	4.02	17.07	1.68	2.35	3.65	6.00
23.77		55	3.69	21.34	1.83	2.56	3.05	5.61
36.57		50	3.35	21.34	1.83	2.56	3.05	5.61
37.18	Φ3	45	3.02	24.38 (Toe)	1.83	2.56	0	2.56
37.49		40	2.68	30.48	2.51	3.52	0	3.52
49.98		35	2.35	33.53	2.59	3.63	0	3.63
57.91		30	2.01	37.19 (Φ3)	2.51	3.52	0	3.52
58.52	Φ4	25	1.52	42.67	2.36	3.31	0	3.31
58.52		20	1.34	54.86	1.83	2.56	0	2.56
58.52		15	1.0	58.52 (Φ4)	3.35	4.69	0	4.69
58.83		0	0	58.83	3.20	4.48	0	4.48

Vertical force acting along base of Barrage (weir)
Pond level + 51.8m R.L. (Density of concrete in water 1.4)

Effective head
51.82m – 45.11m = 6.71m

Table-2: Computation of uplift Pressure & downward force of under sluice section

Uplift Pressure				Downward Force				
Horizontal distance in (m) from U.S.	Piling Point	Potential %	Uplift force (m) in water	Horizontal distance in (m)	Thickness of concrete in (m)	wt. of concrete (m) in water	wt. of water (m)	Downward force (m) water
1	2	3	4	5	6	7	8	9
(0)		100	7.32	0	1.83	2.56	5.48	8.04
0.91		95	6.95	0.91 (Φ1)	1.83	2.56	5.48	8.04
0.91		90	6.58	4.88	0.91	1.28	5.48	6.76
0.91	Φ1	80	5.85	9.14	0.91	1.28	5.48	6.76
1.22		75	5.49	14.02	1.83	2.56	5.48	8.04
1.22		70	5.12	14.63 (Φ2)	1.83	2.56	5.48	8.04
14.02		65	4.75	17.07	1.22	1.70	5.48	7.18
14.63	Φ2	60	4.39	21.34	1.83	2.56	4.88	7.44
24.38		55	4.02	23.16	1.68	2.35	4.88	7.29
35.96		50	3.66	24.38 (Toe)	1.83	2.56	0	2.56
36.58		45	3.29	30.48	2.59	3.63	0	3.63
36.58	Φ3	40	2.93	36.58 (Φ3)	2.59	3.63	0	3.63
50.29		35	2.56	42.67	2.52	3.52	0	3.52
57.91		30	2.19	54.86	1.83	2.56	0	2.56
58.52	Φ4	25	1.83	58.52 (Φ4)	32.0	4.37	0	4.37
58.52		20	1.46	58.83	32.0	4.37	0	4.37
58.52		15	1.10				0	
58.52		10	0.73				0	
58.52		5	0.366				0	
58.83		0	0				0	

Vertical force acting along base of undersluice
Pond level + 51.8m R.L. (Density of concrete in water 1.4)

Effective head
51.82m – 44.50m = 7.32m

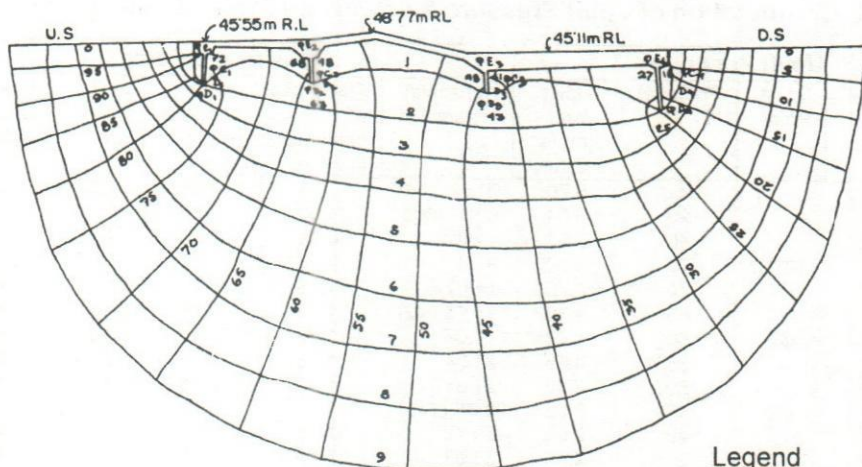


Fig-1: Flow Net Barrage section

Legend

Lenth of cut of wall

D1=6.1m

D2=6.1m

D3=6.1m

D4=7.62m

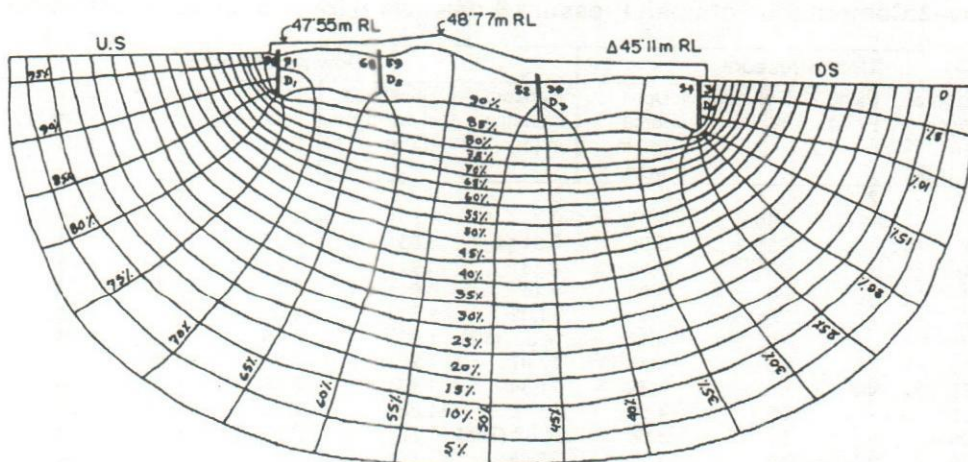


Fig-2: Flow Net Barrage section

Legend

Lenth of cut of wall

D1=6.1m

D2=6.1m

D3=6.1m

D4=7.62m

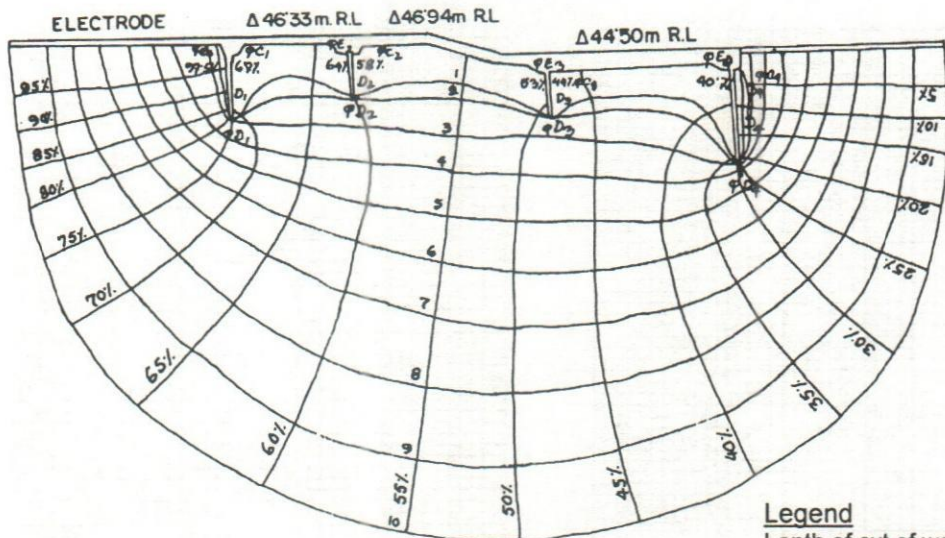


Fig - 4: Flow Net under sluice

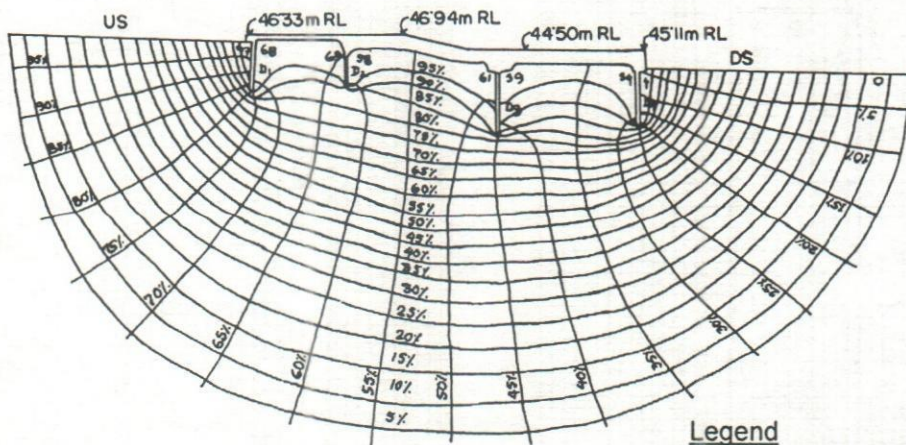


Fig - 5: Flow Net under sluice

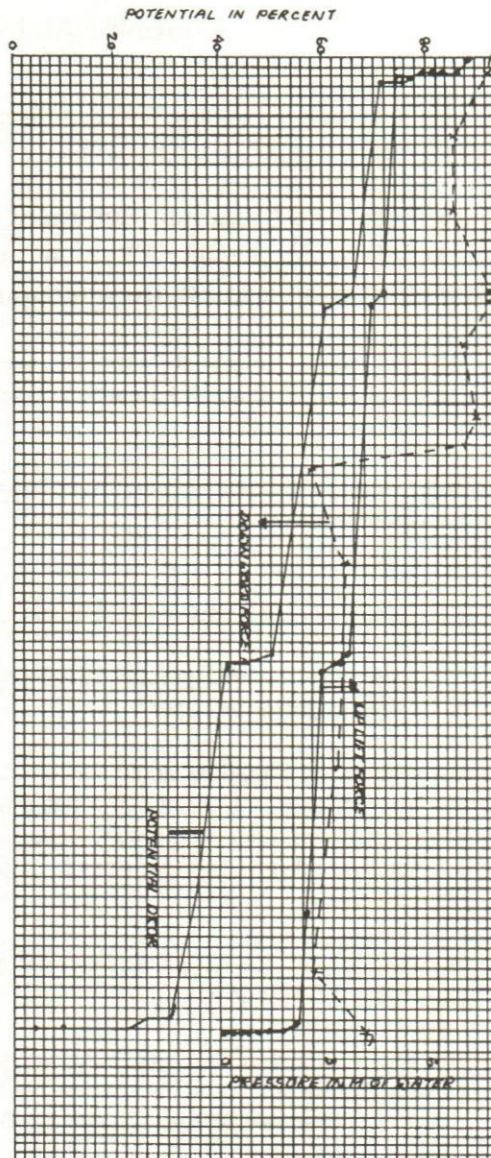
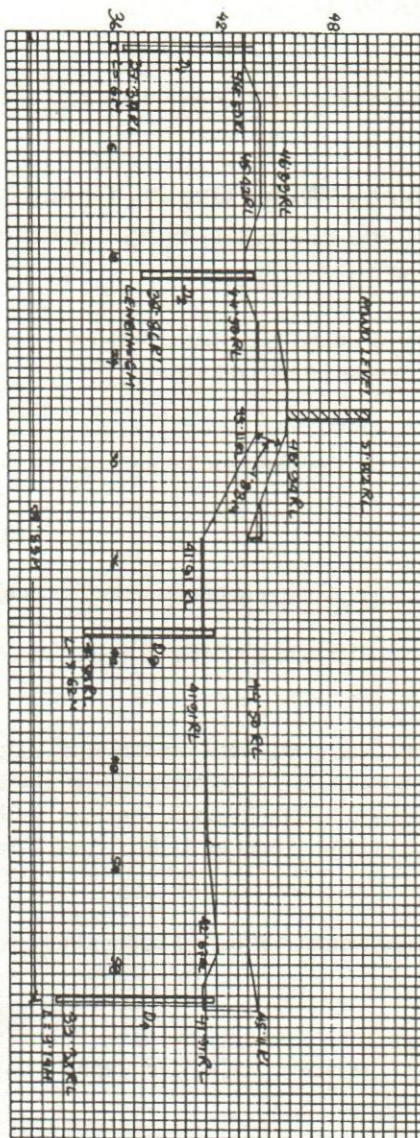


Fig-6 : Uplift pressure by electric analogy, profile of under sluice

GENERAL INFORMATION

The Technical journal of River Research Institute is published yearly. The journal publishes Scientific research papers in the fields of:

Hydraulics, Geo-technics, Sediment Technology, Water Quality, Concrete and building Materials, Physical and Mathematical Modeling, Ground Water Utilization and Environmental Engineering.

The Editorial Board, Technical journal of River Research Institute is responsible for the final acceptance of any paper and the Board's decision is final in case of any controversy.

The following guidelines should be followed strictly by the authors in submitting the manuscript of paper:

- The authors should be submitted their papers in two copies along with the diskette (3.5 inch).
- All words of the manuscript must be written in American Standard English and SI unit should be used throughout the paper.
- The manuscript should be single spaced computer typed using MS-word font size Arial 10 for text and MS-excel for graphs. The paper size should be B5 Env (176 mm x 250 mm) with page margin top, bottom, left, right, header, footer 1 inch, 0.5 inch, 1 inch, 0.5 inch, 0.5 inch, 0.5 inch respectively. The font sizes for caption & sub caption should be 11 & 10 Arial (bold) respectively.
- The manuscript of a full paper must not exceed 5000 words (16 journal pages) including tables, graphs, figures etc.
- The paper should contain minimum number of tables, graphs and figures and the size of these should be such that they can be read easily i.e. The tables, figures and graphs should contain in paper size B5 Env 176 mm x 250 mm.
- The manuscript of the paper should contain the title of the paper, Abstract, Introduction, Literature review, Materials and method or Methodology, results and discussion, conclusion, recommendation, acknowledgement (if any) and references.
- The title of the paper should not exceed 90 characters (capital) without spaces and font size should be Arial 12 with bold.
- The name of the author (s) should appear just below the title of the paper in the centre position and designation & address should appear as the footnote at the bottom of 1st page of the paper.
- All references of the published literature used in the paper should be arranged at the end of the text according to the alphabetical order of the author's last name and followed by the

Printed by:
Khan Art Block
Niltuly, Faridpur.
Phone: .0631- 62173, 62685
E-mail: kmsalim@bdonline.com

